Department of Mathematics and Statistics

A Generalized Fractal Dynamics Option Pricing Model with Transaction Costs

Francisca Angkola

This thesis is presented for the Degree of
Doctor of Philosophy
of
Curtin University

December 2016

Declaration

To the best of my knowledge and belief, this thesis contains no material previously published by any other person except where due acknowledgement has been made.

This thesis contains no material which has been accepted for the award of any other degree or diploma in any university.

.....
Francisca Angkola
December 2016

Abstract

Option pricing is an area which has been studied by many researchers worldwide with the aim of developing a much more realistic model than existing ones. Despite recent improvements, limitations still exist due to the various assumptions attached to the model itself. This research attempts to relax the assumptions of the stock return and volatility dynamics and construct a generalized pricing model that takes into account proportional transaction costs. This better reflects the financial market and thus improves the existing option pricing model. This thesis consists of three stages of work including deriving the general option pricing model with transaction costs for constant and stochastic volatility, performing numerical analysis for the general models, and applying the models to the real option data to verify its validity.

In the first part of this thesis, we derive the partial differential equation of the general European call option model which takes into account transaction costs. In addition to assuming a log-normal diffusion process, the general model also considers the fractal stock dynamic diffusion processes such as fractional Brownian motion and mixed fractional Brownian motion. We further extend this derivation to a general stochastic volatility model which assumes various volatility diffusion processes for different stock dynamic diffusion including the fractal dynamic processes.

The second part of this thesis focuses on the numerical analysis for the solution of the general model with constant and stochastic volatility processes, taking into account transaction costs. The use of finite element method in solving partial differential equations of the financial problems is demonstrated. The numerical results are then used to analyse the influence of various additional parameters on the European call option price.

Finally, we compare these general models using European call option market data. This is an important stage in determining which is the best performing model. The results show that there is no significant difference in assuming fractal dynamics as the stock diffusion process in the general constant volatility model. However, the inclusion of a stochastic volatility model improves the performance of the model against the real data. The effect of taking into account fractal dynamics in stock returns and/or volatility also becomes

more apparent when applied to stochastic volatility model. Adopting mixed fractional Brownian motion in both stock returns and volatility best models the market data. Last but not least, we also conclude our main contributions and discuss further research that may be done relating to this topic.

List of publications

The following papers were published or submitted for publication during the PhD candidature:

- S. Li, C. Luong, F. Angkola, and Y. H. Wu, "Optimal Asset Portfolio with Stochastic Volatility under the Mean-Variance Utility with State-Dependent Risk Aversion," *Journal of Industrial and Management Optimization*, vol. 12, no. 4, pp. 1521-1533, 2016.

- F. Angkola, Y. H. Wu, B. Wiwatanapataphee, and Y. Zhang, "Numerical Analysis of European Call Option under Fractional and Mixed Fractional Brownian Motion with Transaction Costs," *under review*

- Y. Zhang, Y. H. Wu, B. Wiwatanapataphee, and F. Angkola, "Asset Liability Management for an Ordinary Insurance System with Proportional Reinsurance in a CIR Stochastic Interest Rate and Heston Stochastic Volatility Framework," *under review*

Acknowledgements

The research reported in this thesis was carried out during which I was a PhD student at the Department of Mathematics and Statistics of Curtin University from March 2013 to December 2016. I would like to express my deepest gratitude and appreciation for all forms of help and support that I have received from my supervisor, co-supervisor, professors, families, friends and colleagues during this period of time.

I would like to express my genuine thanks to my supervisor, Prof. Yong Hong Wu, for his never-ending assistance during the period of my research. Prof. Wu continuously guides me in my research and constantly helps me with any relating matter. Thank you for always being there and patiently standing by me.

I would also like to thank my co-supervisor, Dr. Ee Ling Grace Aw, for her constant support during the period of my research. She is always willing to help whenever I have questions. I greatly appreciate her physical and mental support as well as sharing valuable life lessons from time to time.

I would like to express my warm thanks to Prof. Benchawan Wiwanathaphee for her tremendous help in the past two years. Prof. Wiwanathaphee keenly assisted my research every step of the way despite having to know me for a short period of time. Not only has she taught me new knowledge and helped me with Matlab programs, she also encouraged me to promptly finish my thesis.

I would like to give thanks to all my friends, in particular Li Shuang, Dewi Tjia, Elayaraja Aruchunan, Shican Liu, Siti, Dr. Hong Ben Yee, Dr. Yan Zhang, Dr. Yanli Zhou and Dr. Sabarina Shafie for their support and positive encouragements during this period of time.

In addition, I also thank all of the staffs and friends in the Department of Mathematics & Statistics for ensuring a friendly and comfortable working environment. My earnest thanks to the administrative staff - Jeannie Darmago, Marcus Tey, Petrina Beeton, Aimee Tournay, Joyce Yang, Cheryl Cheng and many others - for always being there to help with my never-ending queries.

Finally, I wholeheartedly thank my family: my parents, Syafei and Lily, and my two younger sisters, Elizabeth and Pauline, who endlessly support and encourage everything I do and will do in the future. Thank you for always believing in me and being the pillars that I could always rely on.

Contents

List of Figures

List of Tables

CHAPTER 1

Introduction

1.1 Motivation and background

For many decades, the financial markets have raised a lot of questions and caused confusion for many. No one is clear as to how the market behaves. For many years, researchers have attempted to comprehend this but in reality, the financial market is highly volatile and its behaviour is sometimes wild and unpredictable. In addition, factors such as high volume trading and computer mishap complicate matters. The introduction of derivatives, which originated from the need to reduce the risk of future loss, does not assist in making it easier to understand the financial market. However, derivative markets serve an important role and many traders rely on it, particularly for hedging purposes.

The idea of option trading had been developed at least as early as the 1600's as described by Joseph De La Vega (as cited in [22]) from the evidence of Netherlands having active involvement in trading option. Weber [23] suggested that the practice of such trading had occurred even earlier and provided detailed history and the origin of derivative markets. The revolution in trading and pricing derivative securities however, began in 1973 when the Chicago Board of Options Exchange started trading of options in exchanges. Options have nevertheless been actively traded in over-the-counter markets in earlier years [76]. The invention of profit charts in around 1870 [23] allowed the first pioneering attempt by Louis Bachelier [41] in 1990 to understand the complicated world of derivatives from a mathematical point of view. Bachelier [41] proposed an option pricing formula and assumed an arithmetic Brownian motion with drift (as cited in [20]). Gradually, similar formulas were since then developed with further adjustment to drift, distribution of dynamics and other improvements as presented by Sprenkle, Boness and Samuelson (as cited in [20]). However, it was not until 1973 that a complete option pricing formula, well-known as Black-Scholes Merton model, was developed by Fischer Black, Myron Scholes and Merton themselves [26, 55]. The celebrated model simplifies the complicated world of option pricing to an elegant formula of calculating European option. The formula made it

easy for everyone to calculate the option price and together with the addition of trading program, opened up to new possibilities of the financial market and along with that the derivative markets rapidly grew.

The Black-Scholes model describes the European option price with five important components consisting of strike price (K), constant risk free rate which may be measured using government bonds (r), price of underlying security (S_t), time to maturity ($T - t$) and constant volatility of the asset (σ). The formula is constructed based on the strict assumptions of perfect markets, constant risk free rate and volatility, log-normal distribution of share price dynamics, no dividends, continuous delta hedging and divisible number of shares as well as the possibility of short selling [26]. These 'ideal conditions' allow for such simplicity of the closed-form option pricing formula. However, it comes with the great compensation of not having to fit the reality of the financial market. Since the discovery of Black-Scholes Merton model, many researchers have begun to further develop the model on other derivative products as well as modifying it to better reflect the market. Stewart [35] suggested, the derivative system is relatively complex to work based on hunches and gut feelings, yet the current mathematical models do not adequately represent the reality of the market. Hence, Stewart [35] reinforced that the world economy requires more mathematics than less.

In view of these, the motivation of this research is to address the drawbacks and improve the model by modifying some of the strict assumptions in an attempt to better understand the derivative market, specifically the European option. First, assumptions such as perfect market, continuous hedging and no paid dividends are clearly unrealistic. In the real financial market, it is impossible to achieve a perfect market without anomalies such as transaction costs. Continuous hedging would also be too costly especially when transaction cost is taken into account. Second, the constant volatility parameter assumed in the Black-Scholes-Merton model is unmistakably one of the problematic parameter. Not only is it difficult to measure, it is obvious that the volatility in real financial market is not constant. In order to resolve the problem of constant volatility, the volatility may be modeled as a deterministic function (local volatility) or assumed to follow a stochastic process [76]. The drawback of local volatility model stems from its restrictive use to describe the behaviour of the volatility variations [76], whereas the stochastic volatility process complicates the model. This is the same argument for the assumption of constant risk free rate. Last but not least, the log-normal distribution assumption of stock price dynamics (geometric Brownian motion) dictates that the stock price or underlying security is log-normally distributed. However, numerous empirical studies and behavioural finance have shown that this has not always been the case. The distribution of stock re-

turn has been shown to have a thicker tail than a normal distribution would, and display observations of wide and non-periodic cyclical fluctuations [81]. Along with the evidence of volatility clustering [56], these may be an indication of non-linear dynamics. XSP Index daily log-returns [68] also shows this characteristic of volatility clustering, where large changes are clustered together (Figure 1.1). This, in turn, suggests that the distribution may be non-normal and Fama [21] and Mandelbrot [8] suggested possible alternatives of non-normal distribution of stock prices.

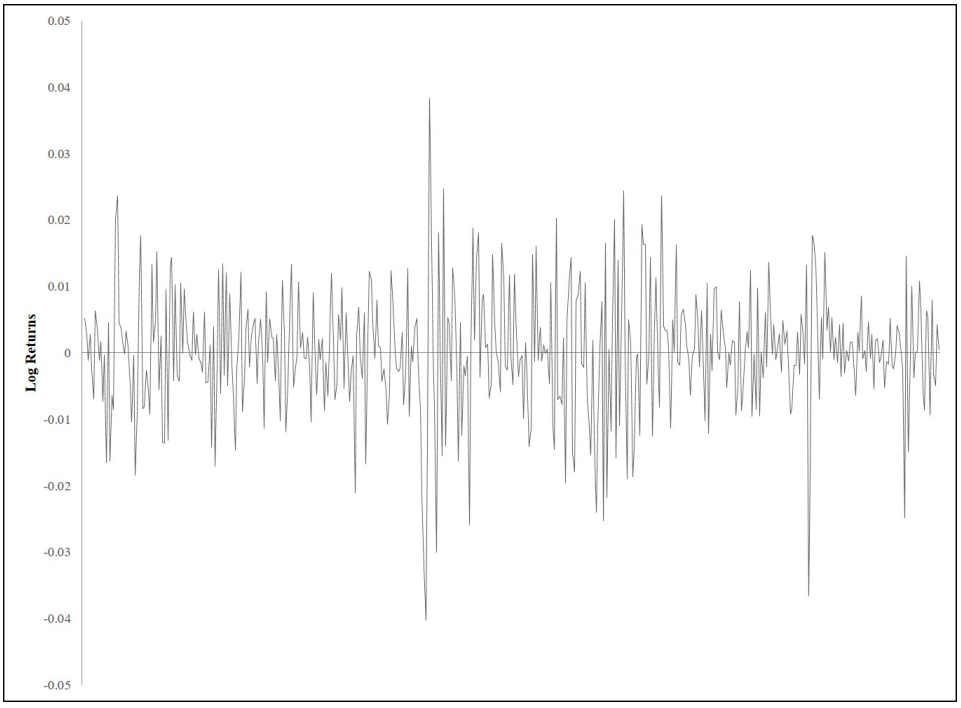

Figure 1.1: XSP Index daily log-returns

It was not until 1966 when Mandelbrot [9] proposed that the stock price dynamic is non-linear and the possibility that long range dependence may exist. Long range dependence represents a special form of non-linear dynamics called 'fractals' [6]. The existence of long range dependence indicates that the past history value influences the future value of stock. This however, contradicts the no-arbitrage property assumed in many development of financial models. This drives the research attention towards long range dependence in stock price and how it should be included in the option pricing formula instead of assuming random walk. Mandelbrot [11] proposed fractional Brownian motion (fBm) as an alternative for Brownian motion in order to capture the long range dependence property in the stock market. It is apparent that fBm is still Gaussian and self-similar (Figure 1.2). There are also other possible diffusion processes available that may be considered.

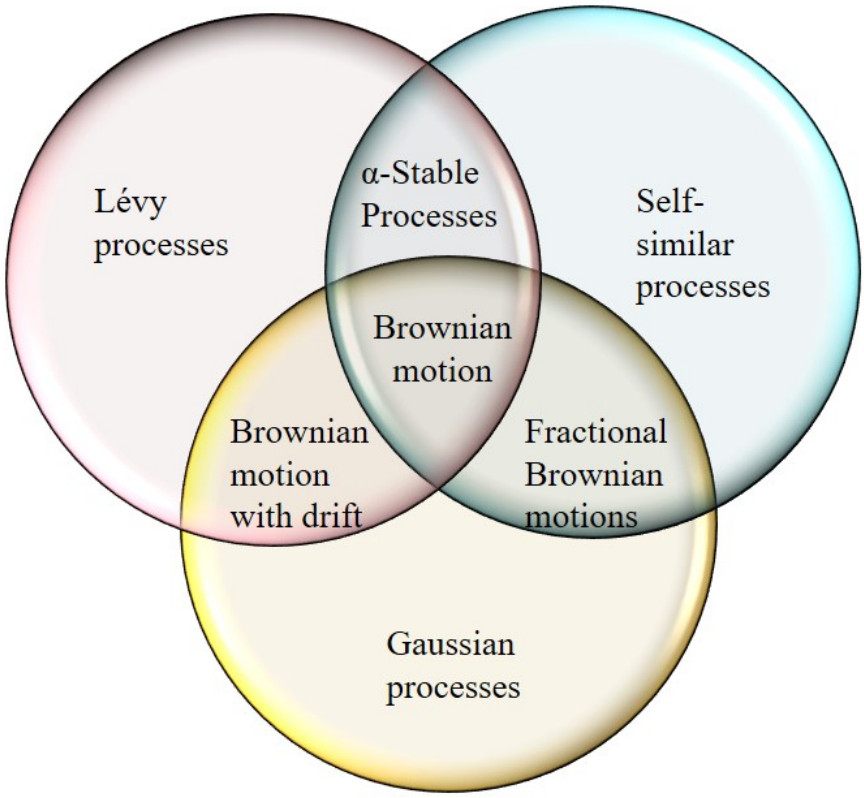

Figure 1.2: Venn diagram of various financial processes [57]

1.2 Objectives and contributions

Motivated by the growing interest to better understand the derivatives market, this thesis aims to develop a sophisticated model that will closely reflect the real market and then validate the model in various aspects. This goal is accomplished through achievement of the following specific objectives:

(i) Propose a general European option pricing model with proportional transaction costs assuming different stock dynamic processes with a stochastic volatility process

(ii) Derive the partial differential equation of the general stochastic volatility model of the European call option with the transaction costs being taken into account

(iii) Employ the finite element method on the general models to obtain the European call option price

(iv) Compare the various models by analysing the effect of additional parameters on the call option price, which distinguish each specific model from the Black-Scholes Merton model

(v) Calibrate each of the different models against the real data to attain the parameters which minimise the sum of squared errors (SSE) on each model

(vi) Use the calibrated parameters to determine the SSE on a new set of data to determine the best model for describing the market

In the process of achieving these objectives, we have also contributed to the following:

(i) Demonstrate the use of the finite element method to perform numerical analysis in finance

(ii) Analyse the significance of various parameters in the model

(iii) Determine which models are better in describing the market

(iv) Demonstrate how the analytical formula of the model may be used in practice

1.3 Innovation and significance

The introduction of the Black-Scholes Merton model has led to intensive research on financial derivative using mathematical modeling to better explain the behaviour of the market. One of the arguments in relation to the share market is the possible existence of long range dependence. However, there are many controversial theories surrounding the idea of long range dependence in finance, whether it exists in the share return or its volatility, or even exists in both cases. Furthermore, the next challenge is to determine how to include this in the model. Hence in this thesis, we have derived the general constant and stochastic volatility model to calculate the European call option price. The generalized model allows for an overall approach of viewing the problem, instead of having strict initial assumptions of the share return dynamic and volatility. In addition to relaxing the assumptions on the stock dynamics and volatility, the generalized model also takes into account transaction costs. The cost parameters introduced are relevant in practice as it plays a significant role in the derivative market. This model will then be calibrated against the real data to determine which model better reflects the market. The results assist in validating the idea of long range dependence in share market.

1.4 Outline of the thesis

This thesis consists of seven chapters as outlined in Figure 1.3. Chapter 1 is a brief introduction on option pricing. Chapter 2 of this thesis discusses the extensive studies that have been performed by many researchers in the financial market, starting from understanding how the share market behaves and later extending these knowledges to the derivatives market. The use of 'fractal' dynamics which captures the possibility of long memory in shares is examined and extended to the derivative model. In Chapter 3, the general stochastic volatility model with transaction costs is constructed and the partial differential equation of European call option price is derived. Numerical analysis on the derived partial differential equation (PDE) general model with constant volatility and stochastic volatility are performed in Chapter 4 and Chapter 5 respectively, in order to study the effect of various parameters involved in the model. In Chapter 6, the suitability of each model is validated by performing calibration of the various models with the actual call option price data. Chapter 7 concludes the main contributions of this thesis and provides recommendations for further research work.

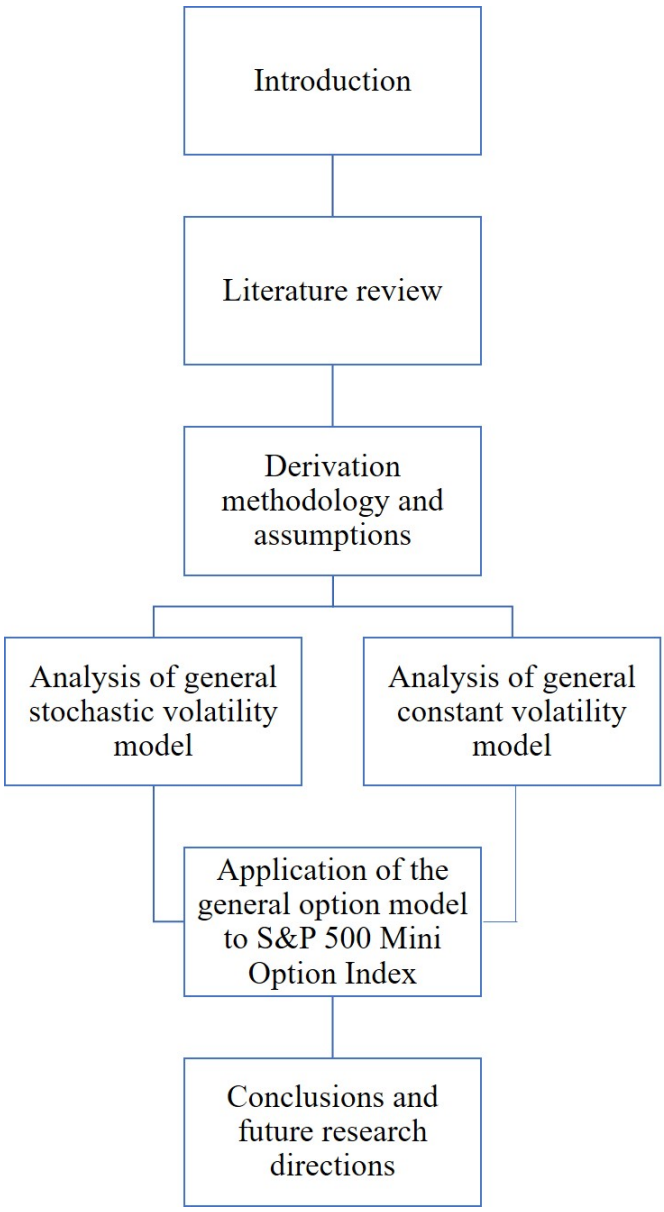

Figure 1.3: Outline of the thesis

CHAPTER 2

Literature review

2.1 General

As previously mentioned, stock returns are not normally distributed, having shown features of leptokurtosis and volatility clustering. Mandelbrot [11] first suggested the possibility of long memory existence in the market and introduced fractional Brownian motion to capture this dependence. In order to understand the purpose and scope of this research, we review the studies that have been conducted so far and discuss the evidence from previous literature in relation to the long memory (persistence) in the market as well as how to incorporate this persistence in the calculation of option price. This chapter examines the challenges of adopting fractional Brownian motion in finance and the proposed strategies in the literature and the existing option pricing models.

2.2 Long memory and fractional Brownian motion

The notion of 'long range dependence' or 'long memory' started when Hurst [32] and later along with Black and Simaika [33] studied the long term storage capacity in reservoirs (as cited in [78]). The studies resulted in the existence of long-term dependence of storage capacity which is measured by the 'Hurst' parameter. $H > \frac{1}{2}$ presents an aggregation behaviour which could describe the 'cluster' phenomena (memory and persistence) [25].

Fractional Brownian motion was initially introduced by Kolmogrov in 1940 (as cited in [46]). It is known as a generalized Gaussian process or a two-sided Brownian motion stochastic process $\{B_t^H, t \in \Re\}$ described by its Hurst parameter $H \in (0, 1)$ and its

integral representation according to Mandelbrot [11] is defined as the following:

$$\begin{aligned} B_0^H =& 0 \\ B_t^H =& \frac{1}{\Gamma(H+\frac{1}{2})} \int_{\Re} \Big((t-s)_+^{H-\frac{1}{2}} - (-s)_+^{H-\frac{1}{2}} \Big) dB(s) \\ =& \frac{1}{\Gamma(H+\frac{1}{2})} \int_{-\infty}^{0} \Big((t-s)^{H-\frac{1}{2}} - (-s)^{H-\frac{1}{2}} \Big) dB(s) + \\ & \frac{1}{\Gamma(H+\frac{1}{2})} \int_{0}^{t} (t-s)^{H-\frac{1}{2}} dB(s). \end{aligned} \tag{2.1}$$

Other integral representations of fBm are discussed in [25]. Fractional Brownian motion, on a complete probability space (Ω, F, P), also has the following properties:

(i) $E(B_t^H) = 0, \quad \forall t \in \Re$

(ii) $Cov(B_t^H, B_s^H) = \frac{1}{2}(|t|^{2H} + |s|^{2H} - |t-s|^{2H}), \quad \forall s, t \in \Re$

From its covariance property, it is possible to attain its increment properties as follows:

$$E[B_t^H - B_s^H] = E[B_t^H] - E[B_s^H] = 0, \quad \forall t, s \in \Re, \tag{2.2}$$

$$\begin{aligned} E[(B_t^H - B_s^H)^2] =& E[(B_t^H - B_s^H)(B_t^H - B_s^H)] \\ =& E[(B^H)^2] - 2E[(B_t^H B_s^H)] + E[(B_s^H)^2] \\ =& t^{2H} - 2.\frac{1}{2}[|t|^{2H} + |s|^{2H} - |t-s|^{2H}] + s^{2H} \\ =& |t-s|^{2H}, \quad \forall t, s \in \Re. \end{aligned} \tag{2.3}$$

The first and second moments of the increments depend only on the lag of t and s, thus indicating that fractional Brownian motion has stationary increments. Let $0 < s < t$, then

$$\begin{aligned} E[(B_t^H - B_s^H)(B_s^H - B_0^H)] =& E[B_t^H B_s^H] - E[B_t^H B_0^H] - E[B_s^H B_s^H] + E[B_s^H B_0^H] \\ =& \frac{1}{2}[t^{2H} + s^{2H} - (t-s)^{2H}] - s^{2H} \\ =& \frac{1}{2}[t^{2H} - s^{2H} - (t-s)^{2H}]. \end{aligned} \tag{2.4}$$

Equation (2.4) indicates correlated increments when $H \neq \frac{1}{2}$. When $H > \frac{1}{2}$, fBm increment is positively correlated to the historical increments and thus depicts a persistent nature. On the other hand, when $H < \frac{1}{2}$, fBm depicts an anti-persistent behaviour where the current increment will behave in contrary to the past evolution. $H = \frac{1}{2}$ indicates independent increments which is the property of the classical Brownian motion.

These behaviour may also be described by looking at the increment of fBm in terms of its integral representations,

$$\begin{aligned}\Delta B_t^H =& B_{t+\Delta t}^H - B_t^H \\ =& \frac{1}{\Gamma(H+\frac{1}{2})}\int_{-\infty}^{t}\Big((t+\Delta t-s)^{H-\frac{1}{2}} - (t-s)^{H-\frac{1}{2}}\Big)dB(s) + \\ & \frac{1}{\Gamma(H+\frac{1}{2})}\int_{t}^{t+\Delta t}(t+\Delta t-s)^{H-\frac{1}{2}}dB(s)\end{aligned} \tag{2.5}$$

Equation (2.5) separates the interpretation of fractional Brownian motion into two parts. The second term captures the current innovation from t to $t+\Delta t$, whereas the first integral term measures the moving average of the past historical shocks. The first integral may be positive or negative depending on the value of H, and the weighting kernel $f(x) = x^{H-\frac{1}{2}}$. If $H < \frac{1}{2}$, the weighting kernel is a downward-sloping hyperbola function and hence the first term of equation (2.5) will yield a negative increment. On the other hand when $H > \frac{1}{2}$, the first term yields positive increments consistent with the persistent behaviour due to the historical shocks.

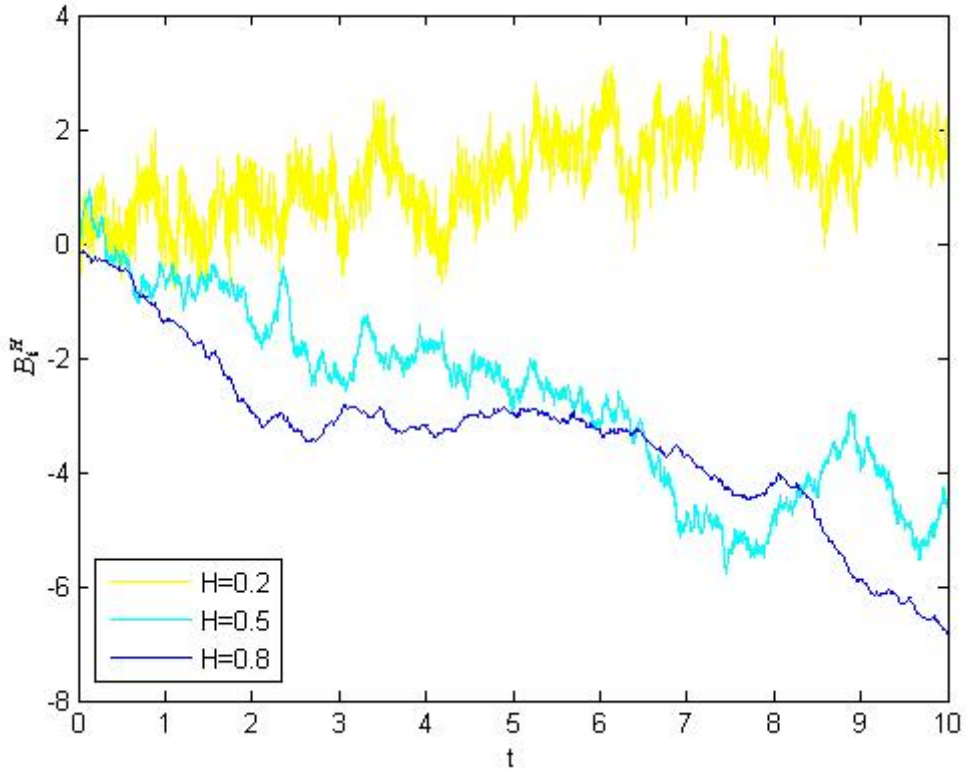

Figure 2.1: Fractional Brownian motion path for different values of Hurst parameter

The path of fractional Brownian motion varies for different values of Hurst parameter (H), i.e. lower, equal and higher than 0.5. The path of fBm for higher Hurst parameter is smoother compared to those of lower value of H. For $H > \frac{1}{2}$, the path also deviates more from the mean compared to the others, thus reinforces its persistent characteristics (Figure 2.1).

Numerous empirical and behavioural finance studies on stock returns of various stock markets have indicated the presence of long memory. Mandelbrot's studies [10] of long memory in stock price is based on the classical (Rescaled Range Statistic) R/S analysis and results in a H value of approximately 0.55 (as cited in [48]). Greene and Fielits [48] studied the long memory of 200 daily stock return series listed on the New York Stock Exchange using the same technique and found that many series are characterized by long term dependence. The forecastability of long horizon stock returns may be due to time variation in expected returns or speculative bubbles, but it may also be an indication of long memory [50]. This was further investigated by Henry [50] through the analysis of various international stock indices. Evidence of long memory was also found in some firms' return series but not in stock indices [40]. Others [1,19,53,60] have attained mixed results with some showing weak evidence of long memory. Dajcman [59] concluded that the Hurst parameter only increases in accordance with major financial market disruptions.

Besides calculating the Hurst parameter, there are other ways of identifying the existence of long range dependence such as analysing the autocovariance function (ACF). By definition [62], when the autocovariance function of a stochastic process declines at least exponentially as lag increases, it indicates that the stochastic process has short memory. If ACF declines hyperbolically, the stochastic process has an intermediate memory as long as the infinite sum of all absolute values of the autocovariance still exists. If the latter condition is not satisfied, the stochastic process is said to have long memory [62]. The autocovariance function of the increment of fBm is given as follows:

$$\begin{aligned}\rho_H(\tau) =& Cov(B^H(t+\tau) - B^H(t+\tau-1), B^H(t) - B^H(t-1)) \\ =& \frac{1}{2}[(\tau+1)^{2H} + (\tau-1)^{2H} - 2\tau^{2H}]\end{aligned} \tag{2.6}$$

For $H > \frac{1}{2}$,

$$\sum_{\tau=1}^{\infty} \rho_\tau = \infty. \tag{2.7}$$

For $H < \frac{1}{2}$,

$$\sum_{\tau=1}^{\infty} |\rho_\tau| < \infty. \tag{2.8}$$

From equations (2.7) and (2.8), we may conclude that fBm has long memory when $H > \frac{1}{2}$ and intermediate memory when $H < \frac{1}{2}$. Therefore, when analysing the long memory, one has to consider the influence of the entire history instead of just looking at a finite past, because limiting observations to a finite past is only feasible for intermediate memory processes [62]. In reality, considering the entire historical influence may be difficult in practice.

The measurement of long term dependence has always incurred a problem as statistical test may not be powerful enough to detect the dependence given the limited time span of available data [81]. However, despite no conclusive answer of the existence of long memory, historical records still exhibit distinct non-periodic cyclical patterns which are indications of the presence of significant power of low frequencies (long-range dependence) [69]. When in doubt of whether long memory exists, one should question whether the markets are actually efficient [48]. An efficient market is where the price reflects all the available and relevant information, and the arrival of new information is promptly arbitraged away [48]. This is also indicated by Bayraktar *et al.* [19] who showed that after the introduction of computer trading, which leads to the increase in efficiency in the market, the measured H value drops closer to 0.5. In reality, this does not always occur. Therefore, it is sensible to consider the existence of long memory in the financial market.

2.3 Non-semimartingale property of fBm for $H > \frac{1}{2}$ and arbitrage opportunities

The idea of fractional Brownian motion and long memory in stock market was very appealing. However, fBm process does not have a semimartingale property for when $H \neq \frac{1}{2}$. An elegant proof of the non-semimartingale property of fBm through the computation of p-variation of B^H is detailed in [42] and [25]. Another approach of analysing the non-semimartingale property of fBm as the one presented in [78] is as follows:

A process $\{X_t, F_t, t \geq 0\}$ is semimartingale if

$$X_t = X_0 + M_t + A_t,$$

where X_0 is F_0-measurable, M is a F_t local martingale with $M_0 = 0$ and A_t is a process of locally bounded variation. This implies that a semimartingale process has a locally bounded variation. Let $X_t = B_t^H$, the quadratic variation is infinite for $H < \frac{1}{2}$ and zero for $H > \frac{1}{2}$. Thus, fBm is not a semimartingale process for $H \neq \frac{1}{2}$. The issue with

this is that the extensively used Itô calculus, developed for semimartingales to solve for stochastic integral, does not apply here. Similarly, the non-semimartingale property of fBm indicates that arbitrage opportunities are possible as proved in [42]. This is, however, inevitable since long memory depicted in fBm implies that the future value of the market is predictable by its historical value. As a result, the researches on fBm as a process used in finance came to a halt. It was not until Duncan *et al.* [64] presented a solution to the problem by introducing a stochastic integration calculus with respect to Wick product ($\diamond$) that motivated further research in this area. The use of Wick product allows the stochastic integral problems to be solved as such that it shows close proximity to the Itô calculus, thus named as fractional Wick Itô integrals. Although this brought new insights towards the use of fBm in describing the stock market evolution, it has not entirely solved the problem of arbitrage. Delbaen and Schachermayer [29] had proven that irrespective of the integration theory, a weak arbitrage called free lunch with vanishing risk is still present in continuous time market models unless the underlying stock S_t is a semimartingale process. Cheridito [52] has also successfully constructed arbitrage strategies in fractional Black-Scholes model when Wick Itô and pathwise integration methods were used.

2.4 Fractional integration

When restricting $f(s)$ to only deterministic integrands, the definition of stochastic integral with respect to fractional Brownian motion does not differ to the one previously developed for standard Brownian motion. Thus, no new integration methods would be necessary. The deterministic integrands may be approximated by the sequence $\sum_{i=1}^{n} \zeta_i I_{[t_i,t_{i+1}]}$ being a piecewise constant and hence may be directly multiplied with the discrete fractional Brownian motion increment $(B^H_{t_{i+1}} - B^H_{t_i})$. As the partitions $|\pi| \to 0$ of the interval $[0,t]$, the Riemann sums converge to a random variable in the mean square sense, and thus the fractional integral of $f(s)$ may be defined as the following:

$$\int_0^t f(s) dB^H_s := \lim_{|\pi|\to 0} \sum_{i\in\pi} \zeta_i (B^H_{t_{i+1}} - B^H_{t_i}). \tag{2.9}$$

However, when the integrands are no longer deterministic or they are of infinite variation, the convergence of Riemann sums in the mean square sense may not be available [31]. In order to define this type of stochastic integrals, one may either alter the Riemann sums or change the definition of convergence. These developed integration theories only apply for $H > \frac{1}{2}$. Further extension for all $H \in (0,1)$ requires the S-transform approach. This extension of Wick-Based approach to $H \in (0,1)$ is famously known as Wick Itô Skorohod

integrals. More detailed discussion and derivation are in [12], [13] and [25].

2.4.1 Wick-based approach

It was mentioned in the previous section that Duncan *et al.* [64] has developed the stochastic integration method based on the Wick product instead of using the ordinary product multiplication. The idea of Wick product is used parallel to fractional white noise calculus as discussed in [75] and [25]. When the integrand $F(s)$ is no longer deterministic, the stochastic fractional integral of Wick-based type is defined as follows:

$$\int_0^t F(s)dB_s^H := \lim_{|\pi|\to 0} \sum_{i\in\pi} F(t_i)\diamond(B_{t_{i+1}}^H - B_{t_i}^H). \tag{2.10}$$

The Wick-based approach is shown to be parallel to the classical Brownian integration theory and the expectation of $\int_0^t F(s)dB_s^H$ is zero which is a convenient feature and thus is the reason why this approach was first introduced [62]. However, the use of Wick-Based integral approach may be difficult to justify from a modeling point of view. Nevertheless, this integral method is still useful in describing the financial market due to its conformity with Itô calculus and many results have been obtained using this idea [46, 62].

Let the stochastic differential equation of a stock price (S_t) be

$$dS_t = \mu S_t dt + \sigma S_t dB_t^H, \tag{2.11}$$

where μ and σ are constants. The analytical solution based on Wick-Based integration approach is

$$S_t = S_0 e^{\mu t + \sigma B_t^H - \frac{1}{2}\sigma^2 t^{2H}}, \quad t \geq 0. \tag{2.12}$$

2.4.2 Pathwise integrals

Another approach of fractional integration is based on the pathwise sense. In this case, the stochastic integral is still defined as Riemann sums using ordinary product, but instead altering the definition of convergence. There are two ways of relaxing the definition of convergence. The first method is by postulating pathwise convergence which then results in a deterministic integral that converges in the Riemann-Stieltjes sense, thus known as pathwise integration. However, when using this method, the integrand has to satisfy pathwise Hölder continuinity. The pathwise integral for $H > \frac{1}{2}$ is defined as follows:

$$\int_0^t F(s)dB_s^H := \lim_{|\pi|\to 0} \sum_{i\in\pi} F(t_i)(B_{t_{i+1}}^H - B_{t_i}^H). \tag{2.13}$$

Alternatively, one may use fractional Stratonovich integral where the convergence definition is based on the convergence in probability, thus allowing for a wider class of integrands. The integral definition for $H > \frac{1}{2}$ is as follows:

$$\int_0^t F(s)dB_s^H := \lim_{|\pi|\to 0} \sum_{i\in\pi} F\Big(\frac{t_{i+1}+t_i}{2}\Big)(B_{t_{i+1}}^H - B_{t_i}^H). \tag{2.14}$$

However, since pathwise and Stratonovich integrals are based on the same concept of altering the definition of convergence, they are usually treated as a single approach to fractional integration. Rostek [62] and Biagini *et al.* [25] provided detailed description of these alternative integral methods and outlined the difference between these methods compared to the Wick-based approach. The pathwise sense is a more natural approach to modeling, but it does not produce a zero mean desirable property as the Wick-based approach. For the same stochastic differential equation (2.11), the analytical solution based on the pathwise sense is

$$S_t = S_0 e^{\mu t + \sigma B_t^H}, \quad t \geq 0. \tag{2.15}$$

2.5 Strategies to solve arbitrage

Despite the introduction of Wick-Based stochastic integration approach with the zero mean property, it has not solved the problem of arbitrage for continuous market model such as the Black-Scholes model for option pricing. Many studies [25, 52, 62] have shown arbitrage possibilities when fBm is used in continuous dynamic hedging regardless of any integration theory used, Wick-based or pathwise sense. This will always be true provided that the definition of arbitrage, self-financing and admissibility remain unchanged [62]. This drives the research to continue finding strategies to solve the arbitrage problems by altering the underlying definitions. Hu and Øksendal [75], and Elliot and Van Der Hoek [58] took similar approach of modifying the definition of portfolio value and the property of self financing by extending the idea of Wick product in constructing the portfolio (Π_t) such that

$$\Pi_t = X_1 \diamond S_t + X_2 D_t. \tag{2.16}$$

At first glance, this model provides an encouraging result as it manages to exclude arbitrage opportunities and the approaches used are mathematically correct. Motivated by this result, Necula [16] managed to construct a complete fractional Black-Scholes model. However, the use of Wick product on financial concepts received many criticism in terms of its economic interpretation. The use of this Wick product beyond pure integration

approach and the economic interpretation of Wick self-financing property was first questioned by Sottinen and Valkeila [66]. The Wick self-financing definition contradicts economic intuition for both definitions [58, 75] and this was further discussed by Bjork and Hult [63]. Later, Øksendal [7] suggested that a way of looking at the economic intuition of Wick-based portfolio value is based on market observers and the process S_t is viewed as the fundamental firm value. This unusual approach is introduced in order to validate the use of Wick product for both integral theory and portfolio construction. Despite this approach being reasonable, the setting seems to be quite artificial [15]. Bender [15] viewed these approaches as restrictions of the class of trading strategies and thus concluded that the answer to the arbitrage problem would be to search for feasible restrictions of these.

Another type of strategy is introduced to solve the problem of arbitrage is the regularization of fractional Brownian motion proposed by Rogers [42] and Cheridito [51]. This strategy is constructed by replacing the weighting kernel of the integral representation of fBm so that the resulting stochastic process still adopts the desirable fBm property, yet it becomes semimartingale. Other researchers [4, 14, 49, 67] have also attempted semimartingale approximation approach to fractional Brownian motion in order to maintain the no-arbitrage requirement. Cheridito [51] further proposed mixed fractional Brownian motion (mfBm) and proved that this process is semimartingale for $H \in (\frac{3}{4}, 1)$, but questioned the regularization of such use.

Instead of seeking strategies for fBm to satisfy the semimartingale requirement, both Guasoni [54] and Rostek [62] took a slightly different approach and introduced market imperfections to avoid the existence of arbitrage. Guasoni [54] had successfully proved that the existence of transaction costs eliminate arbitrage possibilities. In light of this, Rostek [62] suggested a dynamically incomplete market which assumed that a single investor will not be able to proceed two consecutive transactions infinitesimally fast, thus restricting their tradability based on their risk preferences.

2.6 Mixed fractional Brownian motion

Mixed fractional Brownian motion (mfBm), which was first introduced by Cheridito [51], is constructed via the linear combination of Brownian motion (B_t) and fractional Brownian motion (B_t^H). The stochastic differential equation of stock price S_t assuming mfBm is

$$dS_t = \mu S_t dt + \sigma S_t(\gamma dB_t + dB_t^H), \tag{2.17}$$

where μ, σ and γ are constants. Subsequently, the analytic solution is presented as

$$S_t = S_0 e^{\mu t + \sigma(\gamma B_t + B_t^H)}. \tag{2.18}$$

As previously discussed, a mixed fractional Brownian motion process is semimartingale only when $H \in (\frac{3}{4}, 1)$, given that B_t and B_t^H are independent to each other. Thus, the arbitrage problem still exists for $H \in (\frac{1}{2}, \frac{3}{4})$. However, mixed market is arbitrage free without any conditions on the dependence of B_t and B_t^H if restricted to self-financing Markov type strategies with smooth B_t and B_t^H [78]. After the introduction of mfBm, numerous researchers have taken this idea to apply it in different concepts of financial model [70, 71]. Dominique and Rivera-Solis [17] also tested mfBm model for the case of S&P 500 Index and argued that this process offers a more realistic view of financial data due to its ability to capture the local variability. Mishura and Shevchenko [77] also reinforced the motivation of adopting mixed fractional Brownian motion which is to capture the two distinguishable sources of randomness in the financial market. One being the noise from the stock exchange with thousand of agents which may be captured by the geometric Brownian motion process. The other random source is from the financial and economical situation which may be represented by the fractional Brownian motion.

2.7 Fractional models for option pricing

In order to include long memory in derivatives such as option, the log-normal distribution of stock dynamic assumption is modified to follow geometric fractional Brownian motion. The problem of arbitrage may be solved using strategies as those mentioned in Section 2.5. A fractional Black-Scholes model developed by Necula [16], using the idea of Wick portfolio value, is considered to have no intuitive economic interpretation. In order to adopt the Wick-based portfolio strategy, the definitions of S_t as the firm value and consideration in terms of market observers should instead be used for interpretation of the model. The corresponding results will still be the same as presented by Necula [16]. However, since this strategy is difficult to be justified, other strategies are preferable. Wang [72] constructed a European call option pricing model assuming geometric fractional Brownian motion as its stock dynamic, solving fractional integration based on the pathwise sense and taking into account proportional transaction costs to eliminate the arbitrage problems. Later, Wang *et al.* [73] further constructed a European call option pricing model in which mixed fractional Brownian motion stock dynamic was assumed. The partial differential equation for both models [72,73] are attained using Leland's discrete hedging strategy [34] and with further assumptions of surely positive gamma $\left(\frac{\partial^2 c}{\partial S^2}\right)$, the analytical model of min-

imum European call option price are given. Summarising Wang *et al.* derivation [72, 73], we take a slightly different approach of constructing the derivation of partial differential equation of European call option price assuming a general case where both fBm and mfBm stock dynamics are considered, as well as taking into account the transaction costs.

Consider a stock price dynamic S_t which follows a general 'fractal' diffusion process and thus the stochastic differential equation follows:

$$dS_t = \mu S_t dt + \sigma S_t(\gamma dW_t + (1-\gamma)dB_t^H) \tag{2.19}$$

where μ, σ, γ are constants, dW_t and dB_t^H represent Brownian motion and fractional Brownian motion, respectively. Note that when $\gamma = 0$, the stock price dynamics will follow geometric fractional Brownian motion, whereas when $\gamma = 1$, equation (2.19) follows a geometric Brownian motion. In other cases where $\gamma \in (0, 1)$, equation (2.19) follows a mixed fractional Brownian motion.

Let $c(t, S_t)$ be the value of a European call on the underlying share (S) at time, t, with exercise date (T) and exercise price (K). In order to derive the PDE for the call option value (c), we consider a portfolio consisting of one unit of short selling of the European call option and X_1 units of share, such that

$$\Pi = -c + X_1 S_t, \tag{2.20}$$

where S_t is the price of one unit share which follows the general diffusion process as described by the stochastic differential equation (2.19) in which $\mu, \sigma, \gamma \in \Re$, $H > \frac{1}{2}$ and dB_t^H is independent of dW_t.

Applying the delta neutral concept in which the portfolio remains unchanged when small changes occur in the shares prices, we have

$$\frac{\partial \Pi}{\partial S} = 0$$

which gives

$$-\frac{\partial c}{\partial S} + X_1 = 0$$

and hence

$$X_1 = \frac{\partial c}{\partial S}. \tag{2.21}$$

Let k be the transaction cost of buying or selling the share measured by the percentage of transaction amount, then the total transaction cost of buying or selling υ units of share

at price S is $k|\upsilon|S$.

Assuming trading can only occur at time t and $t+dt$ but never in between, the change in portfolio after trading, taking into account transaction costs, is as follows:

$$d\Pi = -dc + X_1 dS - k|\upsilon|S. \tag{2.22}$$

Using Taylor expansion and equation (2.19), we get

$$\begin{aligned} dc =& \frac{\partial c}{\partial t}dt + \frac{\partial c}{\partial S}dS + \frac{1}{2}\frac{\partial^2 c}{\partial t^2}dt^2 + \frac{1}{2}\frac{\partial^2 c}{\partial S^2}dS^2 + \frac{1}{2}\frac{\partial^2 c}{\partial t \partial S}dtdS + O(dt^2) \\ =& \frac{\partial c}{\partial t}dt + \frac{\partial c}{\partial S}\Big[\mu S_t dt + \sigma S_t(\gamma dW_t + (1-\gamma)dB_t^H)\Big] + \frac{1}{2}\frac{\partial^2 c}{\partial t^2}dt^2 \\ &+ \frac{1}{2}\frac{\partial^2 c}{\partial S^2}\Big[(\mu S_t dt + \sigma S_t(\gamma dW_t + (1-\gamma)dB_t^H))(\mu S_t dt + \sigma S_t(\gamma dW_t + (1-\gamma)dB_t^H))\Big] \\ &+ \frac{1}{2}\frac{\partial^2 c}{\partial t \partial S}dt\Big[\mu S_t dt + \sigma S_t(\gamma dW_t + (1-\gamma)dB_t^H)\Big] + O(dt^2) \end{aligned} \tag{2.23}$$

From [72], the fractional Brownian motion has the following continuum property

$$\lim_{h\to 0}\sup_{0\le t\le A-h}\frac{|B^H(t+h) - B^H(t)|}{h^H\sqrt{2log(\frac{h}{A})^{-1}}}. \tag{2.24}$$

Thus by keeping only the leading order entries in equation (2.23), we get

$$\begin{aligned} dc =& \Big(\frac{\partial c}{\partial t} + \frac{\partial c}{\partial S}\mu S\Big)dt + \frac{\partial c}{\partial S}\Big[\sigma S_t(\gamma dW_t + (1-\gamma)dB_t^H)\Big] \\ &+ \frac{1}{2}\frac{\partial^2 c}{\partial S^2}S^2\Big[\sigma^2\gamma^2 dW_t^2 + 2\sigma^2\gamma(1-\gamma)dW_t dB_t^H + \sigma^2(1-\gamma)^2 dB_t^{2H}\Big] + O(dt^{H+1}) \end{aligned} \tag{2.25}$$

Hence by substituting equation (2.25) to equation (2.22), we have

$$\begin{aligned} d\Pi =& -\Big(\frac{\partial c}{\partial t} + \frac{\partial c}{\partial S}\mu S\Big)dt - \frac{\partial c}{\partial S}\Big(\sigma S(\gamma dW_t + (1-\gamma)dB_t^H)\Big) \\ &- \frac{1}{2}\frac{\partial^2 c}{\partial S^2}S^2\Big(\sigma^2\gamma^2 dW_t^2 + 2\sigma^2\gamma(1-\gamma)dW_t dB_t^H + \sigma^2(1-\gamma)^2 dB_t^{2H}\Big) \\ &+ X_1(\mu S dt + \sigma S(\gamma dW_t + (1-\gamma)dB_t^H)) - k|\upsilon|S + O(dt^{H+1}) \\ =& -\Big(\frac{\partial c}{\partial t} + \frac{\partial c}{\partial S}\mu S - X_1\mu S\Big)dt - \frac{\partial c}{\partial S}\sigma S\Big(\gamma dW_t + (1-\gamma)dB_t^H\Big) \\ &+ X_1\sigma S(\gamma dW_t + (1-\gamma)dB_t^H) - \frac{1}{2}\frac{\partial^2 c}{\partial S^2}S^2\Big(\sigma^2\gamma^2 dW_t^2 + 2\sigma^2\gamma(1-\gamma)dW_t dB_t^H \\ &+ \sigma^2(1-\gamma)^2 dB_t^{2H}\Big) - k|\upsilon|S + O(dt^{H+1}). \end{aligned} \tag{2.26}$$

Using equation (2.21), we get from equation (2.26) that

$$d\Pi = -\frac{\partial c}{\partial t}dt - \frac{1}{2}\frac{\partial^2 c}{\partial S^2}S^2\sigma^2\Big(\gamma^2 dW_t^2 + 2\gamma(1-\gamma)dW_t dB_t^H + (1-\gamma)^2 dB_t^{2H}\Big) - k|\upsilon|S. \tag{2.27}$$

Obviously, the return of the portfolio is stochastic. To derive the PDE for the option price, we use the hedging strategy that the expected return of the portfolio is equal to the return of the portfolio that is earning bank interest, namely

$$E[d\Pi] = r\Pi dt. \tag{2.28}$$

From equation (2.27), we get

$$\begin{aligned} E[d\Pi] = &-\frac{\partial c}{\partial t}dt - \frac{1}{2}\frac{\partial^2 c}{\partial S^2}S^2\sigma^2\Big(\gamma^2 E[dW_t^2] + 2\gamma(1-\gamma)E[dW_t dB_t^H] + (1-\gamma)^2 E[dB_t^{2H}]\Big) \\ &- E[k|\upsilon|S]. \end{aligned} \tag{2.29}$$

Based on the properties of expectation of the standard Brownian motion and fractional Brownian motion process, we have

$$E[dB_t^H dB_t^H] = (dt)^{2H}, \tag{2.30}$$

$$E[dW_t dW_t] = dt, \tag{2.31}$$

$$E[dB_t^H dW_t] = 0. \tag{2.32}$$

Now we consider the expectation of the transaction cost. The number of share held at time t is $\dfrac{\partial c}{\partial S}(S,t)$, but after re-hedging at time $t+dt$, the number of share held at time $t+dt$ is $\dfrac{\partial c}{\partial S}(S+dS, t+dt)$. Therefore, the number of the share bought, υ, is the difference in the number of shares held before and after re-hedging, namely

$$\upsilon = \frac{\partial c}{\partial S}(S+dS, t+dt) - \frac{\partial c}{\partial S}(S,t). \tag{2.33}$$

Using Taylor expansion and keeping only the leading order terms, we have

$$\begin{aligned} \upsilon =& \frac{\partial^2 c}{\partial S^2}dS + \frac{\partial^2 c}{\partial S \partial t}dt + ... \\ =& \frac{\partial^2 c}{\partial S^2}S\sigma[\gamma dW_t + (1-\gamma)dB_t^H] + O(dt). \end{aligned} \tag{2.34}$$

Hence,

$$\begin{aligned} & E[k|\upsilon|S] \\ &= kSE\Big|\frac{\partial^2 c}{\partial S^2} S\sigma(\gamma dW_t + (1-\gamma)dB_t^H)\Big| \\ &= kS^2\sigma\Big|\frac{\partial^2 c}{\partial S^2}\Big| E|\gamma dW_t + (1-\gamma)dB_t^H| \\ &= kS^2\sigma\Big|\frac{\partial^2 c}{\partial S^2}\Big| \sqrt{\frac{2}{\pi}} \sqrt{\gamma^2 dt + (1-\gamma)^2 dt^{2H}}. \end{aligned} \tag{2.35}$$

Note that we have determined the expectation of absolute value of the random variables using the properties of the standard Brownian motion and fractional Brownian motion.

Substituting equations (2.30)-(2.32) and (2.35) into equation (2.29), then (2.28), and using equations (2.20) and (2.21), we obtain

$$\begin{aligned} & \frac{\partial c}{\partial t} + \frac{1}{2}\frac{\partial^2 c}{\partial S^2} S^2\sigma^2\Big(\gamma^2 + (1-\gamma)^2 dt^{2H-1}\Big) \\ & + kS^2\sigma\Big|\frac{\partial^2 c}{\partial S^2}\Big| \sqrt{\frac{2}{\pi dt}} \sqrt{\gamma^2 + (1-\gamma)^2 dt^{2H-1}} + r\frac{\partial c}{\partial S} S - rc = 0. \end{aligned} \tag{2.36}$$

2.8 Long memory in volatility and fractional volatility model

In Section 2.2, evidence of long memory in market return was discussed through the definition of Hurst parameter and autocorrelation function. Evidence from previous literature in regards to long memory in share return measured from Hurst parameter were quite varied. There are no definite answer of correct measurement of Hurst parameter, whether it is measured by using the most popular R/S statistic test, the Lo's modified R/S or any parametric and semi-parametric methods. Some investigations suggest that long memory in stock return only exist for firms' share and not for stock indices. These inconclusive results may even be due to the difficulty in measuring long memory as a result of limited data span. When analysing from the autocovariance function point of view, the ACF of returns is typically insignificant at lower lags [56]. However, the ACF of absolute returns remains positive for longer lags and decays slowly to zero which may be regarded as a typical manifestation of volatility clustering [56]. This may be an indication of persistent (long memory) characteristic in the volatility of stock return. Ding *et al.* [82] also found the existence of long memory stochastic volatility in stock returns. Similar results were shown by Grau-Carles [53] and Assaf [1] who attained weak evidence of long memory in stock return but significant evidence of persistence in absolute return, which measures volatility.

The trouble when assuming long memory in stock return is that fBm has a non semi-martingale property and consequently the free of arbitrage assumption is violated. However, when long memory is included in volatility, the standard integration theory may still be applied. This inspires many researchers to continue in the direction of including long memory in volatility models [82]. Comte and Renault [27] studied a stochastic volatility model assuming long memory and mean reversion in continuous time Hull and White setting by incorporating fractional Brownian motion in the stock return diffusion process. Together with Countin [28], they later further constructed a long memory volatility model in terms of affine process. This idea was then further pursued by Chronopoulou and Viens [2] in discrete and continuous time settings. Wang *et al.* [74] proposed a European option pricing model taking into account transaction costs under the fractional long memory stochastic volatility model using the idea of reference point. Assuming fBm diffusion processes for both stock return as well as its volatility, Wang *et al.* [74] constructed a partial differential equation and later developed the analytical solution by assuming positive gamma. Others [3, 39, 47] have also studied long memory stochastic volatility model in both stock returns and volatility, but instead took a different approach of using semimartingale approximation strategy to solve the problem of arbitrage.

2.9 Concluding remarks

This chapter acknowledges the various researches that take into account long memory in option pricing. Despite the challenges surrounding fractional Brownian motion, numerous strategies have been introduced to resolve them. Consequently this assists in providing insights on what should be considered to further improve the current existing models, the assumptions and methodology used, as well as the interpretation of results.

CHAPTER 3

Derivation methodology and assumptions

3.1 General

Since the introduction of long memory and fractional Brownian motion in finance, many still question its application in finance due to its non-martingale property, in spite of its ability to capture long range dependence in stock returns. Although this problem has been solved through the introduction of Wick-based product, this has not entirely resolved the arbitrage problem when it is applied to other continuous financial market models in particular derivatives. Wang *et al.* [72, 73] derived the European call option price formula by assuming fractional Brownian motion and mixed fractional Brownian motion with transaction costs and hence generated the partial differential equation similar to equation (2.36) for each assumed model. This derivation was later expanded by Wang *et al.* [74] to include long memory in the volatility dynamics. The idea of memoryless stochastic volatility option model has been long developed since its introduction by Hull and White [38] in 1987 which assumes a log-normal variance stochastic diffusion process. Following their work, many researchers concentrated on developing a better, more realistic stochastic volatility model which reflects closely to the derivatives market such as the Stein and Stein model [24], the Scott model [43] and the more popular and widely used Heston model [61]. Mariani *et al.* [44,45] further considered an approach of including transaction costs in the derivation of a stochastic volatility model assuming log-normal stock and volatility diffusion process. Wang *et al.* [72–74] later established an approach of taking into account the transaction cost in pricing the European call option to eliminate the arbitrage problem, which arises due to adopting fractional Brownian motion stock dynamic process.

In this chapter, we first derive the partial differential model of a typical Hull-White model assuming a square root log-normal volatility process as well as including proportional transaction costs. Since transaction costs are included, we will use the same idea employed by Wang *et al.* [74], who adopted Leland's methodology, to model stochas-

tic volatility model with proportional transaction costs using discrete hedging at every timestep δt. We will proceed in constructing the partial differential equation of a European call option assuming general diffusion process of stock and volatility dynamics as well as taking into account transaction costs.

3.2 Derivation of the Hull-White stochastic volatility model with transaction costs

The derivation of the Hull-White stochastic volatility model in a continuous setting is outlined in [37, 38]. However, since the Hull-White model does not take into account transaction costs, we will apply Leland's discrete hedging method similar to the one employed in Wang *et al.* [74] to derive the partial differential equation of a European call option price taking into account transaction costs. Firstly, we assume that a European call option may be replicated by a portfolio Π_t consisting of the underlying stock S_t (risky asset) and the risk-free bond B_t. Hence, the resulting portfolio (Π_t) is

$$\Pi_t = X_1 S_t + X_2 B_t, \tag{3.1}$$

where X_1 is the number of units of the underlying asset and X_2 is the number of units of the riskless bond.

Since the European call price can be replicated by the portfolio value, the value of European call option is

$$c_t = X_1 S_t + X_2 B_t. \tag{3.2}$$

In the Hull-White stochastic volatility model [38], the stock S_t and its volatility σ_τ are assumed to follow a geometric Brownian motion dynamic diffusion process in which the stochastic differential equation of each is given as

$$dS_t = \mu S_t dt + f(\sigma_t) dW_{S_t}, \tag{3.3}$$

where $f(Y) = \sqrt{Y}$ and

$$d\sigma_\tau = \alpha \sigma_\tau d\tau + \beta \sigma_\tau dW_{\sigma_\tau}, \tag{3.4}$$

where W_{S_t} & W_{σ_τ} are independent.

The subsequent analytic solutions of equation (3.3) and equation (3.4) based on Itô lemma

are

$$S_t = S_0 e^{(\mu - \frac{1}{2}\sigma)t + \int_0^t \sqrt{\sigma_\tau} dW_{S_\tau}}, \tag{3.5}$$

$$\sigma_\tau = \sigma_0 e^{(\alpha - \frac{1}{2}\beta^2)\tau + \beta W_{\sigma_\tau}}, \quad 0 \leq \tau \leq t, \tag{3.6}$$

where
μ, σ, α and $\beta \in \Re$, $H_1 \geq H \geq \frac{1}{2}$,
W_{S_t} is the standard Brownian motion which governs the stock price dynamics,
W_{σ_t} is the standard Brownian motion which governs the volatility process.

The analytic solution for the non-risky asset bond B_t is given as

$$B_t = B_0 e^{rt}, \tag{3.7}$$

and the proportional transaction cost is defined by

$$k|\nu|S_t, \tag{3.8}$$

where k is the transaction cost per unit dollar and ν is the number of shares bought ($\nu > 0$) or sold ($\nu < 0$).

We assume that trading only occurs at t and $t+\delta t$, but never in between, and by adopting Leland's mean self-financing delta-hedging strategy at every δt timestep, the change in portfolio when proportional transaction costs are considered will be

$$\delta \Pi_t = X_1 \delta S_t + X_2 \delta B_t - k|\delta X_1|S_t. \tag{3.9}$$

At time $t+\delta t$, according to Kahneman and Tversky [5,18] and similar to Wang *et al.* [74], we have

$$S_{t+\delta t} = S e^{(\mu - \frac{1}{2}\sigma)\delta t + \int_t^{t+\delta t} \sqrt{\sigma_\tau} dW_{S_\tau}}, \tag{3.10}$$

$$\sigma_\tau = \sigma e^{(\alpha - \frac{1}{2}\beta^2)\delta\tau + \beta \delta W_{\sigma_\tau}}, \quad t \leq \tau \leq t + \delta t. \tag{3.11}$$

Kahneman and Tversky [5, 18] suggested that financial market traders are uncertainty averse and instead tend to use heuristics for judging or decision such as anchoring-adjustment strategy. This implies that many traders are prone to discover 'trends' of the past and expect similar trend of continuation. De Long *et al.* [36] indicated that these behaviours reflect those of positive-feedback traders. Numerous researches in experimental psychology indicate that traders tend to find it difficult to judge, hence forecast accurately, when provided with both newly received information together with prior or

base rate data [74]. This may be the reason why one tends to see over or under reaction when new information are publicised. Therefore, similar to the assumption and method employed by Wang *et al.* [74], it is rational to assume that the traders will use the idea of natural "anchor", thus assigning the previous reference point S_0 and σ_0 as a new reference point as S and σ in equations (3.10) and (3.11).

Subsequently, the change in S and σ at every timestep is defined as follows:

$$\begin{aligned}
\delta S_t \triangleq & S_{t+\delta t} - S \\
=& S[e^{(\mu-\frac{1}{2}\sigma)\delta t+\int_t^{t+\delta t}\sqrt{\sigma_\tau}dW_{S_\tau}} - 1] \\
=& S\Big[1 + (\mu-\frac{1}{2}\sigma)\delta t + \int_t^{t+\delta t}\sqrt{\sigma_\tau}dW_{S_\tau} + \frac{1}{2}\Big((\mu-\frac{1}{2}\sigma)^2\delta t^2 \\
& + 2(\mu-\frac{1}{2}\sigma)\delta t\int_t^{t+\delta t}\sqrt{\sigma_\tau}dW_{S_\tau} + \Big(\int_t^{t+\delta t}\sqrt{\sigma_\tau}dW_{S_\tau}\Big)^2\Big) + O(\delta t^2) - 1\Big] \\
=& S\Big[(\mu-\frac{1}{2}\sigma)\delta t + \int_t^{t+\delta t}\sqrt{\sigma_\tau}dW_{S_\tau} + \frac{1}{2}\Big(\int_t^{t+\delta t}\sqrt{\sigma_\tau}dW_{S_\tau}\Big)^2 + O(\delta t\sqrt{\delta t})\Big],
\end{aligned} \tag{3.12}$$

$$\begin{aligned}
\delta\sigma_t \triangleq & \sigma_\tau - \sigma \\
=& \sigma[e^{(\alpha-\frac{1}{2}\beta^2)\delta\tau+\beta\delta W_{\sigma_\tau}} - 1] \\
=& \sigma\Big[1 + (\alpha-\frac{1}{2}\beta^2)\delta\tau + \beta\delta W_{\sigma_\tau} + \frac{1}{2}\Big((\alpha-\frac{1}{2}\beta^2)^2\delta\tau^2 + 2(\alpha-\frac{1}{2}\beta^2)\delta\tau\beta\delta W_{\sigma_\tau} + \beta^2\delta W_{\sigma_\tau}^2\Big) \\
& + O(\delta\tau^2) - 1\Big] \\
=& \sigma\Big[(\alpha-\frac{1}{2}\beta^2)\delta\tau + \beta\delta W_{\sigma_\tau} + \frac{1}{2}\beta^2\delta W_{\sigma_\tau}^2 + O(\delta\tau\sqrt{\delta\tau})\Big].
\end{aligned} \tag{3.13}$$

In order to construct the partial differential equation of a European call option, we assume a mean-self financing delta hedging strategy in discrete timestep where

$$E[\delta\Pi_t - \delta c_t] = 0. \tag{3.14}$$

If the European call option is replicated by the portfolio, then the expectation of the change in call option and portfolio has to equal zero, hence the equation (3.14). As

$$\begin{aligned}
\delta c(t, S_t, \sigma_t) =& \frac{\partial c}{\partial t}\delta t + \frac{\partial c}{\partial S}\delta S + \frac{\partial c}{\partial \sigma}\delta\sigma + \frac{1}{2}\Big[\frac{\partial^2 c}{\partial t^2}(\delta t)^2 + \frac{\partial^2 c}{\partial S^2}(\delta S)^2 + \frac{\partial^2 c}{\partial \sigma^2}(\delta\sigma)^2 \\
& + 2\frac{\partial^2 c}{\partial S\partial t}(\delta S)(\delta t) + 2\frac{\partial^2 c}{\partial S\partial\sigma}(\delta S)(\delta\sigma) + 2\frac{\partial^2 c}{\partial\sigma\partial t}(\delta\sigma)(\delta t) + O(\delta t^2)\Big],
\end{aligned} \tag{3.15}$$

and using equation (3.9), one has

$$\begin{aligned}E[\delta\Pi_t - \delta c_t] =& E\Big[X_1\delta S + X_2\delta B - k|\delta X_1|S \\ &- \Big(\frac{\partial c}{\partial t}\delta t + \frac{\partial c}{\partial S}\delta S + \frac{\partial c}{\partial \sigma}\delta\sigma + \frac{1}{2}\Big(\frac{\partial^2 c}{\partial t^2}(\delta t)^2 + \frac{\partial^2 c}{\partial S^2}(\delta S)^2 + \frac{\partial^2 c}{\partial \sigma^2}(\delta\sigma)^2 \\ &+ 2\frac{\partial^2 c}{\partial S\partial t}(\delta S)(\delta t) + 2\frac{\partial^2 c}{\partial S\partial \sigma}(\delta S)(\delta\sigma) + 2\frac{\partial^2 c}{\partial \sigma\partial t}(\delta\sigma)(\delta t)\Big) + O(\delta t^2)\Big)\Big].\end{aligned} \tag{3.16}$$

From equation (3.2), we define

$$\frac{\partial c}{\partial S} = X_1, \tag{3.17}$$

$$\frac{\partial^2 c}{\partial S^2} = \frac{\partial X_1}{\partial S}. \tag{3.18}$$

Similarly from equation (3.7), the following is attained:

$$\delta B_t = rB_t\delta t. \tag{3.19}$$

Substituting equations (3.17)-(3.19) into (3.16), we have

$$\begin{aligned}E[\delta\Pi_t - \delta c_t] =& E\Big[X_2 rB\delta t - k|\delta X_1|S - \Big(\frac{\partial c}{\partial t}\delta t + \frac{\partial c}{\partial \sigma}\delta\sigma + \frac{1}{2}\frac{\partial^2 c}{\partial S^2}(\delta S)^2 + \frac{1}{2}\frac{\partial^2 c}{\partial \sigma^2}(\delta\sigma)^2 \\ &+ \frac{\partial^2 c}{\partial S\partial\sigma}(\delta S)(\delta\sigma)\Big) + O(\delta t\sqrt{\delta t})\Big] \\ =& E\Big[\Big(X_2 rB - \frac{\partial c}{\partial t}\Big)\delta t\Big] - \frac{\partial c}{\partial\sigma}E[\delta\sigma] - \frac{1}{2}\frac{\partial^2 c}{\partial S^2}E[\delta S^2] - \frac{1}{2}\frac{\partial^2 c}{\partial\sigma^2}E[\delta\sigma^2] \\ &- \frac{\partial^2 c}{\partial S\partial\sigma}E[\delta S\delta\sigma] - E[k|\delta X_1|S].\end{aligned} \tag{3.20}$$

In order to complete the equation (3.20) above, we need to calculate the expectations of $\delta\sigma$, δS^2, $\delta\sigma^2$ and the expectation of the transaction costs. Since we assume that there are no correlation between the stock return and its volatility,

$$E[\delta S\delta\sigma] = 0. \tag{3.21}$$

We define

$$\begin{aligned}
\delta S^2 =& S^2[e^{(\mu-\frac{1}{2}\sigma)\delta t+\int_t^{t+\delta t}\sqrt{\sigma_\tau}dW_{S_\tau}}-1]^2\\
=& S^2[e^{2(\mu-\frac{1}{2}\sigma)\delta t+2\int_t^{t+\delta t}\sqrt{\sigma_\tau}dW_{S_\tau}}-2e^{(\mu-\frac{1}{2}\sigma)\delta t+\int_t^{t+\delta t}\sqrt{\sigma_\tau}dW_{S_\tau}}+1]\\
=& S^2\Big[1+2(\mu-\frac{1}{2}\sigma)\delta t+2\int_t^{t+\delta t}\sqrt{\sigma_\tau}dW_{S_\tau}+2\Big((\mu-\frac{1}{2}\sigma)^2\delta t^2\\
&+2(\mu-\frac{1}{2}\sigma)\delta t\int_t^{t+\delta t}\sqrt{\sigma_\tau}dW_{S_\tau}+\Big(\int_t^{t+\delta t}\sqrt{\sigma_\tau}dW_{S_\tau}\Big)^2\Big)-2\Big(1+(\mu-\frac{1}{2}\sigma)\delta t\\
&+\int_t^{t+\delta t}\sqrt{\sigma_\tau}dW_{S_\tau}+\frac{1}{2}(\mu-\frac{1}{2}\sigma)^2\delta t^2+(\mu-\frac{1}{2}\sigma)\delta t\int_t^{t+\delta t}\sqrt{\sigma_\tau}dW_{S_\tau}\\
&+\frac{1}{2}\Big(\int_t^{t+\delta t}\sqrt{\sigma_\tau}dW_{S_\tau}\Big)^2\Big)+O(\delta t^2)+1\Big]\\
=& S^2\Big[(\mu-\frac{1}{2}\sigma)^2\delta t^2+2(\mu-\frac{1}{2}\sigma)\delta t\int_t^{t+\delta t}\sqrt{\sigma_\tau}dW_{S_\tau}+\Big(\int_t^{t+\delta t}\sqrt{\sigma_\tau}dW_{S_\tau}\Big)^2+O(\delta t^2)\Big]\\
=& S^2\Big[\Big(\int_t^{t+\delta t}\sqrt{\sigma_\tau}dW_{S_\tau}\Big)^2+O(\delta t\sqrt{\delta t})\Big].
\end{aligned}$$

Based on the Itô isometry, we get

$$\begin{aligned}
E[(\delta S)^2] =& S^2E\Big[\Big(\int_t^{t+\delta t}\sqrt{\sigma_\tau}dW_{S_\tau}\Big)^2+O(\delta t\sqrt{\delta t})\Big]\\
=& S^2E\Big[\Big(\int_t^{t+\delta t}\sigma_\tau d\tau\Big)^2\Big]\\
=& S^2\sigma\delta t.
\end{aligned}\tag{3.22}$$

Using equation (3.13), we calculate the expectation of $\delta\sigma$

$$\begin{aligned}
E[\delta\sigma] =& E\Big[\sigma\Big((\alpha-\frac{1}{2}\beta^2)\delta\tau+\beta\delta W_{\sigma_\tau}+\frac{1}{2}\beta^2\delta W_{\sigma_\tau}^2+O(\delta\tau\sqrt{\delta\tau})\Big)\Big]\\
=& \sigma\Big[(\alpha-\frac{1}{2}\beta^2)\delta t+\frac{1}{2}\beta^2\delta t\Big]\\
=& \alpha\sigma\delta t.
\end{aligned}\tag{3.23}$$

We define

$$\begin{aligned}
\delta\sigma^2 =&\sigma^2[e^{(\alpha-\frac{1}{2}\beta^2)\delta\tau+\beta\delta W_{\sigma_\tau}}-1]^2\\
=&\sigma^2[e^{2((\alpha-\frac{1}{2}\beta^2)\delta\tau+\beta\delta W_{\sigma_\tau})}-2e^{(\alpha-\frac{1}{2}\beta^2)\delta\tau+\beta\delta W_{\sigma_\tau}}+1]\\
=&\sigma^2\Big[1+2(\alpha-\frac{1}{2}\beta^2)\delta\tau+2\beta\delta W_{\sigma_\tau}+2\Big((\alpha-\frac{1}{2}\beta^2)^2\delta\tau^2+2(\alpha-\frac{1}{2}\beta^2)\beta\delta\tau\delta W_{\sigma_\tau}\\
&+\beta^2\delta W_{\sigma_\tau}^2\Big)-2\Big(1+(\alpha-\frac{1}{2}\beta^2)\delta\tau+\beta\delta W_{\sigma_\tau}+\frac{1}{2}(\alpha-\frac{1}{2}\beta^2)^2\delta\tau^2\\
&+(\alpha-\frac{1}{2}\beta^2)\beta\delta\tau\delta W_{\sigma_\tau}+\frac{1}{2}\beta^2\delta W_{\sigma_\tau}^2\Big)+O(\delta t^2)+1\Big]\\
=&\sigma^2\Big[(\alpha-\frac{1}{2}\beta^2)^2\delta\tau^2+2(\alpha-\frac{1}{2}\beta^2)\beta\delta\tau\delta W_{\sigma_\tau}+\beta^2\delta W_{\sigma_\tau}^2+O(\delta t^2)\Big]\\
=&\sigma^2\Big[\beta^2\delta W_{\sigma_\tau}^2+O(\delta t\sqrt{\delta t})\Big],
\end{aligned}$$

thus

$$\begin{aligned}
E[(\delta\sigma)^2] =&\sigma^2E\Big[\beta^2\delta W_{\sigma_\tau}^2+O(\delta t\sqrt{\delta t})\Big]\\
=&\sigma^2\beta^2\delta t.
\end{aligned}\tag{3.24}$$

The expectation of proportional transaction costs incurred is calculated as

$$E[k|\delta X_1|S] =kSE|\delta X_1|.\tag{3.25}$$

By Taylor's expansion and using equation (3.12), we get

$$\begin{aligned}
\delta X_1(t,S(t),\sigma(t)) =&\frac{\partial X_1}{\partial t}\delta t+\frac{\partial X_1}{\partial S}\delta S+\frac{\partial X_1}{\partial\sigma}\delta\sigma+O(\delta t^2)\\
=&\frac{\partial X_1}{\partial S}\delta S+O(\delta t)\\
=&\frac{\partial X_1}{\partial S}S\Big(\int_t^{t+\delta t}\sqrt{\sigma_\tau}dW_{S_\tau}\Big)+O(\delta t).
\end{aligned}$$

Based on the property of Brownian motion, we get that $\int_t^{t+\delta t}\sqrt{\sigma_\tau}dW_{S_\tau}\sim N(0,\sigma\delta t)$. Therefore, we have to attain $E\Big|\int_t^{t+\delta t}\sqrt{\sigma_\tau}dW_{S_\tau}\Big|$, by first letting $X=\int_t^{t+\delta t}\sqrt{\sigma_\tau}dW_{S_\tau}$, where $X\sim N(0,\sigma\delta t)$. Then by substituting the mean and variance of X,

$$\begin{aligned}
E|X| =&\int_{-\infty}^{0}(-X)\frac{1}{\sqrt{\sigma\delta t}\sqrt{2\pi}}e^{-\frac{X^2}{2\sigma\delta t}}dX+\int_0^{\infty}(X)\frac{1}{\sqrt{\sigma\delta t}\sqrt{2\pi}}e^{-\frac{X^2}{2\sigma\delta t}}dX\\
=&\frac{1}{\sqrt{2\pi}}\sqrt{\sigma\delta t}\Big[e^{-\frac{X^2}{2\sigma\delta t}}\Big|_{-\infty}^{0}-e^{-\frac{X^2}{2\sigma\delta t}}\Big|_0^{\infty}\Big]\\
=&\sqrt{\frac{2}{\pi}}\sqrt{\sigma\delta t}.
\end{aligned}\tag{3.26}$$

Therefore, the expectation of proportional transaction costs is

$$\begin{aligned} kSE|\delta X_1| =& kS^2\Big|\frac{\partial X_1}{\partial S}\Big|E\Big|\int_t^{t+\delta t}\sqrt{\sigma_\tau}dW_{S_\tau}\Big| \\ =& kS^2\Big|\frac{\partial X_1}{\partial S}\Big|\sqrt{\frac{2}{\pi}}\sqrt{\sigma\delta t}. \end{aligned} \tag{3.27}$$

Finally, we substitute equations (3.21)-(3.24) and (3.27) into (3.20), and hence we have

$$\begin{aligned} E[\delta\Pi_t - \delta c_t] =& \Big(X_2 rB - \frac{\partial c}{\partial t}\Big)\delta t - \frac{\partial c}{\partial \sigma}\alpha\sigma\delta t - \frac{1}{2}\frac{\partial^2 c}{\partial S^2}S^2\sigma\delta t - \frac{1}{2}\frac{\partial^2 c}{\partial \sigma^2}\sigma^2\beta^2\delta t \\ & - kS^2\Big|\frac{\partial^2 c}{\partial S^2}\Big|\sqrt{\frac{2}{\pi}}\sqrt{\sigma\delta t}. \end{aligned} \tag{3.28}$$

Applying the mean-self financing delta hedging strategy in discrete setting as in equation (3.14), we get

$$\begin{aligned} &\Big(X_2 rB - \frac{\partial c}{\partial t}\Big)\delta t - \frac{\partial c}{\partial \sigma}\alpha\sigma\delta t - \frac{1}{2}\frac{\partial^2 c}{\partial S^2}S^2\sigma\delta t - \frac{1}{2}\frac{\partial^2 c}{\partial \sigma^2}\sigma^2\beta^2\delta t - kS^2\Big|\frac{\partial^2 c}{\partial S^2}\Big|\sqrt{\frac{2}{\pi}}\sqrt{\sigma\delta t} = 0, \\ &X_2 rB - \frac{\partial c}{\partial t} - \frac{\partial c}{\partial \sigma}\alpha\sigma - \frac{1}{2}\frac{\partial^2 c}{\partial S^2}S^2\sigma - \frac{1}{2}\frac{\partial^2 c}{\partial \sigma^2}\sigma^2\beta^2 - kS^2\Big|\frac{\partial^2 c}{\partial S^2}\Big|\sqrt{\frac{2\sigma}{\pi\delta t}} = 0. \end{aligned} \tag{3.29}$$

Since the call option price is assumed to equal the portfolio, $X_2 rB$ may be replaced by $rc - r\frac{\partial c}{\partial S}S$. Thus, equation (3.29) may be written as

$$rc - r\frac{\partial c}{\partial S}S - \frac{\partial c}{\partial t} - \frac{\partial c}{\partial \sigma}\alpha\sigma - \frac{1}{2}\frac{\partial^2 c}{\partial S^2}S^2\sigma - \frac{1}{2}\frac{\partial^2 c}{\partial \sigma^2}\sigma^2\beta^2 = kS^2\Big|\frac{\partial^2 c}{\partial S^2}\Big|\sqrt{\frac{2\sigma}{\pi\delta t}}. \tag{3.30}$$

Note that equation (3.30) above reduces to the Hull-Whilte PDE [38] when $k = 0$, i.e. no transaction costs are present.

3.3 Derivation of the general model with transaction costs

The derivation of general model is similar to the one employed in Section 3.2 with the construction of a portfolio (Π_t) of equation (3.1), consisting of a risky (S_t) and non-risky asset (B_t) which follows equation (3.7). The modifications are made on the assumption of stock and its volatility dynamic diffusion process to consider long memory, such that the corresponding stochastic differential equation (SDE) is given as

$$dS_t = \mu S_t dt + f(\sigma_t)[\gamma S_t dW_{S_t} + (1-\gamma)S_t dB_t^H], \tag{3.31}$$

where $f(Y) = \sqrt{Y}$ and

$$d\sigma_\tau = \alpha\sigma d\tau + \beta\sigma[\varepsilon dW_{\sigma_\tau} + (1-\varepsilon)dB_\tau^{H_1}], \tag{3.32}$$

where B_t^H & $B_t^{H_1}$ are independent and W_{S_τ} & W_{σ_τ} are also independent.

Different approach for solving the SDEs above were previously discussed in Section 2.4. The Wick-based approach provides a desirable zero-mean property for the integration of fractional Brownian motion, whereas the pathwise sense does not. However, both approaches will still lead us towards the arbitrage problem since our purpose is to apply this in the construction of derivative models. Considering that pathwise sense integral is a more natural approach to modeling compared to the Wick-based integral, we will proceed with the integration method as detailed in Section 2.4.2. In order to eliminate the arbitrage problem arising from the predictability nature of fractional Brownian motion, we later include the proportional transaction costs incurred in hedging when constructing the derivative model. Hence, the subsequent analytic solution of equation (3.31) and equation (3.32) are as follows:

$$S_t = S_0 e^{\mu t + \gamma \int_0^t \sqrt{\sigma_\tau} dW_{S_\tau} + (1-\gamma)\int_0^t \sqrt{\sigma_\tau} dB_\tau^H}, \tag{3.33}$$

$$\sigma_\tau = \sigma_0 e^{\alpha\tau + \beta[\varepsilon W_{\sigma_\tau} + (1-\varepsilon)B_\tau^{H_1}]}, \quad 0 \le \tau \le t, \tag{3.34}$$

where the additional parameters
γ and $\varepsilon \in \Re$, $H_1 \ge H \ge \frac{1}{2}$,
$\int_0^t \sqrt{\sigma_\tau} dB_\tau^H$ is a pathwise integral with respect to the fractional Brownian motion B_t^H with constant Hurst exponent (H),
$B_\tau^{H_1}$ is fractional Brownian motion with constant Hurst exponent (H_1),
W_{S_t} is independent of B_t^H and
W_{σ_τ} is independent of $B_\tau^{H_1}$.

The purpose of the general model in this case is to consider all types of diffusion processes. Notice when γ is equal to 1, the stock diffusion process follows a geometric Brownian motion. On the other hand, when γ is equal to zero, the stock dynamic follows a fractional Brownian motion. As discussed in Section 2.6, when $\gamma \in (0,1)$, the process is a mixed fractional Brownian motion. The same relationship of ε is imposed on the diffusion process of stock volatility. The general model enables us to assess the effect of each of the parameters involved and to analyse the resulting models.

The derivation is similar to the one described in previous Section 3.2 using the idea of mean-self financing delta hedging such that $E[\delta\Pi_t - \delta c_t]$. However, since the dynamic diffusion assumptions are different, we need to recalculate the expectations of $\delta\sigma$, δS^2, $\delta\sigma^2$ and the expectation of transaction costs accordingly. We still assume there are no correlation between the stock return and its volatility. The proportional transaction costs incurred are as equation (3.8) and if trading only occurs at t and $t+\delta t$, the change in portfolio after $t+\delta t$ will still be the same as stated in equation (3.9).

The change in value of the share price (δS) and its volatility ($\delta\sigma$) after trading, between t and $t+\delta t$, is given by

$$S_{t+\delta t} = Se^{\mu\delta t+\gamma\int_t^{t+\delta t}\sqrt{\sigma_\tau}dW_{S_\tau}+(1-\gamma)\int_t^{t+\delta t}\sqrt{\sigma_\tau}dB_\tau^H}, \tag{3.35}$$

$$\sigma_\tau = \sigma e^{\alpha(\tau-t)+\beta[\varepsilon(W_\sigma(\tau)-W_\sigma(t))+(1-\varepsilon)(B_{H_1}(\tau)-B_{H_1}(t))]}, \quad t\le\tau\le t+\delta t. \tag{3.36}$$

$$\begin{aligned}
\delta S_t \triangleq & S_{t+\delta t} - S_t \\
=& S[e^{\mu\delta t+\gamma\int_t^{t+\delta t}\sqrt{\sigma_\tau}dW_{S_\tau}+(1-\gamma)\int_t^{t+\delta t}\sqrt{\sigma_\tau}dB_\tau^H} - 1] \\
=& S\Big[1+\mu\delta t+\gamma\int_t^{t+\delta t}\sqrt{\sigma_\tau}dW_{S_\tau}+(1-\gamma)\int_t^{t+\delta t}\sqrt{\sigma_\tau}dB_\tau^H \\
&+\frac{1}{2}\Big(\mu^2\delta t^2+\gamma^2\Big(\int_t^{t+\delta t}\sqrt{\sigma_\tau}dW_{S_\tau}\Big)^2+(1-\gamma)^2\Big(\int_t^{t+\delta t}\sqrt{\sigma_\tau}dB_\tau^H\Big)^2 \\
&+2\mu\gamma\delta t\int_t^{t+\delta t}\sqrt{\sigma_\tau}dW_{S_\tau}+2\gamma(1-\gamma)\int_t^{t+\delta t}\sqrt{\sigma_\tau}dW_{S_\tau}\int_t^{t+\delta t}\sqrt{\sigma_\tau}dB_\tau^H \\
&+2\mu(1-\gamma)\delta t\int_t^{t+\delta t}\sqrt{\sigma_\tau}dB_\tau^H\Big)+O(\delta t^{2H})-1\Big] \\
=& S\Big[\mu\delta t+\gamma\int_t^{t+\delta t}\sqrt{\sigma_\tau}dW_{S_\tau}+(1-\gamma)\int_t^{t+\delta t}\sqrt{\sigma_\tau}dB_\tau^H+\frac{1}{2}\gamma^2\Big(\int_t^{t+\delta t}\sqrt{\sigma_\tau}dW_{S_\tau}\Big)^2 \\
&+\frac{1}{2}(1-\gamma)^2\Big(\int_t^{t+\delta t}\sqrt{\sigma_\tau}dB_\tau^H\Big)^2+\gamma(1-\gamma)\int_t^{t+\delta t}\sqrt{\sigma_\tau}dW_{S_\tau}\int_t^{t+\delta t}\sqrt{\sigma_\tau}dB_\tau^H \\
&+O(\delta t^{H+1})\Big],
\end{aligned} \tag{3.37}$$

$$
\begin{aligned}
\delta\sigma_t \triangleq&\sigma_\tau - \sigma \\
=&\sigma[e^{\alpha\delta\tau+\beta\varepsilon\delta W_\sigma(\tau)+\beta(1-\varepsilon)\delta B_{H_1}(\tau)} - 1] \\
=&\sigma\Big[1+\alpha\delta\tau+\beta\varepsilon\delta W_\sigma(\tau)+\beta(1-\varepsilon)\delta B_{H_1}(\tau)+\frac{1}{2}\Big(\alpha^2\delta\tau^2+\beta^2\varepsilon^2\delta W_\sigma(\tau)^2 \\
&+\beta^2(1-\varepsilon)^2\delta B_{H_1}(\tau)^2+2\alpha\beta\varepsilon\delta\tau\delta W_\sigma(\tau)+2\alpha\beta(1-\varepsilon)\delta\tau\delta B_{H_1}(\tau) \\
&+2\beta^2\varepsilon(1-\varepsilon)\delta W_\sigma(\tau)\delta B_{H_1}(\tau)\Big)+O(\delta\tau^{2H_1})-1\Big] \\
=&\sigma\Big[\alpha\delta\tau+\beta\varepsilon\delta W_\sigma(\tau)+\beta(1-\varepsilon)\delta B_{H_1}(\tau)+\frac{1}{2}\beta^2\varepsilon^2\delta W_\sigma(\tau)^2+\frac{1}{2}\beta^2(1-\varepsilon)^2\delta B_{H_1}(\tau)^2 \\
&+\beta^2\varepsilon(1-\varepsilon)\delta W_\sigma(\tau)\delta B_{H_1}(\tau)+O(\delta\tau^{H_1+1})\Big],
\end{aligned}
\tag{3.38}
$$

$$
\begin{aligned}
\delta S^2 =&S^2[e^{\mu\delta t+\gamma\int_t^{t+\delta t}\sqrt{\sigma_\tau}dW_{S\tau}+(1-\gamma)\int_t^{t+\delta t}\sqrt{\sigma_\tau}dB_\tau^H}-1]^2 \\
=&S^2[e^{2(\mu\delta t+\gamma\int_t^{t+\delta t}\sqrt{\sigma_\tau}dW_{S_\tau}+(1-\gamma)\int_t^{t+\delta t}\sqrt{\sigma_\tau}dB_\tau^H)}-2e^{\mu\delta t+\gamma\int_t^{t+\delta t}\sqrt{\sigma_\tau}dW_{S_\tau}+(1-\gamma)\int_t^{t+\delta t}\sqrt{\sigma_\tau}dB_\tau^H}+1] \\
=&S^2\Big[1+2\Big(\mu\delta t+\gamma\int_t^{t+\delta t}\sqrt{\sigma_\tau}dW_{S_\tau}+(1-\gamma)\int_t^{t+\delta t}\sqrt{\sigma_\tau}dB_\tau^H\Big)+2\Big(\mu^2\delta t^2 \\
&+\gamma^2\Big(\int_t^{t+\delta t}\sqrt{\sigma_\tau}dW_{S_\tau}\Big)^2+(1-\gamma)^2\Big(\int_t^{t+\delta t}\sqrt{\sigma_\tau}dB_\tau^H\Big)^2+2\mu\gamma\delta t\int_t^{t+\delta t}\sqrt{\sigma_\tau}dW_{S_\tau} \\
&+2\gamma(1-\gamma)\int_t^{t+\delta t}\sqrt{\sigma_\tau}dW_{S_\tau}\int_t^{t+\delta t}\sqrt{\sigma_\tau}dB_\tau^H+2\mu(1-\gamma)\delta t\int_t^{t+\delta t}\sqrt{\sigma_\tau}dB_\tau^H\Big) \\
&-2-2\Big(\mu\delta t+\gamma\int_t^{t+\delta t}\sqrt{\sigma_\tau}dW_{S_\tau}+(1-\gamma)\int_t^{t+\delta t}\sqrt{\sigma_\tau}dB_\tau^H\Big)-\Big(\mu^2\delta t^2 \\
&+\gamma^2\Big(\int_t^{t+\delta t}\sqrt{\sigma_\tau}dW_{S_\tau}\Big)^2+(1-\gamma)^2\Big(\int_t^{t+\delta t}\sqrt{\sigma_\tau}dB_\tau^H\Big)^2+2\mu\gamma\delta t\int_t^{t+\delta t}\sqrt{\sigma_\tau}dW_{S_\tau} \\
&+2\gamma(1-\gamma)\int_t^{t+\delta t}\sqrt{\sigma_\tau}dW_{S_\tau}\int_t^{t+\delta t}\sqrt{\sigma_\tau}dB_\tau^H+2\mu(1-\gamma)\delta t\int_t^{t+\delta t}\sqrt{\sigma_\tau}dB_\tau^H\Big) \\
&+O(\delta t^{2H})+1\Big] \\
=&S^2\Big[\gamma^2\Big(\int_t^{t+\delta t}\sqrt{\sigma_\tau}dW_{S_\tau}\Big)^2+(1-\gamma)^2\Big(\int_t^{t+\delta t}\sqrt{\sigma_\tau}dB_\tau^H\Big)^2 \\
&+2\gamma(1-\gamma)\int_t^{t+\delta t}\sqrt{\sigma_\tau}dW_{S_\tau}\int_t^{t+\delta t}\sqrt{\sigma_\tau}dB_\tau^H+O(\delta t^{H+1})\Big].
\end{aligned}
$$

Ren *et al.* [30] proved that if $f(\tau)$ is a deterministic function, the following is true

$$
E\Big[\Big(\int_t^{t+\delta t}\sigma_\tau dB_H(\tau)\Big)^2\Big]=H(2H-1)E\Big[\int_t^{t+\delta t}\int_t^{t+\delta t}\sigma_u\sigma_v|u-v|^{2H-2}dudv\Big]. \tag{3.39}
$$

Given that σ_τ is constant, as stated by Wang *et al.* [74],

$$
\lim_{\delta t\to 0}\frac{E\Big[\Big(\int_t^{t+\delta t}\sigma_\tau dB_H(\tau)\Big)^2\Big]}{\delta t^{2H}}=E[\sigma_t^2]=\sigma_t^2. \tag{3.40}
$$

Since W_{S_t} and B_t^H are independent and by using the resulting equation (3.40), we get

$$E[(\delta S)^2] = S^2\Big[\gamma^2\sigma\delta t + (1-\gamma)^2\sigma(\delta t)^{2H}\Big]. \tag{3.41}$$

Now using equation (3.38) to find the expectation of $\delta\sigma$, we have

$$\begin{aligned} E[\delta\sigma] =& E\Big[\sigma\Big(\alpha\delta\tau + \beta\varepsilon\delta W_\sigma(\tau) + \beta(1-\varepsilon)\delta B_{H_1}(\tau) + \frac{1}{2}\beta^2\varepsilon^2\delta W_\sigma(\tau)^2 \\ &+ \frac{1}{2}\beta^2(1-\varepsilon)^2\delta B_{H_1}(\tau)^2 + \beta^2\varepsilon(1-\varepsilon)\delta W_\sigma(\tau)\delta B_{H_1}(\tau) + O(\delta\tau^{H_1+1})\Big)\Big] \\ =& \sigma[\alpha\delta t + \frac{1}{2}\beta^2\varepsilon^2\delta t + \frac{1}{2}\beta^2(1-\varepsilon)^2(\delta t)^{2H_1}]. \end{aligned} \tag{3.42}$$

$$\begin{aligned} \delta\sigma^2 =& \sigma^2[e^{\alpha\delta\tau+\beta\varepsilon\delta W_\sigma(\tau)+\beta(1-\varepsilon)\delta B_{H_1}(\tau)} - 1]^2 \\ =& \sigma^2[e^{2(\alpha\delta\tau+\beta\varepsilon\delta W_\sigma(\tau)+\beta(1-\varepsilon)\delta B_{H_1}(\tau))} - 2e^{\alpha\delta\tau+\beta\varepsilon\delta W_\sigma(\tau)+\beta(1-\varepsilon)\delta B_{H_1}(\tau)} + 1] \\ =& \sigma^2\Big[1 + 2\Big(\alpha\delta\tau + \beta\varepsilon\delta W_\sigma(\tau) + \beta(1-\varepsilon)\delta B_{H_1}(\tau)\Big) + 2\Big(\alpha^2\delta\tau^2 + \beta^2\varepsilon^2\delta W_\sigma(\tau)^2 \\ &+ \beta^2(1-\varepsilon)^2\delta B_{H_1}(\tau)^2 + 2\alpha\beta\varepsilon\delta\tau\delta W_\sigma(\tau) + 2\alpha\beta(1-\varepsilon)\delta\tau\delta B_{H_1}(\tau) \\ &+ 2\beta^2\varepsilon(1-\varepsilon)\delta W_\sigma(\tau)\delta B_{H_1}(\tau)\Big) - 2 - 2\Big(\alpha\delta\tau + \beta\varepsilon\delta W_\sigma(\tau) + \beta(1-\varepsilon)\delta B_{H_1}(\tau)\Big) \\ &- \Big(\alpha^2\delta\tau^2 + \beta^2\varepsilon^2\delta W_\sigma(\tau)^2 + \beta^2(1-\varepsilon)^2\delta B_{H_1}(\tau)^2 + 2\alpha\beta\varepsilon\delta\tau\delta W_\sigma(\tau) \\ &+ 2\alpha\beta(1-\varepsilon)\delta\tau\delta B_{H_1}(\tau) + 2\beta^2\varepsilon(1-\varepsilon)\delta W_\sigma(\tau)\delta B_{H_1}(\tau)\Big) + O(\delta t^{2H_1}) + 1\Big] \\ =& \sigma^2\Big[\beta^2\varepsilon^2\delta W_\sigma(\tau)^2 + \beta^2(1-\varepsilon)^2\delta B_{H_1}(\tau)^2 + 2\alpha\beta\varepsilon\delta\tau\delta W_\sigma(\tau) + 2\alpha\beta(1-\varepsilon)\delta\tau\delta B_{H_1}(\tau) \\ &+ 2\beta^2\varepsilon(1-\varepsilon)\delta W_\sigma(\tau)\delta B_{H_1}(\tau) + O(\delta t^{2H_1})\Big] \\ =& \sigma^2\Big[\beta^2\varepsilon^2\delta W_\sigma(\tau)^2 + \beta^2(1-\varepsilon)^2\delta B_{H_1}(\tau)^2 + 2\beta^2\varepsilon(1-\varepsilon)\delta W_\sigma(\tau)\delta B_{H_1}(\tau) + O(\delta t^{H_1+1})\Big]. \end{aligned}$$

From the property of fractional Brownian motion discussed in Section 2.2 and the independence property of $W_\sigma(\tau)$ and $B_{H_1}(\tau)$, we attain the following

$$E[(\delta\sigma)^2] = \sigma^2\beta^2[\varepsilon^2\delta t + (1-\varepsilon)^2(\delta t)^{2H_1}]. \tag{3.43}$$

The proportional transaction cost is similarly defined as the previous section by using equation (3.37) and Taylor's expansion,

$$\begin{aligned} \delta X_1(t, S(t), \sigma(t)) =& \frac{\partial X_1}{\partial t}\delta t + \frac{\partial X_1}{\partial S}\delta S + \frac{\partial X_1}{\partial \sigma}\delta\sigma + O(\delta t^2) \\ =& \frac{\partial X_1}{\partial S}\delta S + O(\delta t) \\ =& \frac{\partial X_1}{\partial S}\Big(\gamma\int_t^{t+\delta t}\sqrt{\sigma_\tau}dW_{S_\tau} + (1-\gamma)\int_t^{t+\delta t}\sqrt{\sigma_\tau}dB_\tau^H\Big), \end{aligned}$$

$$kSE|\delta X_1| = kS^2\Big|\frac{\partial X_1}{\partial S}\Big|E\Big|\gamma\int_t^{t+\delta t}\sqrt{\sigma_\tau}dW_{S_\tau} + (1-\gamma)\int_t^{t+\delta t}\sqrt{\sigma_\tau}dB_\tau^H\Big|. \tag{3.44}$$

In order to solve $E\Big|\gamma\int_t^{t+\delta t}\sqrt{\sigma_\tau}dW_{S_\tau}+(1-\gamma)\int_t^{t+\delta t}\sqrt{\sigma_\tau}dB_\tau^H\Big|$, we first let $X=\gamma\int_t^{t+\delta t}\sqrt{\sigma_\tau}dW_{S_\tau}$ and $Y=(1-\gamma)\int_t^{t+\delta t}\sqrt{\sigma_\tau}dB_\tau^H$.

Let $X\sim N\Big(0,\gamma^2\sigma\delta t\Big)$ and $Y\sim N\Big(0,(1-\gamma)^2\sigma\delta t^{2H}\Big)$,

$$E[X+Y]=0, \tag{3.45}$$

$$\begin{aligned} E[(X+Y)^2] =& E[X^2+2XY+Y^2] \\ =& E[X^2]+2E[XY]+E[Y^2] \\ =& \sigma[\gamma^2\delta t+(1-\gamma)^2\delta t^{2H}]. \end{aligned} \tag{3.46}$$

Thus,

$$X+Y\sim N(0,\sigma(\gamma^2\delta t+(1-\gamma)^2\delta t^{2H})). \tag{3.47}$$

For the mean and expectation of $X+Y$ as given in equation (3.47), solving $E|X+Y|$ is a process similar to that for obtaining equation (3.26) with the corresponding μ and σ. Hence,

$$E\Big|\gamma\int_t^{t+\delta t}\sqrt{\sigma_\tau}dW_{S_\tau}+(1-\gamma)\int_t^{t+\delta t}\sqrt{\sigma_\tau}dB_\tau^H\Big| = \sqrt{\frac{2}{\pi}}\sqrt{\sigma(\gamma^2\delta t+(1-\gamma)^2\delta t^{2H})}. \tag{3.48}$$

Substituting equation (3.48) into equation (3.44), we get

$$kSE|\delta X_1| = kS^2\Big|\frac{\partial X_1}{\partial S}\Big|\sqrt{\frac{2}{\pi}}\sqrt{\sigma(\gamma^2\delta t+(1-\gamma)^2\delta t^{2H})}. \tag{3.49}$$

Substituting equations (3.41)-(3.43) and (3.49) into equation (3.20) and using equation (3.14), we have the following

$$\begin{aligned} &\Big(X_2rB-\frac{\partial c}{\partial t}\Big)\delta t-\frac{\partial c}{\partial\sigma}\sigma\Big(\alpha\delta t+\frac{1}{2}\beta^2\varepsilon^2\delta t+\frac{1}{2}\beta^2(1-\varepsilon)^2(\delta t)^{2H_1}\Big) \\ &-\frac{1}{2}\frac{\partial^2 c}{\partial S^2}S^2\Big(\gamma^2\sigma\delta t+(1-\gamma)^2\sigma(\delta t)^{2H}\Big)-\frac{1}{2}\frac{\partial^2 c}{\partial\sigma^2}\sigma^2\beta^2\Big(\varepsilon^2\delta t+(1-\varepsilon)^2(\delta t)^{2H_1}\Big) \\ &-kS^2\Big|\frac{\partial^2 c}{\partial S^2}\Big|\sqrt{\frac{2}{\pi}}\sqrt{\sigma(\gamma^2\delta t+(1-\gamma)^2\delta t^{2H})}=0, \\ &X_2rB-\frac{\partial c}{\partial t}-\frac{\partial c}{\partial\sigma}\sigma\Big(\alpha+\frac{1}{2}\beta^2\varepsilon^2+\frac{1}{2}\beta^2(1-\varepsilon)^2(\delta t)^{2H_1-1}\Big) \\ &-\frac{1}{2}\frac{\partial^2 c}{\partial S^2}S^2\sigma\Big(\gamma^2+(1-\gamma)^2\delta t^{2H-1}\Big)-\frac{1}{2}\frac{\partial^2 c}{\partial\sigma^2}\sigma^2\beta^2\Big(\varepsilon^2+(1-\varepsilon)^2(\delta t)^{2H_1-1}\Big) \\ &-kS^2\Big|\frac{\partial^2 c}{\partial S^2}\Big|\sqrt{\frac{2}{\pi\delta t}}\sqrt{\sigma(\gamma^2+(1-\gamma)^2\delta t^{2H-1})}=0. \end{aligned} \tag{3.50}$$

$X_2 rB$ may be replaced as $rc - r\frac{\partial c}{\partial S}S$, hence equation (3.50) may be written as

$$\begin{aligned} & rc - rS\frac{\partial c}{\partial S} - \frac{\partial c}{\partial t} - \frac{\partial c}{\partial \sigma}\sigma\Big(\alpha + \frac{1}{2}\beta^2\varepsilon^2 + \frac{1}{2}\beta^2(1-\varepsilon)^2\delta t^{2H_1-1}\Big) \\ & - \frac{1}{2}\frac{\partial^2 c}{\partial S^2}\sigma S^2\Big(\gamma^2 + (1-\gamma)^2\delta t^{2H-1}\Big) - \frac{1}{2}\frac{\partial^2 c}{\partial \sigma^2}\sigma^2\beta^2\Big(\varepsilon^2 + (1-\varepsilon)^2\delta t^{2H_1-1}\Big) \\ & = kS^2\Big|\frac{\partial^2 c}{\partial S^2}\Big|\sqrt{\frac{2\sigma}{\pi\delta t}}\sqrt{\gamma^2 + (1-\gamma)^2\delta t^{2H-1}}. \end{aligned} \tag{3.51}$$

Remark 3.1. Note that when $\alpha = \beta = 0$, then the partial differential equation (3.51) reduces to the PDE of European call option for constant volatility which resembles equation (2.36) with slightly different volatility parameter.

Remark 3.2. For the special case in which $\gamma = 0$ and $\varepsilon = 0$, then equation (3.51) reduces to the partial differential equation in [74].

3.4 Concluding remarks

In this section, we derive the partial differential equation for the price of European call option by assuming a general model of 'fractals' with transaction costs as shown in equation (3.51). We use this to further analyse the general model and investigate how it may be used in the financial market. Wang *et al.* [74] has constructed the analytical solution of a fractional long memory model by assuming a positive value of $\Big|\frac{\partial X_1}{\partial S}\Big|$. We will use the general PDE model to compare the effect of additional parameters in various models and investigate how this may be relevant to the real financial market.

CHAPTER 4

Analysis of the general constant volatility model

4.1 General

In Section 3.3, we have established the general PDE (3.51) for European option price. In this chapter, we will perform numerical analysis on the partial differential equation for the special case with constant volatility using the finite element method in order to further analyse the effect of different parameters in the model as well as its relevance to the real financial market.

The finite element method is a numerical method that is believed to be more reliable than finite difference method. The finite difference method has been widely used in solving numerical PDE problems in finance since it is sufficiently simple and efficient to perform the analysis. However, many studies have claimed that the finite element method is a better and preferable method in numerically solving partial differential equations of greater than second order as it is more accurate and the results converge at a faster rate compare to finite difference method. Thus in this section, we will apply finite element analysis to solve the non-linear PDE (2.36) of the general constant volatility model, to attain the European call option price.

4.2 Numerical analysis of 1D problems

We first need to construct the variational statement for each PDE problem. In this section, we will start by analysing the 1D non-linear PDE problem of equation (2.36). Note that this PDE problem is similar to the 1D generalized model of equation (3.51)

when $\alpha = \beta = 0$. By changing the time $t \to T - t$, equation (2.36) becomes

$$\begin{aligned}&\frac{\partial c}{\partial t} - \frac{1}{2}\frac{\partial^2 c}{\partial S^2}S^2\sigma^2\Big(\gamma^2 + (1-\gamma)^2\delta t^{2H-1}\Big)\\&- r\frac{\partial c}{\partial S}S + rc = kS^2\sigma\Big|\frac{\partial^2 c}{\partial S^2}\Big|\sqrt{\frac{2}{\pi dt}}\sqrt{\gamma^2 + (1-\gamma)^2\delta t^{2H-1}},\end{aligned} \tag{4.1}$$

with initial and boundary conditions as follows:

$$c(0, S) = max(S - K, 0), \tag{4.2}$$

$$c(t, 0) = 0, \quad c(t, S_{max}) = S_{max} - Ke^{-rt}. \tag{4.3}$$

The variational statement of the problem above can be attained by initially multiplying equation (4.1) by a test function $\upsilon \in H^1$ and integrating over Ω, then using the idea of Green's theorem to reduce the second derivative term. The second derivative of the force term (F) is discretised using Central Difference method.

The second derivative on the left hand side of equation (4.1) may be represented as

$$\frac{\partial}{\partial S}\Big(S^2\frac{\partial c}{\partial S}\upsilon\Big) = S^2\upsilon\frac{\partial^2 c}{\partial S^2} + 2S\upsilon\frac{\partial c}{\partial S} + S^2\frac{\partial \upsilon}{\partial S}\frac{\partial c}{\partial S}. \tag{4.4}$$

Using equation (4.4) above, we are able to attain

$$\begin{aligned}&\int_\Omega c_t\upsilon d\Omega - \int_\Omega rS\frac{\partial c}{\partial S}\upsilon d\Omega + \int_\Omega rc\upsilon d\Omega\\&- \frac{1}{2}\sigma^2\Big(\gamma^2 + (1-\gamma)^2\delta t^{2H-1}\Big)\int_\Omega\Big(\frac{\partial}{\partial S}\Big(S^2\frac{\partial c}{\partial S}\upsilon\Big) - 2S\upsilon\frac{\partial c}{\partial S} - S^2\frac{\partial \upsilon}{\partial S}\frac{\partial c}{\partial S}\Big)d\Omega\\&= \int_\Omega kS^2\sigma\Big|\frac{c_{i+1} - 2c_i + c_{i-1}}{(\Delta t)^2}\Big|\sqrt{\frac{2}{\pi dt}}\sqrt{\gamma^2 + (1-\gamma)^2\delta t^{2H-1}}\upsilon d\Omega.\end{aligned}$$

Since dirichlet conditions exist on both boundaries as stated in equation (4.3), the test function (υ) is equal to zero on the boundaries. Hence, the boundary integration term will vanish and the equation simplifies to

$$\begin{aligned}&\int_\Omega c_t\upsilon d\Omega + \int_\Omega rc\upsilon d\Omega + \int_\Omega\Big[-r + \sigma^2\Big(\gamma^2 + (1-\gamma)^2\delta t^{2H-1}\Big)\Big]S\frac{\partial c}{\partial S}\upsilon d\Omega\\&+ \frac{1}{2}\sigma^2\Big(\gamma^2 + (1-\gamma)^2\delta t^{2H-1}\Big)\int_\Omega S^2\frac{\partial \upsilon}{\partial S}\frac{\partial c}{\partial S}d\Omega\\&= \int_\Omega kS^2\sigma\Big|\frac{c_{i+1} - 2c_i + c_{i-1}}{(\Delta t)^2}\Big|\sqrt{\frac{2}{\pi dt}}\sqrt{\gamma^2 + (1-\gamma)^2\delta t^{2H-1}}d\Omega.\end{aligned} \tag{4.5}$$

Therefore, the variational statement may be written as

Find $c \in H^1(\Omega)$ such that for every $t \in [0,T]$, $c(t,0)=0$, $c(t,S_{max}) = S_{max} - Ke^{-rt}$ and

$$\begin{aligned}
&\int_\Omega c_t \upsilon d\Omega + \int_\Omega r c \upsilon d\Omega + \int_\Omega \Big[-r + \sigma^2\Big(\gamma^2 + (1-\gamma)^2 \delta t^{2H-1}\Big)\Big] S \frac{\partial c}{\partial S} \upsilon d\Omega \\
&+ \frac{1}{2}\sigma^2\Big(\gamma^2 + (1-\gamma)^2\delta t^{2H-1}\Big) \int_\Omega S^2 \frac{\partial \upsilon}{\partial S}\frac{\partial c}{\partial S} d\Omega \\
&= \int_\Omega k S^2 \sigma \Big| \frac{c_{i+1} - 2c_i + c_{i-1}}{(\Delta t)^2}\Big| \sqrt{\frac{2}{\pi dt}} \sqrt{\gamma^2 + (1-\gamma)^2 \delta t^{2H-1}} d\Omega, \quad \forall \upsilon \in H_0^1(\Omega).
\end{aligned} \tag{4.6}$$

In order to use the Galerkin finite element method, we first pose the problem into a finite dimension space H_h^1 with basis functions $(\phi_i, i = 1, ..., n)$ to obtain

$$\Big(\frac{\partial c_h}{\partial t}, \upsilon_h\Big) + a(c_h, \upsilon_h) = L(\upsilon_h), \quad \forall \upsilon_h \in H_h^1, \tag{4.7}$$

where

$$\begin{aligned}
a(c_h, \upsilon_h) &= \int_\Omega r c \upsilon d\Omega + \int_\Omega \Big[-r + \sigma^2\Big(\gamma^2 + (1-\gamma)^2 \delta t^{2H-1}\Big)\Big] S \frac{\partial c}{\partial S} \upsilon d\Omega \\
&+ \frac{1}{2}\sigma^2\Big(\gamma^2 + (1-\gamma)^2\delta t^{2H-1}\Big) \int_\Omega S^2 \frac{\partial \upsilon}{\partial S}\frac{\partial c}{\partial S} d\Omega,
\end{aligned} \tag{4.8}$$

$$L(\upsilon_h) = \int_\Omega k S^2 \sigma \Big| \frac{c_{i+1} - 2c_i + c_{i-1}}{(\Delta t)^2}\Big| \sqrt{\frac{2}{\pi dt}} \sqrt{\gamma^2 + (1-\gamma)^2 \delta t^{2H-1}} d\Omega. \tag{4.9}$$

As

$$\upsilon \approx \upsilon_h(s,t) = \sum_{i=1}^n \upsilon_i(t)\phi_i(s), \quad c \approx c_h(s,t) = \sum_{j=1}^n c_j(t)\phi_j(s), \tag{4.10}$$

by adopting the property of inner product, the problem (4.7) reduces to

$$\sum_{j=1}^n \Big(\phi_j(s), \phi_i(s)\Big)\dot{c_j}(t) + \sum_{j=1}^n a\Big(\phi_j(s), \phi_i(s)\Big) c_j(t) = L(\phi_i(s)) \tag{4.11}$$

which can be expressed in matrix form by

$$\mathbf{M}\dot{\mathbf{c}} + \mathbf{A}\mathbf{c} = \mathbf{F}, \quad \mathbf{c}(0) = c_0, \tag{4.12}$$

where $\mathbf{M} = (m_{ij})$ with $m_{ij} = (\phi_i, \phi_j)$,
$\mathbf{A} = (a_{ij})$ with $a_{ij} = a(\phi_i, \phi_j)$,
$\mathbf{F} = (f_i)$ with $f_i = L(\phi_i)$.

By using the backward Euler scheme, equation (4.12) becomes

$$\mathbf{M}\frac{\mathbf{c}^{n+1}-\mathbf{c}^{n}}{\Delta\tau}+\mathbf{A}\mathbf{c}^{n+1}=\mathbf{F}^{(n+1)}. \tag{4.13}$$

The force term $\mathbf{F}$ is nonlinear due to the absolute of the second derivative term. In order to use the backward Euler scheme, we need to do iterations at every each time step. However, for the purpose of this analysis, we will only take the first iteration as the approximation.

4.3 Numerical results of the general constant volatility model

Numerical analysis is carried out based on the finite element method discussed in the previous Section 4.2. We will analyse the effect of various additional parameters assumed in using the fractional Brownian motion and mixed fractional Brownian motion processes in a constant volatility option pricing model. This analysis is important to determine the validity of each model and how it affects the call option price. From the general PDE model of equation (2.36), $\gamma = 1$ assumes geometric Brownian motion, whereas $\gamma = 0$ indicates that the stock dynamic assumes a fractional Brownian motion process. When the value of γ is neither 0 or 1 and $H \in (0.5, 1)$, the model assumes mixed fractional Brownian motion diffusion process. However, before analysing the various assumed models, we will first look at the effect of transaction costs on all of the three models. Table 4.1 lists the parameters used in analysing each model and attaining the proceeding results, unless specified otherwise.

Table 4.1: Values of model parameters

	r	K	σ	γ	H	k	δt	T
gBm	0.05	150	0.15	1	0.5	0.01	$\frac{30}{365}$	$\frac{92}{365}$
fBm	0.05	150	0.15	0	0.55	0.01	$\frac{30}{365}$	$\frac{92}{365}$
MfBm	0.05	150	0.15	0.5	0.55	0.01	$\frac{30}{365}$	$\frac{92}{365}$

4.3.1 Proportional transaction costs (k) and trading days (δt)

In the real market, the cost of buying or selling underlying shares, despite being minimal, still affects the fair price of option. Previous studies of option model assuming log-normal diffusion process, i.e. geometric Brownian motion assumption [34, 65] have raised awareness on the importance of including transaction costs in valuing option prices. Thus in the general option model, we have included transaction costs not only due to its importance, but also to eliminate the no-arbitrage requirement. In this section we will study the effect of proportional transaction costs in all the three models, starting with the classical model which assumes gBm. We will further analyse the transaction costs together with the trading days (δt) as they are closely related. Due to the competitive market nowadays, the assumption of proportional transaction costs ($k = 0.01$) used in this analysis is considered to be sensible. The effect of increasing transaction costs on the price of European call option is shown in Figure 4.1.

It is apparent that an increase in proportional transaction costs increases the price of European call option particularly when the value of share price is near the strike price (Figure 4.1). In addition, the effect of transaction costs is similar for all three models, which reinforces the significance of transaction costs in calculating the call option price to avoid underestimation.

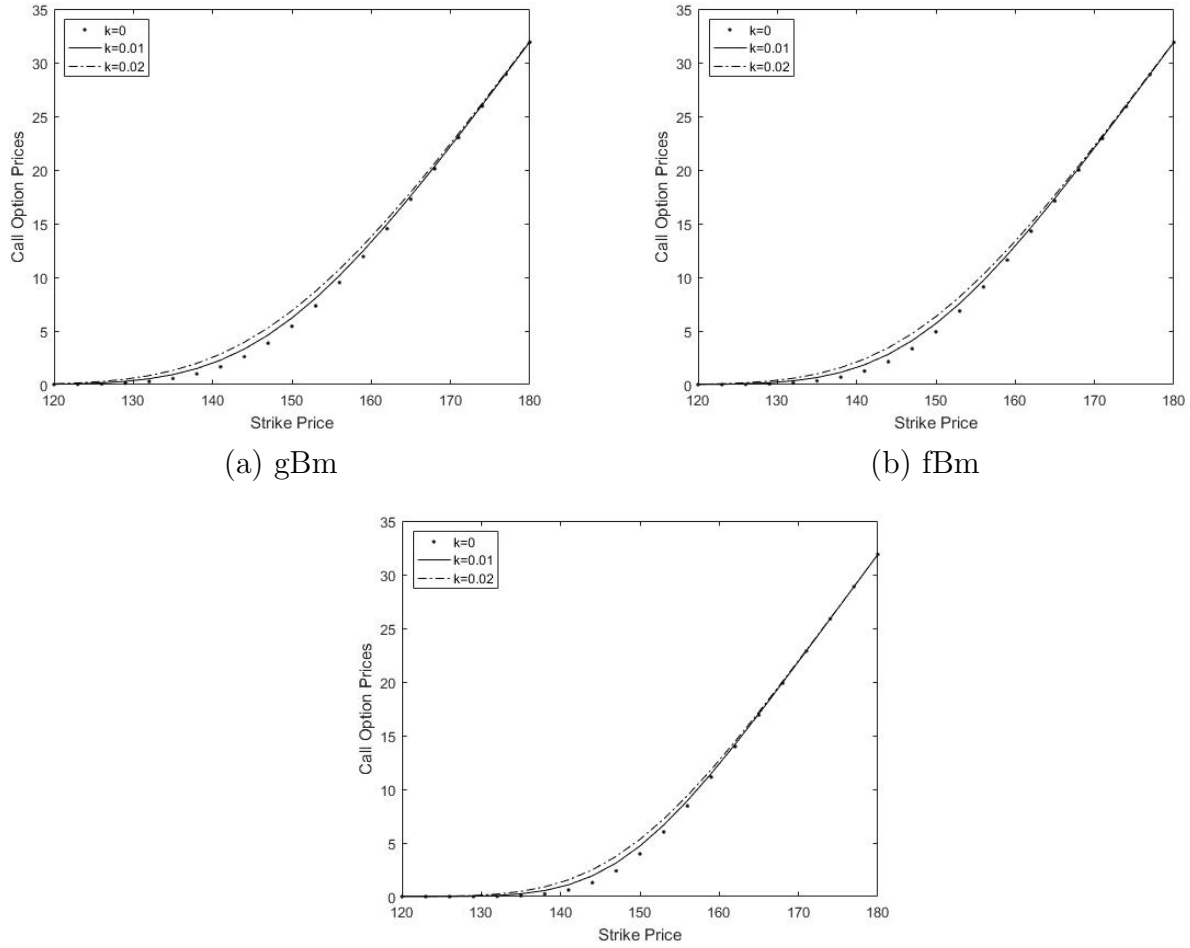

(a) gBm

(b) fBm

(c) mfBm

Figure 4.1: The effect of proportional transaction costs on European call option prices for all the three models.

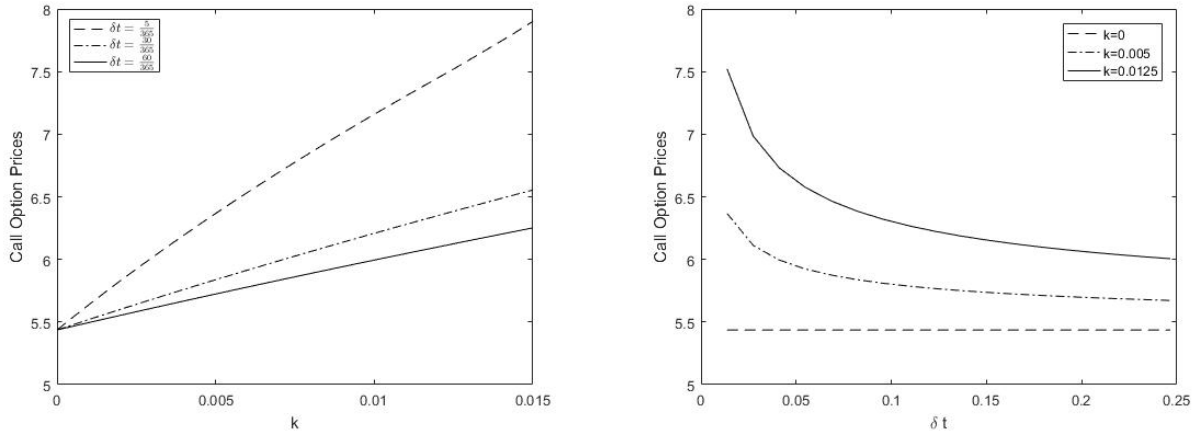

(a) gBm

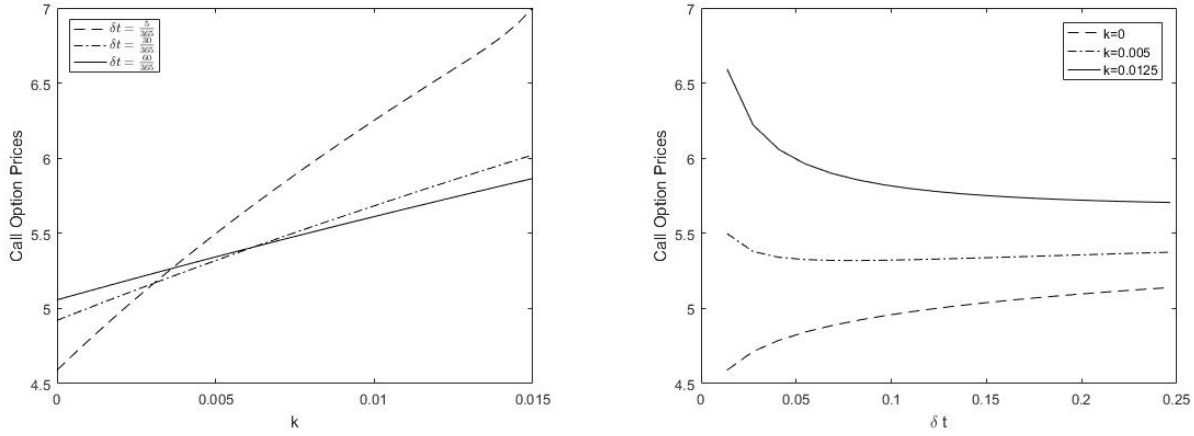

(b) fBm

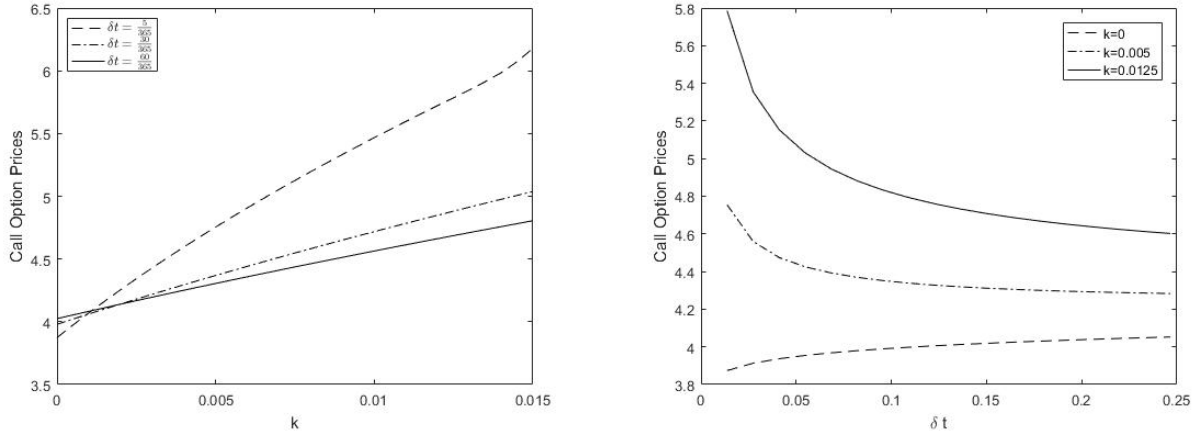

(c) mfBm

Figure 4.2: The effect of different values of k and δt on the European call option price when $S = K = 150$ for the given parameters in Table 4.1 for all the three models.

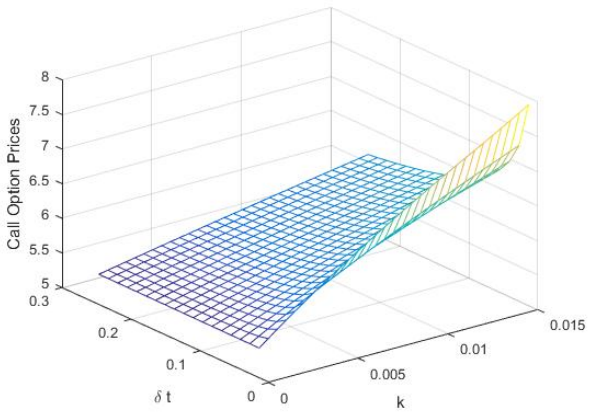

(a) gBm

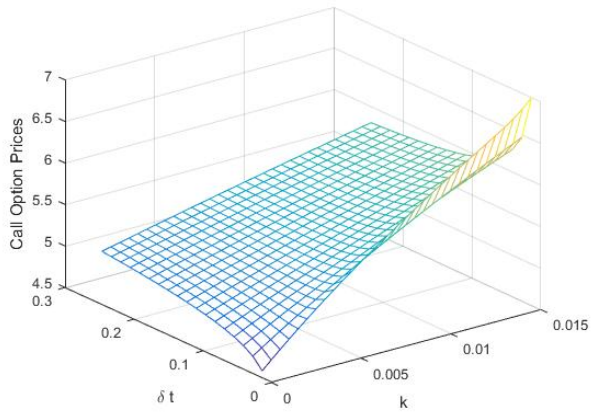

(b) fBm

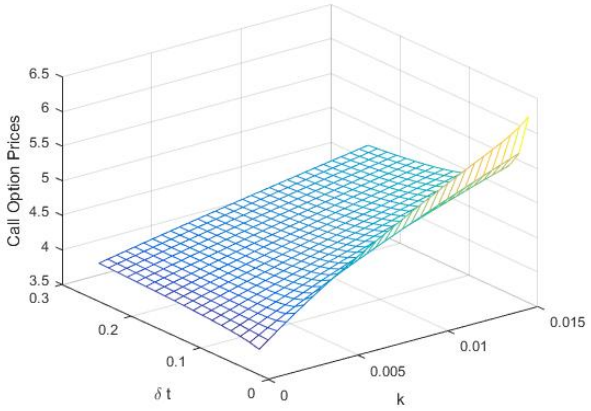

(c) mfBm

Figure 4.3: The relationship between at-the-money ($S = K = 150$) European call option price based on the given parameters in Table 4.1 and the parameters of k and δt for all the three models.

There is a general trend that as the transaction cost (k) increases, so does the price of call option (Figure 4.3). This increase is almost linear although the rate of increase depends on the trading days (δt) (Figure 4.2 and Figure 4.3). The longer the trading days or re-hedging period, the call option price will increase at a slower rate in response to increasing transaction costs. On the other hand, call option price is negatively proportional to δt. This is apparent in Figure 4.2 in which high trading days reduce the price of call option at a hyperbolic rate. The increase of k however, translates the entire curve up, hence the call option price. It is obvious that transaction costs (k) and trading days (δt) are closely related and positively proportional to one another (Figures 4.2 and 4.3). This indicates that since transaction cost has a great impact towards the price of call option, trading should not occur as often because the cost of trading the underlying stock at each transaction will accumulate highly. According to Hoggard *et al.* [65], one may trade as

often as possible given that the cost parameter (κ) is still lower than the bid-spread ratio of the option traded. The cost parameter (κ) of a Black-Scholes model with transaction costs as stated in [65] captures the relationship between k, σ and δt. Therefore, the only parameter that we have control of is δt, as we are able to alter it accordingly. The cost parameter for the general PDE model of equation (2.36) is given as the following:

$$\kappa = \frac{k}{\sigma}\sqrt{\frac{8}{\pi\delta t((1-\gamma)^2\delta t^{2H-1}+\gamma^2)}}. \tag{4.14}$$

In the absence of transaction costs, the European call option values assuming gBm model is unaffected by the change in trading days (δt), but this is not the case when assuming fBm and mfBm model (Figures 4.2 and 4.3). This result is consistent with the argument made by Wang [72] that fractal scaling δt has a significant impact on option pricing. Furthermore, the effect of fractal scaling δt on call option price for fBm is greater than mfBm (Figure 4.2).

4.3.2 Hurst parameter (H) and γ

In order to capture the long memory in stock returns, it was previously discussed that fractional Brownian motion process should be adopted instead of the classical Brownian motion since fBm has the desirable property of correlated increments when $H \neq \frac{1}{2}$. The additional parameter that differentiates between fBm process from the classical Brownian motion is the Hurst parameter (H). Therefore, we here analyse the effect of $H > \frac{1}{2}$ on the European call option price. An increase in H reduces the price of call option when the share price is around the strike price (Figure 4.4).

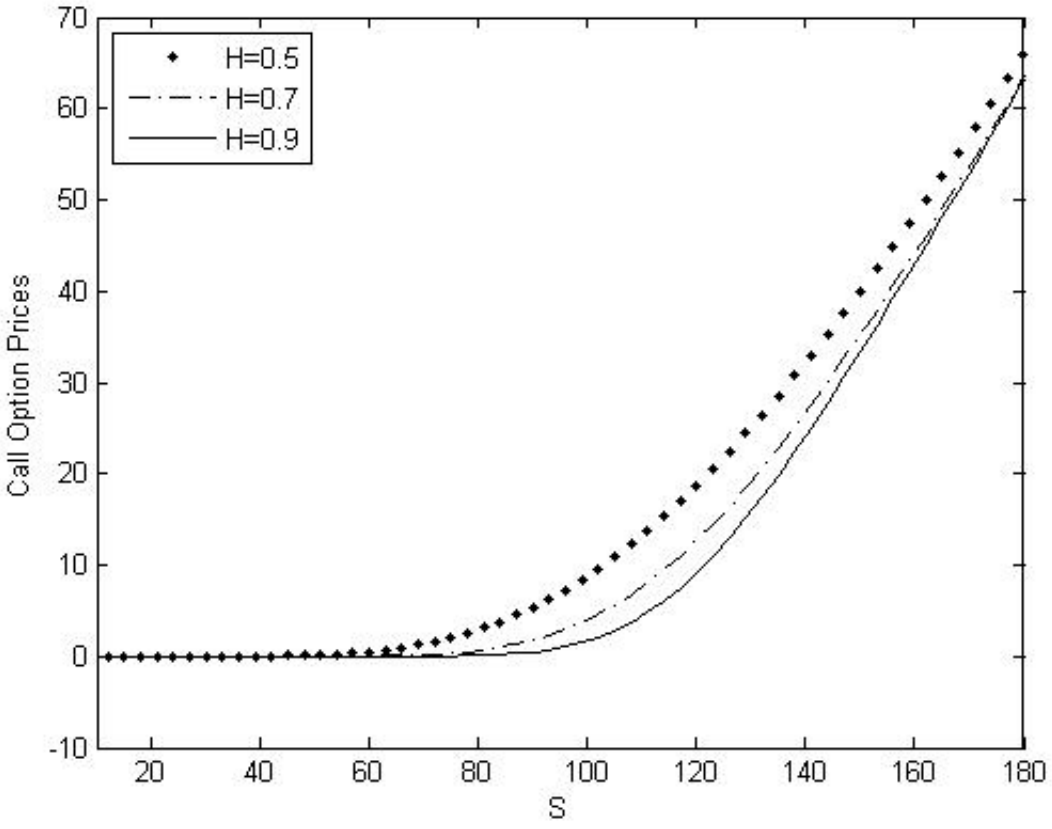

Figure 4.4: The price of European call option for various values of H.

Mixed fractional Brownian motion is constructed through the linear combination of gBm and fBm. The additional parameter introduced in mfBm is γ and we also want to analyse its effect on the European call option price. We will start by assuming the parameters stated in Table 4.1 and test for different values of γ. Note that when $\gamma = 1$, the model assumes the classical Brownian motion. Similarly when $\gamma = 0$, the model follows the fBm diffusion process. Assuming other parameters $(k, \delta t, \sigma)$ are constant as shown in Table 4.1, it is apparent that the call option prices based on mixed fractional Brownian motion, for S values close to K, are lower compared to the other two models (Figure 4.5).

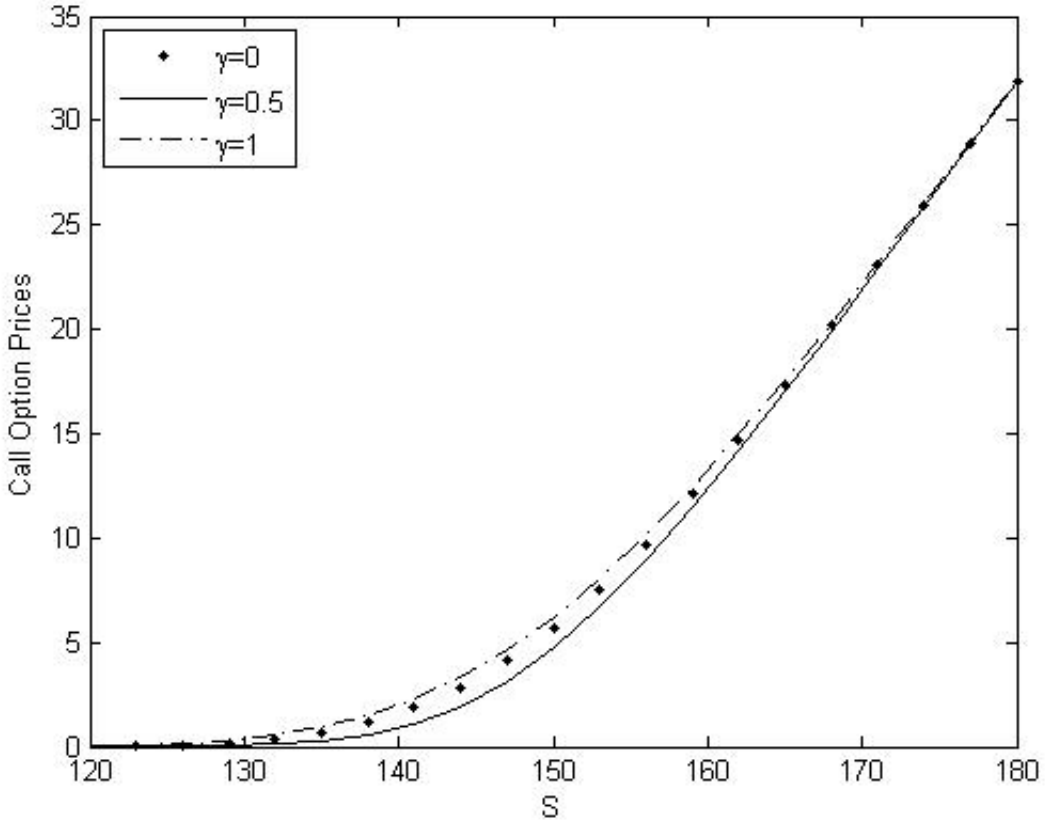

Figure 4.5: The price of European call option for various values of γ.

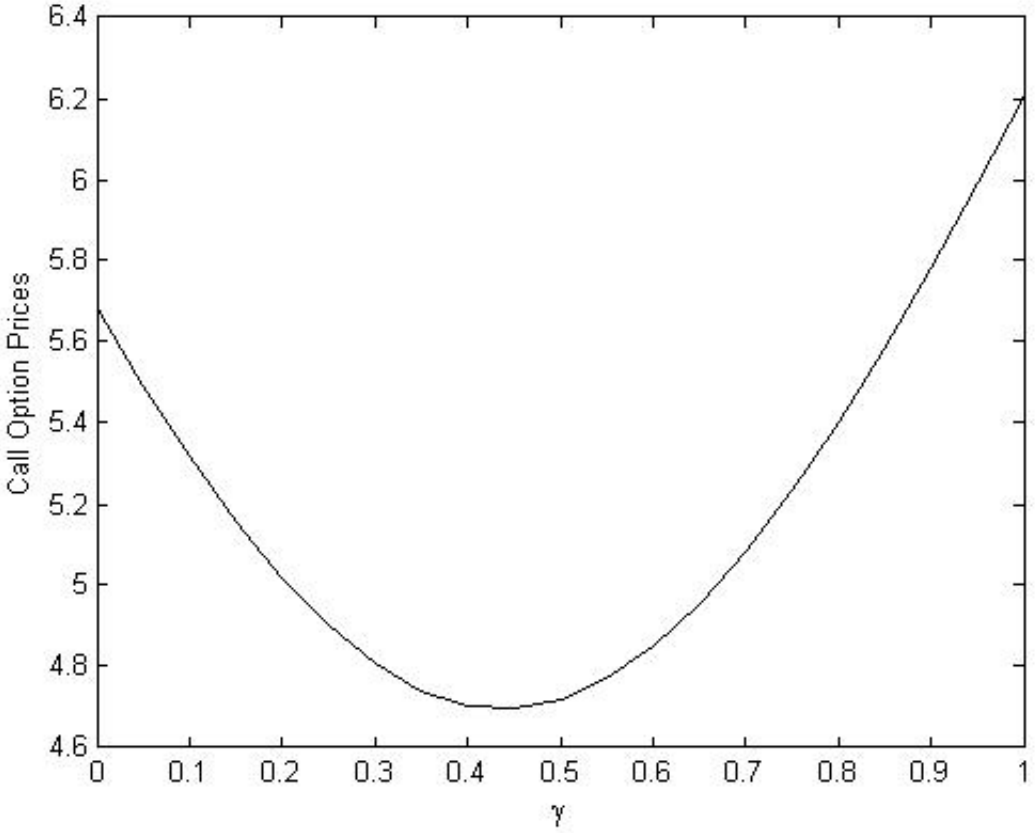

Figure 4.6: The variation of the price of European call option with respect to γ for the chosen parameters in Table 4.1 and $S = 150$.

In order to further analyse the effect of γ on the value of European call price, we plot the variation of the call price with respect to γ for $\gamma \in [0, 1]$ when $S = K = 150$ as shown in Figure 4.6. At moneyness, i.e. $S = K = 150$, the call option price is lowest when γ is approximately 0.45 for the other chosen parameters listed in Table 4.1 (Figure 4.6). The value of call option price when assuming $\gamma = 1$, i.e. gBm, is also much higher compared to the fBm ($\gamma = 0$) or the mfBm model. Therefore, it is important to consider the parameter γ in order not to overestimate the value of call option.

In addition, we also know that besides the additional parameter γ, mfBm also depends on the Hurst parameter (H). When we consider the effect of γ previously, we have kept H constant, equals to 0.55, such that the value of H is identical to the ones assumed in the fBm process. The intention is to further analyse the effect of H in the mfBm model and how sensitive it is compared to when it is adopted in the fBm model.

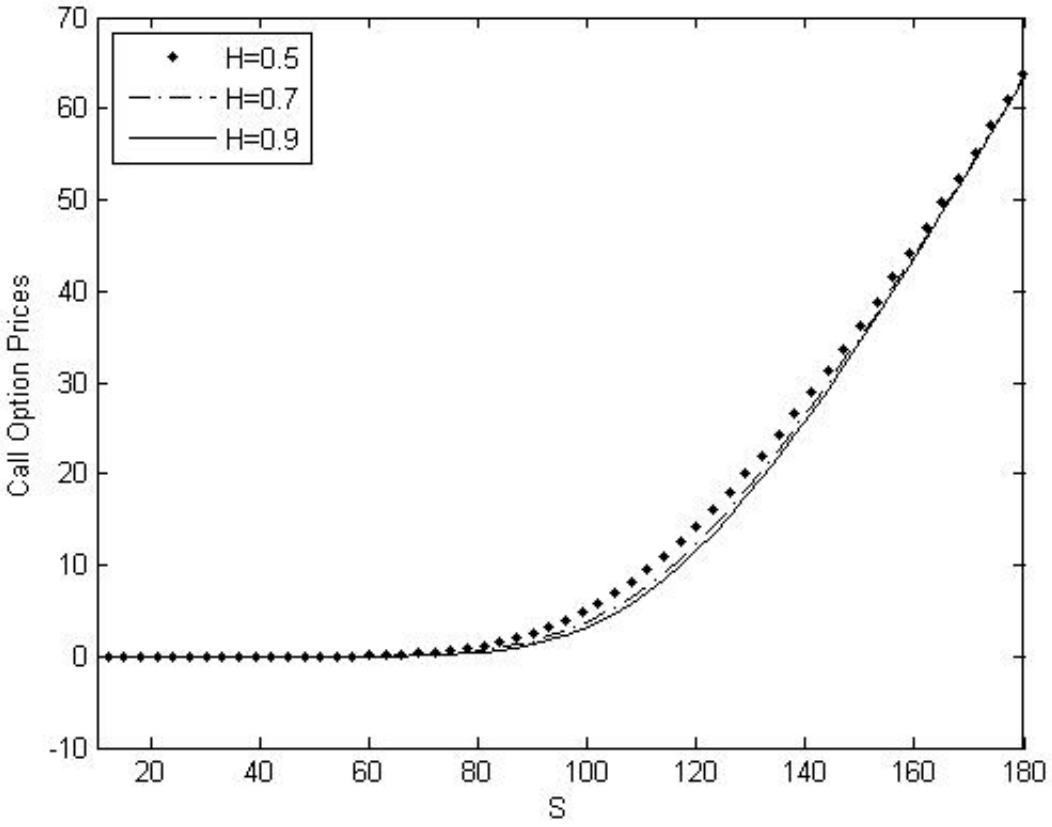

Figure 4.7: The price of European call option assuming mixed fractional Brownian motion when $\gamma = 0.5$ for different values of H.

The effect of changing H in this case (Figure 4.7) is not as significant as in the case of fBm as shown in Figure 4.4. The price of call option decreases much more rapidly for increasing value of H when γ is relatively small (Figures 4.8 and 4.9). As γ increases, the effect of Hurst parameter towards the call option diminishes and disappears as $\gamma = 1$. This is not surprising as $\gamma = 1$ indicates that the model assumes geometric Brownian motion, hence it should not be affected by the change in H.

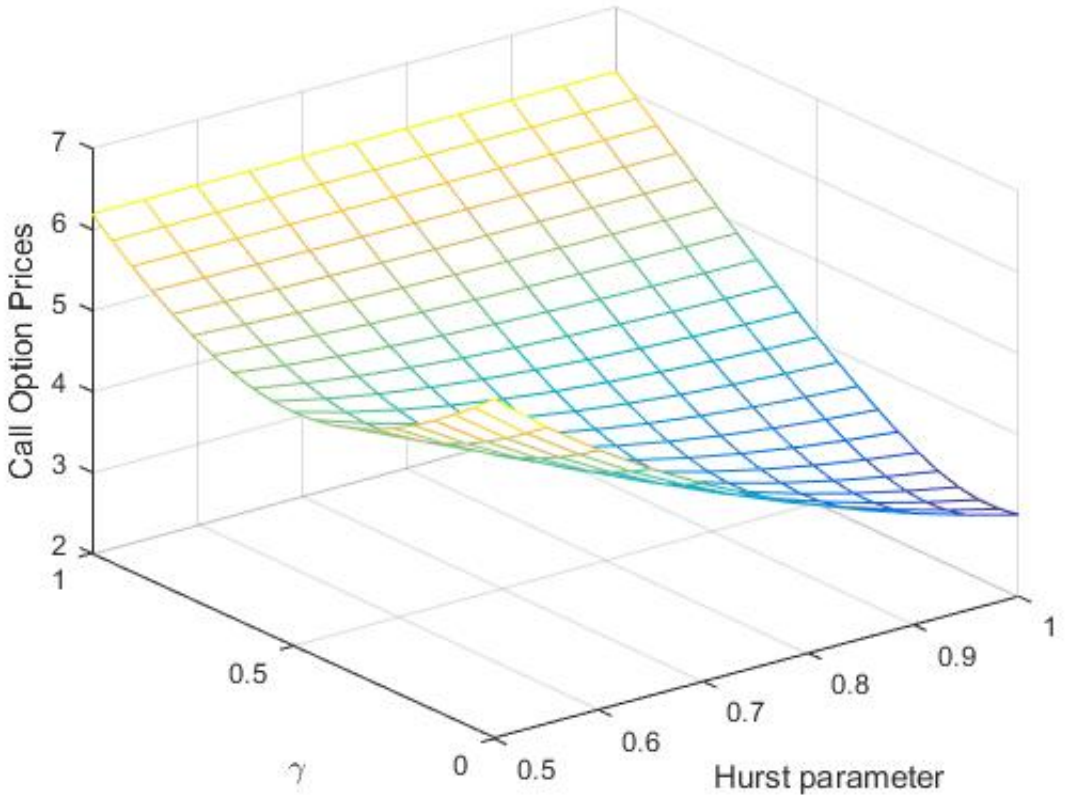

Figure 4.8: The price of European call option for different values of γ and H for the chosen parameters in Table 4.1 and $S = 150$.

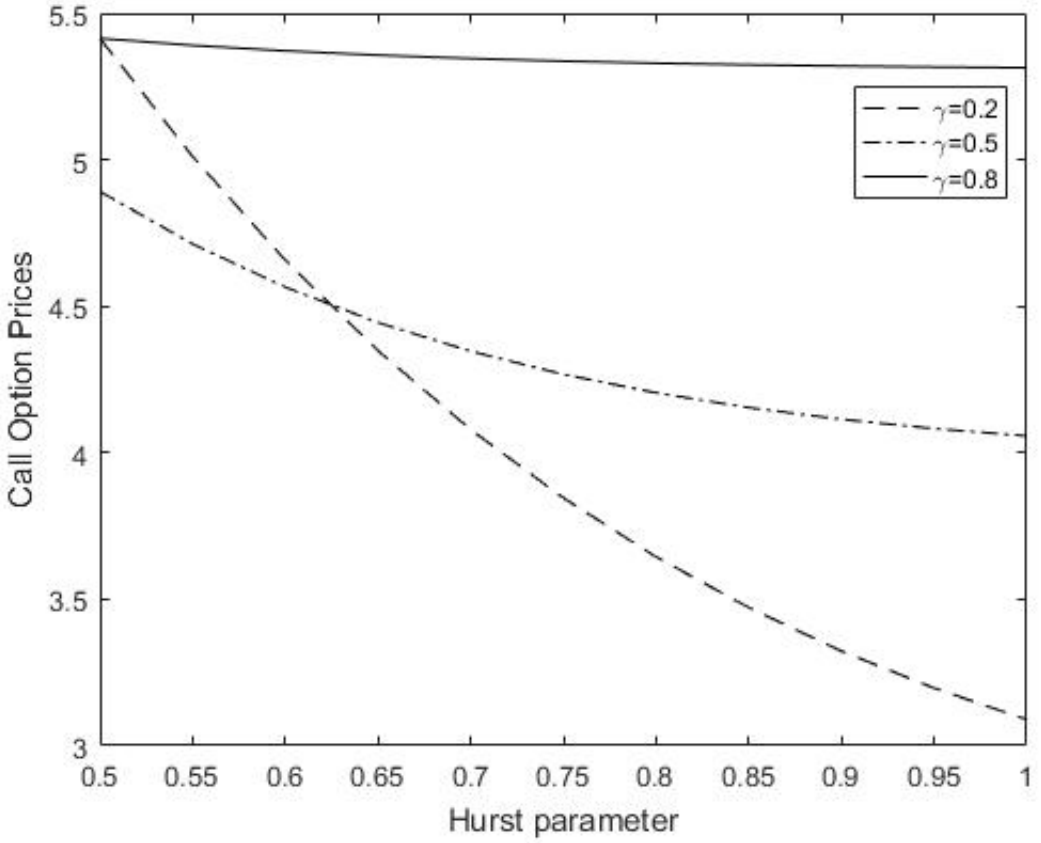

Figure 4.9: The price of European call option against H for different values of γ for the chosen parameters in Table 4.1 and $S = 150$.

We previously concluded that the value of call option price based on γ shows a relationship resembling a parabola where its turning point is at approximately γ equals to 0.45 (Figure 4.6). However, this is calculated based on H value of 0.55 and other chosen parameters listed in Table 4.1. We further investigate whether this relationship applies to all values of $H \in (0.5, 1)$. The resemblance to a parabolic curve shown in Figure 4.6 does not apply to all values of H (Figure 4.10). The curve appears to be more obvious for lower value of H. As H increases, the parabolic relationship between call option price and γ gradually diminishes. This result is also evident from the surface Figure 4.8 which shows the general relationship between H and γ towards the call option price.

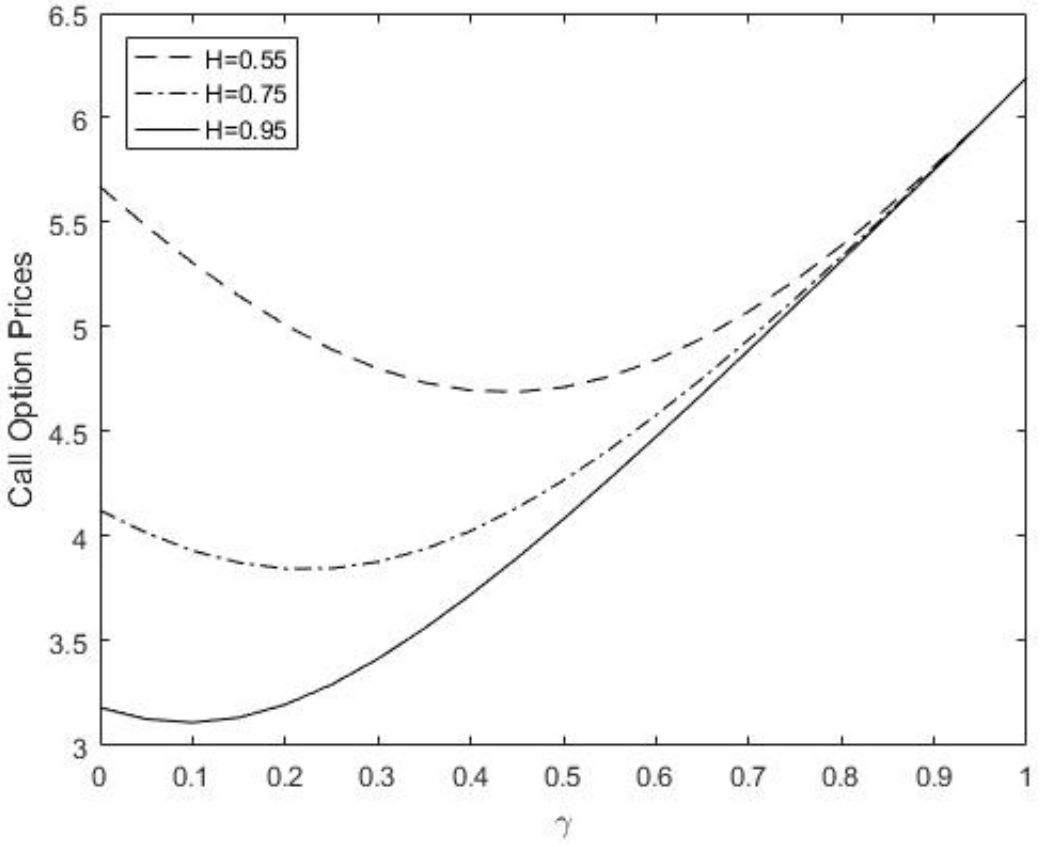

Figure 4.10: The price of European call option against γ for different values of H for the chosen parameters in Table 4.1 and $S = 150$.

4.3.3 Influence of volatility (σ)

Volatility is a crucial parameter in the classical Black-Scholes model and is the trickiest one to be determined, since there is no definite answer. In the classical Black-Scholes model, volatility (σ) is said to be constant. Since this parameter is constant, presumably the value needs to be sufficiently large to capture the average volatility of the whole share market. Realistically, this may not be possible, which is why we will later extend the model to consider stochastic volatility in the next chapter. We start by analysing the effect of constant volatility parameter (σ) on the price of European call option. There is a general trend that when the volatility (σ) increases, so does the value of call option for all the three models (Figure 4.11). The parameter σ significantly affects the call option price for all range of values of S, unlike the other parameters (k, H, γ) which mainly affect the call option price when S is near the strike price (K). This result is reasonable and is consistent with the classical Black-Scholes model.

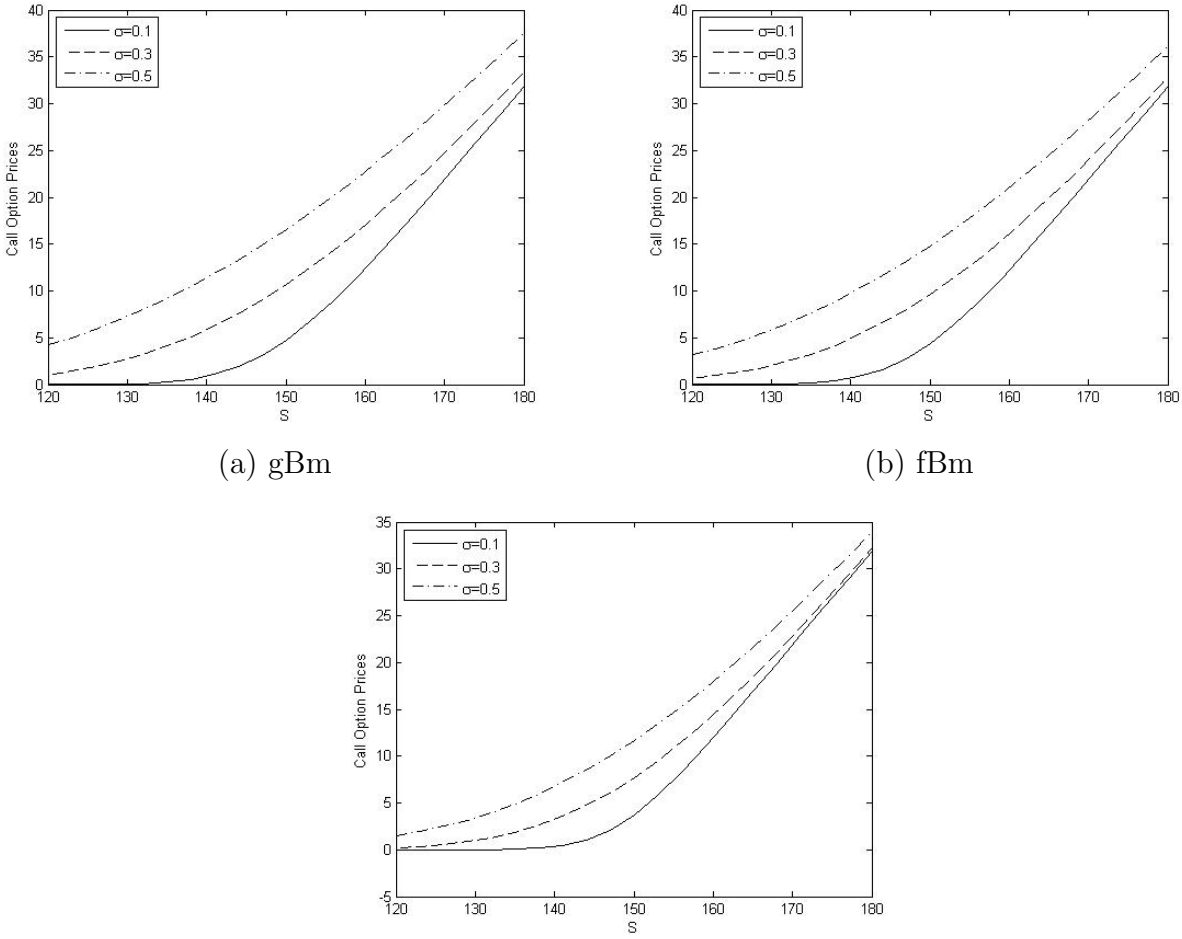

(a) gBm

(b) fBm

(c) mfBm

Figure 4.11: The price of European call option price based on the given parameters in Table 4.1 for different values of σ for all the three models.

4.4 Concluding remarks

This chapter focuses on the numerical analysis and results of the general constant volatility model. Many numerical analysis in finance uses finite difference method due to its simplicity as well as efficiency. However, when faced with a more complicated problem, finite difference method may not be the best choice. Thus, many researchers use a more efficient method known as the finite element method. Since the general call option model introduced in this thesis involves transaction costs, a non-linear partial differential equation is unavoidable. In this chapter, we have demonstrated how the finite element method is employed to solve for one dimension non-linear PDE problems. We adopted the Central Difference method in tackling the absolute value of the second derivative term and treating it as a force term. Several other approaches may well be considered to improve the numerical performance in solving the PDE problems. However, for the purpose of

this numerical analysis, which is to study the effect of additional parameters in the fBm and the mfBm models, we only employ the Backward Euler iteration to approximate the results.

We started off by investigating the effect of various parameters involved in the general constant volatility model. When assuming the fBm and mfBm diffusion processes, we know that in theory, transaction costs need to be considered to eliminate the no-arbitrage requirement. However, proportional transaction costs play a significant role in valuing call option price in all the three models to avoid underestimating the fair value, particularly for those options in which the underlying price (S) is near the strike price (K). This is in line with the studies that have been previously done by many researchers such as Leland [34] and Hoggard *et al.* [65] who have raised the importance of taking into account transaction costs in the option pricing model that assumes gBm diffusion process. In addition, there is a crucial relationship between the transaction costs and the trading or re-hedging days (δt). The effect of high call option price due to the high value of k may be reduced by increasing δt. However, when assuming the gBm model and $k = 0$, δt has no effect on European call option price. When $k = 0$ and fBm and mfBm models are assumed, δt contributes towards the fractal scaling effect.

Moreover, further analysis shows the importance of the Hurst parameter and γ in determining the value of call option price. The inclusion of the Hurst parameter reduces the value of call option price around the strike price. This indicates the possibility of the fBm and the mfBm model being able to better reflect the value of call option price due to the additional parameters. Acknowledging the relationship between these parameters will assist in understanding the appropriate parameters to include, whether it may be fBm or mfBm.

In this chapter, we have also shown the effect of constant volatility parameter (σ). The results show that σ significantly affects the European call option price for all range of values of S. Therefore, it will be difficult to describe the features of call option price with only a constant volatility parameter. Hence, we will extend the numerical analysis to study the effect of various parameters of the general stochastic volatility model in the next chapter.

CHAPTER 5

Analysis of the general stochastic volatility model

5.1 General

In Chapter 3.3, we have constructed the general stochastic volatility model for European call option price taking into account transaction costs. The use of finite element method allows faster convergence especially for the stochastic volatility model which involves two dimensional second order partial differential equation. Hence, similar to the previous chapter, we perform the numerical analysis on the partial differential equation (3.51) using the finite element method to analyse the effect of various parameters, particularly the additional parameters α and β. The effect of transaction costs (k) and trading days (δt) have been observed in Chapter 4, thus these will not be further discussed in this chapter. We acknowledge that the rise in transaction costs (k) increases the call option price and the increase of δt will compensate the high transaction costs. In this chapter, we focus on the effect of stochastic volatility and the parameters that greatly affect the volatility namely α, β, ε and H_1.

5.2 Numerical analysis of the general stochastic volatility model

The numerical analysis for the general stochastic volatility model is similarly performed as the previous Section 4.2 for 1D model. Firstly we need to alter the time $t \to T - t$ of the non-linear PDE problem of equation (3.51) to attain

$$\begin{aligned}&\frac{\partial c}{\partial t} - rS\frac{\partial c}{\partial S} - \frac{\partial c}{\partial \sigma}\sigma\Big(\alpha + \frac{1}{2}\beta^2\varepsilon^2 + \frac{1}{2}\beta^2(1-\varepsilon)^2\delta t^{2H_1-1}\Big)\\&- \frac{1}{2}\frac{\partial^2 c}{\partial S^2}\sigma S^2\Big(\gamma^2 + (1-\gamma)^2\delta t^{2H-1}\Big) - \frac{1}{2}\frac{\partial^2 c}{\partial \sigma^2}\sigma^2\beta^2\Big(\varepsilon^2 + (1-\varepsilon)^2\delta t^{2H_1-1}\Big) + rc\\&= kS^2\Big|\frac{\partial^2 c}{\partial S^2}\Big|\sqrt{\frac{2\sigma}{\pi\delta t}}\sqrt{\gamma^2 + (1-\gamma)^2\delta t^{2H-1}},\end{aligned} \tag{5.1}$$

which satisfies the following initial and boundary conditions:

$$c(0, S, \sigma) = max(S - K, 0), \tag{5.2}$$

$$c(t, 0, \sigma) = 0, \quad \frac{\partial c}{\partial S}(t, S_{max}, \sigma) = 1. \tag{5.3}$$

Note that there are no boundary conditions imposed on σ_{min} and σ_{max}. In order to construct the variational statement of the problem above, we introduce the test function $\upsilon \in H^1$ which is multiplied throughout equation (5.1), then the resulting equation is integrated to get

$$\begin{aligned}&\int\int_\Omega \frac{\partial c}{\partial t}\upsilon d\Omega - \int\int_\Omega rS\frac{\partial c}{\partial S}\upsilon d\Omega - \int\int_\Omega \frac{\partial c}{\partial \sigma}\sigma\Big(\alpha + \frac{1}{2}\beta^2\varepsilon^2 + \frac{1}{2}\beta^2(1-\varepsilon)^2\delta t^{2H_1-1}\Big)\upsilon d\Omega\\&- \int\int_\Omega \frac{1}{2}\frac{\partial^2 c}{\partial S^2}\sigma S^2\Big(\gamma^2 + (1-\gamma)^2\delta t^{2H-1}\Big)\upsilon d\Omega - \int\int_\Omega \frac{1}{2}\frac{\partial^2 c}{\partial \sigma^2}\sigma^2\beta^2\Big(\varepsilon^2 + (1-\varepsilon)^2\delta t^{2H_1-1}\Big)\upsilon d\Omega\\&+ \int\int_\Omega rc\upsilon d\Omega = \int\int_\Omega kS^2\Big|\frac{\partial^2 c}{\partial S^2}\Big|\sqrt{\frac{2\sigma}{\pi\delta t}}\sqrt{\gamma^2 + (1-\gamma)^2\delta t^{2H-1}}\upsilon d\Omega.\end{aligned} \tag{5.4}$$

Similar to that for reducing the second derivative term of $\dfrac{\partial^2 c}{\partial S^2}$ in equation (4.4), we also have

$$\frac{\partial}{\partial \sigma}\Big[\Big(\sigma^2\frac{\partial c}{\partial \sigma}\Big)\upsilon\Big] = \sigma^2\upsilon\frac{\partial^2 c}{\partial \sigma^2} + 2\sigma\upsilon\frac{\partial c}{\partial \sigma} + \sigma^2\frac{\partial \upsilon}{\partial \sigma}\frac{\partial c}{\partial \sigma}. \tag{5.5}$$

Let

$$\begin{aligned}D_1 &= \beta^2(\varepsilon^2 + (1-\varepsilon)^2\delta t^{2H_1-1}),\\D_2 &= \gamma^2 + (1-\gamma)^2\delta t^{2H-1},\\D_3 &= k\sqrt{\frac{2\sigma D_2}{\pi\delta t}}.\end{aligned} \tag{5.6}$$

By using equations (4.4) and (5.5), equation (5.4) may be reduced to

$$\begin{aligned}
&\int\int_{\Omega}\frac{\partial c}{\partial t}\upsilon d\Omega-\int\int_{\Omega}rS\frac{\partial c}{\partial S}\upsilon d\Omega-\int\int_{\Omega}\frac{\partial c}{\partial\sigma}\sigma\Big(\alpha+\frac{1}{2}D_1\Big)\upsilon d\Omega\\
&-\frac{1}{2}D_2\int\int_{\Omega}\sigma\Big[\frac{\partial}{\partial S}\Big(S^2\frac{\partial c}{\partial S}\upsilon\Big)-2S\upsilon\frac{\partial c}{\partial S}-S^2\frac{\partial\upsilon}{\partial S}\frac{\partial c}{\partial S}\Big]d\Omega\\
&-\frac{1}{2}D_1\int\int_{\Omega}\Big[\frac{\partial}{\partial\sigma}\Big(\sigma^2\frac{\partial c}{\partial\sigma}\upsilon\Big)-2\sigma\upsilon\frac{\partial c}{\partial\sigma}-\sigma^2\frac{\partial\upsilon}{\partial\sigma}\frac{\partial c}{\partial\sigma}\Big]d\Omega\\
&+\int\int_{\Omega}rc\upsilon d\Omega=\int\int_{\Omega}D_3S^2\Big|\frac{c_{i+1,j}-2c_{i,j}+c_{i-1,j}}{(\Delta t)^2}\Big|\upsilon d\Omega.
\end{aligned}\tag{5.7}$$

Using equation (5.3), we further simplify the integration of $\frac{\partial}{\partial S}\Big(S^2\frac{\partial c}{\partial S}\upsilon\Big)$ and $\frac{\partial}{\partial\sigma}\Big(\sigma^2\frac{\partial c}{\partial\sigma}\upsilon\Big)$, we get

$$\int_{\sigma_{min}}^{\sigma_{max}}\int_{0}^{S_{max}}\frac{\partial}{\partial S}\Big(S^2\frac{\partial c}{\partial S}\upsilon\Big)dSd\sigma=\int_{\sigma_{min}}^{\sigma_{max}}S_{max}^2\upsilon d\sigma,\tag{5.8}$$

$$\begin{aligned}
\int_{0}^{S_{max}}\int_{\sigma_{min}}^{\sigma_{max}}\frac{\partial}{\partial\sigma}\Big(\sigma^2\frac{\partial c}{\partial\sigma}\upsilon\Big)d\sigma dS&=\int_{0}^{S_{max}}\sigma^2\frac{\partial c}{\partial\sigma}\upsilon\Big|_{\sigma_{min}}^{\sigma_{max}}dS\\
&=\int_{0}^{S_{max}}\sigma_{max}^2\frac{\partial c}{\partial\sigma}\upsilon dS-\int_{0}^{S_{max}}\sigma_{min}^2\frac{\partial c}{\partial\sigma}\upsilon dS.
\end{aligned}\tag{5.9}$$

The integral in (5.8) is simplified to having no unknown term because of the Neumann boundary, thus this term will be moved to the right hand side of the equation. On the other hand, equation (5.9) still has the unknown c, therefore it still stays on the left hand side and will be treated as the integration on the boundaries σ_{min} and σ_{max}. Hence, substituting these into equation (5.7), we have

$$\begin{aligned}
&\int\int_{\Omega}\frac{\partial c}{\partial t}\upsilon d\Omega-\int\int_{\Omega}rS\frac{\partial c}{\partial S}\upsilon d\Omega-\int\int_{\Omega}\frac{\partial c}{\partial\sigma}\sigma\Big(\alpha+\frac{1}{2}D_1\Big)\upsilon d\Omega+\int\int_{\Omega}D_2\sigma S\upsilon\frac{\partial c}{\partial S}d\Omega\\
&+\int\int_{\Omega}\frac{1}{2}D_2\sigma S^2\frac{\partial\upsilon}{\partial S}\frac{\partial c}{\partial S}d\Omega-\frac{1}{2}D_1\int_{0}^{S_{max}}\sigma_{max}^2\frac{\partial c}{\partial\sigma}\upsilon dS+\frac{1}{2}D_1\int_{0}^{S_{max}}\sigma_{min}^2\frac{\partial c}{\partial\sigma}\upsilon dS\\
&+D_1\int\int_{\Omega}\sigma\upsilon\frac{\partial c}{\partial\sigma}d\Omega+\int\int_{\Omega}\frac{1}{2}D_1\sigma^2\frac{\partial\upsilon}{\partial\sigma}\frac{\partial c}{\partial\sigma}d\Omega+\int\int_{\Omega}rc\upsilon d\Omega\\
&=\int\int_{\Omega}D_3S^2\Big|\frac{c_{i+1,j}-2c_{i,j}+c_{i-1,j}}{(\Delta t)^2}\Big|\upsilon d\Omega+\frac{1}{2}D_2\int_{\sigma_{min}}^{\sigma_{max}}\sigma S_{max}^2\upsilon d\sigma.
\end{aligned}\tag{5.10}$$

Thus, we may write the variational statement as the following:

Find $c \in H^1(\Omega)$ such that for every $t \in [0,T]$, $c(t,0,\sigma) = 0$ and

$$\begin{aligned}
&\int\int_\Omega \frac{\partial c}{\partial t}\upsilon d\Omega + \int\int_\Omega \Big(- r + D_2\sigma\Big) S\frac{\partial c}{\partial S}\upsilon d\Omega + \int\int_\Omega \frac{\partial c}{\partial \sigma}\sigma\Big(- \alpha + \frac{1}{2}D_1\Big)\upsilon d\Omega \\
&+ \int\int_\Omega \frac{1}{2}D_2\sigma S^2\frac{\partial \upsilon}{\partial S}\frac{\partial c}{\partial S}d\Omega - \frac{1}{2}D_1\int_0^{S_{max}} \sigma_{max}^2\frac{\partial c}{\partial \sigma}\upsilon dS + \frac{1}{2}D_1\int_0^{S_{max}} \sigma_{min}^2\frac{\partial c}{\partial \sigma}\upsilon dS \\
&+ \int\int_\Omega \frac{1}{2}D_1\sigma^2\frac{\partial \upsilon}{\partial \sigma}\frac{\partial c}{\partial \sigma}d\Omega + \int\int_\Omega rc\upsilon d\Omega \\
&= \int\int_\Omega D_3S^2\Big|\frac{c_{i+1,j} - 2c_{i,j} + c_{i-1,j}}{(\Delta t)^2}\Big|\upsilon d\Omega + \frac{1}{2}D_2\int_{\sigma_{min}}^{\sigma_{max}} \sigma S_{max}^2\upsilon d\sigma, \quad \forall \upsilon \in H_0^1(\Omega).
\end{aligned} \tag{5.11}$$

Adopting the Galerkin finite element method as described on the previous Section 4.2, the problem stated may be reduced to

$$\mathbf{M}\dot{\mathbf{c}} + \mathbf{A}\mathbf{c} = \mathbf{F}, \quad \mathbf{c}(0) = c_0, \tag{5.12}$$

where

$$\begin{aligned}
\mathbf{M} &= \sum_{e=1}^{E}\int\int_{\Omega_e} \phi_j\phi_i d\Omega, \\
\mathbf{A} &= \sum_{e=1}^{E}\int\int_{\Omega_e} \Big[(-r + D_2\sigma)S\phi_{j_S}^{'}\phi_i + (-\alpha + \frac{1}{2}D_1)\sigma\phi_{j_\sigma}^{'}\phi_i + \frac{1}{2}D_2\sigma S^2\phi_{i_S}^{'}\phi_{j_S}^{'} \\
&\quad + \frac{1}{2}D_1\sigma^2\phi_{i_\sigma}^{'}\phi_{j_\sigma}^{'} + r\phi_j\phi_i\Big]d\Omega - \sum_{Be=1}^{BE}\int_{\partial\Omega_{4e}} \frac{1}{2}D_1\sigma_{max}^2\phi_{j_\sigma}^{'}\phi_i dS + \sum_{Be=1}^{BE}\int_{\partial\Omega_{2e}} \frac{1}{2}D_1\sigma_{min}^2\phi_{j_\sigma}^{'}\phi_i dS, \\
\mathbf{F} &= \sum_{e=1}^{E}\int\int_{\Omega_e} D_3S^2\Big|\frac{c_{i+1,j} - 2c_{i,j} + c_{i-1,j}}{(\Delta t)^2}\Big|\phi_i d\Omega + \sum_{Be=1}^{BE}\int_{\partial\Omega_{3e}} \frac{1}{2}D_2\sigma S_{max}^2\phi_i d\sigma.
\end{aligned}$$

Note that the second derivative term in the force term ($\mathbf{F}$) is discretised using Central Difference method.

For this finite element analysis, we use a structured triangular mesh which consists of 6 nodes per element as shown in Figure 5.1. The nodes allocation on each triangular element is shown as in Figure 5.2.

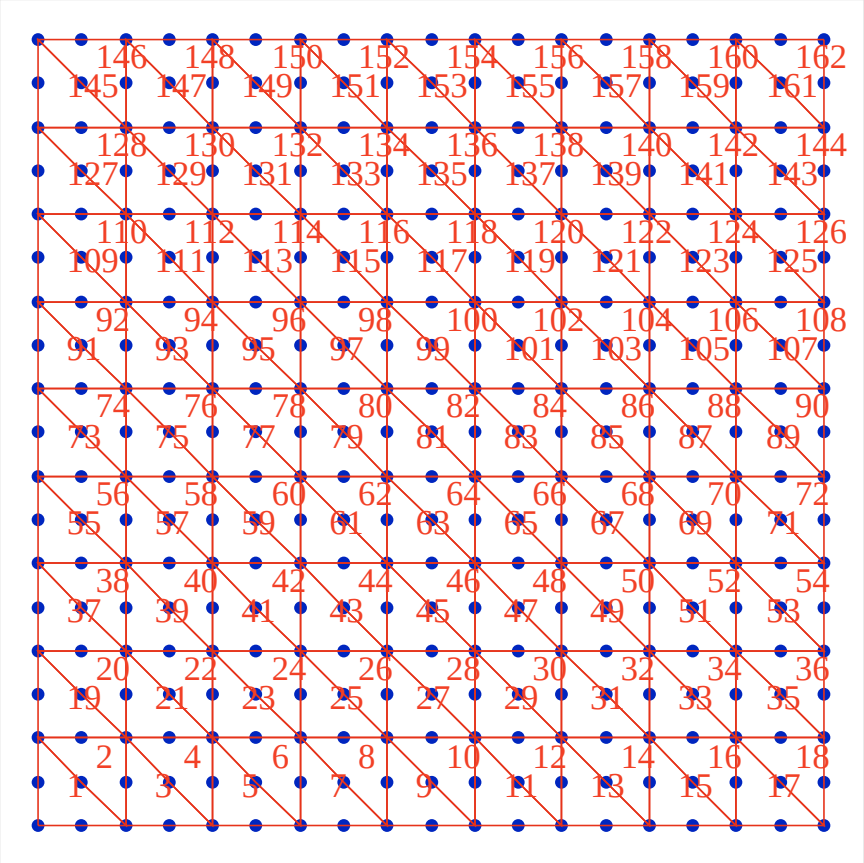

Figure 5.1: Triangular Mesh

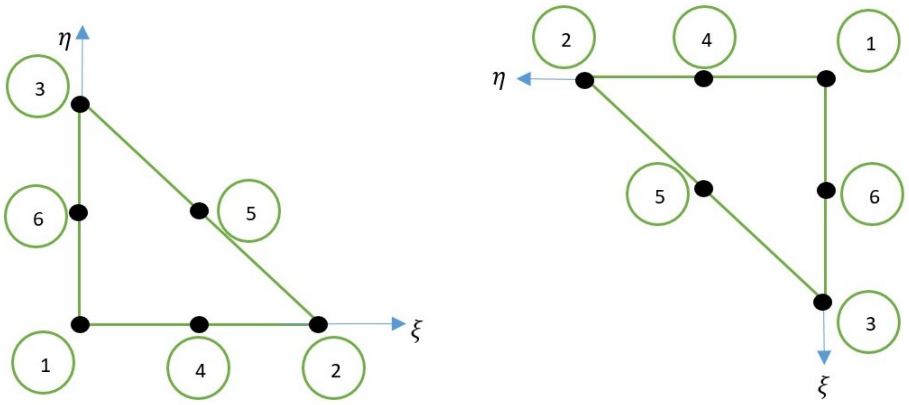

Figure 5.2: Nodes allocation

The six basis functions on reference to a standard triangle are

$$\begin{aligned} N_1(\xi,\eta) &= (1-\xi-\eta)(1-2\xi-2\eta), \\ N_2(\xi,\eta) &= \xi(2\xi-1), \\ N_3(\xi,\eta) &= \eta(2\eta-1), \\ N_4(\xi,\eta) &= 4\xi(1-\xi-\eta), \\ N_5(\xi,\eta) &= 4\xi\eta, \\ N_6(\xi,\eta) &= 4\eta(1-\xi-\eta). \end{aligned} \tag{5.13}$$

The numerical solution to PDE (5.1) is attained by solving the system of equation (5.12) using the backward Euler scheme, i.e.

$$\mathbf{M}\frac{\mathbf{c}^{n+1}-\mathbf{c}^{n}}{\Delta\tau}+\mathbf{A}\mathbf{c}^{n+1}=\mathbf{F}^{(n+1)}, \tag{5.14}$$

corresponding to $\mathbf{M}$, $\mathbf{A}$ and $\mathbf{F}$. Integration are performed on each triangular element by applying the Gaussian Quadrature of degree three.

5.3 Numerical results of the general stochastic volatility model

The same numerical analysis using backward Euler finite element method is performed on the non-linear PDE as of equation (5.1). In this case, the volatility is also stochastic, thus equation (5.1) depends on both share price and volatility. From the numerical analysis performed in Section 5.2, we are able to consider the additional parameters that arise from assuming the different models. The general stochastic volatility model may result in various types of models depending on the assumptions made specifically on γ, ε, H and H_1. Since we have validated the importance of transaction costs and trading days based on the general constant volatility model, we here use the same assumption of k. The effect of k and δt are the same in which k increases the value of call option price and we may adjust δt accordingly to compensate for the increase in costs. In the previous Section 4.2, we only assumed a constant volatility. However, in this chapter, we extend our analysis to the stochastic volatility model, thus the influence of the additional parameters ε, H_1, α and β comes into effect. Note that when we assume $\gamma = 1$, $H = 0.5$, $\varepsilon = 1$ and $H_1 = 0.5$, the general stochastic volatility model will reduce to the Hull-White PDE model with transaction costs as in equation (3.30).

Table 5.1: Values of model parameters for the general stochastic volatility model

S_t	σ_τ	r	K	k	δt	T	γ	ε	H	H_1	α	β
gBm	gBm	0.05	150	0.01	$\frac{30}{365}$	$\frac{92}{365}$	1	1	0.5	0.5	0.1	0.05
gBm	fBm	0.05	150	0.01	$\frac{30}{365}$	$\frac{92}{365}$	1	0	0.5	0.65	0.1	0.05
gBm	mfBm	0.05	150	0.01	$\frac{30}{365}$	$\frac{92}{365}$	1	0.5	0.5	0.65	0.1	0.05
fBm	gBm	0.05	150	0.01	$\frac{30}{365}$	$\frac{92}{365}$	0	1	0.55	0.5	0.1	0.05
fBm	fBm	0.05	150	0.01	$\frac{30}{365}$	$\frac{92}{365}$	0	0	0.55	0.65	0.1	0.05
fBm	mfBm	0.05	150	0.01	$\frac{30}{365}$	$\frac{92}{365}$	0	0.5	0.55	0.65	0.1	0.05
mfBm	gBm	0.05	150	0.01	$\frac{30}{365}$	$\frac{92}{365}$	0.5	1	0.55	0.5	0.1	0.05
mfBm	fBm	0.05	150	0.01	$\frac{30}{365}$	$\frac{92}{365}$	0.5	0	0.55	0.65	0.1	0.05
mfBm	mfBm	0.05	150	0.01	$\frac{30}{365}$	$\frac{92}{365}$	0.5	0.5	0.55	0.65	0.1	0.05

As previously discussed in Section 2.8, since there is a more apparent evidence of long memory in the absolute return, i.e. the volatility of stock return, it is reasonable to model long memory stochastic volatility. Ding *et al.* [82] and Comte *et al.* [27, 28] have also considered long memory stochastic volatility model assuming log-normal stock dynamic return. In this section, we will start by analysing the stochastic volatility model

assuming that S_t follows the geometric Brownian motion process and we will test for different diffusion processes of σ_τ. The analysis is later extended to different assumptions of stock dynamic processes which follows fBm and mfBm as well as various volatility diffusion processes.

5.3.1 S_t assumed geometric Brownian motion

Assuming that the share return still follows geometric Brownian motion, we analyse the effect of altering the volatility diffusion models. Note that in this case when the volatility model assumes the gBm process, the PDE of stochastic volatility model of equation (3.51) simplifies to the PDE of Hull-White model with transaction costs as discussed in Section 3.2. Mariani *et al.* [44, 45] constructed a PDE of an option pricing model which includes transaction costs and stochastic volatility with the assumptions of gBm for both stock return and volatility in which they are correlated. Numerical results have also been obtained from the derivation constructed by Mariani *et al.* [45]. However, the derivation method is slightly different and the resulting PDE in [45] does not have the $\frac{\partial c}{\partial \sigma}$ component. Comte *et al.* [27, 28] considered the possibility of long memory existence in the volatility by assuming a stock return diffusion process which follows gBm, and a volatility diffusion process which follows the fBm model. Comte and Renault [27] first took an approach using GARCH, but later further extended the discussion in terms of the affine processes [28]. They did not construct a PDE model of the option pricing model. In this thesis, we first compare the option pricing model with transaction costs by assuming log-normal (gBm) stock dynamic process, but for different assumptions of volatility diffusion processes.

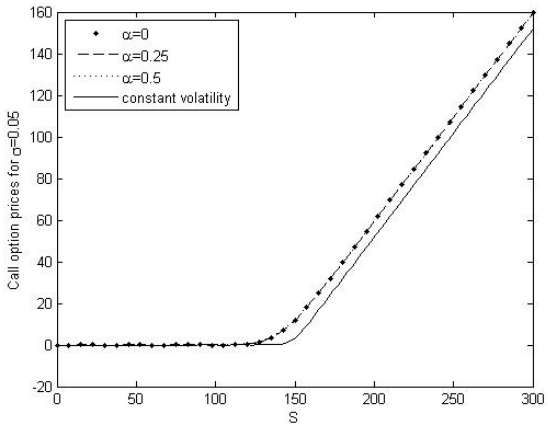

(a) $\sigma = 0.05$

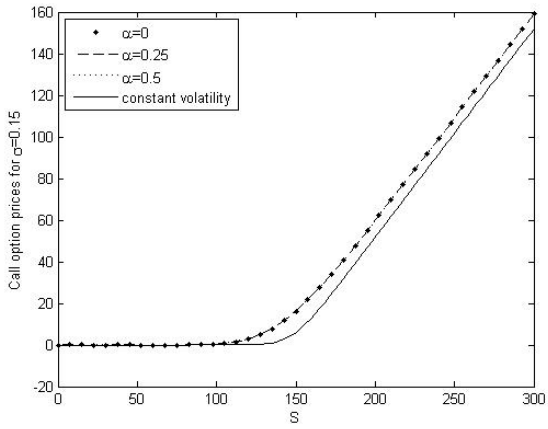

(b) $\sigma = 0.15$

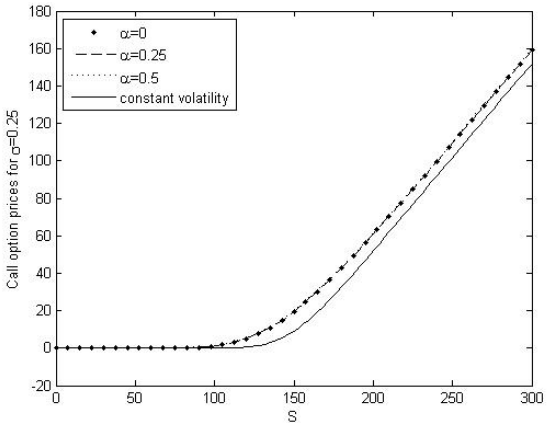

(c) $\sigma = 0.25$

Figure 5.3: The price of European call option price when S_t follows gBm with the parameter values given in Table 5.1 for different values of α at specific values of σ which follows gBm, i.e. $\varepsilon = 1$.

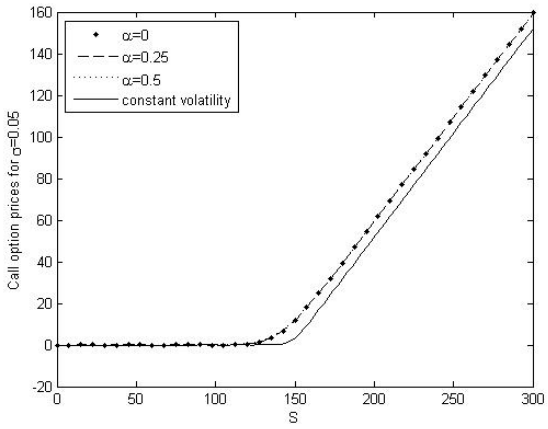

(a) $\sigma = 0.05$

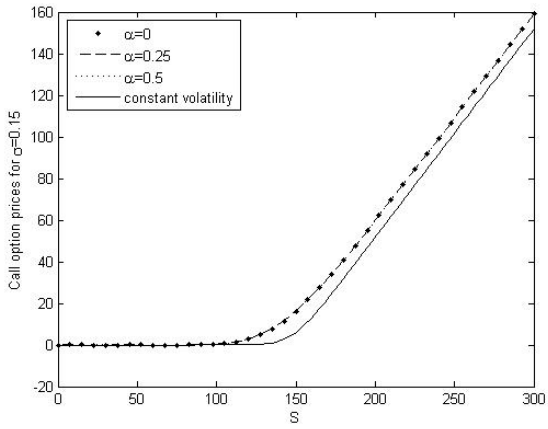

(b) $\sigma = 0.15$

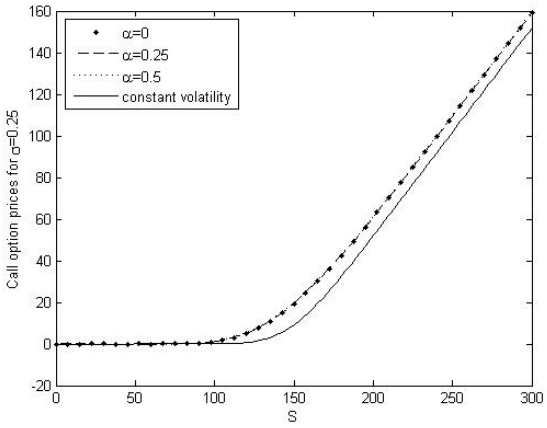

(c) $\sigma = 0.25$

Figure 5.4: The price of European call option price when S_t follows gBm with the parameter values given in Table 5.1 for different values of α at specific values of σ which follows fBm, i.e. $\varepsilon = 0$.

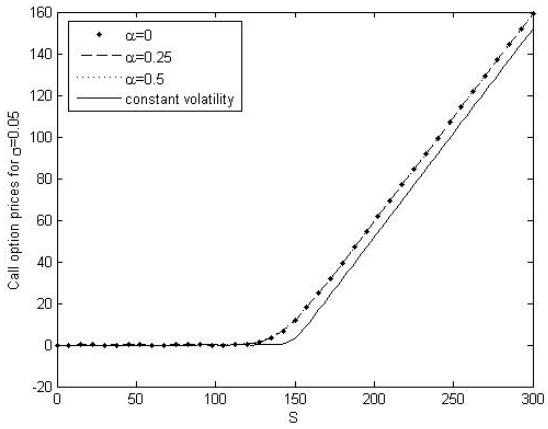

(a) $\sigma = 0.05$

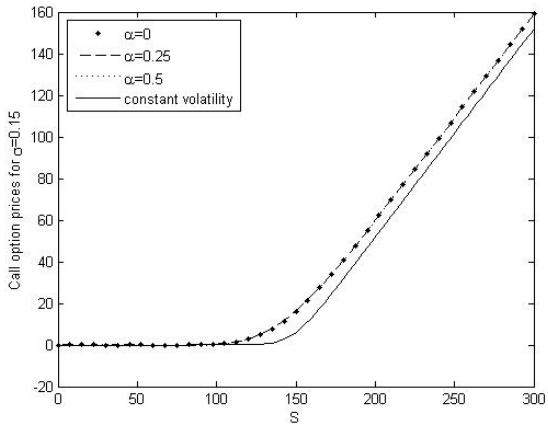

(b) $\sigma = 0.15$

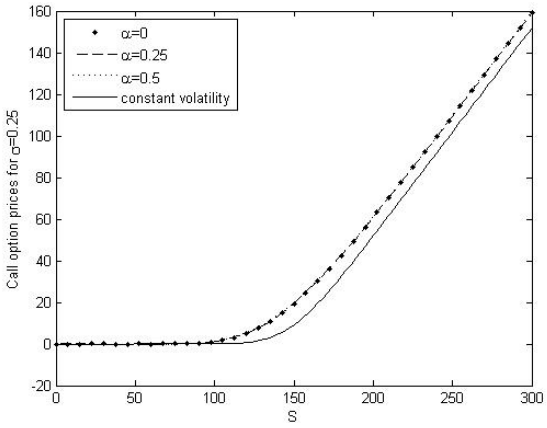

(c) $\sigma = 0.25$

Figure 5.5: The price of European call option price when S_t follows gBm with the parameter values given in Table 5.1 for different values of α at specific values of σ which follows mfBm, i.e. $\varepsilon = 0.5$.

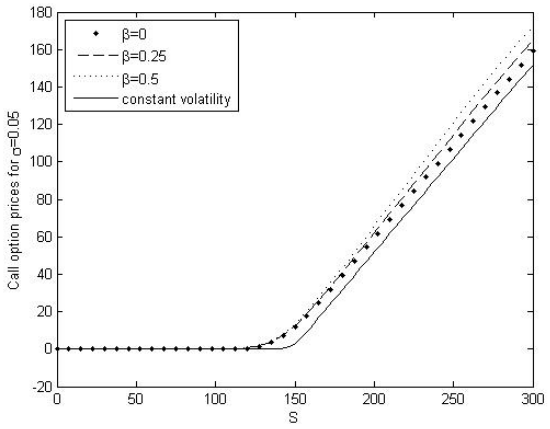

(a) $\sigma = 0.05$

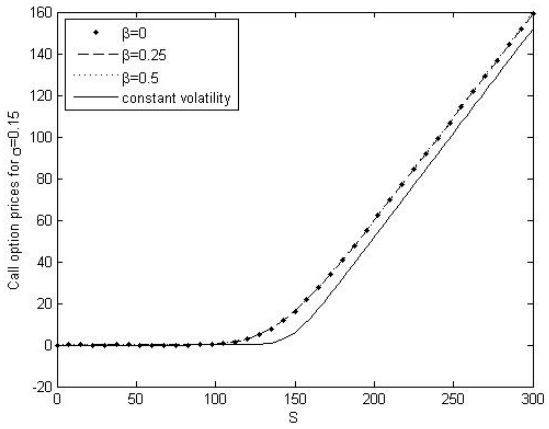

(b) $\sigma = 0.15$

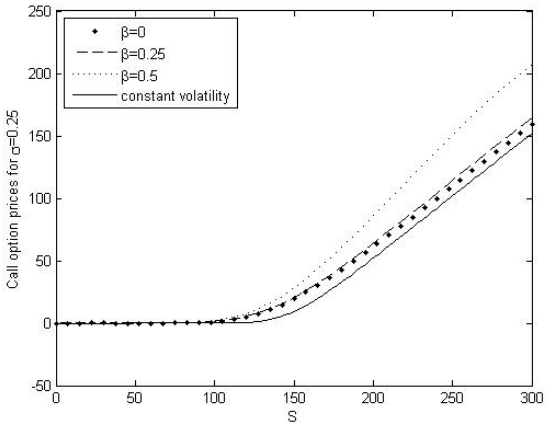

(c) $\sigma = 0.25$

Figure 5.6: The price of European call option price when S_t follows gBm with the parameter values given in Table 5.1 for different values of β at specific values of σ which follows gBm, i.e. $\varepsilon = 1$.

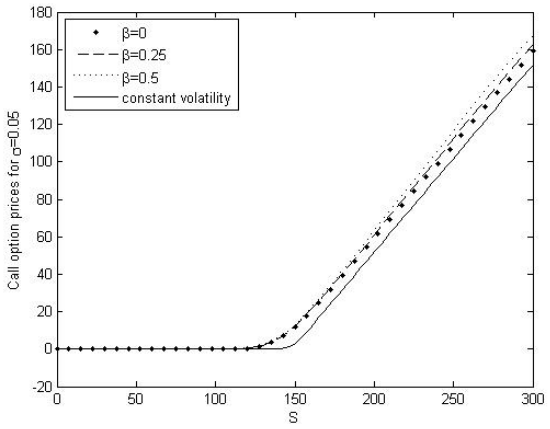

(a) $\sigma = 0.05$

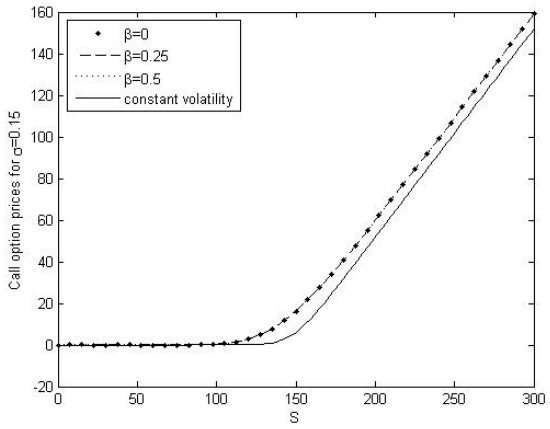

(b) $\sigma = 0.15$

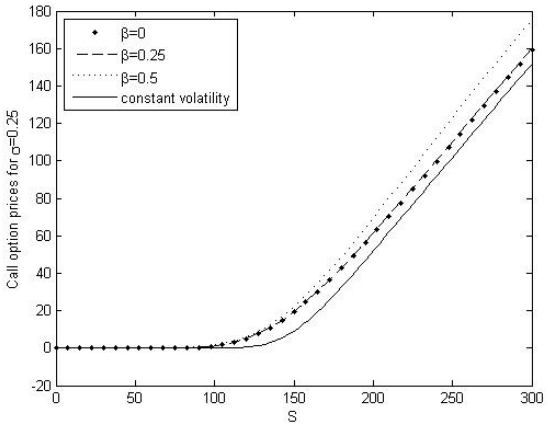

(c) $\sigma = 0.25$

Figure 5.7: The price of European call option price when S_t follows gBm with the parameter values given in Table 5.1 for different values of β at specific values of σ which follows fBm, i.e. $\varepsilon = 0$.

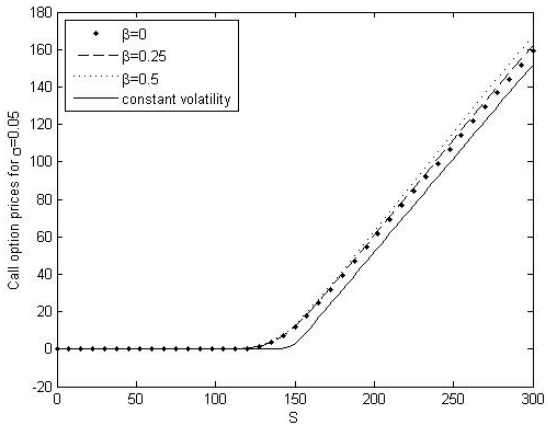

(a) $\sigma = 0.05$

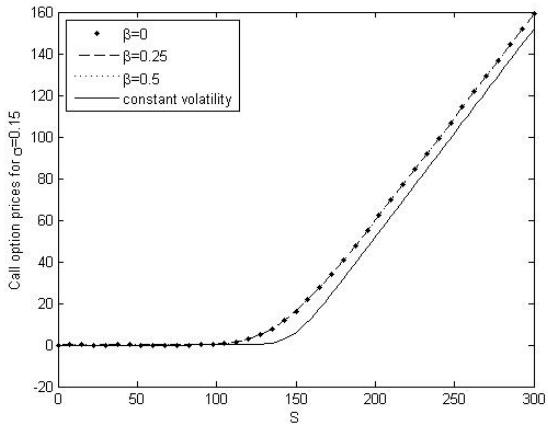

(b) $\sigma = 0.15$

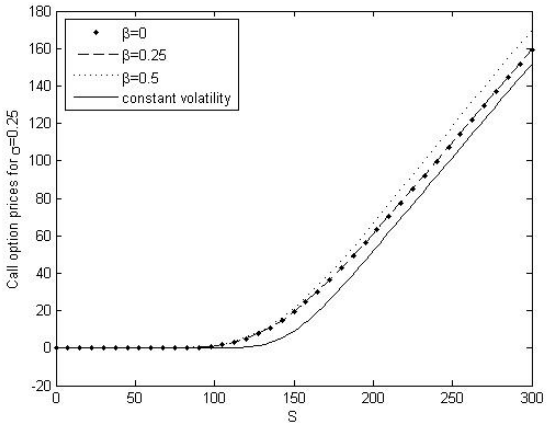

(c) $\sigma = 0.25$

Figure 5.8: The price of European call option price when S_t follows gBm with the parameter values given in Table 5.1 for different values of β at specific values of σ which follows mfBm, i.e. $\varepsilon = 0.5$.

The assumed volatility diffusion which is described by equation (3.32) depends on the parameter α, β, ε and H_1. The results show that there is a significant difference between assuming constant and stochastic volatility (Figures 5.3-5.8). By further comparing Figures 5.3-5.5 and Figures 5.6-5.8, it is apparent that the effect of increasing β is more significant compared to increasing α. The influence of $\alpha \in [0, 0.5]$ on the European call option price for different values of σ is insignificant. On the other hand, the effect of β is significant, particularly for $\sigma = 0.25$, although this is not true when $\sigma = 0.15$. There is also a general trend that increasing β increases the value of European call option price for high values of S (Figures 5.6-5.8). When assuming different assumptions of the volatility diffusion processes, the effect of increasing β on the call option price diminishes from assuming gBm, fBm and mfBm respectively. This trend is apparent by comparing Figures

5.6-5.8, particularly for $\sigma = 0.25$ where the influence of β is the most obvious.

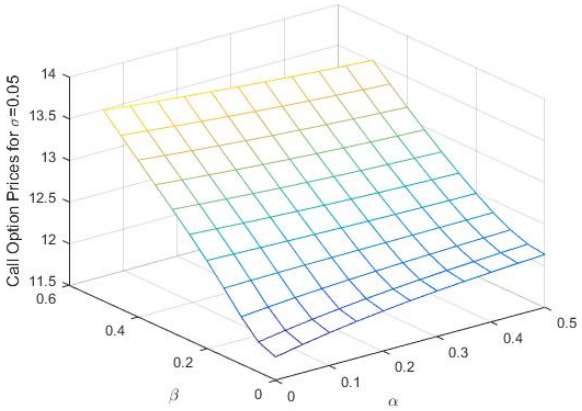

(a) $\sigma = 0.05$

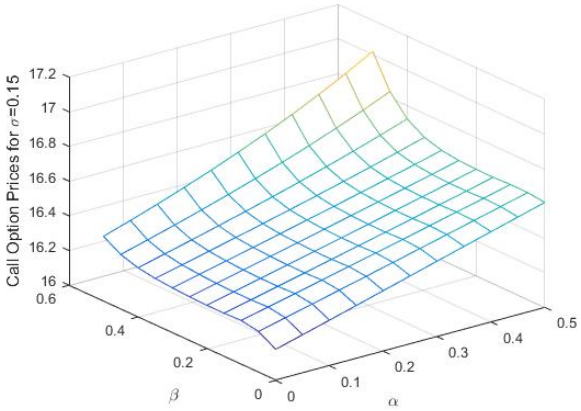

(b) $\sigma = 0.15$

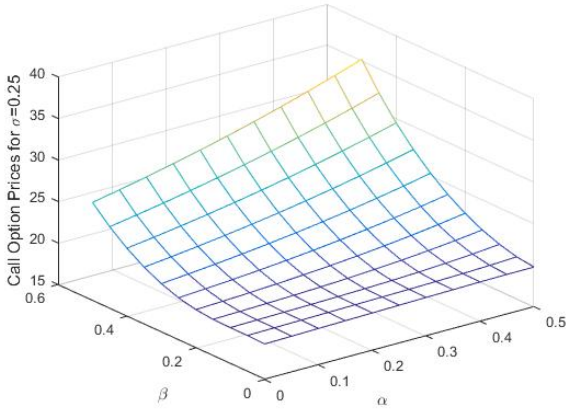

(c) $\sigma = 0.25$

Figure 5.9: The price of at-the-money ($S = K = 150$) European call option price when S_t follows gBm with the parameter values given in Table 5.1 for a range of α and β values assuming that σ follows gBm, i.e. $\varepsilon = 1$.

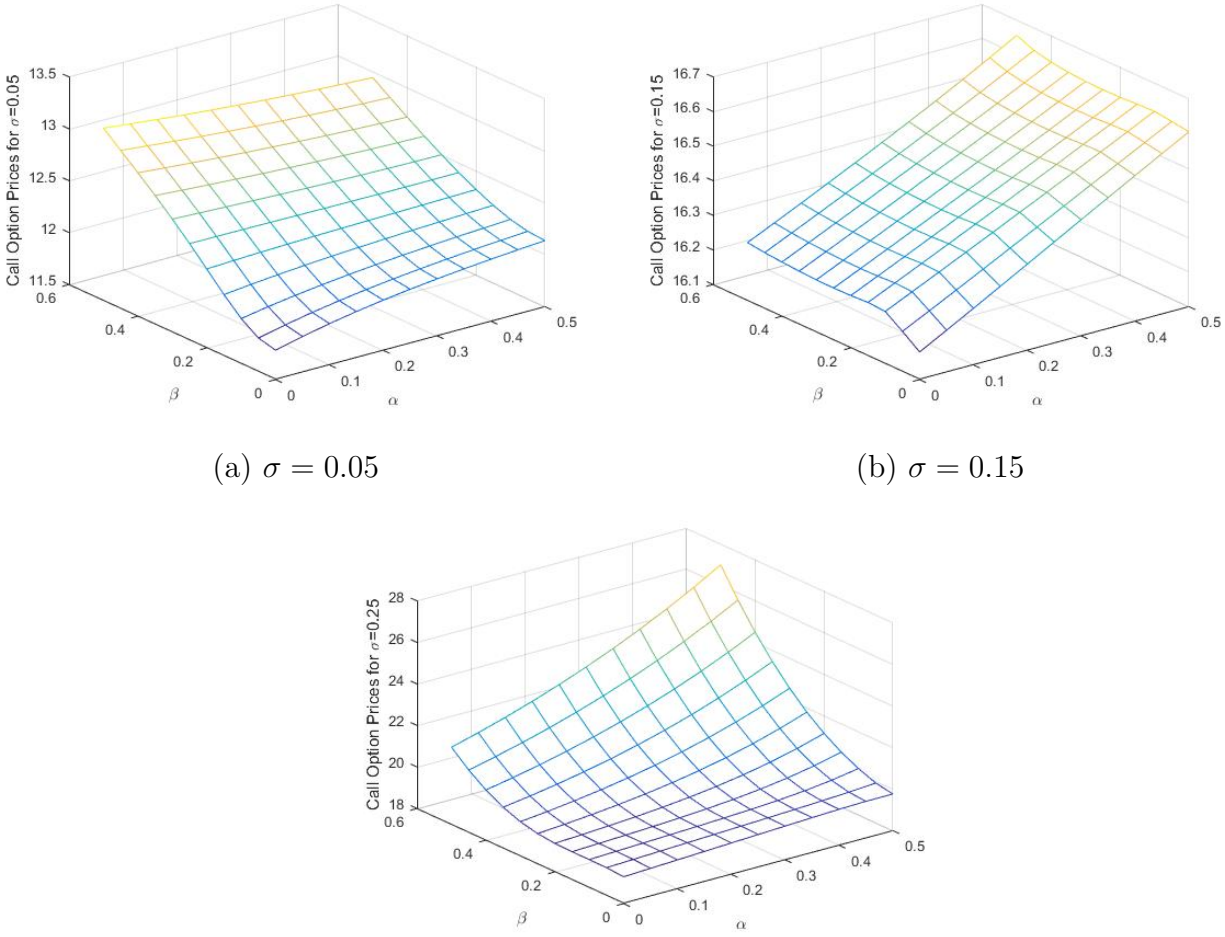

(a) $\sigma = 0.05$

(b) $\sigma = 0.15$

(c) $\sigma = 0.25$

Figure 5.10: The price of at-the-money ($S = K = 150$) European call option price when S_t follows gBm with the parameter values given in Table 5.1 for a range of α and β values assuming that σ follows fBm, i.e. $\varepsilon = 0, H_1 = 0.65$.

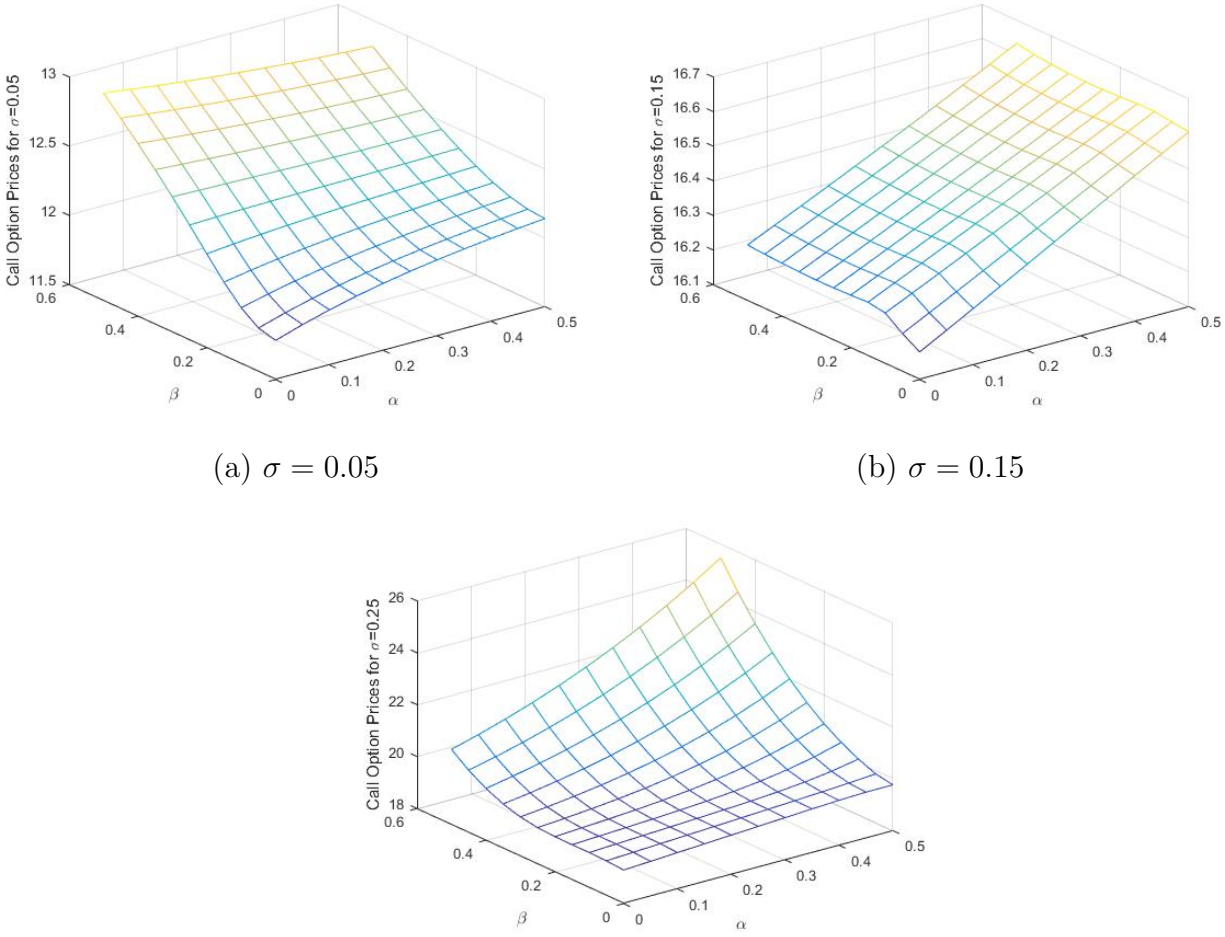

(a) $\sigma = 0.05$

(b) $\sigma = 0.15$

(c) $\sigma = 0.25$

Figure 5.11: The price of at-the-money ($S = K = 150$) European call option price when S_t follows gBm with the parameter values in Table 5.1 for a range of α and β values assuming that σ follows mfBm, i.e. $\varepsilon = 0.5, H_1 = 0.65$.

We next analyse the influence of both α and β on the call option price at $S = K = 150$. By analysing Figures 5.9-5.11 part (a) and (c), it is apparent that the effect of increasing β is greater than the effect of increasing α. This applies for all three assumptions of volatility diffusion processes. However, for $\sigma = 0.25$, from Figures 5.9-5.11 part (c), the increase in call option price is more significant compared to part (a), shown from the range of values of call option price as well as the steep surface curve. The same result is also visible by comparing Figures 5.6-5.8 parts (a) and (c), as previously described above. However, the effects of α and β on the call option price when $\sigma = 0.15$ are not as significant as when $\sigma = 0.05$ and $\sigma = 0.25$ (Figures 5.9-5.11 part (b)). This trend is applicable to all the three considered volatility diffusion processes (gBm, fBm and mfBm). For $\sigma = 0.25$, the price of European call option increases significantly for higher values of α and β, as shown

by the curve feature in Figures 5.9-5.11 part (c). From comparing all the three assumed volatility diffusion processes, the values of call option price assuming the mfBm volatility diffusion process are the lowest for $\alpha \in [0, 0.5]$ and $\beta \in [0, 0.5]$, followed by the fBm and the gBm (Figure 5.9-Figure 5.11).

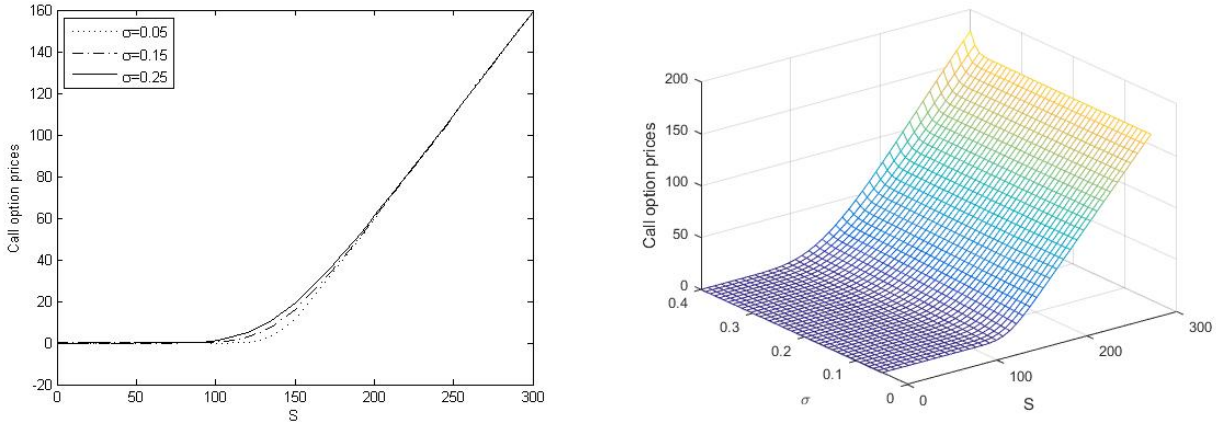

(a) σ_τ assumed gBm

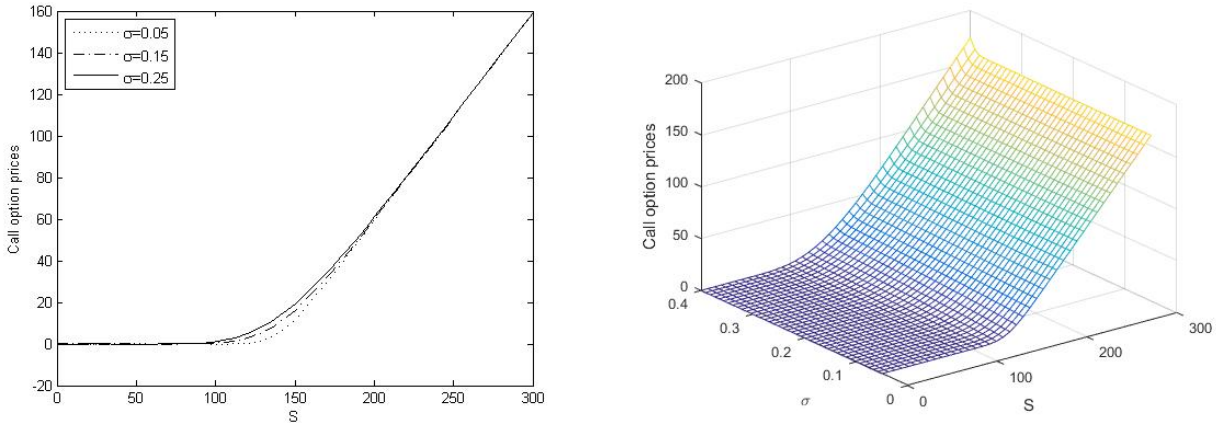

(b) σ_τ assumed fBm

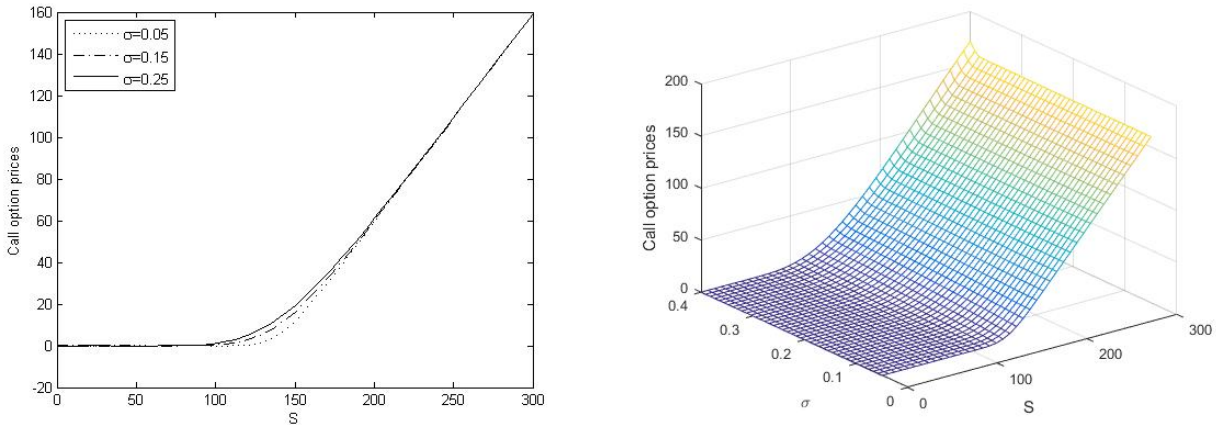

(c) σ_τ assumed mfBm

Figure 5.12: The effect of different values of σ on the European call option price over a range of S values for three different assumptions of the volatility diffusion process as stated in Table 5.1 assuming S_t follows the gBm model.

It is apparent that whatever the assumed volatility diffusion is, σ changes and may take different values unlike the model discussed in Section 4.3 with constant σ (Figure 5.12). Using the PDE (3.51), we compare the effect of using the stochastic volatility model against a constant volatility model. The results are also consistent with Figures 5.3-5.8 for any different values of α and β. We can see that there is no significant difference between using the three volatility diffusion assumptions (Figure 5.13), as reinforced in Figure 5.14. However, we know from Figures 5.3-5.11 that as α and β increase, so does the price of European call option. Thus, we want to further analyse the effect of ε and H_1 on European call option for different combination parameter values of α and β.

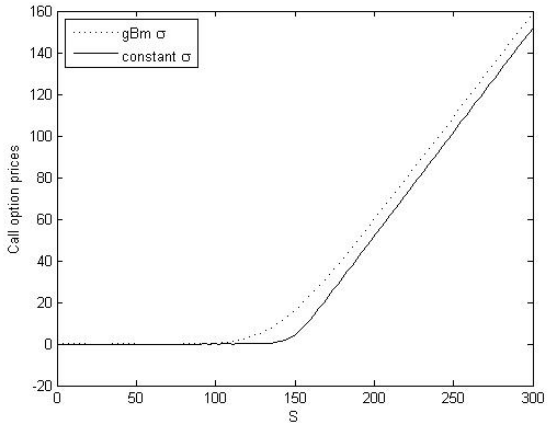

(a) gBm

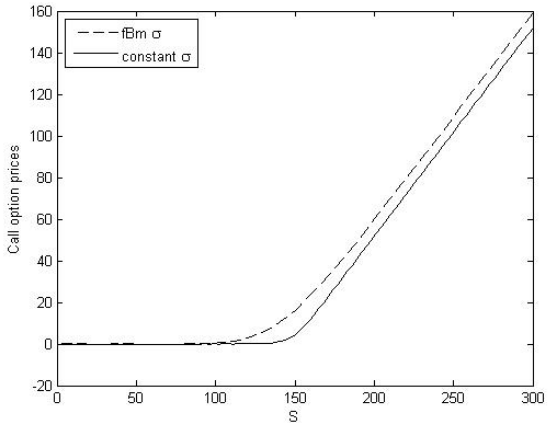

(b) fBm

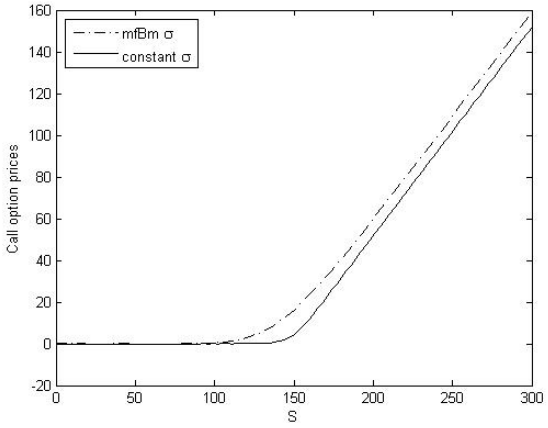

(c) mfBm

Figure 5.13: The comparison of European call option price when using constant volatility and stochastic volatility with three different assumptions of the volatility diffusion processes for $\sigma = 0.15$.

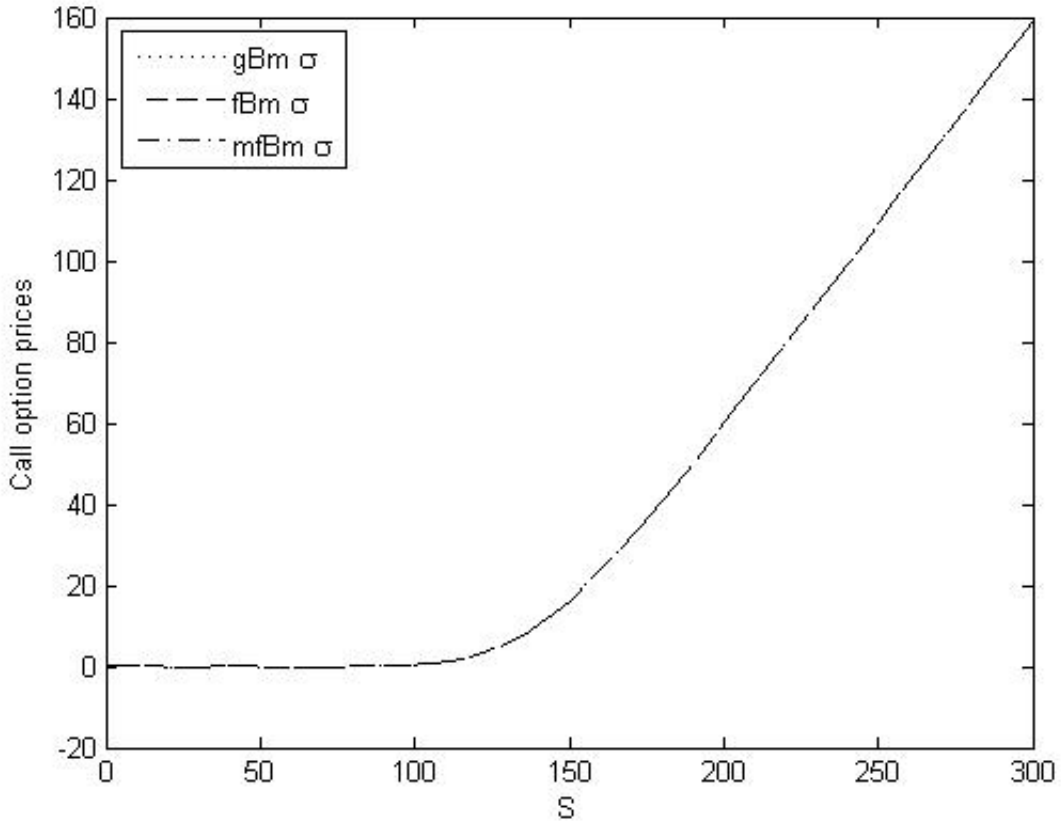

Figure 5.14: The European call option price assuming S_t follows gBm and three different types of volatility diffusion processes using the chosen parameters in Table 5.1.

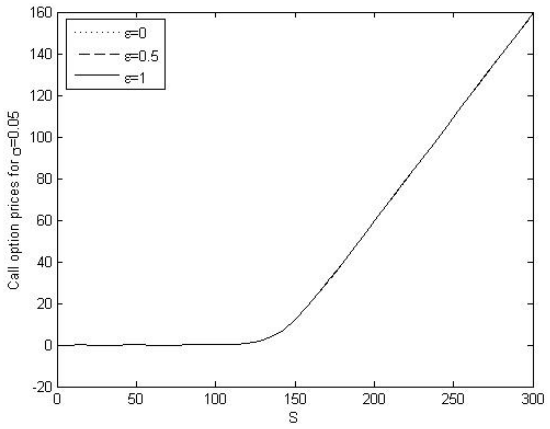

(a) $\sigma = 0.05$

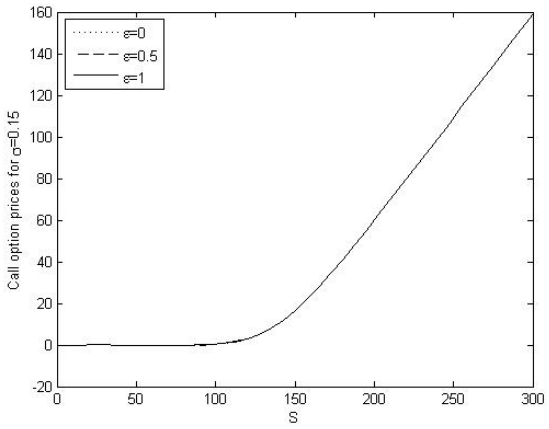

(b) $\sigma = 0.15$

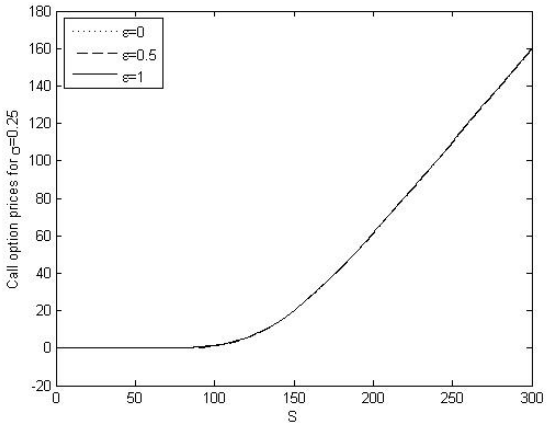

(c) $\sigma = 0.25$

Figure 5.15: The effect of ε on European call option price for different values of σ assuming S_t follows gBm and other chosen parameters in Table 5.1, except altering $\alpha = 0.5$.

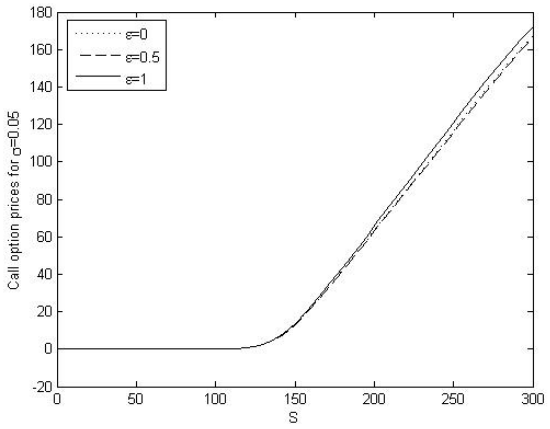

(a) $\sigma = 0.05$

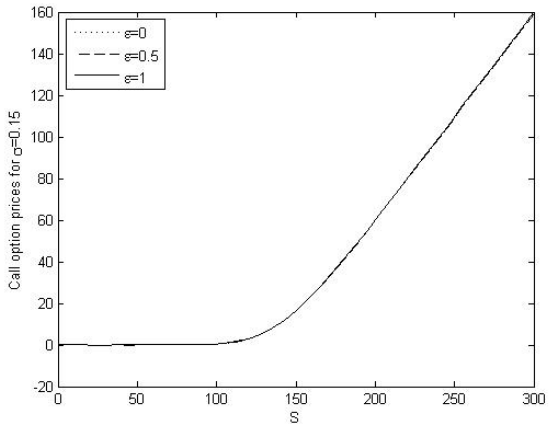

(b) $\sigma = 0.15$

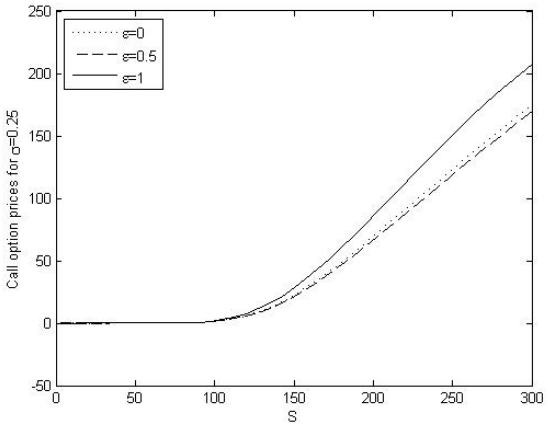

(c) $\sigma = 0.25$

Figure 5.16: The effect of ε on European call option price for different values of σ assuming S_t follows gBm and other chosen parameters in Table 5.1, except altering $\beta = 0.5$.

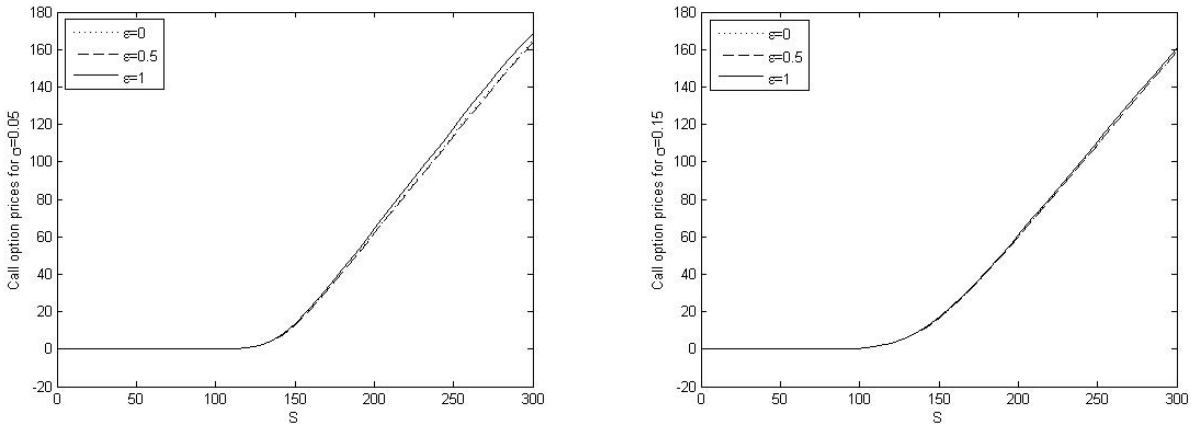

(a) $\sigma = 0.05$ (b) $\sigma = 0.15$

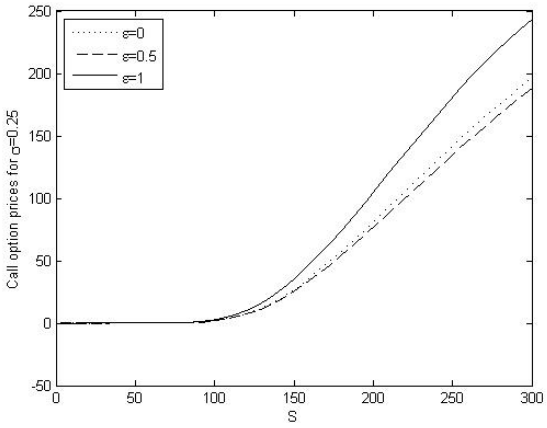

(c) $\sigma = 0.25$

Figure 5.17: The effect of ε on European call option price for different values of σ assuming S_t follows gBm and other chosen parameters in Table 5.1, except altering $\alpha = \beta = 0.5$.

We have shown that by using parameters $\alpha = 0.1$ and $\beta = 0.05$, there is no apparent change in assuming the three different volatility diffusion processes (Figure 5.14). Therefore, we want to first analyse the effect of ε for different combinations of α and β values. Figure 5.15 reinforces the previous results that the effect of increasing α is not significant. On the other hand, high value of β enhances the effect of ε on the call option price, as shown in Figure 5.16. The results show that the effect of ε when $\sigma = 0.15$ is negligible, but not when $\sigma = 0.05$ and $\sigma = 0.25$. The results also show that there are significant difference between assuming gBm ($\varepsilon = 1$) and fBm ($\varepsilon = 0$) when β is high, particularly for high value of $\sigma = 0.25$ and only slightly between fBm and mfBm. These differences are enhanced when assuming high values of α and β (Figure 5.17). It is apparent that when $\varepsilon = 0.5$, the value of call option price for high range of S values is lower compared to when assuming $\varepsilon = 1$ or $\varepsilon = 0$. Thus, assuming the gBm volatility diffusion process would result

in a larger value of call option price for high range of S values compared to fBm and mfBm.

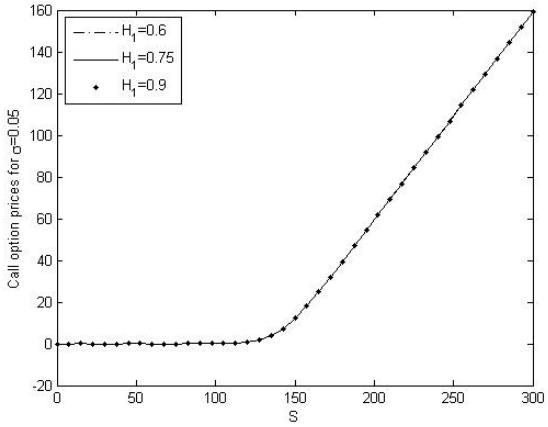

(a) $\sigma = 0.05$

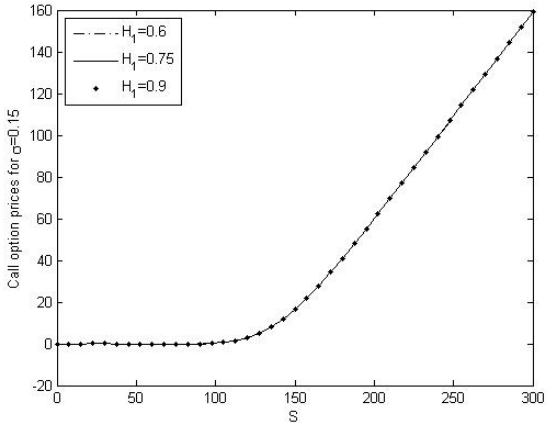

(b) $\sigma = 0.15$

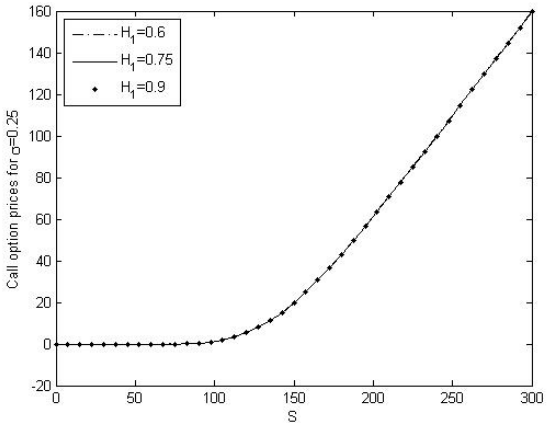

(c) $\sigma = 0.25$

Figure 5.18: The effect of H_1 on European call option price for different values of σ assuming S_t follows gBm and other chosen parameters in Table 5.1, except altering $\alpha = 0.5$.

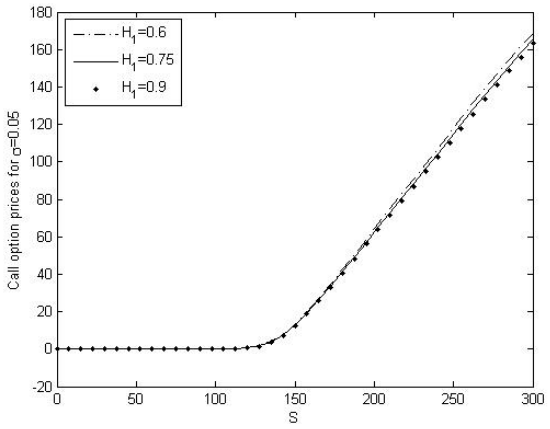

(a) $\sigma = 0.05$

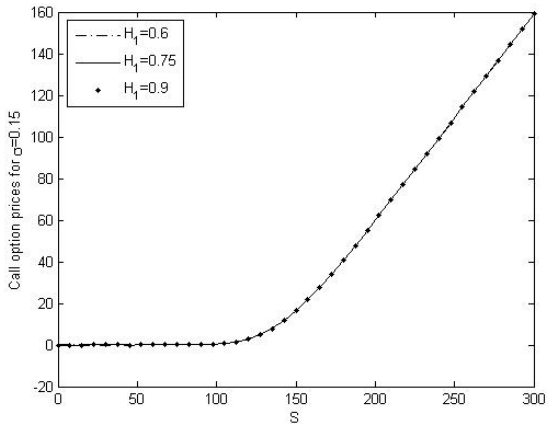

(b) $\sigma = 0.15$

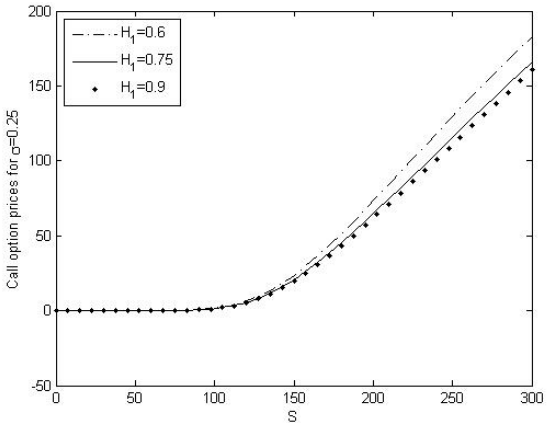

(c) $\sigma = 0.25$

Figure 5.19: The effect of H_1 on European call option price for different values of σ assuming S_t follows gBm and other chosen parameters in Table 5.1, except altering $\beta = 0.5$.

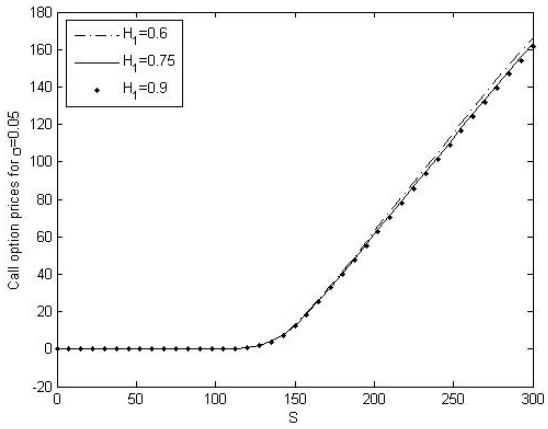

(a) $\sigma = 0.05$

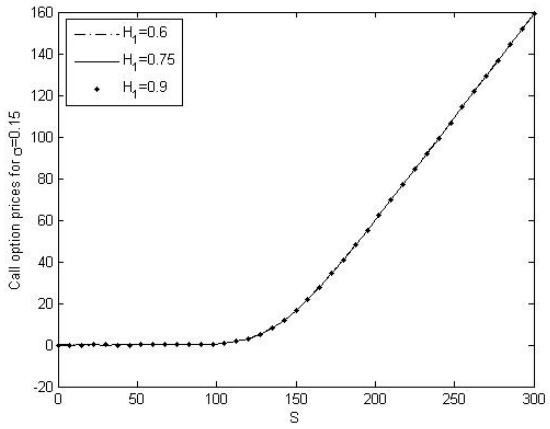

(b) $\sigma = 0.15$

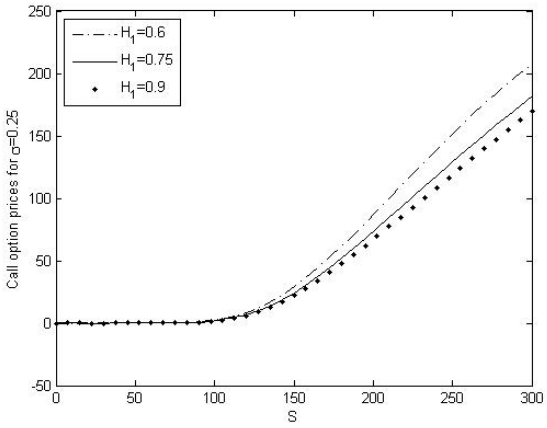

(c) $\sigma = 0.25$

Figure 5.20: The effect of H_1 on European call option price for different values of σ assuming S_t follows gBm and other chosen parameters in Table 5.1, except altering $\alpha = \beta = 0.5$.

Similar to the results above, the influence of H_1 becomes more apparent for greater values of β rather than α, also more when both α and β are high (Figures 5.18-5.20). The results show that the higher the Hurst parameter (H_1) in the volatility diffusion process, the lower is the call option price for large values of share price. However, this effect is not as significant for $\sigma = 0.15$, as shown in part (b) of Figures 5.18-5.20.

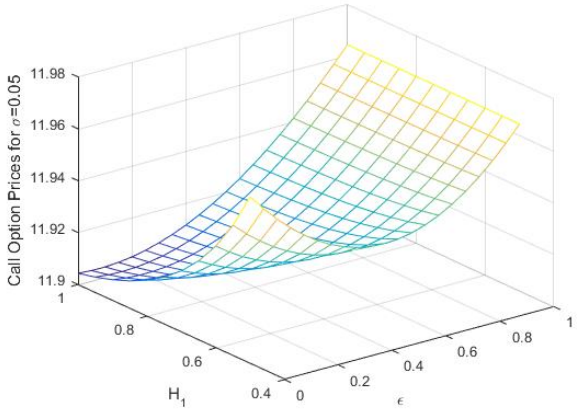

(a) $\sigma = 0.05$

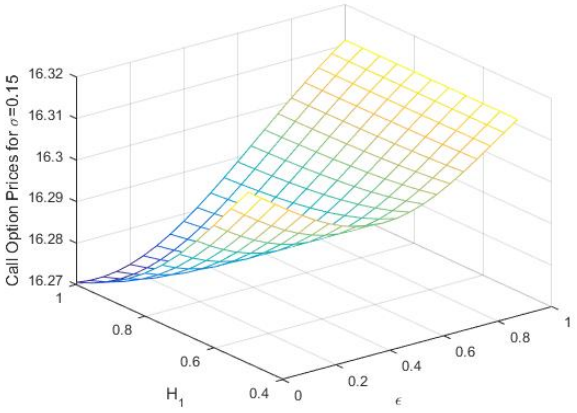

(b) $\sigma = 0.15$

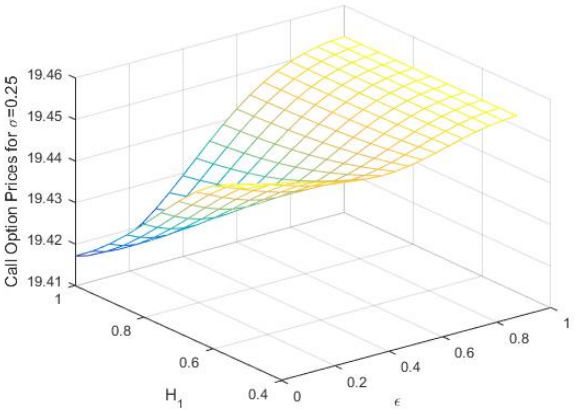

(c) $\sigma = 0.25$

Figure 5.21: The effect of ε and H_1 on European call option price for different values of σ assuming $S = K = 150$ and other chosen parameters in Table 5.1 when S_t follows gBm.

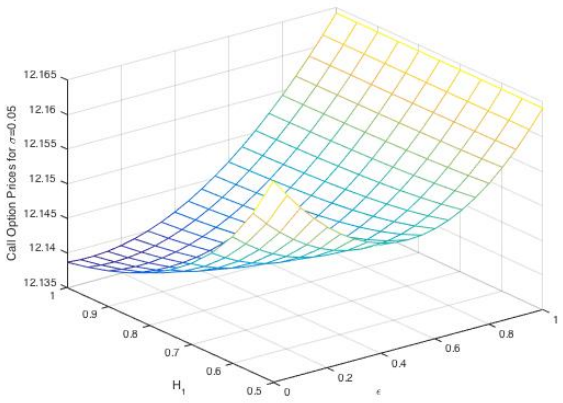

(a) $\sigma = 0.05$

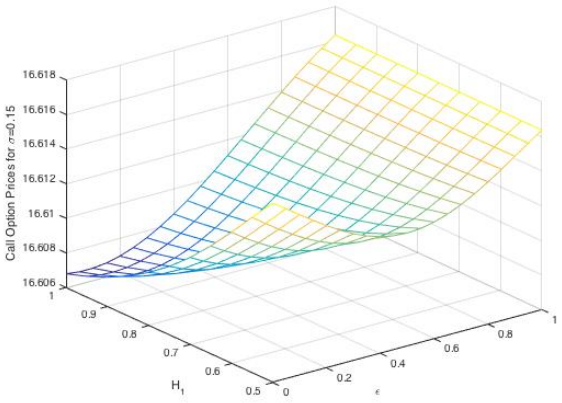

(b) $\sigma = 0.15$

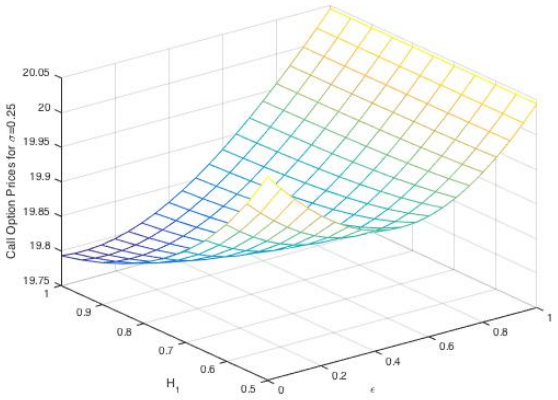

(c) $\sigma = 0.25$

Figure 5.22: The effect of ε and H_1 on European call option price for different values of σ assuming $S = K = 150$, $\alpha = 0.5$ and other chosen parameters in Table 5.1 when S_t follows gBm.

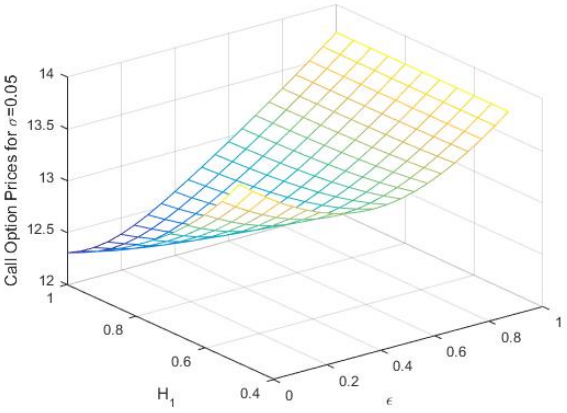

(a) $\sigma = 0.05$

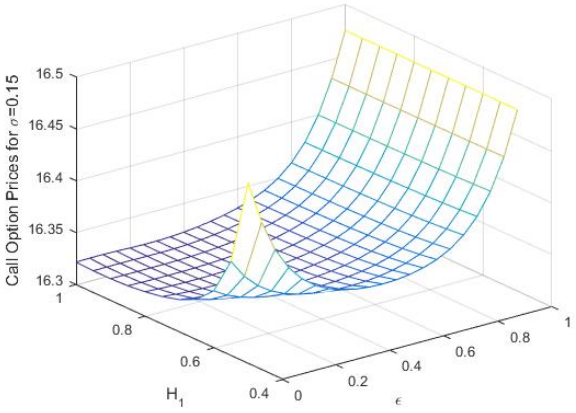

(b) $\sigma = 0.15$

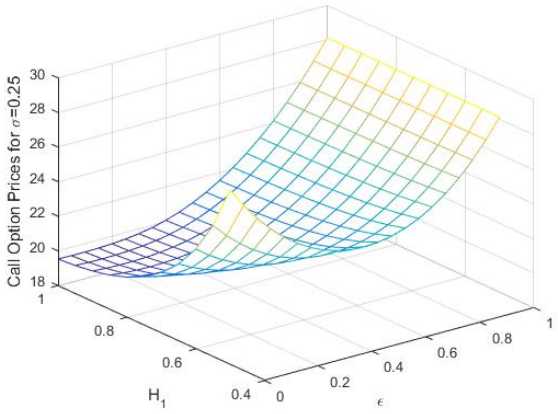

(c) $\sigma = 0.25$

Figure 5.23: The effect of ε and H_1 on European call option price for different values of σ assuming $S = K = 150$, $\beta = 0.5$ and other chosen parameters in Table 5.1 when S_t follows gBm.

We further analyse the relationship between ε and H_1 on the European call option price. Although ε and H_1 have influenced on the European call price, the difference in value is insignificant (Figure 5.21). The difference become greater as β increases, but not so much when α increases, as previously concluded. The relationship between H_1 and ε is similar to the ones between γ and H in Section 4.3.2. The results also show that greater value of β increases the steepness of curve at low value of ε (Figures 5.21-5.24). For greater value of $\sigma = 0.25$, the difference also becomes more significant, but not when $\sigma = 0.15$. These results are also consistent with Figures 5.9-5.11 which show the relationships between α, β and their effects on the call option price.

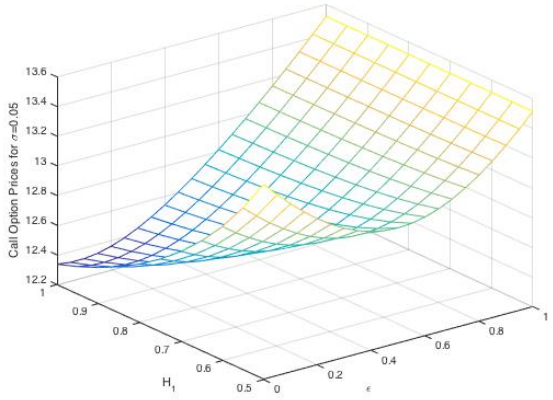

(a) $\sigma = 0.05$

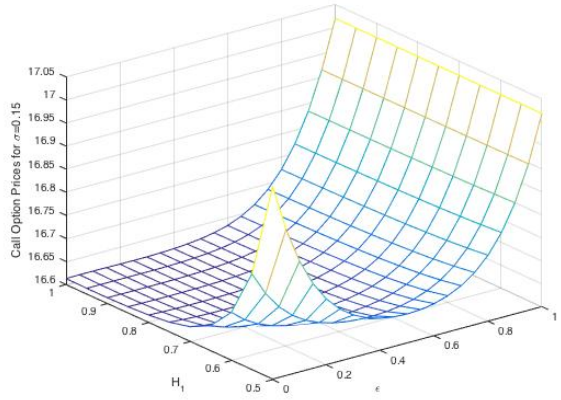

(b) $\sigma = 0.15$

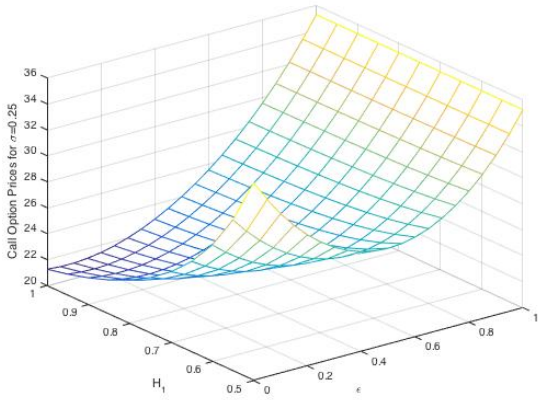

(c) $\sigma = 0.25$

Figure 5.24: The effect of ε and H_1 on European call option price for different values of σ assuming $S = K = 150$, $\alpha = \beta = 0.5$ and other chosen parameters in Table 5.1 when S_t follows gBm.

From analysing the different parameters of the stochastic volatility model which assumed gBm stock return dynamic and different volatility diffusion processes, it is obvious that the parameters α and β play a more significant role compared to ε and H_1. The influences of ε and H_1 are also dependent on how high the values of α and β are, particularly β. Thus, the decisions on whether to assume gBm, fBm or mfBm as the volatility diffusion processes in this stochastic volatility model, hugely depend on the values of α and β.

5.3.2 S_t assumed fractional Brownian motion

As previously mentioned in Section 2.8, Wang *et al.* [74] has introduced a fractional long memory stochastic volatility model with transaction costs which assumes fBm for both stock return and volatility. In this thesis, we will again numerically analyse the effect of considering stochastic volatility model which assumes fBm stock return and other possible volatility diffusion assumptions as detailed in Table 5.1.

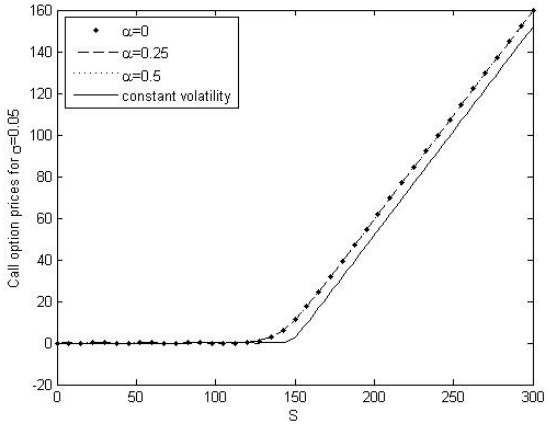

(a) $\sigma = 0.05$

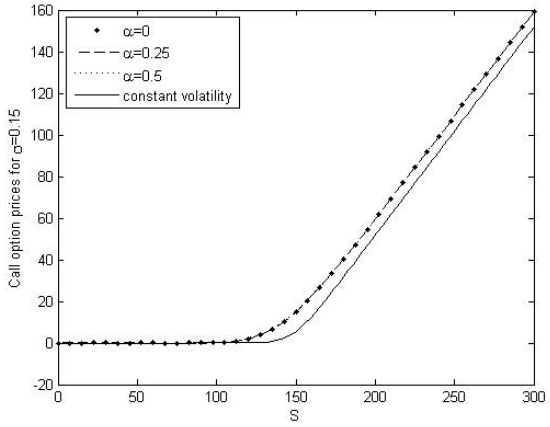

(b) $\sigma = 0.15$

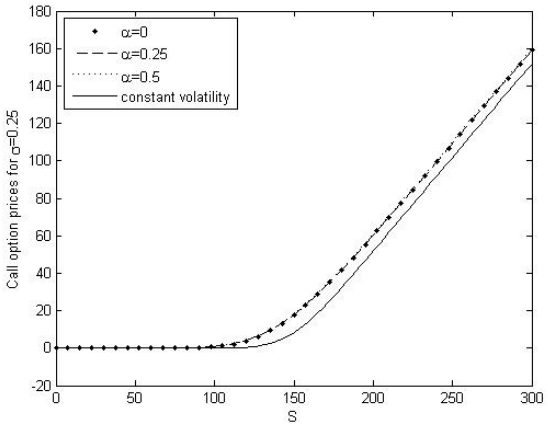

(c) $\sigma = 0.25$

Figure 5.25: The price of European call option price based on the given parameters in Table 5.1 for different values of α at specific values of σ which follows gBm, i.e. $\varepsilon = 1$ and S_t which follows fBm.

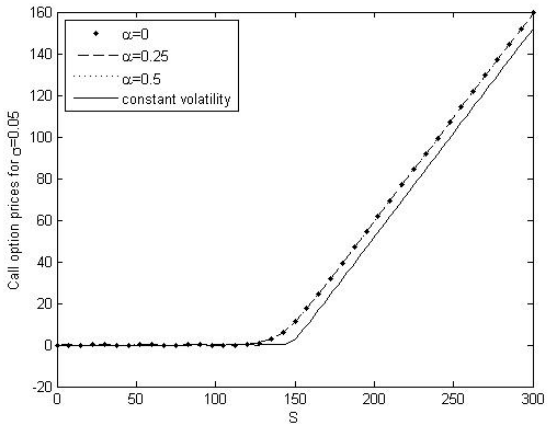

(a) $\sigma = 0.05$

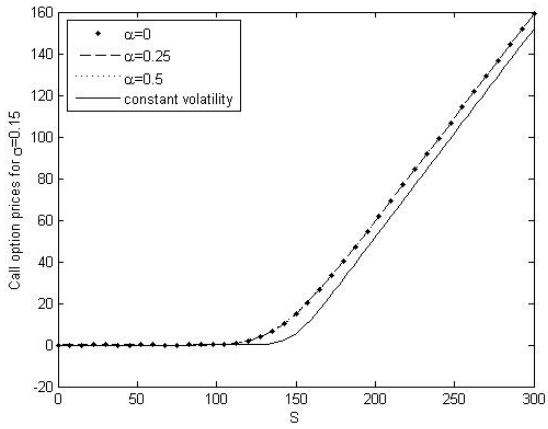

(b) $\sigma = 0.15$

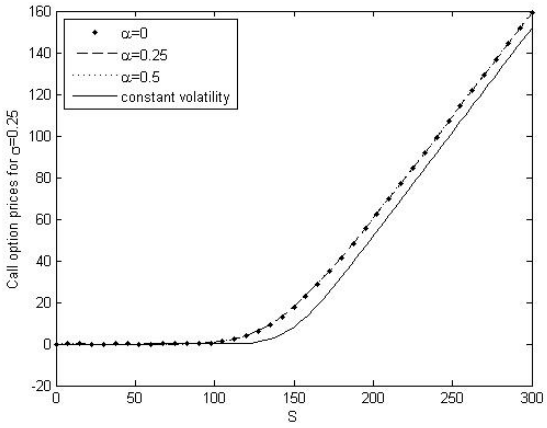

(c) $\sigma = 0.25$

Figure 5.26: The price of European call option price based on the given parameters in Table 5.1 for different values of α at specific values of σ which follows fBm, i.e. $\varepsilon = 0$ and S_t which follows fBm.

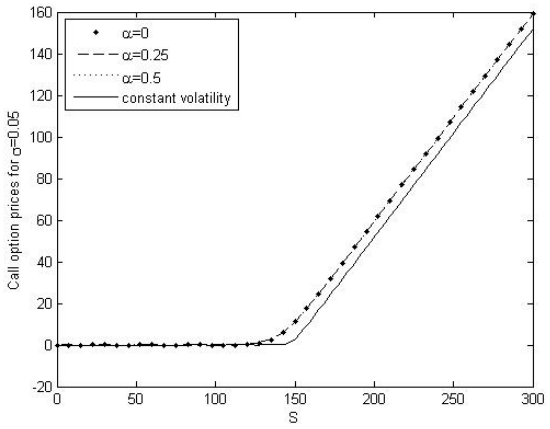

(a) $\sigma = 0.05$

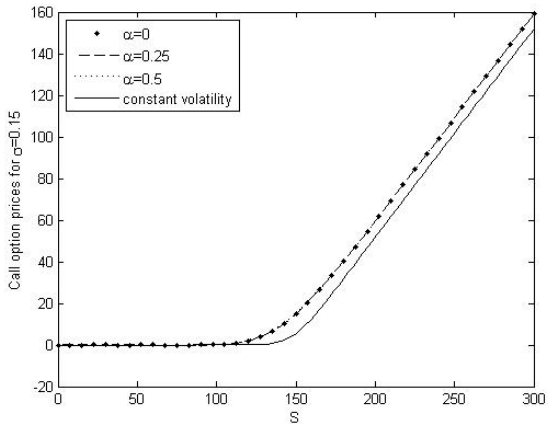

(b) $\sigma = 0.15$

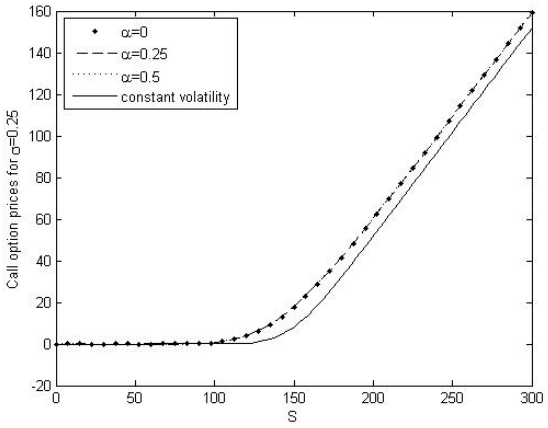

(c) $\sigma = 0.25$

Figure 5.27: The price of European call option price based on the given parameters in Table 5.1 for different values of α at specific values of σ which follows mfBm, i.e. $\varepsilon = 0.5$ and S_t which follows fBm.

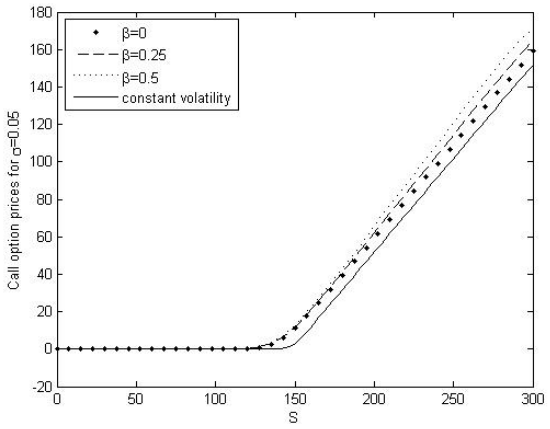

(a) $\sigma = 0.05$

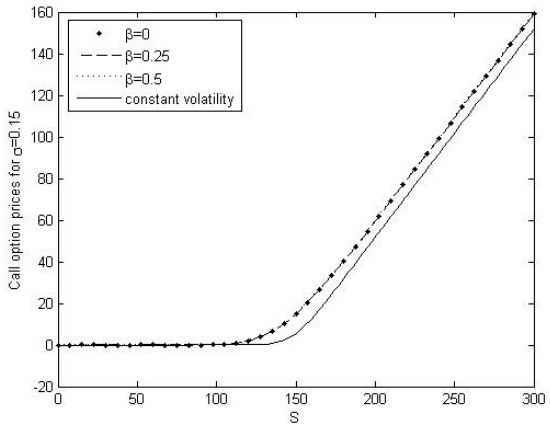

(b) $\sigma = 0.15$

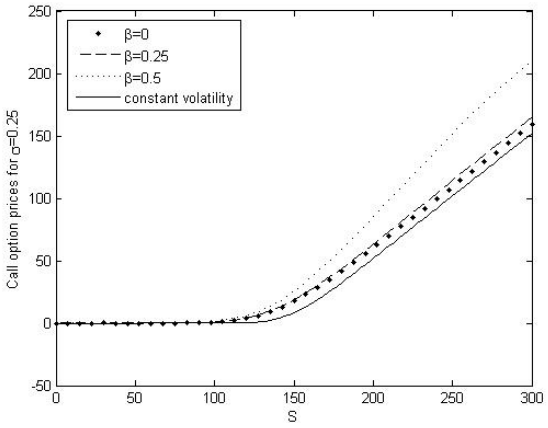

(c) $\sigma = 0.25$

Figure 5.28: The price of European call option price based on the given parameters in Table 5.1 for different values of β at specific values of σ which follows gBm, i.e. $\varepsilon = 1$ and S_t which follows fBm.

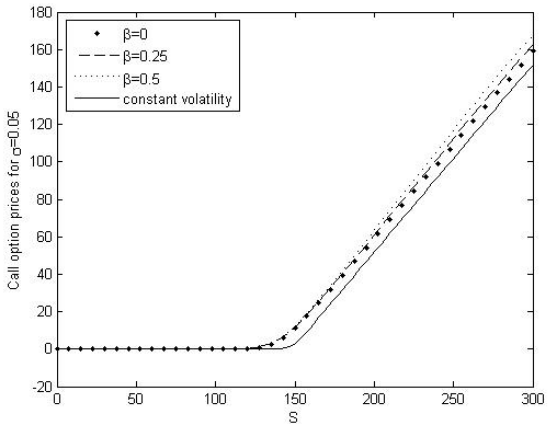

(a) $\sigma = 0.05$

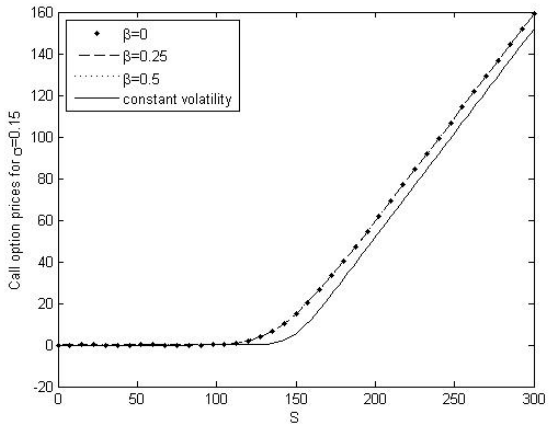

(b) $\sigma = 0.15$

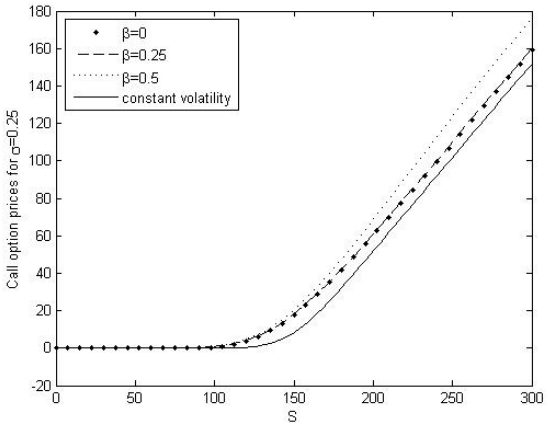

(c) $\sigma = 0.25$

Figure 5.29: The price of European call option price based on the given parameters in Table 5.1 for different values of β at specific values of σ which follows fBm, i.e. $\varepsilon = 0$ and S_t which follows fBm.

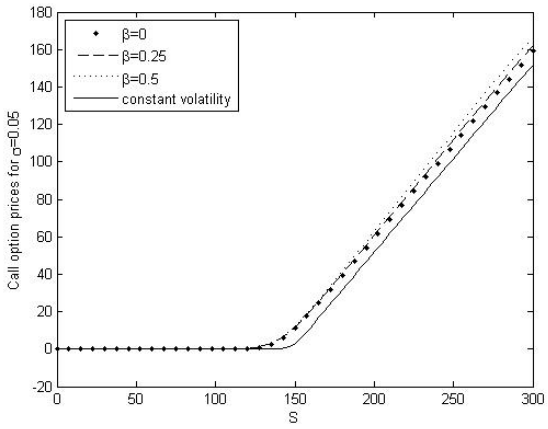

(a) $\sigma = 0.05$

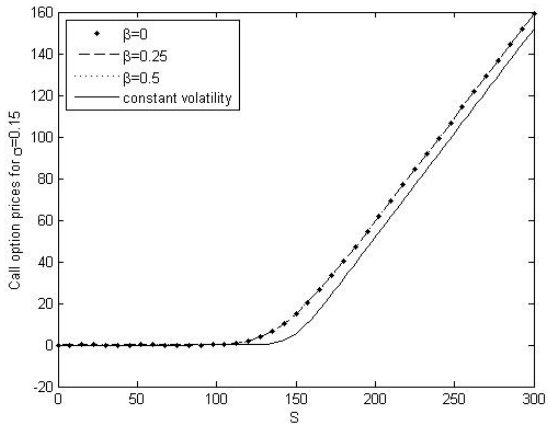

(b) $\sigma = 0.15$

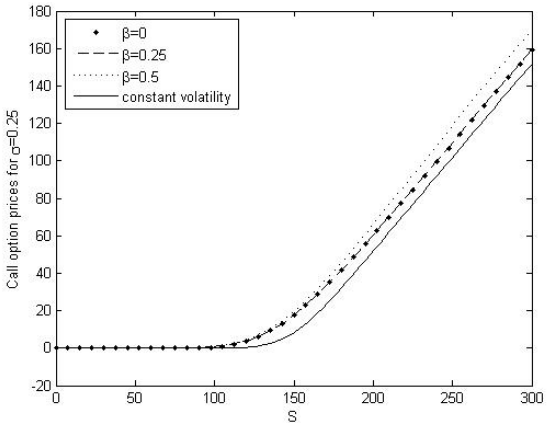

(c) $\sigma = 0.25$

Figure 5.30: The price of European call option price based on the given parameters in Table 5.1 for different values of β at specific values of σ which follows mfBm, i.e. $\varepsilon = 0.5$ and S_t which follows fBm.

The effect of increasing $\alpha \in [0, 0.5]$ is insignificant to the value of call option price (Figures 5.25-5.27). This also applies for all assumption of volatility diffusion processes and also at different values of σ. However, it is obvious that β has a significant influence towards the value of call option price, particularly for higher value of $\sigma = 0.25$ (Figures 5.28-5.30). For $\sigma = 0.15$, there are no apparent influence of β on the call option price no matter what volatility diffusion processes were assumed. The surface figure of α-β-call option price reinforces the previous results on the effects of α and β (Figures 5.31-5.33). These results are consistent with the ones shown in Subsection 5.3.1 on parameters α and β.

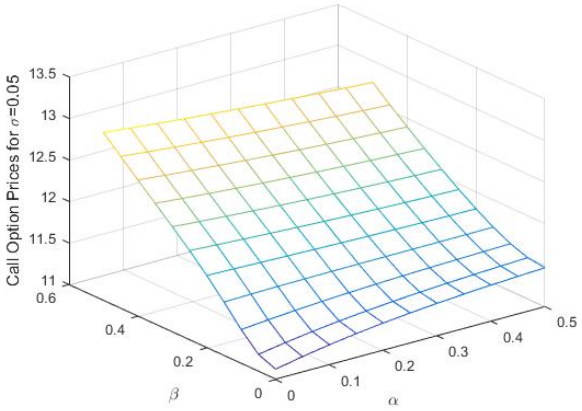

(a) $\sigma = 0.05$

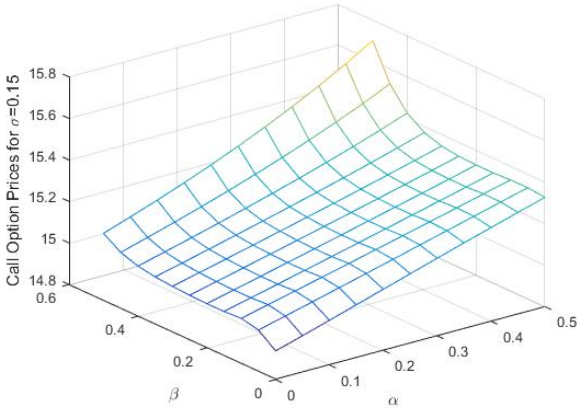

(b) $\sigma = 0.15$

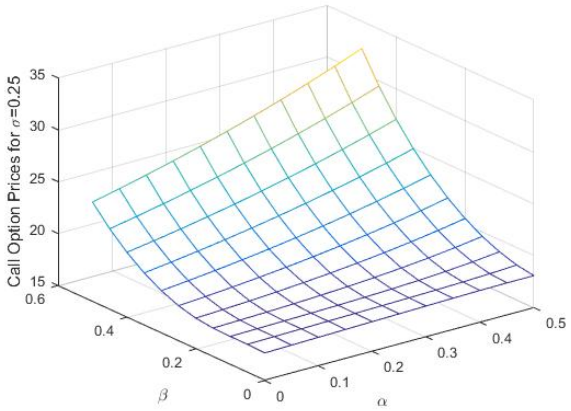

(c) $\sigma = 0.25$

Figure 5.31: The price of at-the-money European call option price based on the given parameters in Table 5.1 for a range of α and β values assuming S_t follows fBm and σ follows gBm, i.e. $\varepsilon = 1, H_1 = 0.5$.

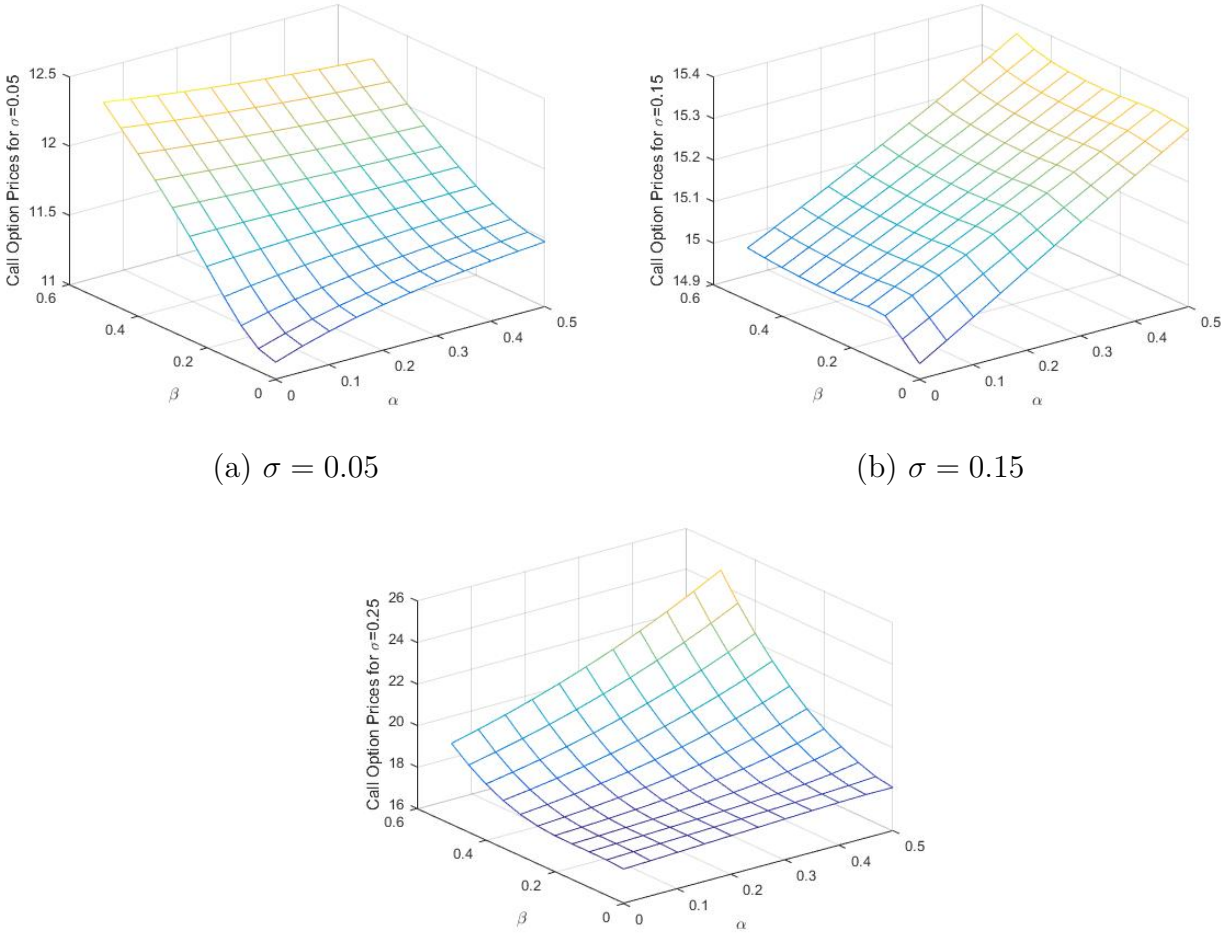

(a) $\sigma = 0.05$

(b) $\sigma = 0.15$

(c) $\sigma = 0.25$

Figure 5.32: The price of at-the-money European call option price based on the given parameters in Table 5.1 for a range of α and β values assuming S_t follows fBm and σ follows fBm, i.e. $\varepsilon = 0, H_1 = 0.65$.

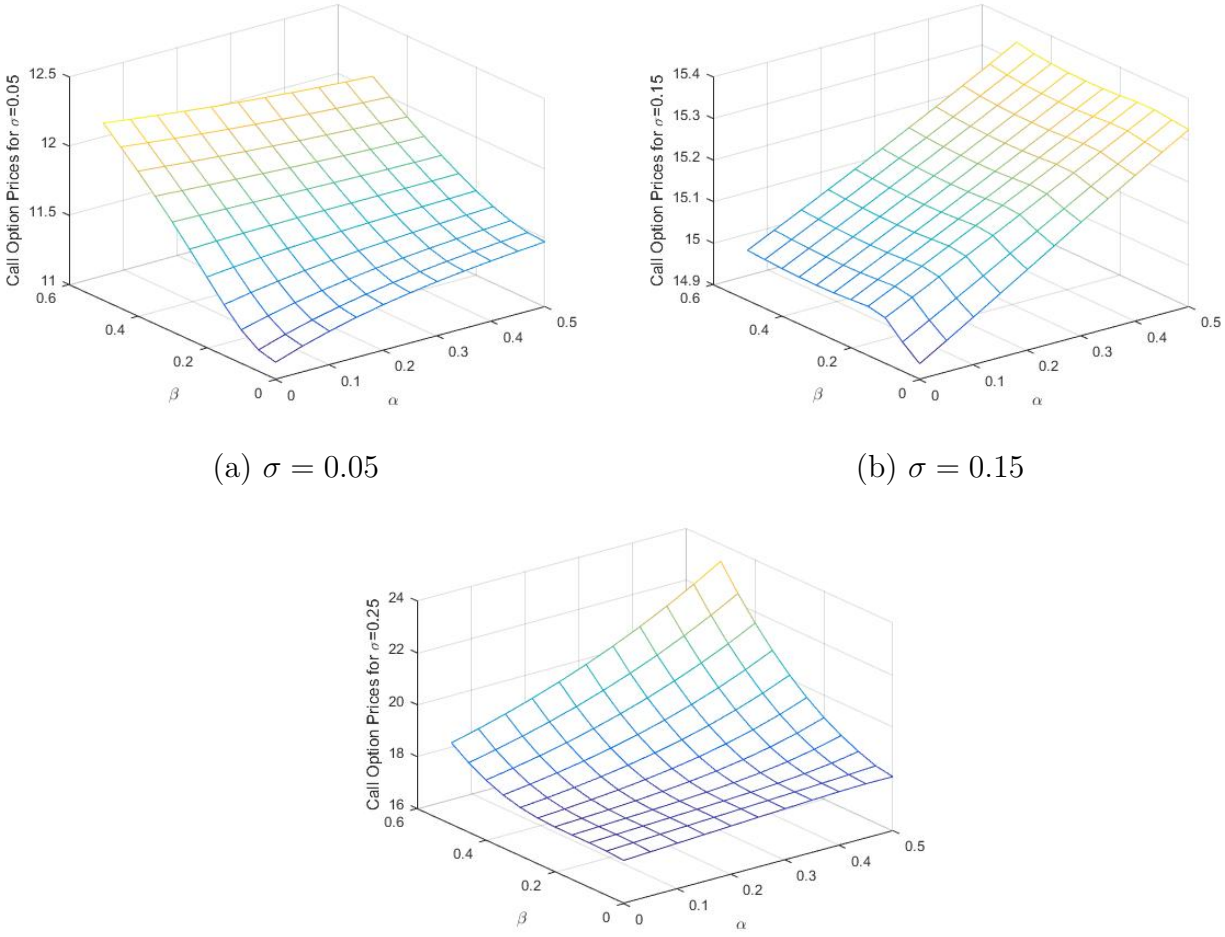

(a) $\sigma = 0.05$

(b) $\sigma = 0.15$

(c) $\sigma = 0.25$

Figure 5.33: The price of at-the-money European call option price based on the given parameters in Table 5.1 for a range of α and β values assuming S_t follows fBm and σ follows gBm, i.e. $\varepsilon = 0.5, H_1 = 0.65$.

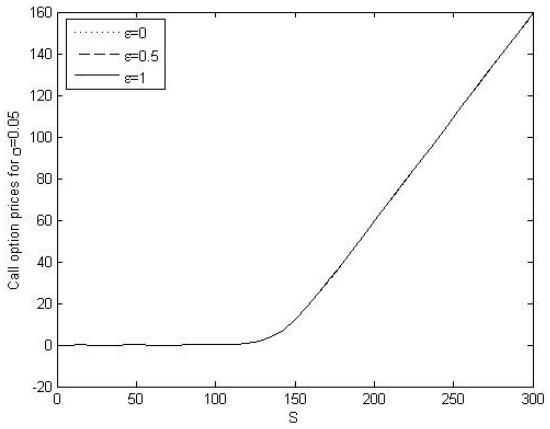

(a) $\sigma = 0.05$

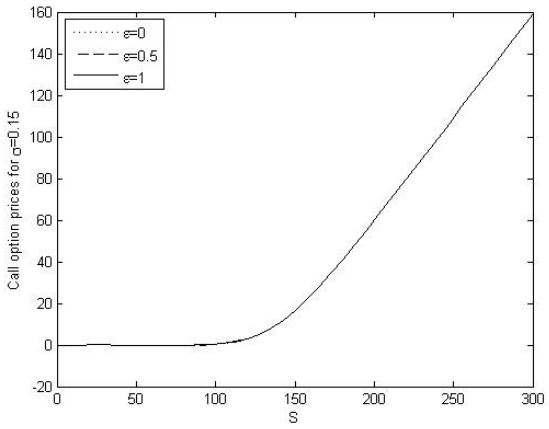

(b) $\sigma = 0.15$

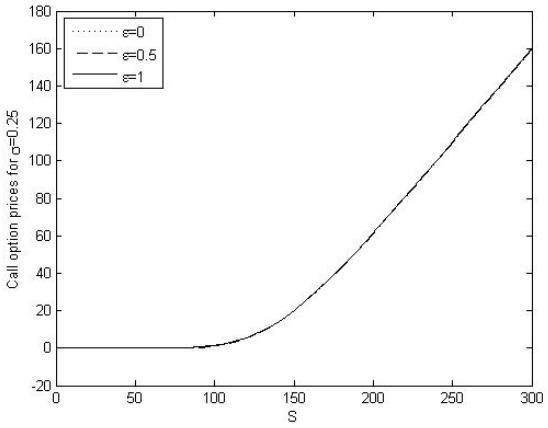

(c) $\sigma = 0.25$

Figure 5.34: The effect of ε on European call option price for different values of σ assuming S_t follows fBm and other chosen parameters in Table 5.1, except altering $\alpha = 0.5$.

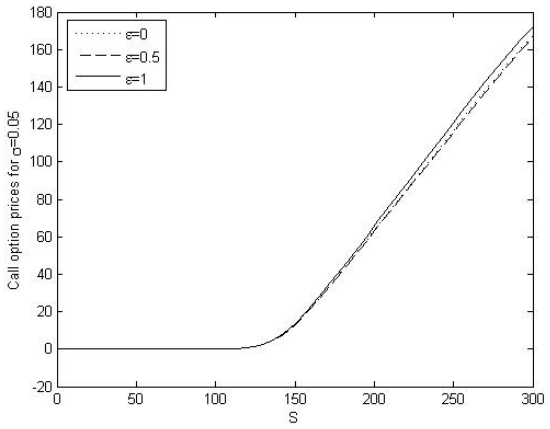

(a) $\sigma = 0.05$

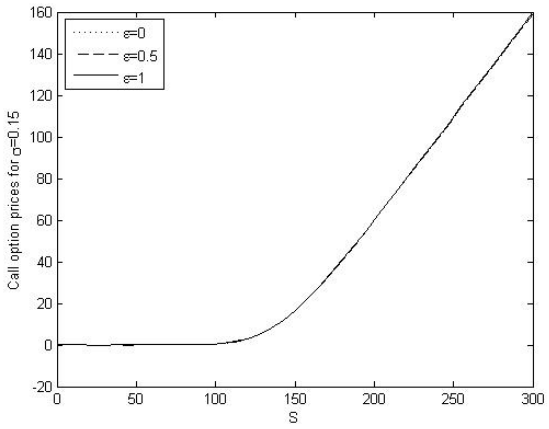

(b) $\sigma = 0.15$

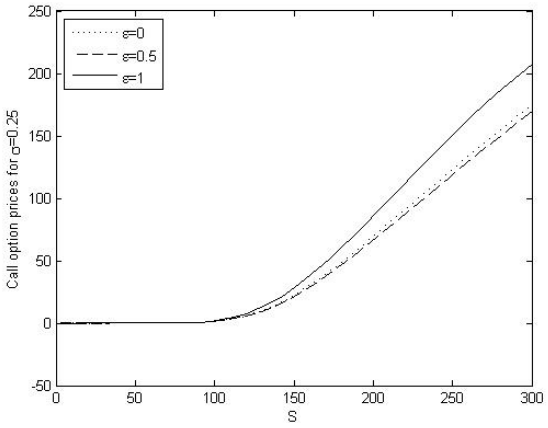

(c) $\sigma = 0.25$

Figure 5.35: The effect of ε on European call option price for different values of σ assuming S_t follows fBm and other chosen parameters in Table 5.1, except altering $\beta = 0.5$.

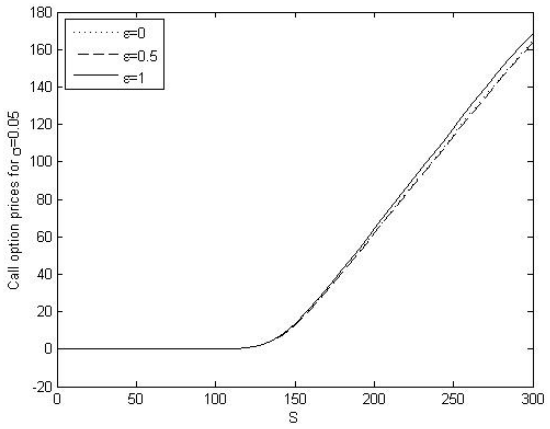

(a) $\sigma = 0.05$

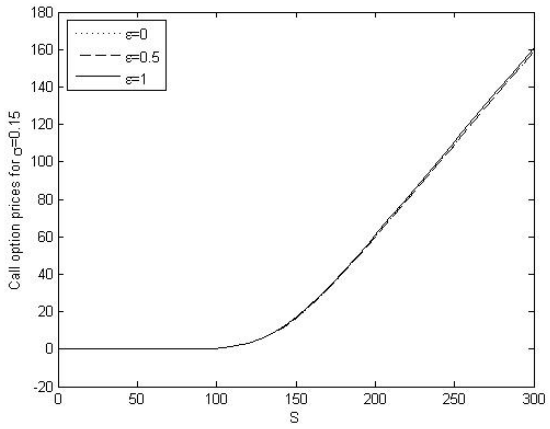

(b) $\sigma = 0.15$

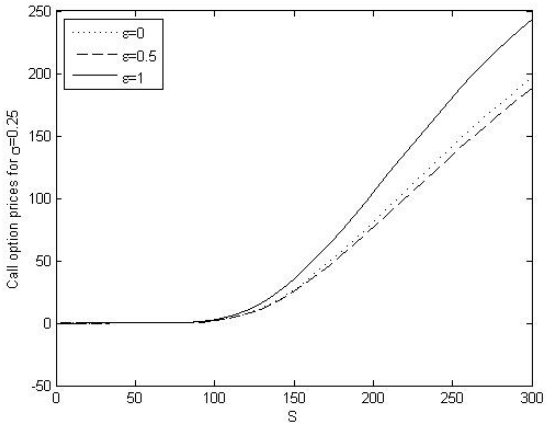

(c) $\sigma = 0.25$

Figure 5.36: The effect of ε on European call option price for different values of σ assuming S_t follows fBm and other chosen parameters in Table 5.1, except altering $\alpha = \beta = 0.5$.

Similar to the previous section, we also want to analyse the effect of ε and H_1. The results are similar to the ones previously discussed in Subsection 5.3.1, where the influence of ε becomes more apparent as β increases, but not so much when α increases (Figures 5.34-5.36). The effect of $\varepsilon = 0.5$ (assuming σ_τ follows mfBm) lowers the call option price compared to when ε is equal to 0 (fBm) and 1 (gBm).

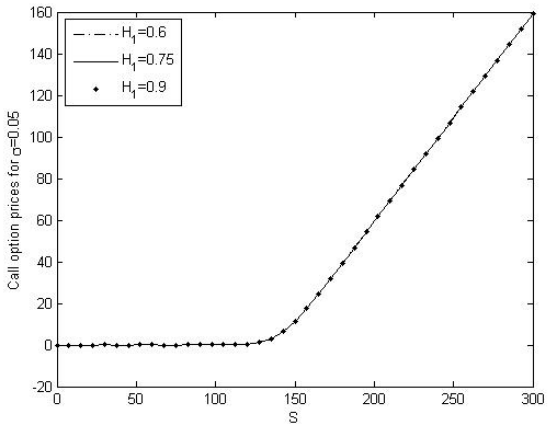

(a) $\sigma = 0.05$

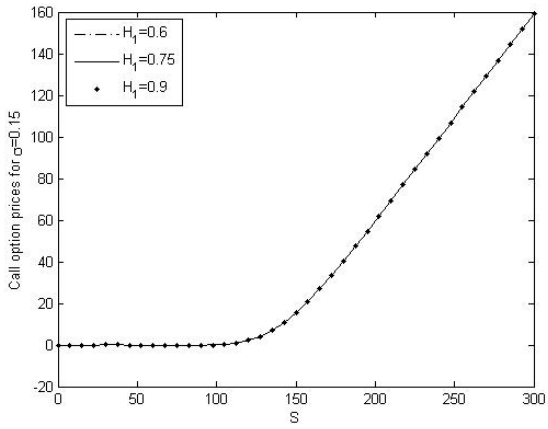

(b) $\sigma = 0.15$

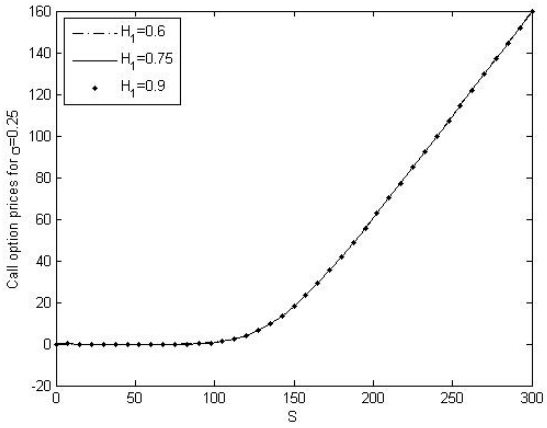

(c) $\sigma = 0.25$

Figure 5.37: The effect of H_1 on European call option price for different values of σ assuming S_t follows fBm and other chosen parameters in Table 5.1, except altering $\alpha = 0.5$.

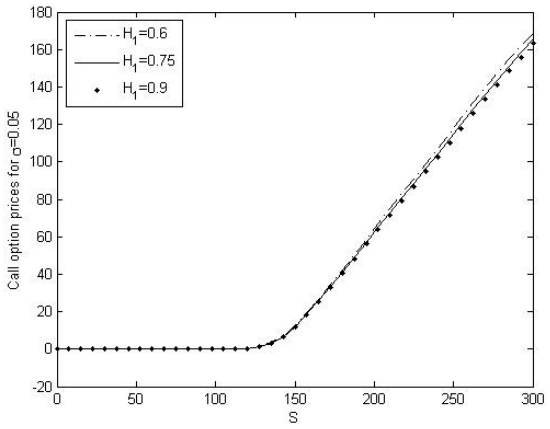

(a) $\sigma = 0.05$

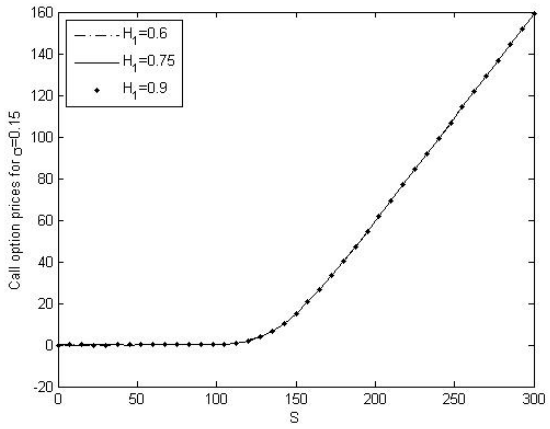

(b) $\sigma = 0.15$

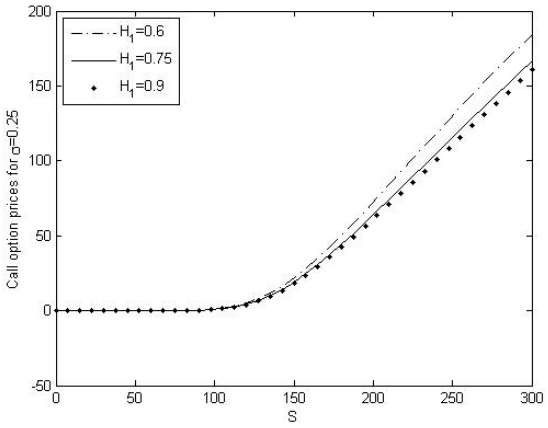

(c) $\sigma = 0.25$

Figure 5.38: The effect of H_1 on European call option price for different values of σ assuming S_t follows fBm and other chosen parameters in Table 5.1, except altering $\beta = 0.5$.

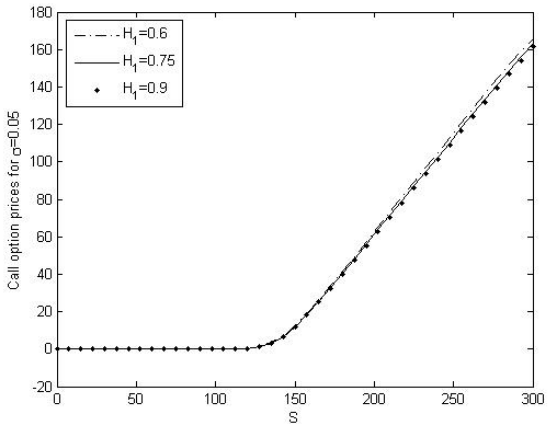

(a) $\sigma = 0.05$

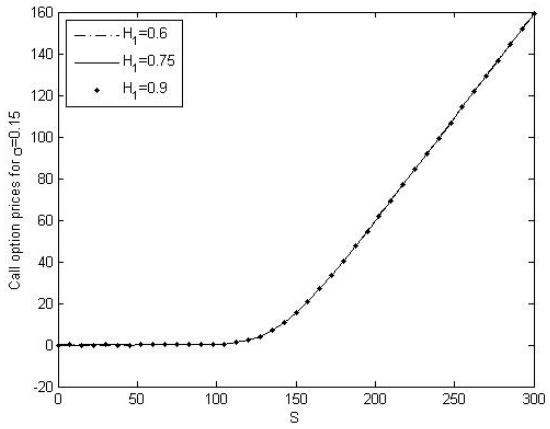

(b) $\sigma = 0.15$

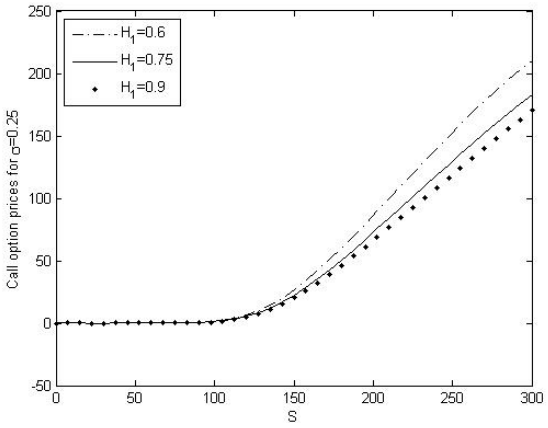

(c) $\sigma = 0.25$

Figure 5.39: The effect of H_1 on European call option price for different values of σ assuming S_t follows fBm and other chosen parameters in Table 5.1, except altering $\alpha = \beta = 0.5$.

The Hurst parameter (H_1) assumed in volatility diffusion processes (σ_τ) affects the European call option price for various combinations of α and β at different values of σ (Figures 5.37-5.39). The effect of H_1 is again similar to the ones previously mentioned in Subsection 5.3.1. The results show that there is a general trend that when Hurst parameter (H_1) increases, the value of call option price for higher values of share price is lower. However, this only becomes apparent when β is large and at particular value of $\sigma = 0.05$ and $\sigma = 0.25$. For the parameter values of α and β assumed in Table 5.1, there are no significant difference in changing the value of H_1.

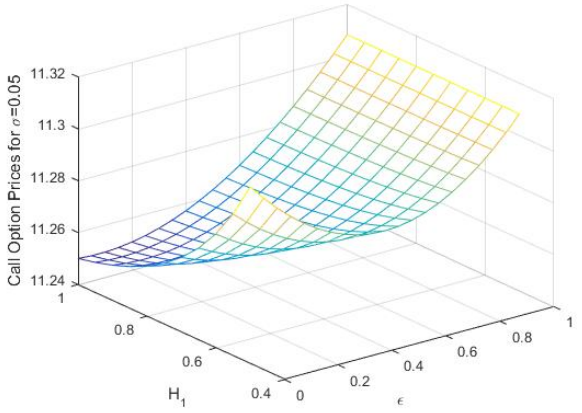

(a) $\sigma = 0.05$

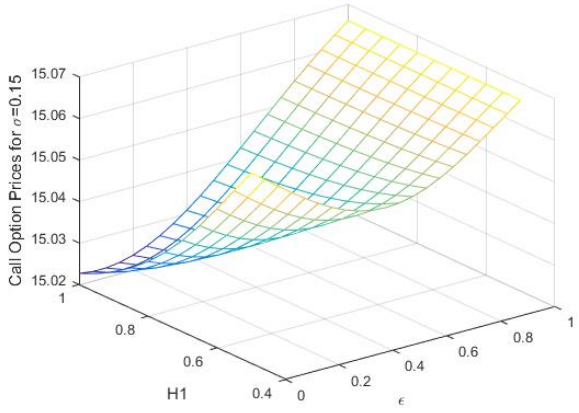

(b) $\sigma = 0.15$

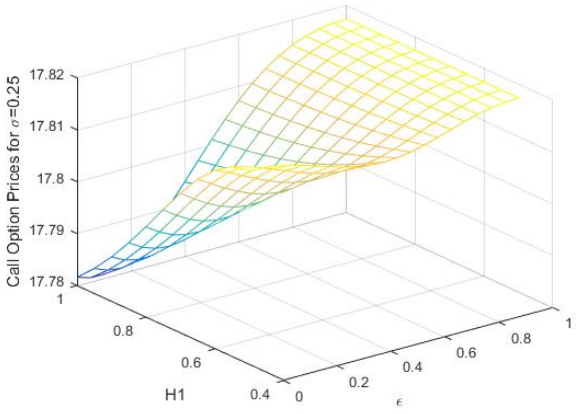

(c) $\sigma = 0.25$

Figure 5.40: The effect of ε and H_1 on European call option price for different values of σ assuming $S = K = 150$ and other chosen parameters in Table 5.1 when S_t follows fBm.

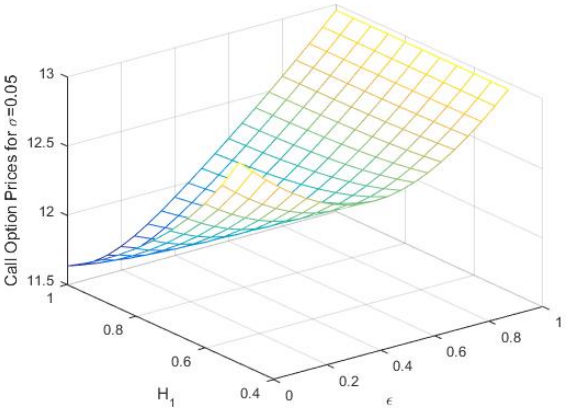

(a) $\sigma = 0.05$

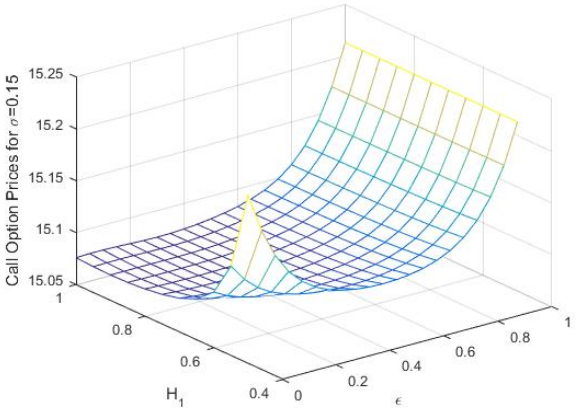

(b) $\sigma = 0.15$

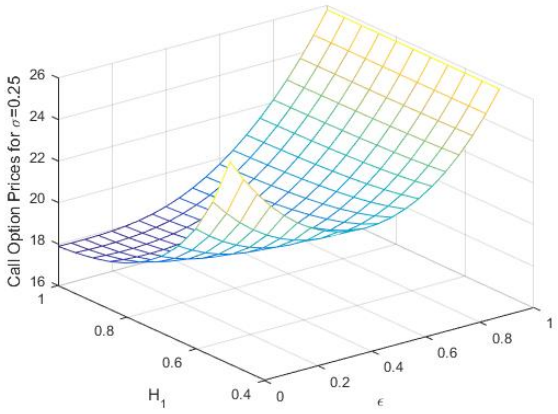

(c) $\sigma = 0.25$

Figure 5.41: The effect of ε and H_1 on European call option price for different values of σ assuming $S = K = 150$, $\beta = 0.5$ and other chosen parameters in Table 5.1 when S_t follows fBm.

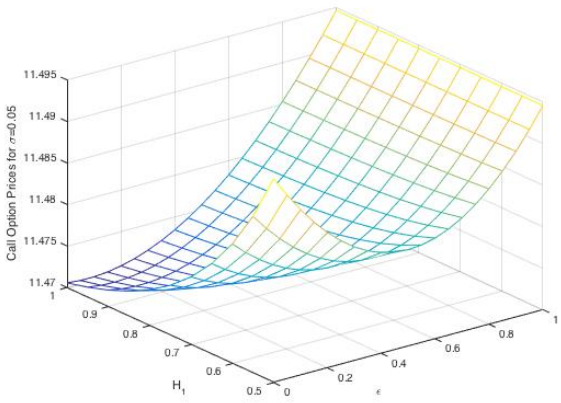

(a) $\sigma = 0.05$

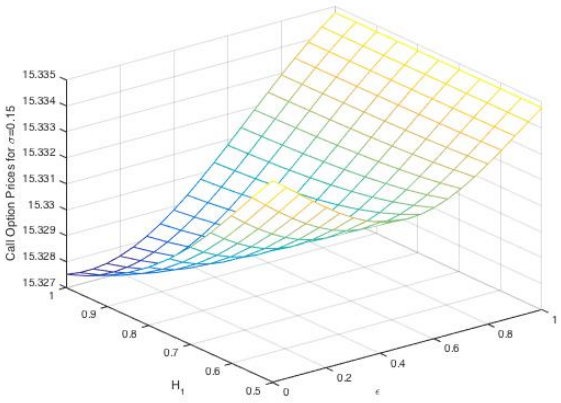

(b) $\sigma = 0.15$

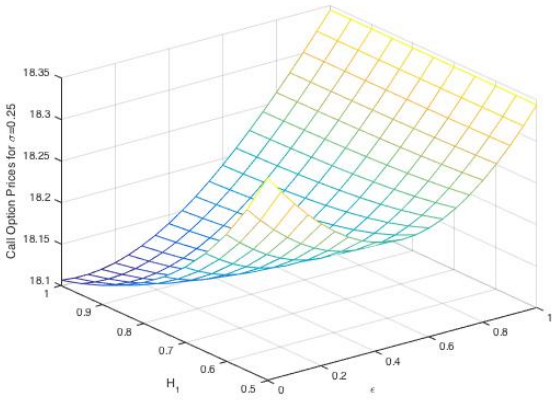

(c) $\sigma = 0.25$

Figure 5.42: The effect of ε and H_1 on European call option price for different values of σ assuming $S = K = 150$, $\alpha = 0.5$ and other chosen parameters in Table 5.1 when S_t follows fBm.

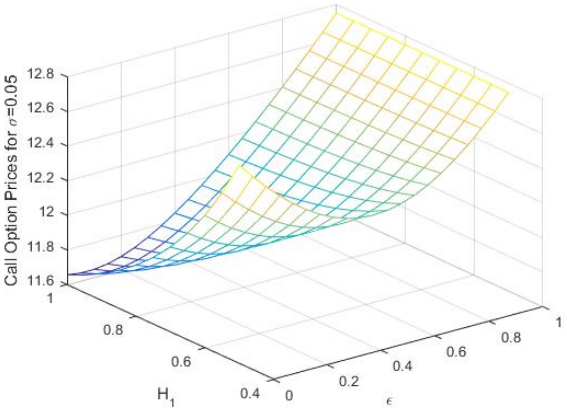

(a) $\sigma = 0.05$

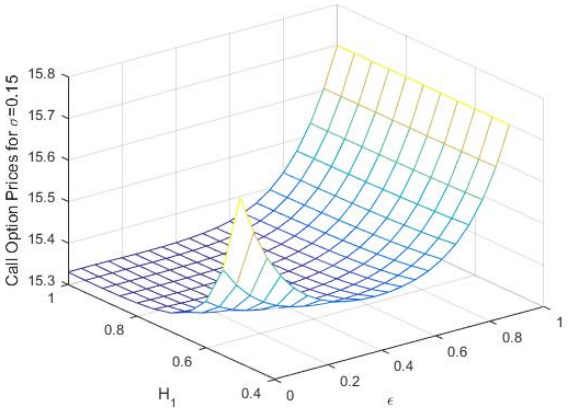

(b) $\sigma = 0.15$

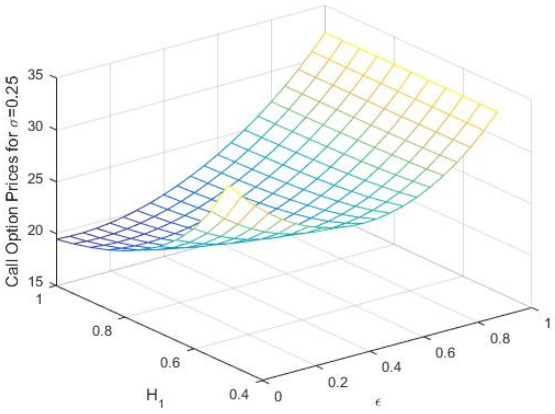

(c) $\sigma = 0.25$

Figure 5.43: The effect of ε and H_1 on European call option price for different values of σ assuming $S = K = 150$, $\alpha = \beta = 0.5$ and other chosen parameters in Table 5.1 when S_t follows fBm.

We may now further analyse the relationship between ε and H_1 and their influences on the European call option price when $S = K = 150$, as shown in Figures 5.40-5.43. The results are consistent with the ones attained when S_t follows gBm in Subsection 5.3.1. The difference in call option value due to the effect of H_1 and ε only becomes significant for high value of β and also at particular values of σ.

5.3.3 S_t assumed mixed fractional Brownian motion

In the previous two Subsections 5.3.1 and 5.3.2, the stock dynamic process in the stochastic volatility model is assumed to be gBm and fBm respectively. In Section 4.3, we have considered the effect of mfBm stock dynamic process. Hence in this subsection, we want to similarly apply this knowledge and take into account the idea of mfBm as the assumed stock dynamic in the stochastic volatility model.

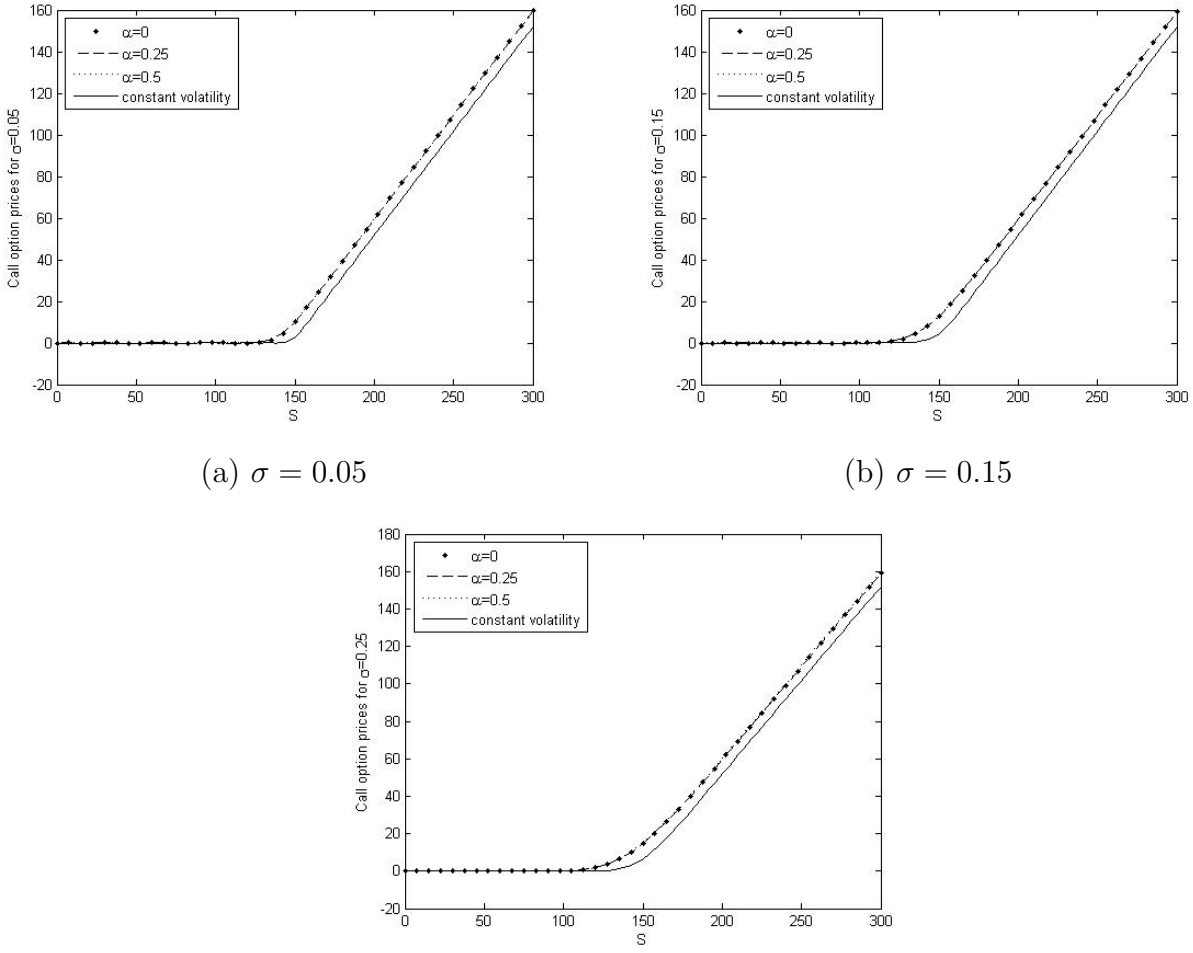

(a) $\sigma = 0.05$

(b) $\sigma = 0.15$

(c) $\sigma = 0.25$

Figure 5.44: The price of European call option price based on the given parameters in Table 5.1 for different values of α at specific values of σ which follows gBm, i.e. $\varepsilon = 1$ and S_t which follows mfBm.

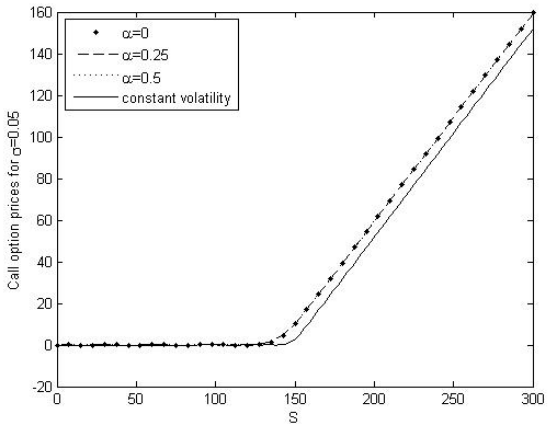

(a) $\sigma = 0.05$

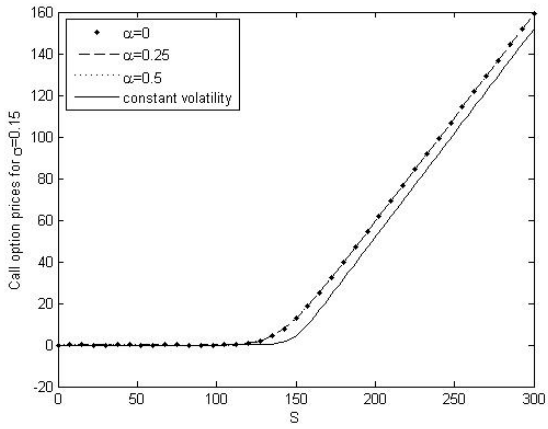

(b) $\sigma = 0.15$

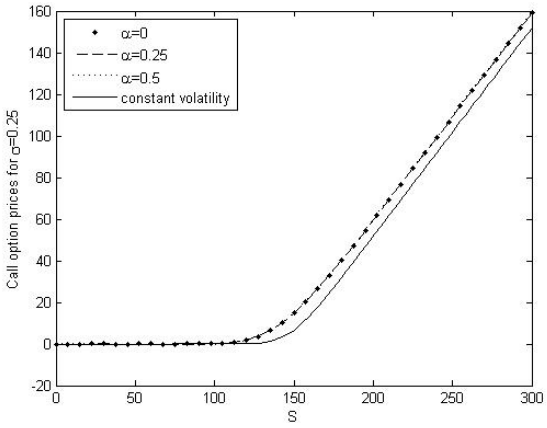

(c) $\sigma = 0.25$

Figure 5.45: The price of European call option price based on the given parameters in Table 5.1 for different values of α at specific values of σ which follows fBm, i.e. $\varepsilon = 0$ and S_t which follows mfBm.

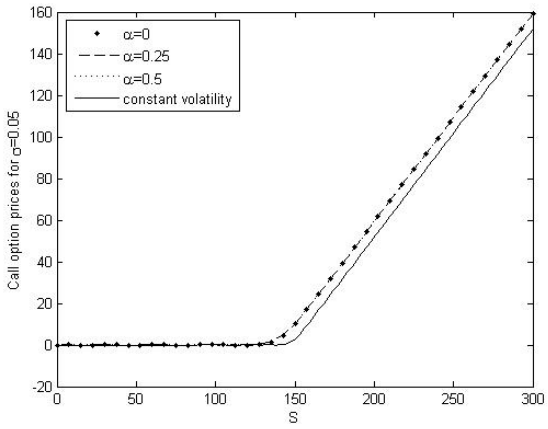

(a) $\sigma = 0.05$

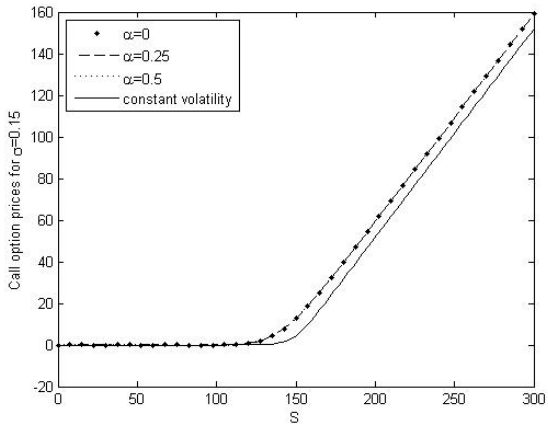

(b) $\sigma = 0.15$

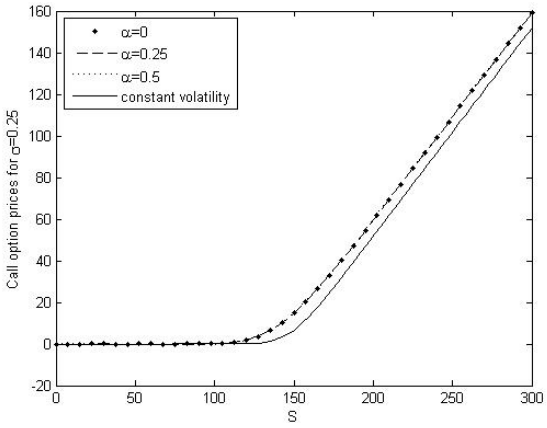

(c) $\sigma = 0.25$

Figure 5.46: The price of European call option price based on the given parameters in Table 5.1 for different values of α at specific values of σ which follows mfBm, i.e. $\varepsilon = 0.5$ and S_t which follows mfBm.

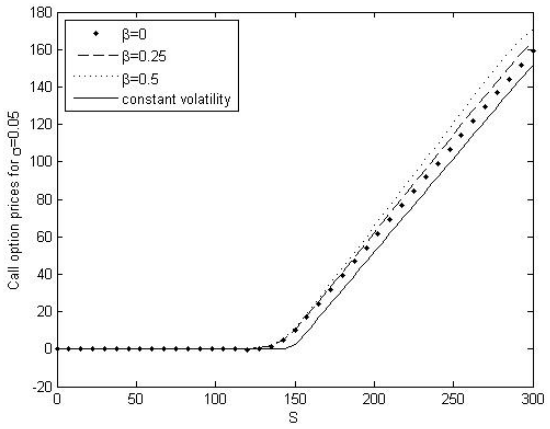

(a) $\sigma = 0.05$

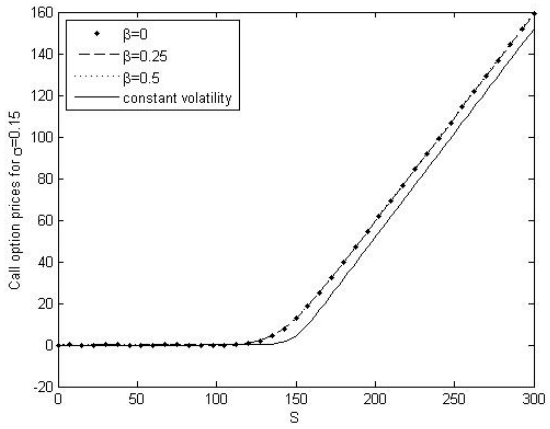

(b) $\sigma = 0.15$

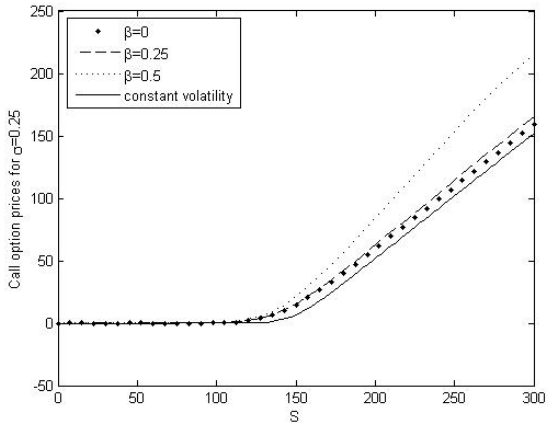

(c) $\sigma = 0.25$

Figure 5.47: The price of European call option price based on the given parameters in Table 5.1 for different values of β at specific values of σ which follows gBm, i.e. $\varepsilon = 1$ and S_t which follows mfBm.

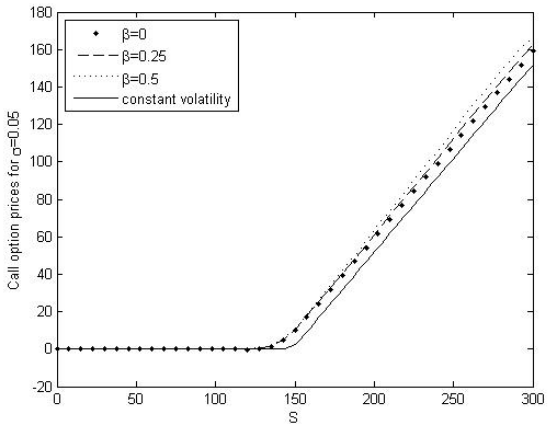

(a) $\sigma = 0.05$

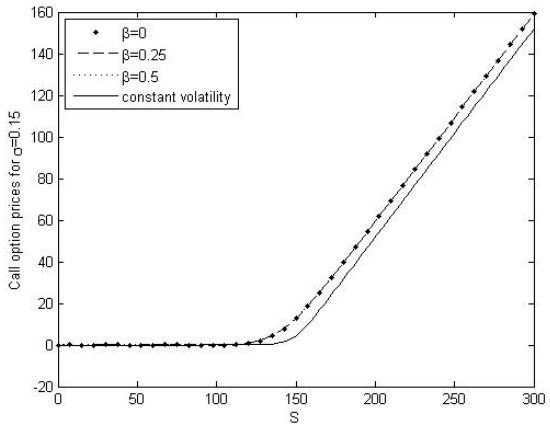

(b) $\sigma = 0.15$

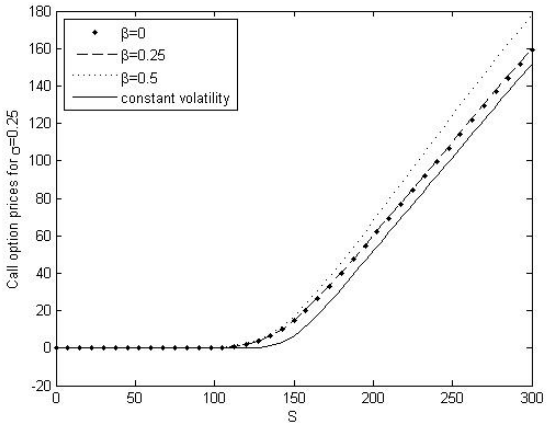

(c) $\sigma = 0.25$

Figure 5.48: The price of European call option price based on the given parameters in Table 5.1 for different values of β at specific values of σ which follows fBm, i.e. $\varepsilon = 0$ and S_t which follows mfBm.

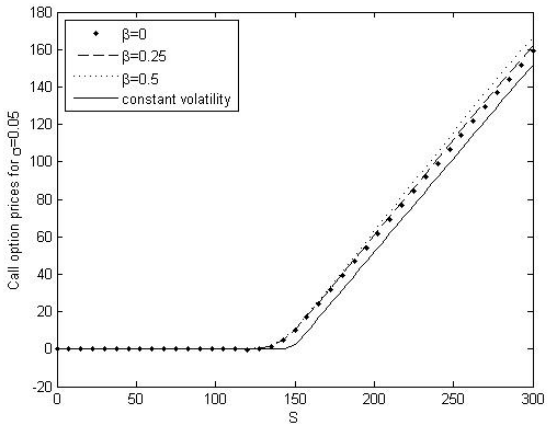

(a) $\sigma = 0.05$

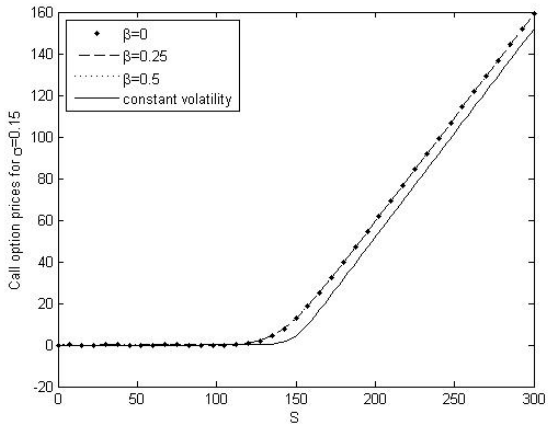

(b) $\sigma = 0.15$

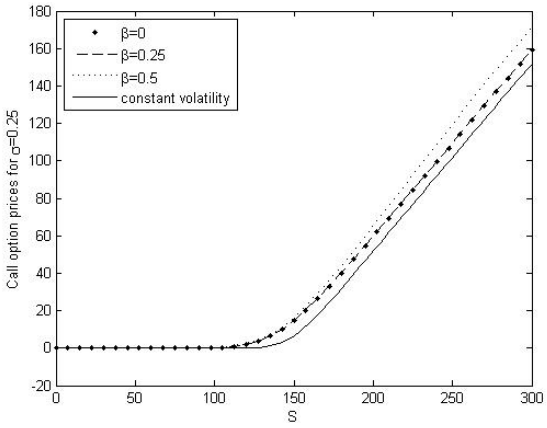

(c) $\sigma = 0.25$

Figure 5.49: The price of European call option price based on the given parameters in Table 5.1 for different values of β at specific values of σ which follows mfBm, i.e. $\varepsilon = 0.5$ and S_t which follows mfBm.

The results show no significant change in call option price between $\alpha \in [0, 0.5]$ (Figures 5.44-5.46). On the other hand, the effect of increasing $\beta \in [0, 0.5]$ has more impact on the call option price as shown in Figures 5.47-5.49. This is true for all volatility diffusion processes assumed, as well as consistent with the results as shown in the previous two Subsections 5.3.1 and 5.3.2.

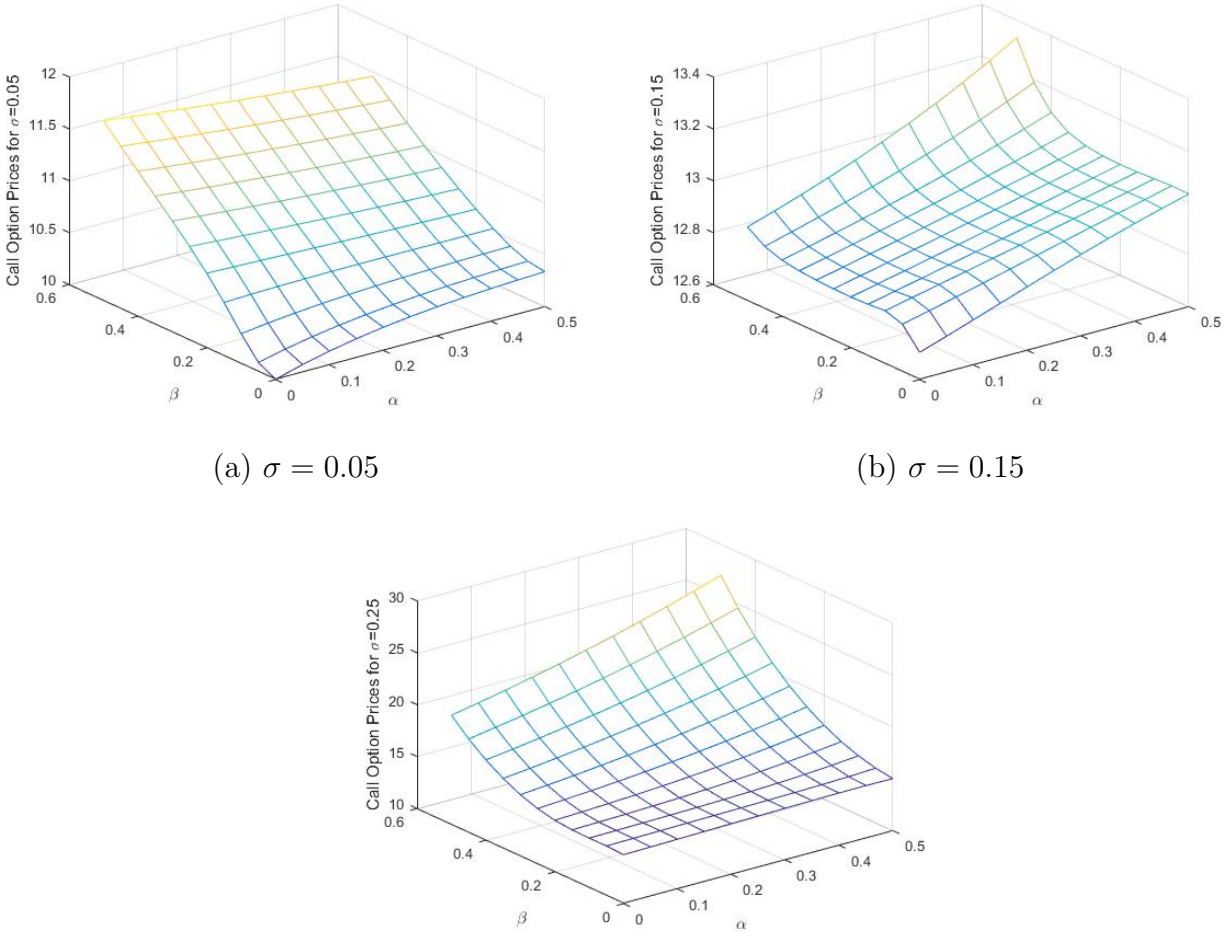

(a) $\sigma = 0.05$

(b) $\sigma = 0.15$

(c) $\sigma = 0.25$

Figure 5.50: The price of at-the-money European call option price based on the given parameters in Table 5.1 for a range of α and β values assuming S_t follows mfBm and σ follows gBm, i.e. $\varepsilon = 1, H_1 = 0.5$.

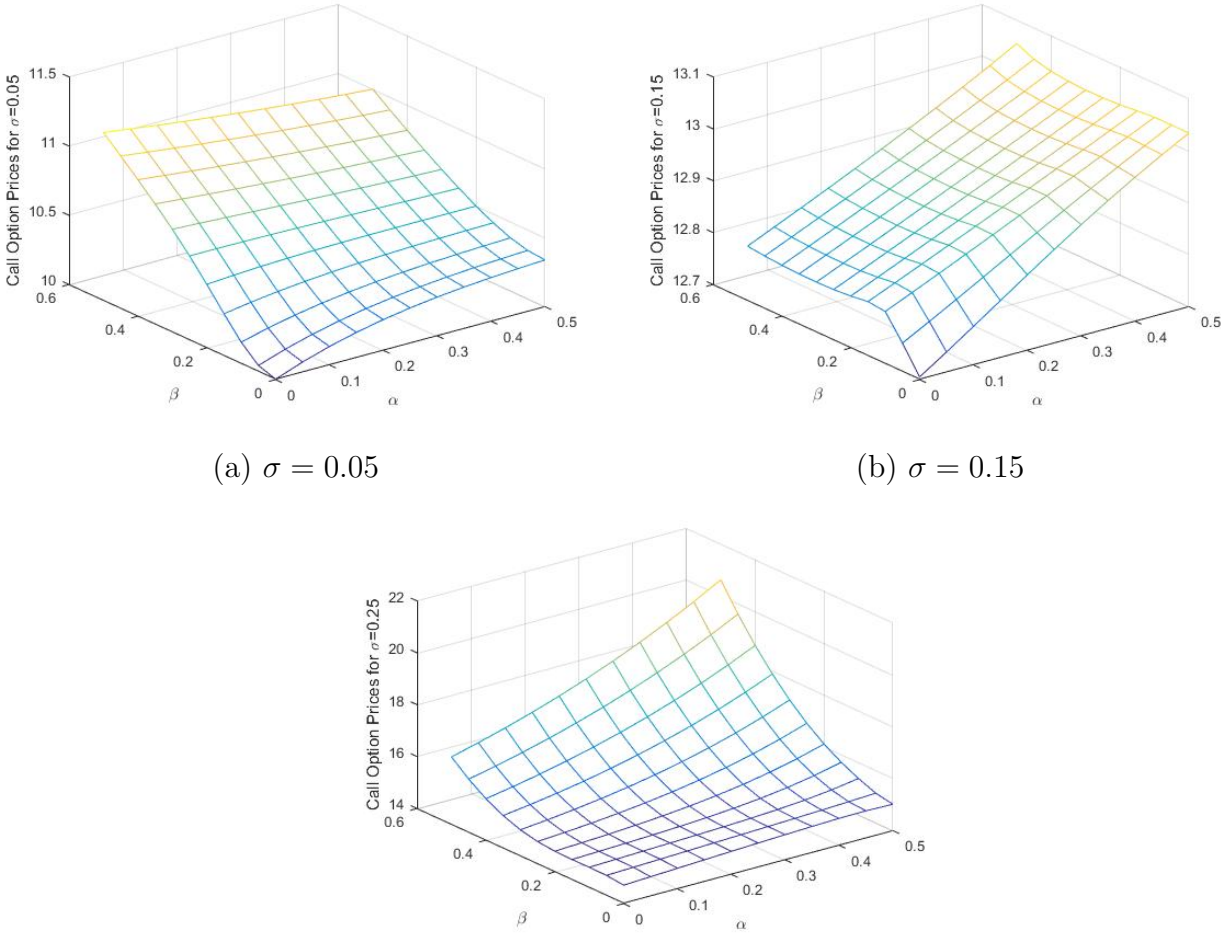

(a) $\sigma = 0.05$

(b) $\sigma = 0.15$

(c) $\sigma = 0.25$

Figure 5.51: The price of at-the-money European call option price based on the given parameters in Table 5.1 for a range of α and β values assuming S_t follows mfBm and σ follows fBm, i.e. $\varepsilon = 0, H_1 = 0.65$.

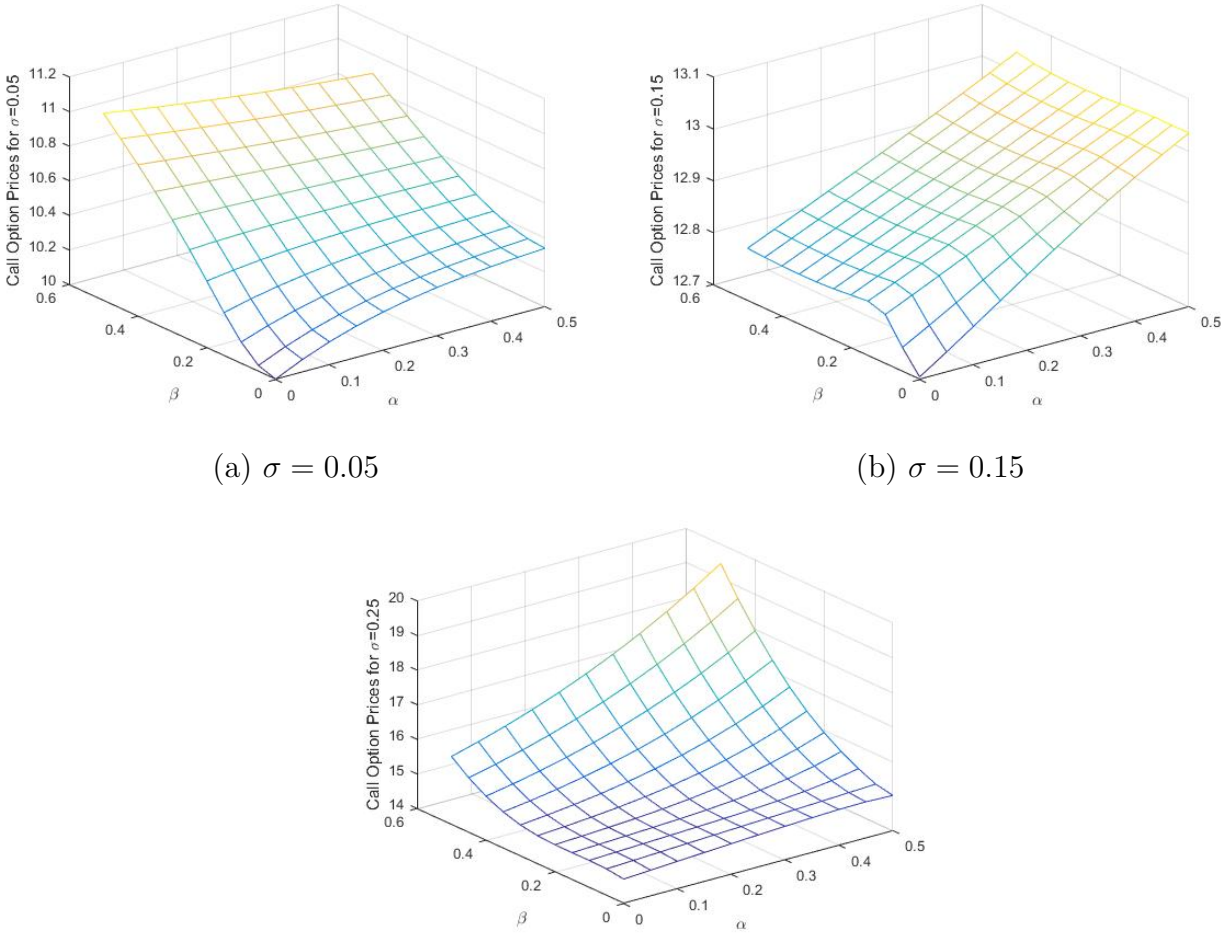

(a) $\sigma = 0.05$

(b) $\sigma = 0.15$

(c) $\sigma = 0.25$

Figure 5.52: The price of at-the-money European call option price based on the given parameters in Table 5.1 for a range of α and β values assuming S_t follows mfBm and σ follows mfBm, i.e. $\varepsilon = 0.5, H_1 = 0.65$.

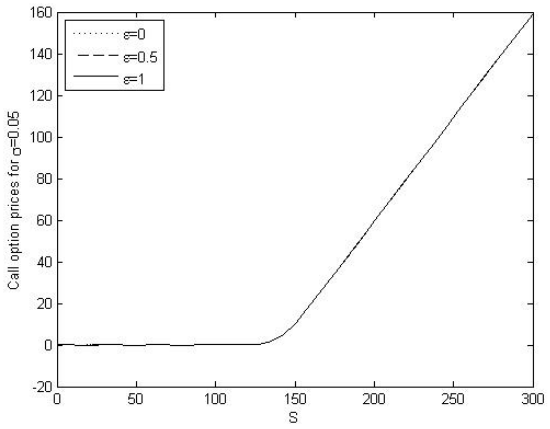

(a) $\sigma = 0.05$

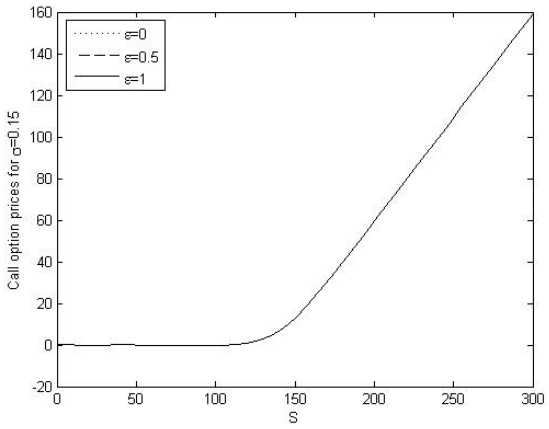

(b) $\sigma = 0.15$

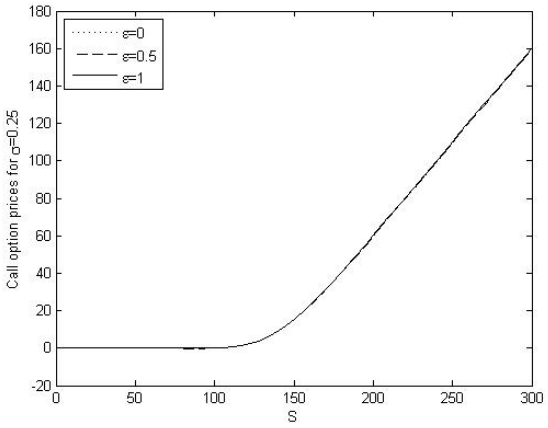

(c) $\sigma = 0.25$

Figure 5.53: The effect of ε on European call option price for different values of σ assuming S_t follows mfBm and other chosen parameters in Table 5.1, except altering $\alpha = 0.5$.

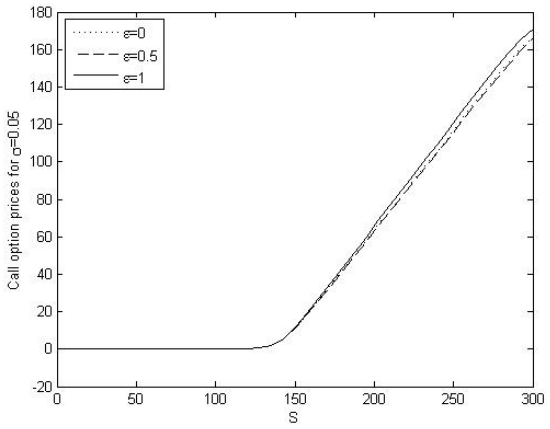

(a) $\sigma = 0.05$

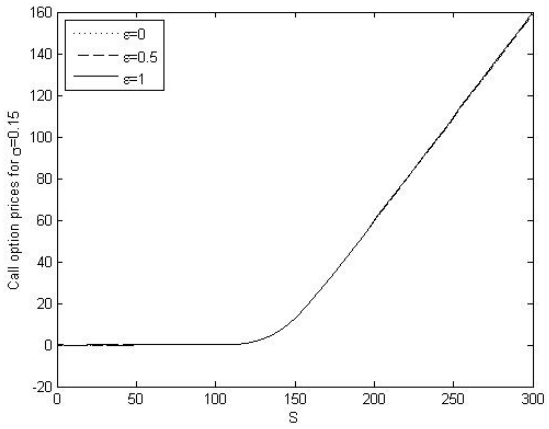

(b) $\sigma = 0.15$

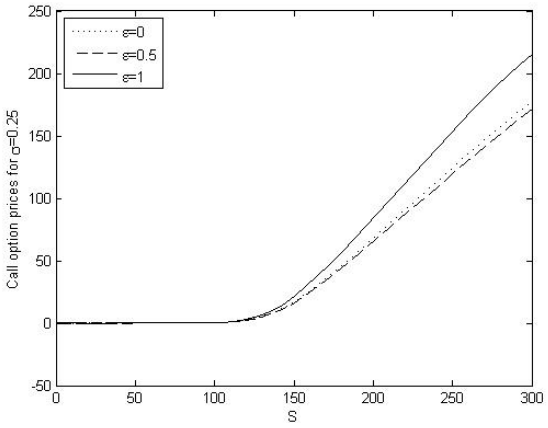

(c) $\sigma = 0.25$

Figure 5.54: The effect of ε on European call option price for different values of σ assuming S_t follows mfBm and other chosen parameters in Table 5.1, except altering $\beta = 0.5$.

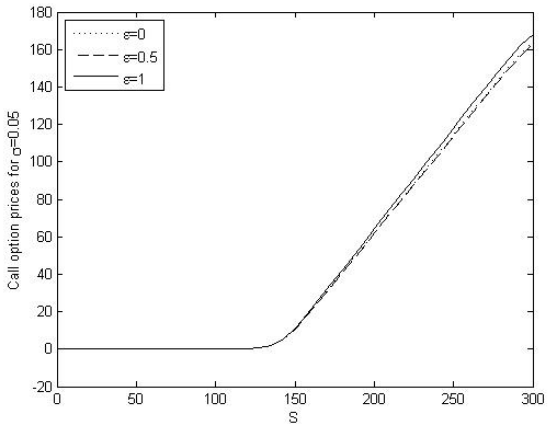

(a) $\sigma = 0.05$

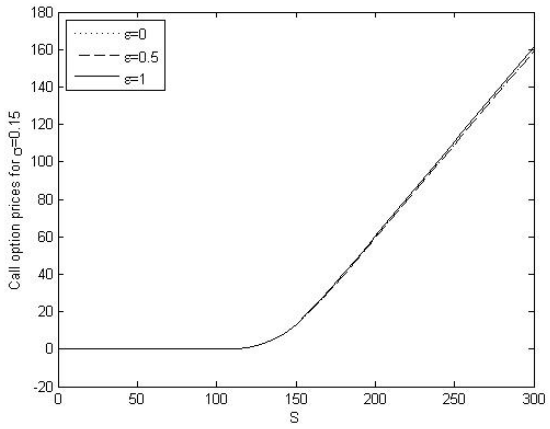

(b) $\sigma = 0.15$

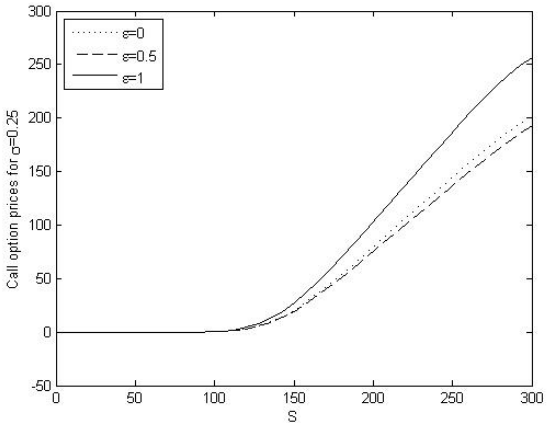

(c) $\sigma = 0.25$

Figure 5.55: The effect of ε on European call option price for different values of σ assuming S_t follows mfBm and other chosen parameters in Table 5.1, except altering $\alpha = \beta = 0.5$.

The influence of increasing α is not as significant as increasing β (Figures 5.50-5.52). These results are consistent with Figures 5.44-5.49. It is apparent that any significant difference only becomes visible when the value of β increases, as shown in Figures 5.54 and 5.55.

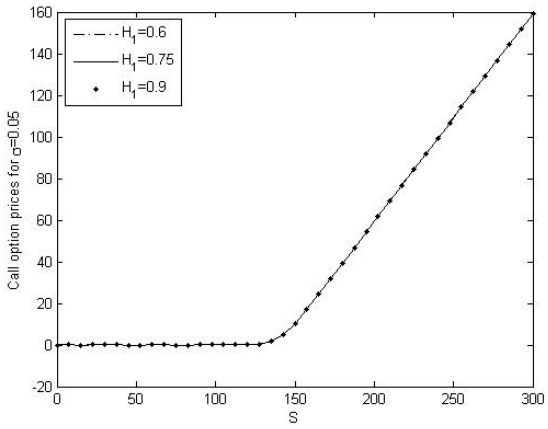

(a) $\sigma = 0.05$

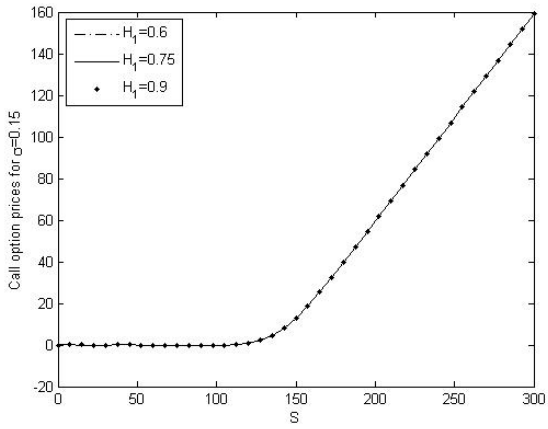

(b) $\sigma = 0.15$

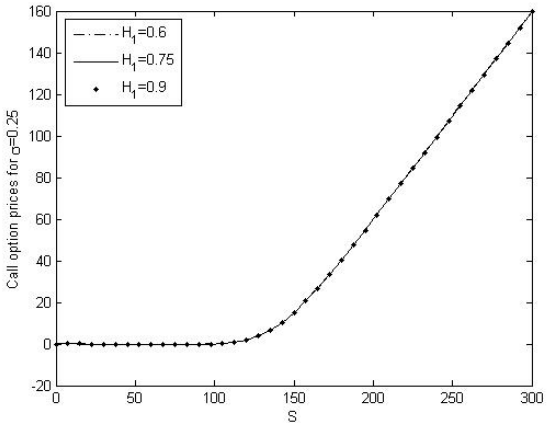

(c) $\sigma = 0.25$

Figure 5.56: The effect of H_1 on European call option price for different values of σ assuming S_t follows mfBm and other chosen parameters in Table 5.1, except altering $\alpha = 0.5$.

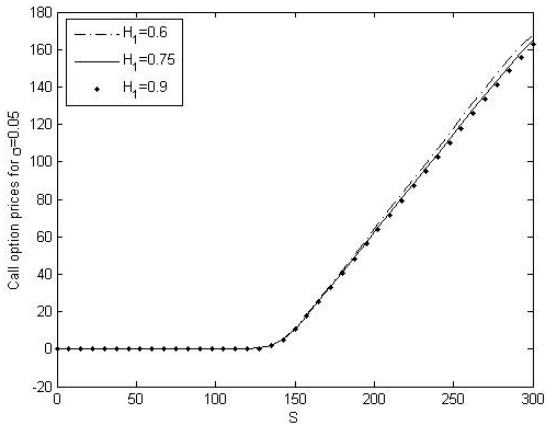

(a) $\sigma = 0.05$

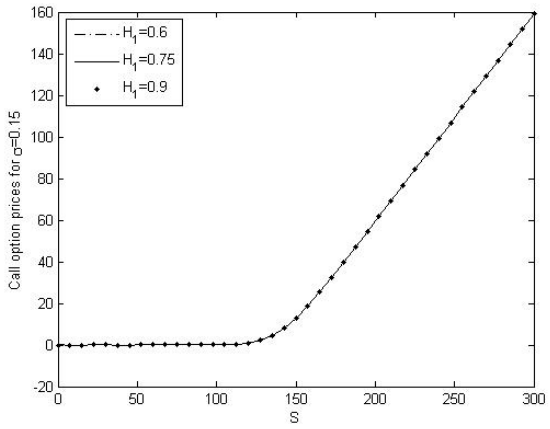

(b) $\sigma = 0.15$

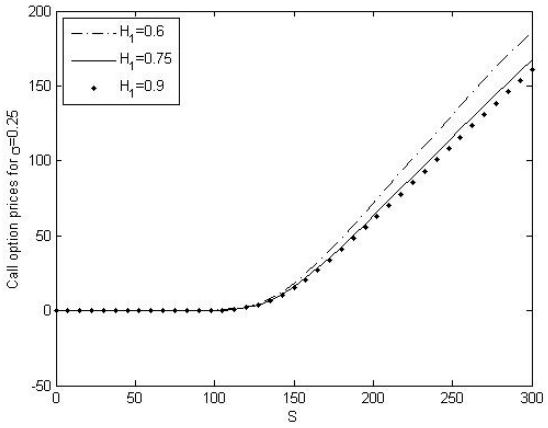

(c) $\sigma = 0.25$

Figure 5.57: The effect of H_1 on European call option price for different values of σ assuming S_t follows mfBm and other chosen parameters in Table 5.1, except altering $\beta = 0.5$.

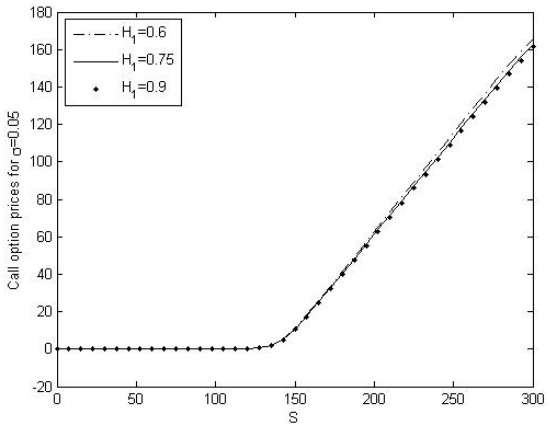

(a) $\sigma = 0.05$

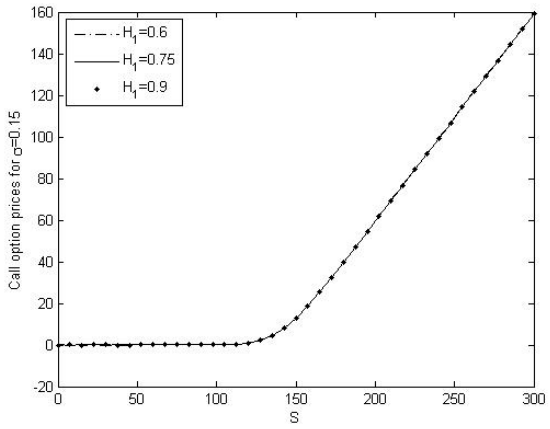

(b) $\sigma = 0.15$

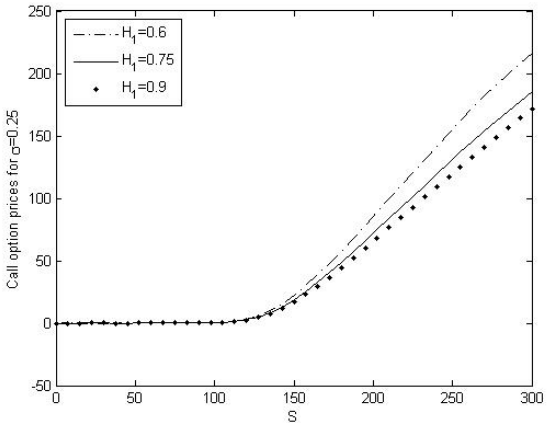

(c) $\sigma = 0.25$

Figure 5.58: The effect of H_1 on European call option price for different values of σ, other chosen parameters in Table 5.1 and altering $\alpha = \beta = 0.5$.

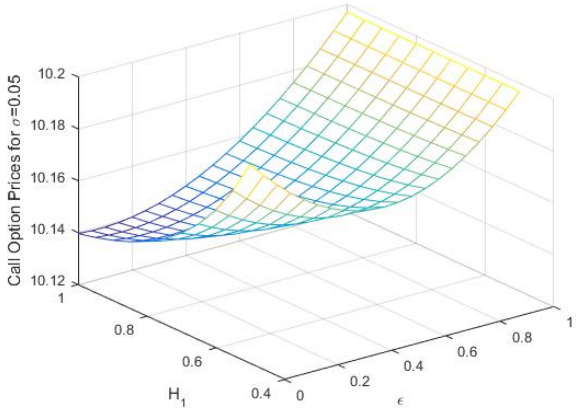

(a) $\sigma = 0.05$

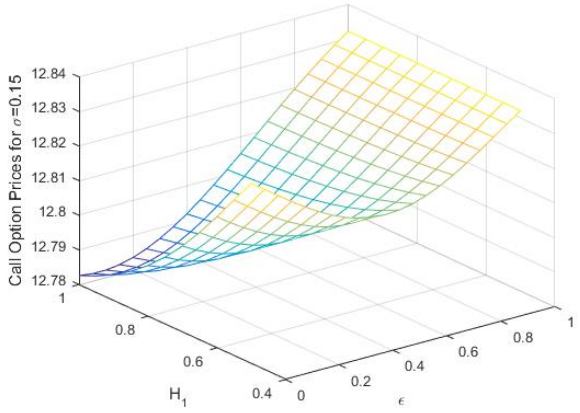

(b) $\sigma = 0.15$

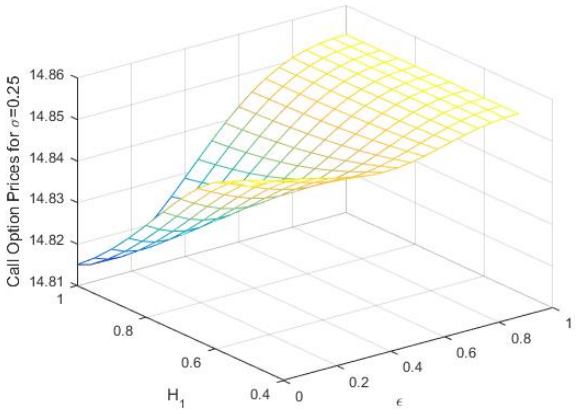

(c) $\sigma = 0.25$

Figure 5.59: The effect of ε and H_1 on European call option price for different values of σ assuming $S = K = 150$ and other chosen parameters in Table 5.1 when S_t follows mfBm.

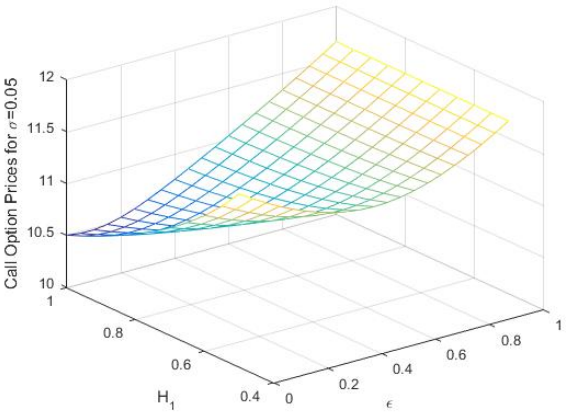

(a) $\sigma = 0.05$

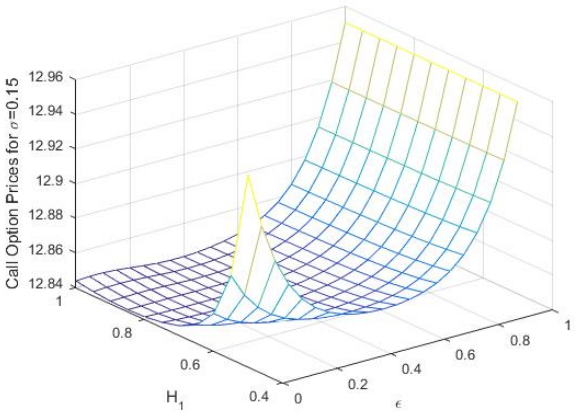

(b) $\sigma = 0.15$

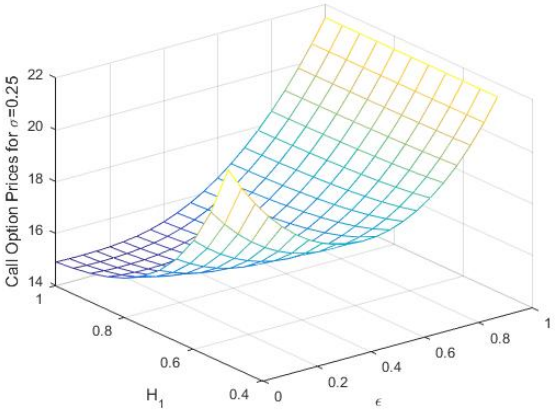

(c) $\sigma = 0.25$

Figure 5.60: The effect of ε and H_1 on European call option price for different values of σ assuming $S = K = 150$, $\beta = 0.5$ and other chosen parameters in Table 5.1 when S_t follows mfBm.

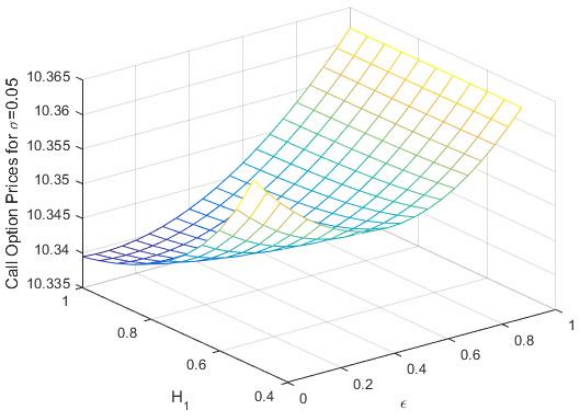

(a) $\sigma = 0.05$

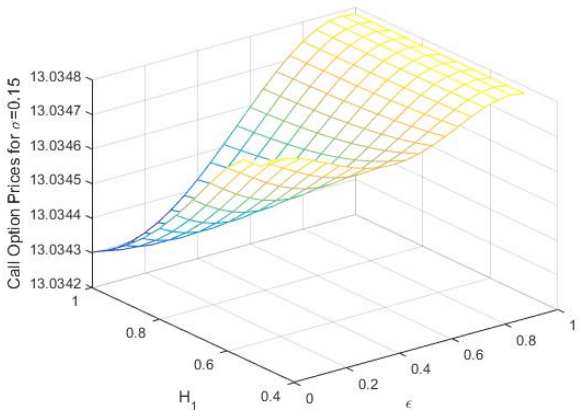

(b) $\sigma = 0.15$

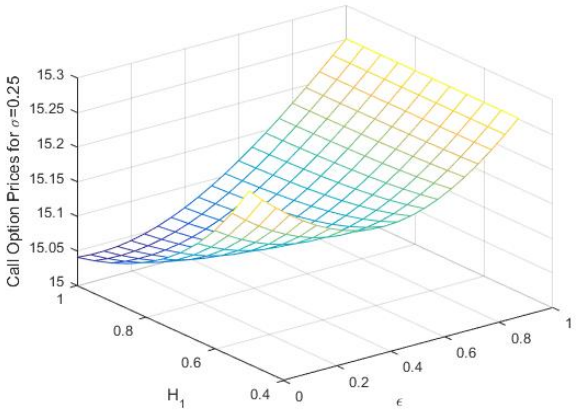

(c) $\sigma = 0.25$

Figure 5.61: The effect of ε and H_1 on European call option price for different values of σ assuming $S = K = 150$, $\alpha = 0.5$ and other chosen parameters in Table 5.1 when S_t follows mfBm.

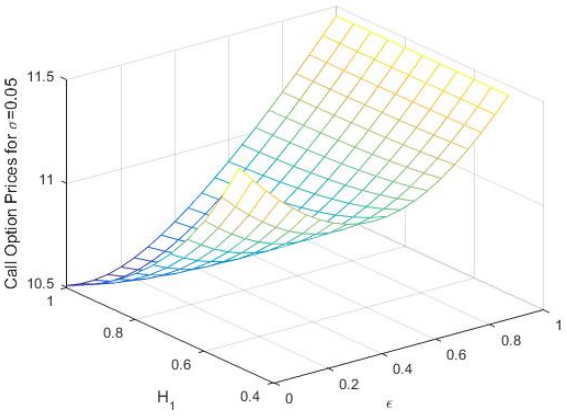

(a) $\sigma = 0.05$

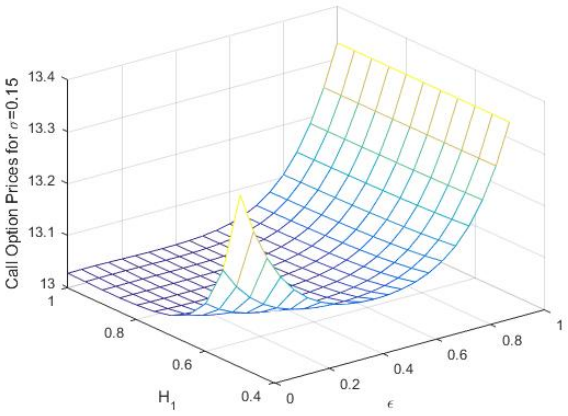

(b) $\sigma = 0.15$

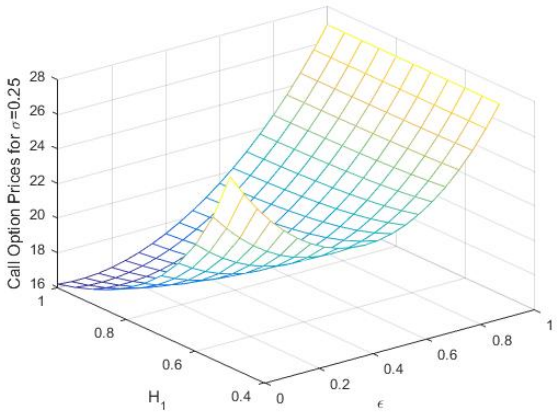

(c) $\sigma = 0.25$

Figure 5.62: The effect of ε and H_1 on European call option price for different values of σ assuming $S = K = 150$, $\alpha = \beta = 0.5$ and other chosen parameters in Table 5.1 when S_t follows mfBm.

The same results are also true when analysing the effect of H_1. Although there is a general trend that greater H_1 means lower value of call option for high range values of S, this is only apparent when β is sufficiently high (Figures 5.56-5.58). From further analysing the influence of both ε and H_1 on the European call price at $S = K = 150$, the results shown in Figures 5.59-5.62 are consistent with the ones discussed above. The results are also similar to the ones attained in Subsections 5.3.1 and 5.3.2.

5.3.4 Comparison of the stochastic volatility models

In the previous Subsections 5.3.1-5.3.3, we have analysed the different stochastic volatility models assuming various stock dynamic processes and σ_τ. The results show that

the effects of parameters α, β, ε and H_1 are similar no matter what the assumptions of stock dynamic processes are. Comparing the results from the three subsections, despite showing similar trends in the influence of its parameters, the results of assuming stock return which follows gBm give higher values of call option compared to the other two assumed stock dynamic processes. This is then followed by fBm S_t. MfBm S_t produces the lowest value of call option price when other chosen parameters are unchanged. The difference is due to the change in assumptions of the stock return model, i.e. the changes in parameters γ and H. This is also reinforced by the results shown in Figures 5.63-5.65. This is once again consistent with the results that we have found in Section 4.3 Figure 4.7.

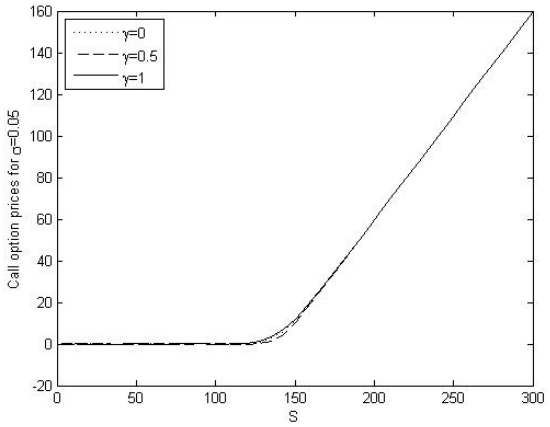

(a) $\sigma = 0.05$

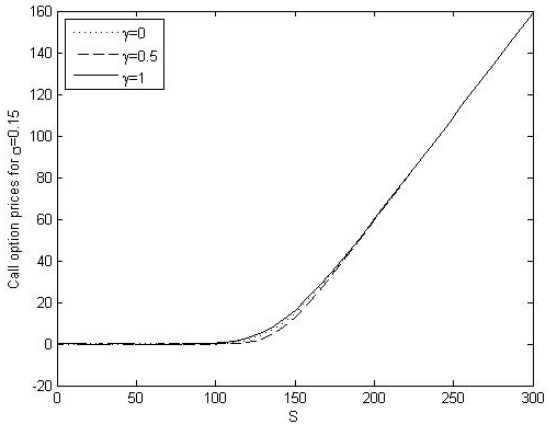

(b) $\sigma = 0.15$

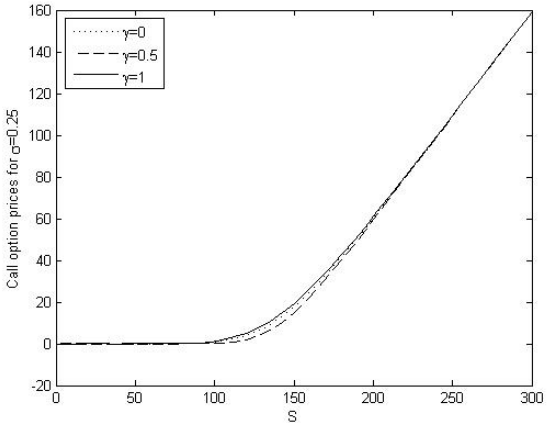

(c) $\sigma = 0.25$

Figure 5.63: The effect of γ on European call option price for different values of σ over a range of S values following the gBm volatility diffusion process and other chosen parameters in Table 5.1.

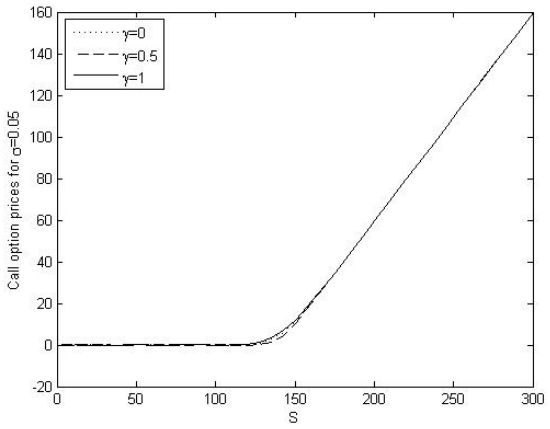

(a) $\sigma = 0.05$

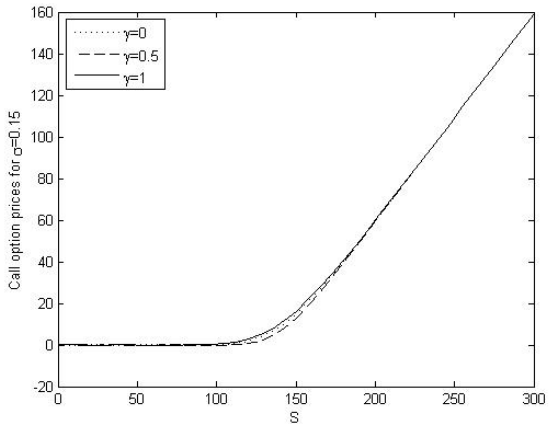

(b) $\sigma = 0.15$

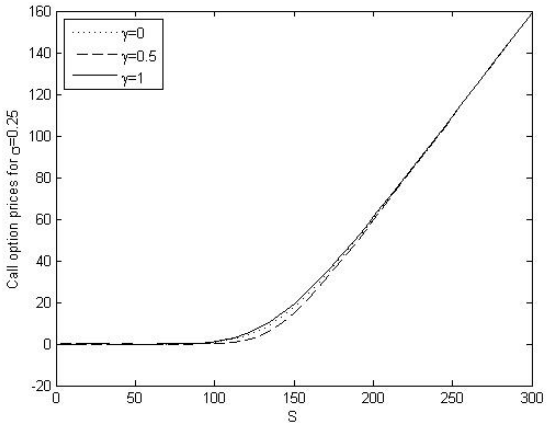

(c) $\sigma = 0.25$

Figure 5.64: The effect of γ on European call option price for different values of σ over a range of S values following the fBm volatility diffusion process and other chosen parameters in Table 5.1.

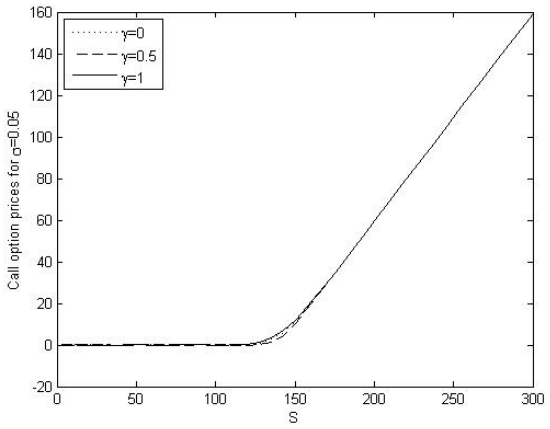

(a) $\sigma = 0.05$

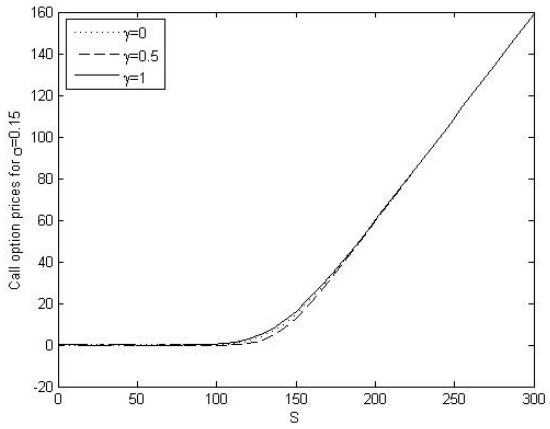

(b) $\sigma = 0.15$

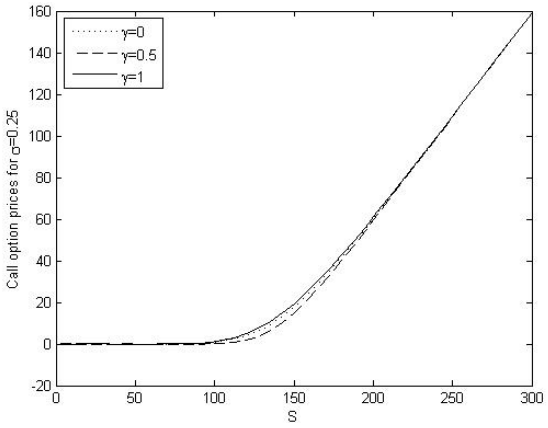

(c) $\sigma = 0.25$

Figure 5.65: The effect of γ on European call option price for different values of σ over a range of S values following the mfBm volatility diffusion process and other chosen parameters in Table 5.1.

Therefore, we may conclude that changing the assumptions of stock return dynamics have significant impact towards the European call option price, particularly when share price is near the strike price. On the other hand, altering the volatility diffusion assumptions mainly affect the value of call option price for large values of S and this becomes apparent when parameters α and β are particularly high.

5.4 Concluding remarks

This chapter discusses the numerical analysis and results of the general stochastic volatility model using the finite element method. In particular with the stochastic volatility model, since the non-linear PDE is based on S and σ, adopting the finite element method will assist in a faster and more accurate numerical analysis. Similar to Chapter 4, we have analysed the various parameters in the stochastic volatility model when assuming different S and σ diffusion processes. We also compare the difference between assuming constant and stochastic volatility model. In the stochastic volatility model, the European call option price depends on the additional parameters α and β instead of only on a constant σ. In this chapter, we have considered different combinations of stock and volatility diffusion models using 'fractal' dynamics and log-normal in both diffusion processes.

The numerical results show that the effects of altering the assumptions of the stock dynamic processes and the stochastic volatility models on the European call option values are similar to that discussed in Chapter 4. The change in assumptions of the stock dynamic diffusions affects mostly the European call option price for S values close to the strike price (K). On the other hand, the effect of changing the volatility diffusion processes influences the European call option price for high values of S. The degree of influence depends on the parameters α, β, σ and other additional parameters (H_1 and ε) when assuming fractional and mixed fractional Brownian motion model. The effect of the parameter β is much greater than the effect of α and this also depends on the range of values of σ. The effect of changing the volatility diffusion process to fBm or mfBm by altering ε reduces the value of the European call option for greater value of S. In addition, increasing H_1 leads to lower values of the call option price. However, the effect of changing ε and H_1 again varies depending on the value of α, β and σ. This chapter assists in better understanding the influence of the additional parameters and how it should be considered in the European option pricing model. This also gives an indication on how the various diffusion processes assumed for S and σ will affect the value of European call option.

CHAPTER 6

Application of the general option model to S&P 500 Mini Option Index

6.1 General

In Chapter 4 and Chapter 5, we have discussed the numerical analysis and results of the general constant and stochastic volatility option models which take into account transaction costs. We have examined the effect of various parameters on the European call option price and their relationships, and this knowledge may be verified against real financial data.

There are still numerous questions surrounding the existence of long memory in stock returns and/or its volatility. Researchers continue to investigate the existence of long memory and examine how this may be included in financial models, particularly derivative models. In this thesis, we have constructed a general model which could capture the possibility of long memory in stock returns and/or its volatility through chosen parameters. In this chapter, we will validate the model by comparing the model predictions with real financial data and predictions by other existing models, in order to determine the model which is superior in modeling the European call option market data.

6.2 Real market vs model

In this section, we will compare the European call option market price against each of the different models assumed. We will start by calibrating the real call option price against the basic Black-Scholes Merton model of assuming gBm diffusion process, constant volatility, no transaction costs and continuous dynamic hedging. In deciding which model best reflects the market data, we employ the sum of squared errors (SSE). A lower SSE value indicates that the model is a better fit in approximating the actual call option price.

The sum of squared errors is calculated by

$$SSE = \sum_{i=1}^{n}((y_i - \hat{y}_i))^2, \tag{6.1}$$

where y_i is the observed market value and $\hat{y}_i$ is the model calculated value of European call option price. In this thesis, we have used XSP (S&P 500 Mini) call option index as the comparison to real observed market data. We have obtained the European call option data of XSP as at 6^{th} of July 2016 sourced from Yahoo Finance [79]. The XSP data is listed in Table 6.1.

Table 6.1: XSP European call options expire as at 16 September 2016 [79]

K	Symbol	Bid	Ask	Price
130	XSP160916C00130000	68.6	78.2	73.4
150	XSP160916C00150000	54.15	63.65	58.9
160	XSP160916C00160000	39.95	49.45	44.7
165	XSP160916C00165000	35.35	44.83	40.09
175	XSP160916C00175000	28.75	37.95	33.35
180	XSP160916C00180000	24.3	33.8	29.05
187	XSP160916C00187000	18.23	27.73	22.98
190	XSP160916C00190000	15.43	24.98	20.205
194	XSP160916C00194000	10.8	20.18	15.49
198	XSP160916C00198000	11.85	13.16	12.505
199	XSP160916C00199000	11.17	12.46	11.815
200	XSP160916C00200000	7.4	16.9	12.15
213	XSP160916C00213000	3.73	4.45	4.09
215	XSP160916C00215000	1.13	2.18	1.655
216	XSP160916C00216000	2.3	3.15	2.725

Note that for the purpose of our analysis, we are only interested in the fair price of European call option. Thus, we take the average of bid and ask price to get the price as in column (5) of Table 6.1. The index price of XSP on 6 July 2016 is noted to be \$208.86 [68]. Note that in the real market, the risk free interest rate is known. In this case, we will use the 3 months US Treasury Bill rate as its assumed risk free rate for our calibration. We are able to attain the 3 months US Treasury Bill rate on 6 July 2016 which is 0.279% [80]. The time to maturity is calculated based on the time period between 6 July 2016 to the date of expiry of the European call option.

6.2.1 Application of the 1D general constant volatility model

We first calibrate the data in Table 6.1 against the analytical classic Black Scholes model. For the purpose of parameter estimations and in order to avoid the errors from the numerical results, we use the analytical results to compare the different models outline above. As previously mentioned in Section 2.2 and 3.3, Wang *et al.* [72–74] have attained the complete analytical solution of European call option pricing assuming fractal dynamics with transaction costs by postulating that $\Gamma = \frac{\partial^2 c}{\partial S^2}$ is always positive for European call option price, similar to when no transaction costs are present. Hence in this chapter, we adopt the analytical approach for parameter estimation. Assuming that Γ is always positive, similar to Wang *et al.* and using equation (4.14), we are able to attain the analytical solution which resembles the Black Scholes model with modified volatility given by:

$$\tilde{\sigma^2} = (\gamma^2 + (1-\gamma)^2 \delta t^{2H-1})[\sigma^2(1+\kappa)]. \tag{6.2}$$

The analytical solution is given as:

$$C(t,S) = SN(d_1) - Ke^{-r(T-t)}N(d_2), \tag{6.3}$$

where

$$d_1 = \frac{ln\frac{S}{K} + (r + \frac{\tilde{\sigma}^2}{2})(T-t)}{\tilde{\sigma}\sqrt{T-t}}, \quad d_2 = d_1 - \tilde{\sigma}\sqrt{T-t}. \tag{6.4}$$

We calibrate the data in Table 6.1 against the classical Black-Scholes model with $\gamma = 1$, $k = 0$, $\delta t = 1e-6$ and constant volatility. Even in the classical Black-Scholes model, the issue lies in choosing the right parameter for calculation especially the volatility parameter (σ). Our approach is to calibrate the call option in Table 6.1 and using the Matlab function 'fminbnd' to find the σ parameter that will give the lowest SSE. The resulting parameter σ of the calibration of Black-Scholes model is summarised in Table 6.2.

In Chapter 4, we concluded that the inclusion of transaction cost (k) and consequently δt are crucial in determining the fair price of call option. Thus, further calibration is performed using the Matlab function 'fmincon' to find the combination of parameters of $k, \delta t$ and σ which will minimise the SSE of the general model assuming gBm stock dynamic process with transaction costs. The transaction cost of trading the shares should be known. However, since we do not have the initial value of k, we will use the calibration against the basic model to first find the approximate value of k. We will then fix this value assuming that the transaction costs are the same throughout the three models. Thereafter, appropriate parameters of H and γ which will minimise the SSE are estimated. Table 6.2 summarises the given parameters and the calibrated parameters.

Table 6.2: Parameters used in the simulation of XSP call option prices and the minimum SSE by different models

	S_0	T	r	k	δt	γ	σ	H	SSE
gBm	208.86	$\frac{72}{365}$	0.00279	0.0	1e-6	1	0.1494	0.5	68.7090
gBm	208.86	$\frac{72}{365}$	0.00279	0.0078	0.0952	1	0.1304	0.5	68.7090
fBm (I)	208.86	$\frac{72}{365}$	0.00279	0.0078	0.0002	0	0.0426	0.5764	68.7090
fBm (II)	208.86	$\frac{72}{365}$	0.00279	0.0078	0.1012	0	0.1505	0.5609	68.7090
mfBm (I)	208.86	$\frac{72}{365}$	0.00279	0.0078	0.0001	0.2067	0.0329	0.5878	68.7090
mfBm (II)	208.86	$\frac{72}{365}$	0.00279	0.0078	0.0421	0.3703	0.1814	0.5306	68.7090

The results in Table 6.2 show that all the three models described in Chapter 4 as well as the classical Black-Scholes model have identical values of sum of squared errors. This indicates that for all models, the parameters listed in Table 6.2 are equally capable in reflecting the real data in Table 6.1. Many other combinations of parameters may be attained as well. However, the first calibrated parameters shown in Table 6.2 for fBm (I) and mfBm (I) are odd, since the δt parameter is significantly small even when transaction

costs are present. The corresponding cost parameter (κ) will also be high and hence in reality these parameters will not be applicable. This argument is reinforced by Hoggard *et al.* [65] who analysed the significance of cost parameter (κ) of equation (4.14) and identified the following cases:

(i) $\kappa >> 1$: The effect of transaction costs (k) is extremely large. Large value of δt is required to counteract the effect of k.

(ii) $\kappa = O(1)$: Assuming the high liquidity in the market nowadays, the effect of transaction costs is still relatively high in practical sense.

(iii) $\kappa << 1$: The transaction costs will affect the price only marginally. Hence, this will be the most realistic case.

Therefore, the alternative parameters for the fBm (II) and mfBm (II) models are instead given. From here, further analysis are required to investigate on which the assumed model will provide a better approximation using the parameters found as listed in Table 6.2.

6.2.2 Application of the 2D general stochastic volatility model

For the application of general stochastic volatility model, we will use the transaction costs ($k = 0.0078$) assumed in the previous section and calibrate other required parameters. Similar to the previous section, for the purpose of parameter calibrations, we will use the analytical solution of European call option price for a general stochastic volatility model by assuming positive $\Gamma = \dfrac{\partial^2 c}{\partial S^2}$ similar to Wang [74]. Using this assumption and the idea of Feynman-Kac, we attain the analytical solution to the PDE problems of equation (3.51) as the following:

$$\begin{aligned}
&C(t,S) = E[SN(d_1) - Ke^{-r(T-t)}N(d_2)],\\
&d_1 = \frac{ln\frac{S}{K} + (r + \frac{\tilde{\sigma}^2}{2})(T-t)}{\tilde{\sigma}\sqrt{T-t}}, \quad d_2 = d_1 - \tilde{\sigma}\sqrt{T-t},\\
&\tilde{\sigma}^2 = \frac{\int_t^T \hat{\sigma}^2 d\tau}{T-t},\\
&\hat{\sigma}^2 = \sigma(\gamma^2 + (1-\gamma)^2\delta t^{2H-1})\left(1 + k\sqrt{\frac{8}{\pi\sigma\delta t(\gamma^2 + (1-\gamma)^2\delta t^{2H-1})}}\right).
\end{aligned} \tag{6.5}$$

The volatility (σ) parameter is assumed to follow the general diffusion process as equation (3.32). Using the proposition as of equation (2.24) similarly to [74], we may write equation (3.32) as

$$\begin{aligned}
d\sigma_\tau &= \alpha\sigma d\tau + \beta\sigma[\varepsilon dW_{\sigma_\tau} + (1-\varepsilon)\delta t^{H-\frac{1}{2}} dW_{\sigma_\tau}]\\
&= \alpha\sigma d\tau + \beta\sigma(\varepsilon + (1-\varepsilon)\delta t^{H_1-\frac{1}{2}})dW_{\sigma_\tau}.
\end{aligned} \tag{6.6}$$

Thus, the corresponding analytical solution of the above equation is

$$\sigma = \sigma_0 e^{\alpha t + \beta(\varepsilon + (1-\varepsilon)\delta t^{H_1-\frac{1}{2}})W_t}, \tag{6.7}$$

where W_t follows a standard Brownian motion.

Table 6.3: Model parameters used in the simulation of XSP call option prices and the minimum SSE by the various stochastic volatility models

Model SSE	δt	σ_0	γ	H	ε	H_1	α	β
gBm S_t-**gBm** σ_τ 68.6762	0.1399	0.0162	1	0.5	1	0.5	0.2699	0.499
gBm S_t-**fBm** σ_τ 68.6844	0.071	0.0155	1	0.5	0	0.5016	0.1416	0.1807
gBm S_t-**mfBm** σ_τ 68.6945	0.0493	0.0144	1	0.5	0.7389	0.8768	0.1327	0.3704
fBm S_t-**gBm** σ_τ 68.6080	0.1515	0.0173	0	0.5049	1	0.5	0.0425	0.4154
fBm S_t-**fBm** σ_τ 68.6968	0.126	0.02	0	0.5404	0	0.81	0.0247	0.2817
fBm S_t-**mfBm** σ_τ 68.6957	0.0882	0.0169	0	0.5111	0.0222	0.6071	0.0388	0.2138
mfBm S_t-**gBm** σ_τ 68.6984	0.1012	0.0297	0.313	0.5111	1	0.5	0.0018	0.3818
mfBm S_t-**fBm** σ_τ 68.6889	0.1944	0.0202	0.0149	0.5314	0	0.9016	0.0002	0.4988
mfBm S_t-**mfBm** σ_τ 68.6927	0.0752	0.032	0.2822	0.5502	0.926	0.863	0.0508	0.4975

The results in Table 6.3 show that all assumed stochastic volatility models are relatively similar in reflecting the real data of XSP. The SSE of each assumed model only varies slightly, thus no conclusion can yet be made on which stochastic model is the most suitable one. Hence, further validations are required, similarly as the case for 1D general constant volatility model. The calibrated parameters shown in Table 6.3 are consistent with the findings in the previous Chapter 5, where we have concluded that the parameter β contributes more significantly on the European call option price compared to α.

From comparing the results of constant volatility model in Table 6.2 and stochastic volatility model in Table 6.3, it is apparent that the latter is better performing. The minimum SSE for the calibration of the constant volatility model results in a constant and a minimum of 68.7090. On the other hand, assuming stochastic volatility model produces a varied lower SSE values for all the assumed models. This indicates that the stochastic volatility models allow for greater flexibility of the parameters that is better suited to the market. The stochastic nature of the model explains the varied outcomes of the SSE values. In this chapter, we have considered 350 simulations of σ path to attain the value of European call option. The number of simulations of σ paths required to achieve convergence when assuming gBm for both stock return and its volatility is sufficient for the purpose of validation (Figure 6.1). However, more simulations should be performed to improve precisions.

6.3 Further validation

In the previous section, we have attained the calibrated parameters which minimise SSE between the real data listed in Table 6.1 and the results obtained by the different models. In this section, we will perform further analysis to validate the models against a different data set as listed in Table 6.4. Table 6.4 shows the XSP European call option index price for various value of strike price (K) as at 6 July 2016 and will expire as at 16 December 2016 [79]. The index price as at 6 July 2016 is \$208.86 [68]. We use this data to examine which models best reflect the real market by using the calibrated parameters from the previous section. Using the model parameters attained, we calculate the sum of squared error between each different models and the real XSP data in Table 6.4.

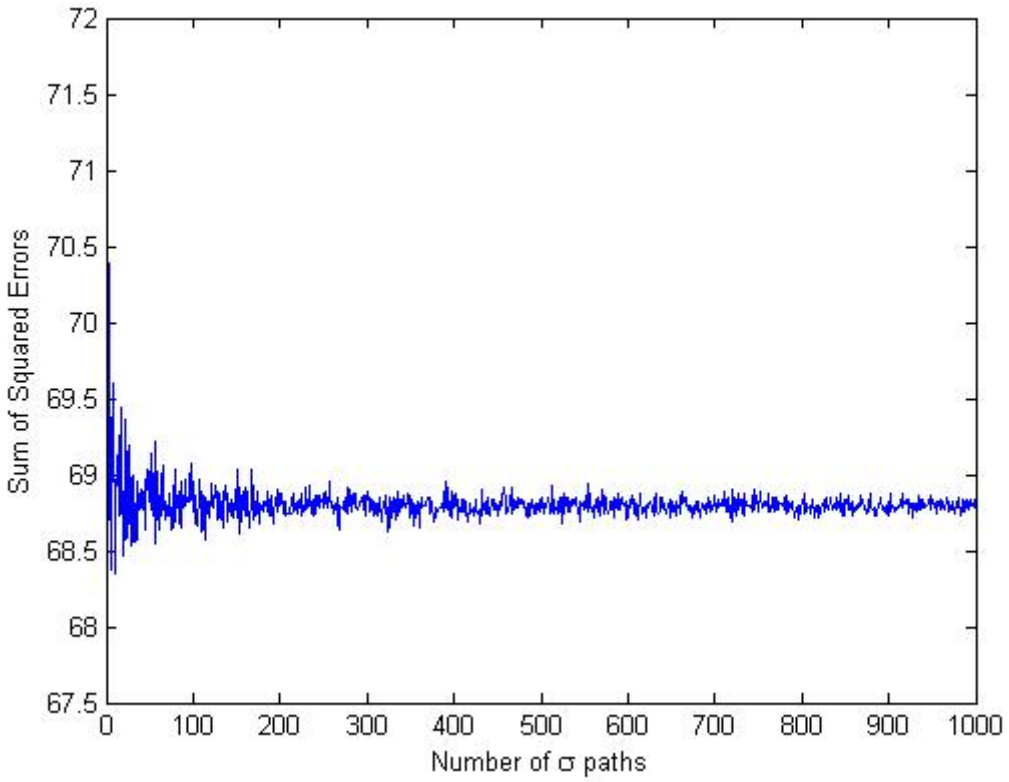

Figure 6.1: Convergence analysis of SSE when numerical analysis is performed assuming gBm for stock return and volatility.

Table 6.4: XSP European call options expire as at 16 December 2016 [79]

K	Symbol	Bid	Ask	Price
170	XSP161216C00170000	35.45	37.25	36.35
175	XSP161216C00175000	31.22	33.08	32.15
180	XSP161216C00180000	29.5	30.7	30.1
181	XSP161216C00181000	28.65	29.5	29.075

Table 6.4: XSP European call options expire as at 16 December 2016 [79]

K	Symbol	Bid	Ask	Price
182	XSP161216C00182000	25.54	27.27	26.405
186	XSP161216C00186000	22.39	24.07	23.23
190	XSP161216C00190000	21.06	22.42	21.74
194	XSP161216C00194000	16.64	18.02	17.33
195	XSP161216C00195000	15.95	17.3	16.625
198	XSP161216C00198000	13.95	15.13	14.54
200	XSP161216C00200000	10.38	11.05	10.715
202	XSP161216C00202000	11.43	12.5	11.965
205	XSP161216C00205000	7.36	8	7.68
206	XSP161216C00206000	8.17	8.88	8.525
210	XSP161216C00210000	7.63	8.29	7.96
214	XSP161216C00214000	5.01	6.04	5.525
215	XSP161216C00215000	4.9	5.53	5.215
218	XSP161216C00218000	3.28	4.49	3.885
220	XSP161216C00220000	2.62	3.25	2.935

6.3.1 Validation on the 1D general constant volatility model

Table 6.5: Parameters used in the simulation of XSP call option prices and the resulting SSE by different models

	S_0	T	r	k	δt	γ	σ	H	SSE
gBm	208.86	$\frac{163}{365}$	0.00279	0.0	1e-6	1	0.1494	0.5	37.9936
gBm	208.86	$\frac{163}{365}$	0.00279	0.0078	0.0952	1	0.1304	0.5	37.7539
fBm (I)	208.86	$\frac{163}{365}$	0.00279	0.0078	0.0002	0	0.0426	0.5764	30.0603
fBm (II)	208.86	$\frac{163}{365}$	0.00279	0.0078	0.1012	0	0.1505	0.5609	37.7239
mfBm (I)	208.86	$\frac{163}{365}$	0.00279	0.0078	0.0001	0.2067	0.0329	0.5878	25.8378
mfBm (II)	208.86	$\frac{163}{365}$	0.00279	0.0078	0.0421	0.3703	0.1814	0.5306	37.7109

The results show that the standard Black-Scholes model with geometric Brownian motion diffusion process ($\gamma = 1$), continuous hedging and no transaction costs, produces the highest resulting SSE compared to the other models when validated against the new data (Table 6.5). When transaction costs are taken into account, the SSE value is slightly lower. However, when we assume fractional Brownian motion as its stock dynamic and use the first calibrated parameters (I), there is a significant drop in SSE to 30.0603 compare to the classical Black Scholes model with or without transaction costs. The SSE drops further when the mixed fractional Brownian motion model with the corresponding first parameters (I) as shown in Table 6.5 is assumed. These results indicate that the model which assumes mfBm better reflects the XSP European call option index data compared

to the one with fractional or geometric Brownian motion diffusion processes. Figure 6.2 also reinforced the results of Table 6.5.

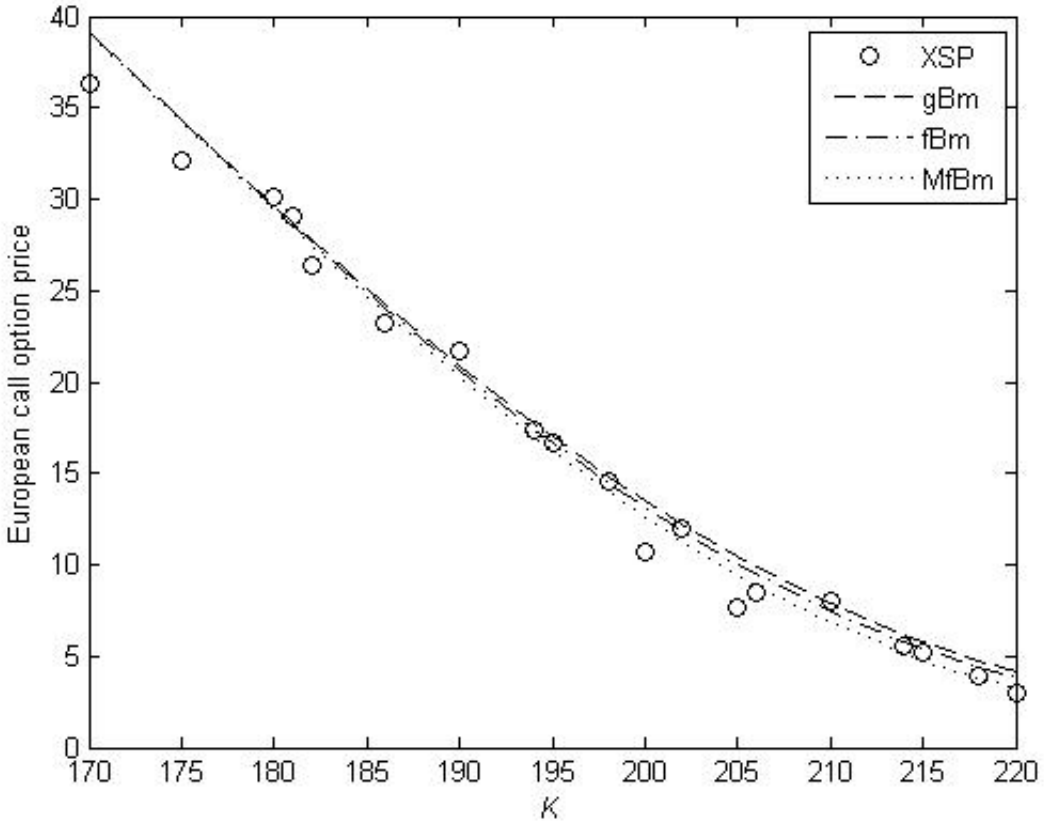

Figure 6.2: XSP European call option data expiring as at 16 December 2016 against the calculated call option price of all the three models using the calibrated parameters for gBm with transaction costs, fBm (I) and mfBm (I) as shown in Table 6.2.

However, as previously mentioned, these parameters are not applicable and the alternative parameters (II) should instead be used for validation. When assuming the second set of parameters for fBm and mfBm, the SSE for both models are lower compared to the original Black-Scholes model which assumes gBm stock dynamic diffusion process. The difference in results is not very significant (Figure 6.3). The results above show no clear answer of which model best reflects the market. Although the SSE is lower when mfBm model is assumed, the difference is not highly significant when using the second set of calibrated parameters compared to the one with the first set of parameters. One possible conclusion is that the additional parameters assumed in both fBm and mfBm models allow for more flexibility in the calibration of parameters, thus provide more alternatives of parameter combinations which would reduce the SSE. Further validations on other

different sets of data are required before we can be certain of which is the better model.

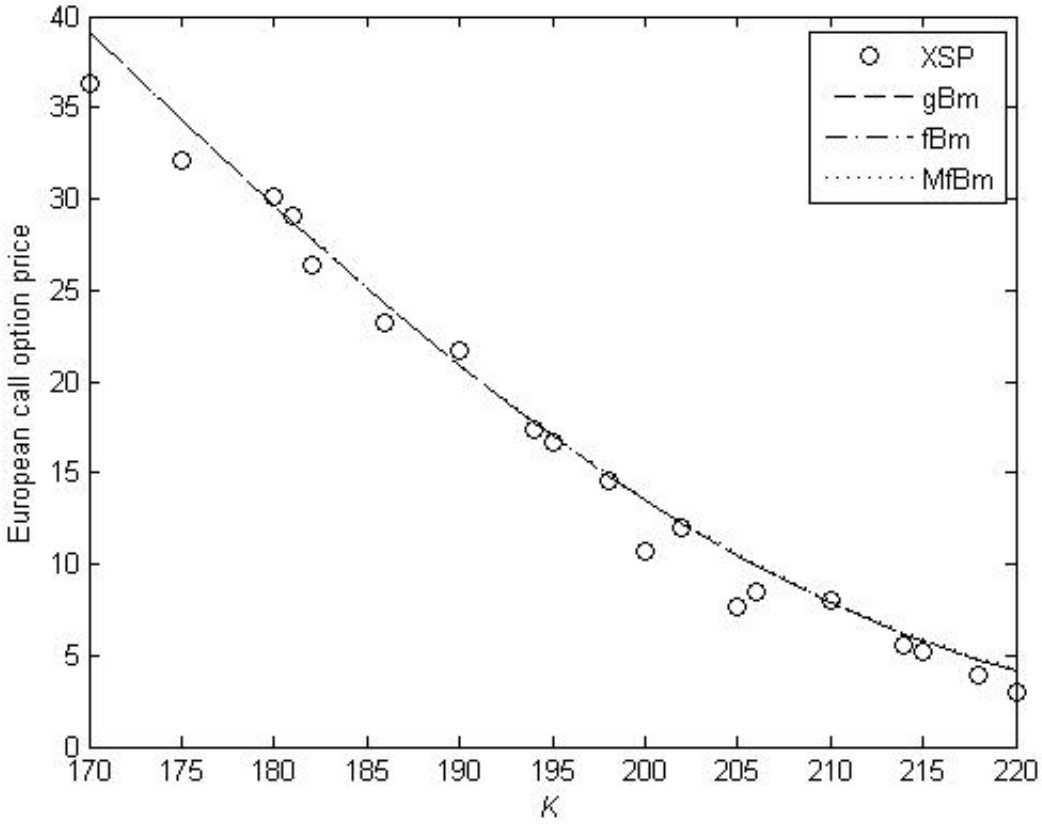

Figure 6.3: XSP European call option data expiring as at 16 December 2016 against the calculated call option price of all the three models using the calibrated parameters for gBm with transaction costs, fBm (II) and mfBm (II) as shown in Table 6.2.

6.3.2 Validation on the 2D general stochastic volatility model

Similar process of validation is applied on the general stochastic volatility models using the same data listed on Table 6.4 and using the same parameters of $S_0 = \$208.86$, $T = \frac{163}{365}$, $r = 0.00279$ and $k = 0.0078$ as the previous subsection. The results are summarised in Table 6.6.

Table 6.6: Parameters used in the simulation of XSP call option prices and the resulting SSE by the various stochastic volatility models

Model SSE	δt	σ_0	γ	H	ε	H_1	α	β
gBm S_t**-gBm** σ_τ 37.2946	0.1399	0.0162	1	0.5	1	0.5	0.2699	0.499
gBm S_t**-fBm** σ_τ 36.4503	0.071	0.0155	1	0.5	0	0.5016	0.1416	0.1807
gBm S_t**-mfBm** σ_τ 35.5018	0.0493	0.0144	1	0.5	0.7389	0.8768	0.1327	0.3704
fBm S_t**-gBm** σ_τ 35.2007	0.1515	0.0173	0	0.5049	1	0.5	0.0425	0.4154
fBm S_t**-fBm** σ_τ 35.1500	0.126	0.02	0	0.5404	0	0.81	0.0247	0.2817
fBm S_t**-mfBm** σ_τ 34.6755	0.0882	0.0169	0	0.5111	0.0222	0.6071	0.0388	0.2138
mfBm S_t**-gBm** σ_τ 34.6224	0.1012	0.0297	0.313	0.5111	1	0.5	0.0018	0.3818
mfBm S_t**-fBm** σ_τ 34.7451	0.1944	0.0202	0.0149	0.5314	0	0.9016	0.0002	0.4988
mfBm S_t**-mfBm** σ_τ 33.8647	0.0752	0.032	0.2822	0.5502	0.926	0.863	0.0508	0.4975

The resulting SSE of the assumed stochastic volatility model is lower compared to those of the constant volatility model shown from the results in Tables 6.5 and 6.6. The reduction in SSE value of assuming stochastic volatility model in Table 6.6 is relatively more significant compared to the one in the constant volatility model in Table 6.5. These results are also reinforced by Figures 6.4-6.6.

For each assumption of stock return dynamic processes, the effect of changing the volatility diffusion processes to include fractal dynamics reduces the SSE of the corresponding model. The results show that assuming the mfBm volatility process also produces the lowest SSE for each case of stock dynamic processes. Hence, this suggests that assuming mfBm volatility diffusion processes improves the ability of the model, regardless of the assumptions of the stock dynamics. The results show that there is a small change in European call option value for different assumptions of volatility diffusion processes, corresponding to each assumption of stock dynamics (Figures 6.4-6.6).

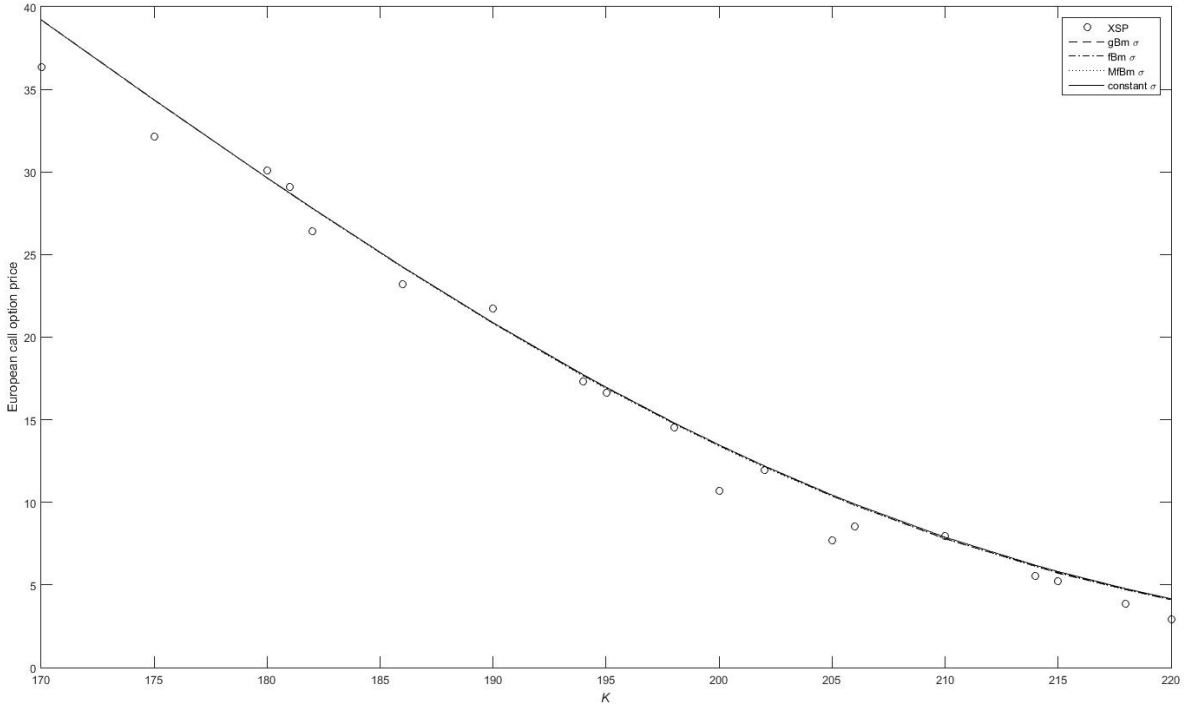

(a) $170 \leq K \leq 220$

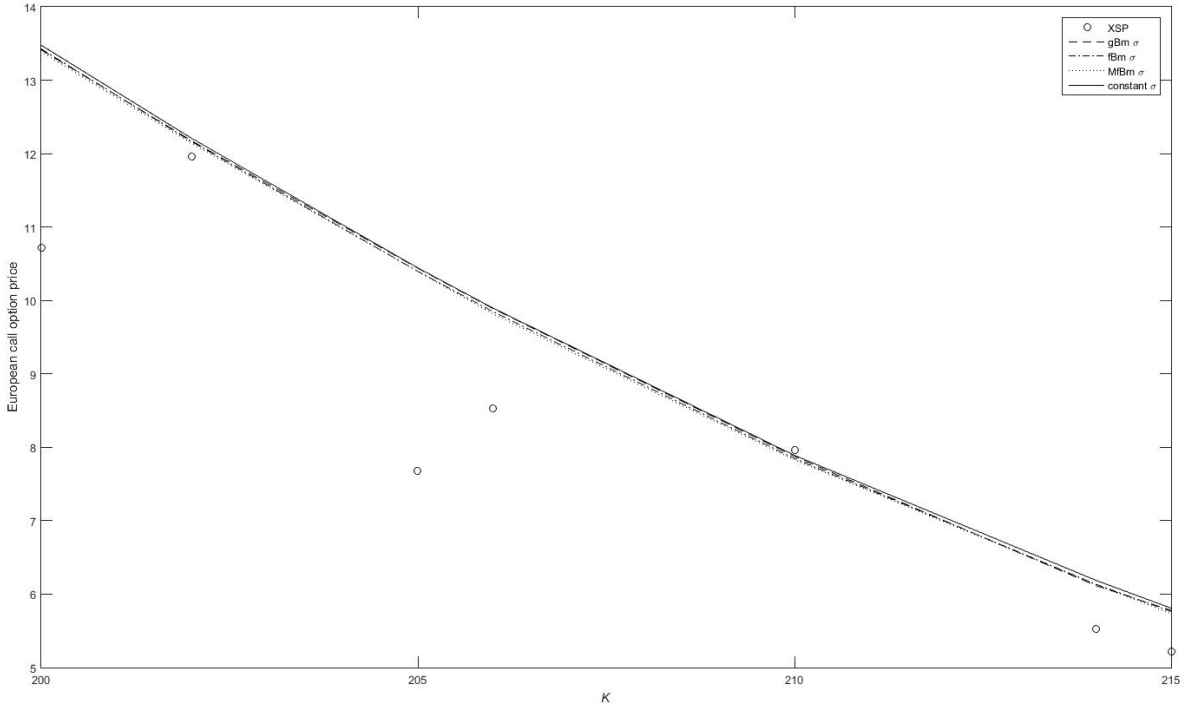

(b) $200 \leq K \leq 215$

Figure 6.4: XSP European call option data expiring as at 16 December 2016 against the calculated call option price of all three different assumptions of σ_τ and constant volatility when stock return follows the gBm model using the calibrated parameters as shown in Table 6.3 and 6.2 respectively.

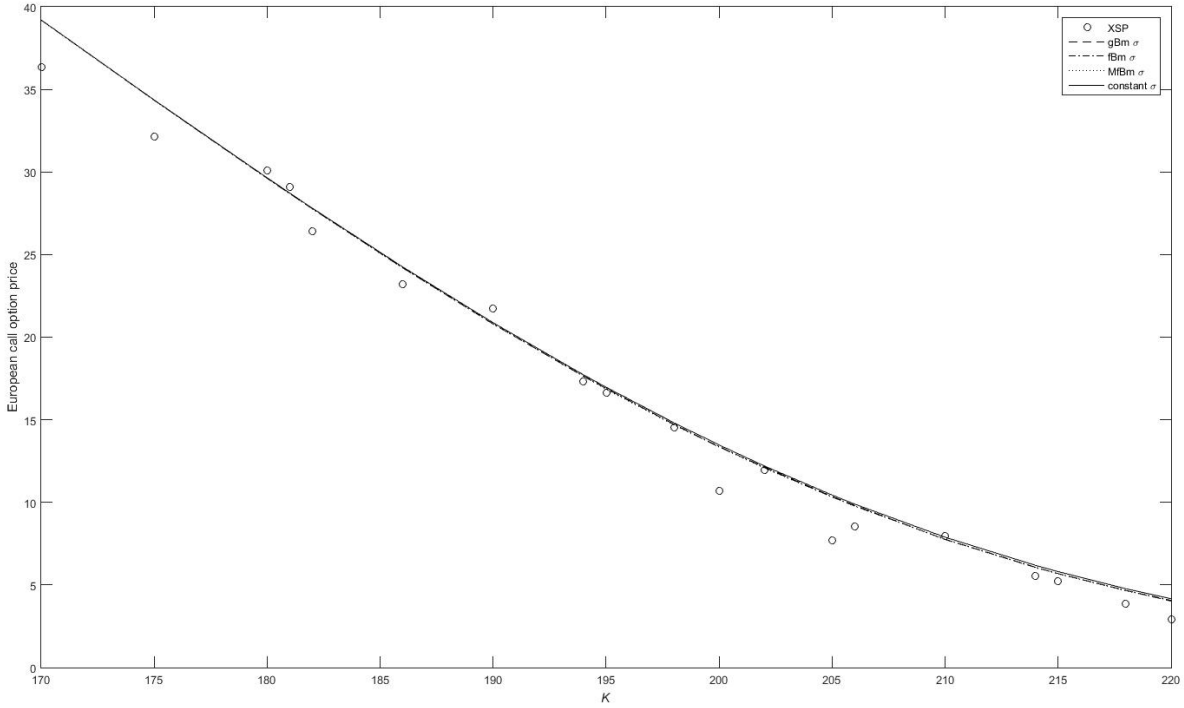

(a) $170 \leq K \leq 220$

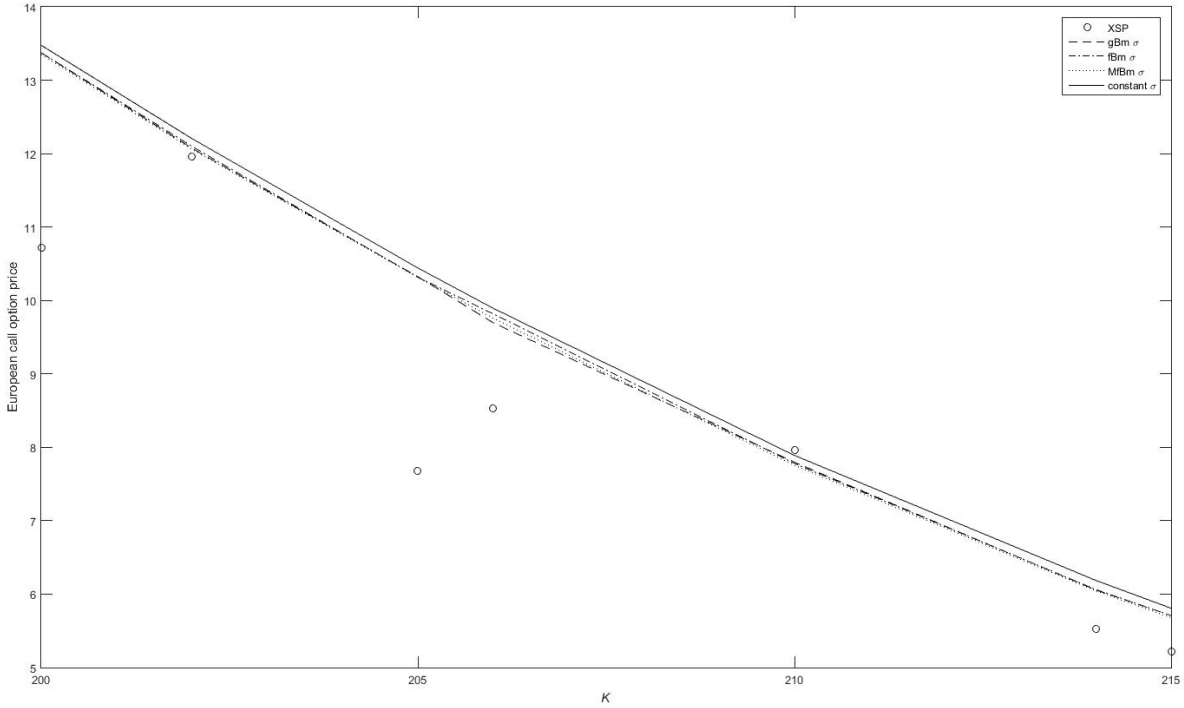

(b) $200 \leq K \leq 215$

Figure 6.5: XSP European call option data expiring as at 16 December 2016 against the calculated call option price of all three different assumptions of σ_τ and constant volatility when stock return follows the fBm model using the calibrated parameters as shown in Table 6.3 and Table 6.2 respectively.

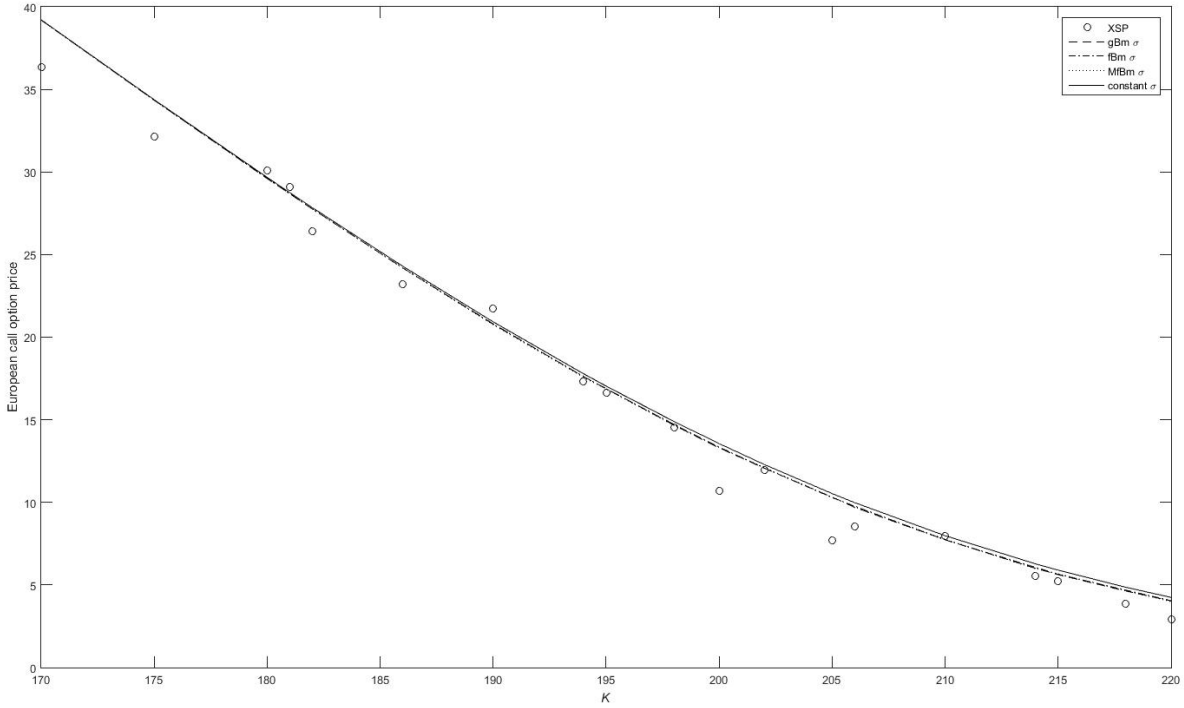

(a) $170 \leq K \leq 220$

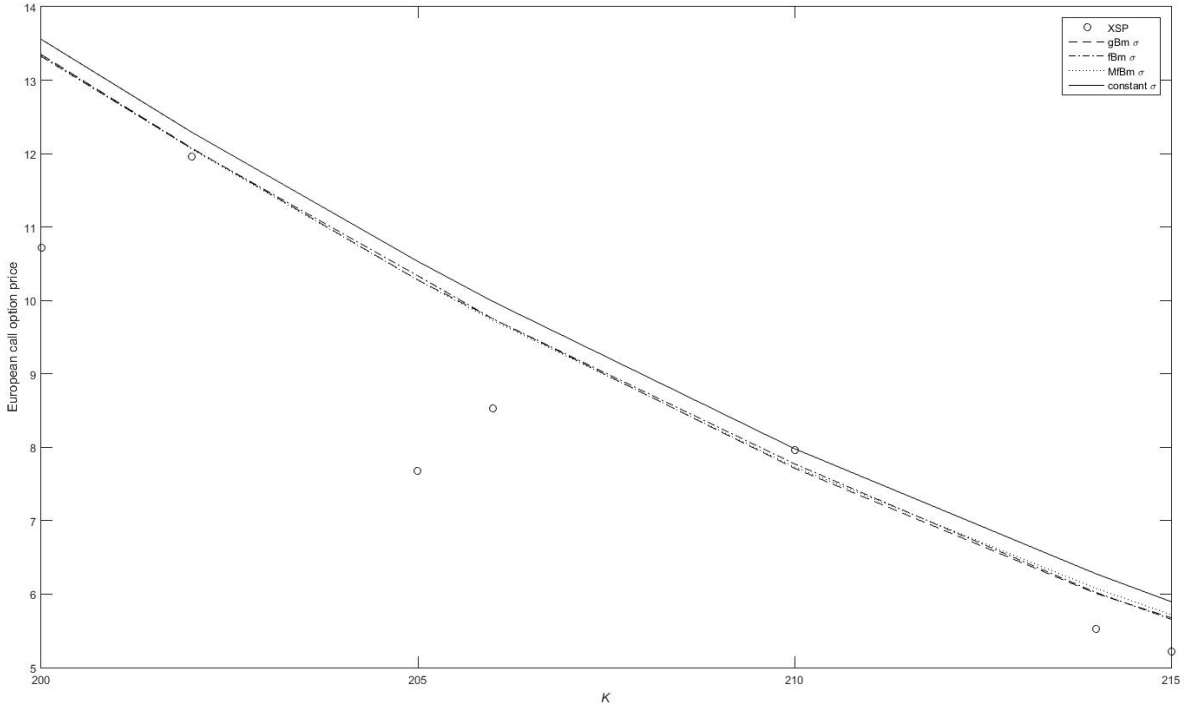

(b) $200 \leq K \leq 215$

Figure 6.6: XSP European call option data expiring as at 16 December 2016 against the calculated call option price of all three different assumptions of σ_τ and constant volatility when stock return follows the mfBm model using the calibrated parameters as shown in Table 6.3 and 6.2 respectively.

For each assumption of volatility diffusion processes, the effect of adopting fractal dynamics in stock return, particularly the mfBm model, reduces the SSE. The results in Table 6.6 also show that assuming a mixed fractional Brownian motion stock return diffusion process, in general, produces the lowest SSE compared to the other S_t model, disregarding any assumptions on its volatility processes. In the previous subsection, we conclude that the effect of altering the stock dynamic diffusion to include fractal dynamics, is almost insignificant. When considering stochastic volatility diffusions process, the effect of changing only the assumed stock return dynamic process becomes more obvious. This result applies for any assumption of its volatility diffusion process. Further analysing Table 6.6 and Figures 6.4-6.9 show that the stock dynamic assumptions have a greater effect on the European call option price compared to changing the volatility diffusion processes. Similar trend is also shown in Chapter 5 when we analyse the various parameters of the general stochastic model.

Furthermore, the combination of mfBm diffusion processes for both stock return and its volatility produces the lowest SSE value (Table 6.6). Hence, this reinforces the significance of considering the general stochastic volatility model in pricing European option as it considers the possibility of fractal dynamics in both stock return and volatility. The effect of fractal dynamics also becomes more apparent when applied to the general stochastic volatility model. The generalized model allows for the flexibility of capturing the real market more closely.

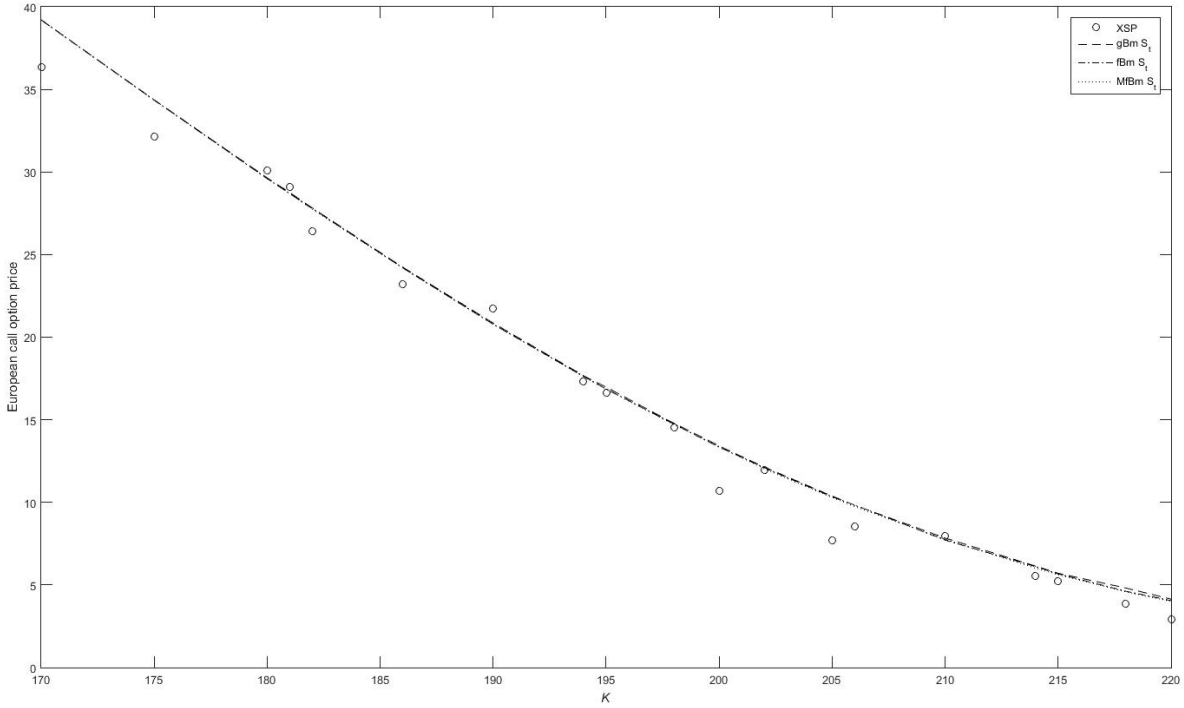

(a) $170 \leq K \leq 220$

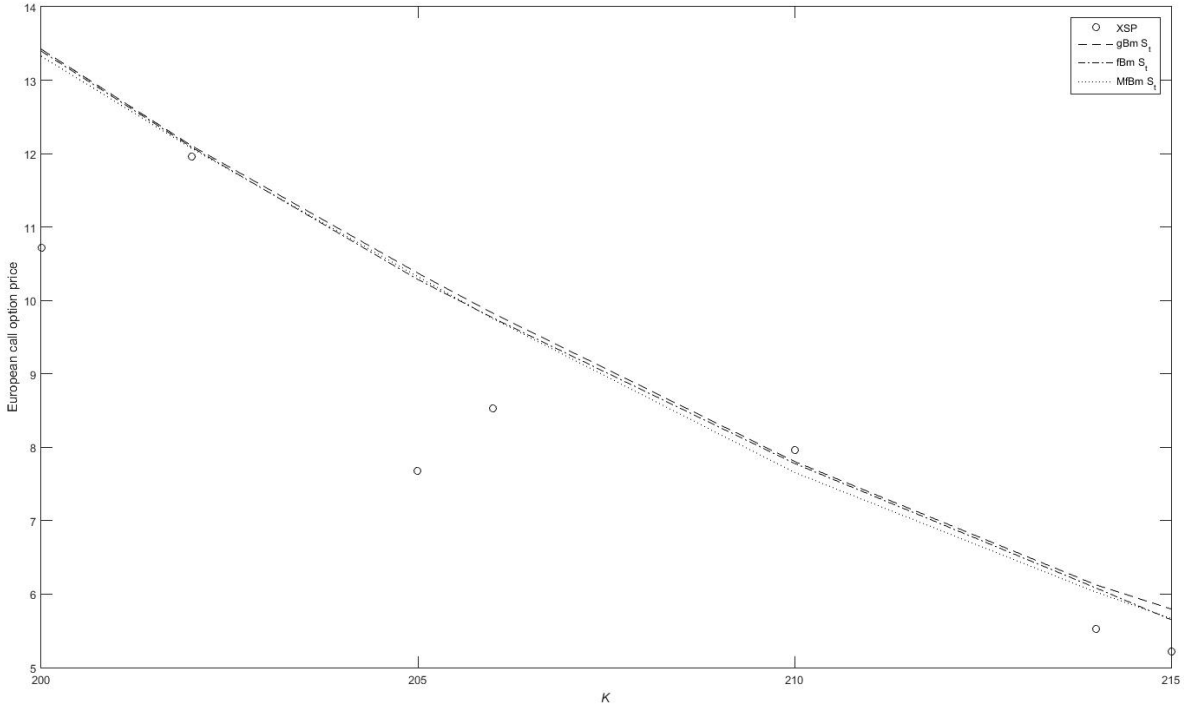

(b) $200 \leq K \leq 215$

Figure 6.7: XSP European call option data expiring as at 16 December 2016 against the calculated call option price of all three different assumptions of S_t when σ_τ follows the gBm model using the calibrated parameters as shown in Table 6.3.

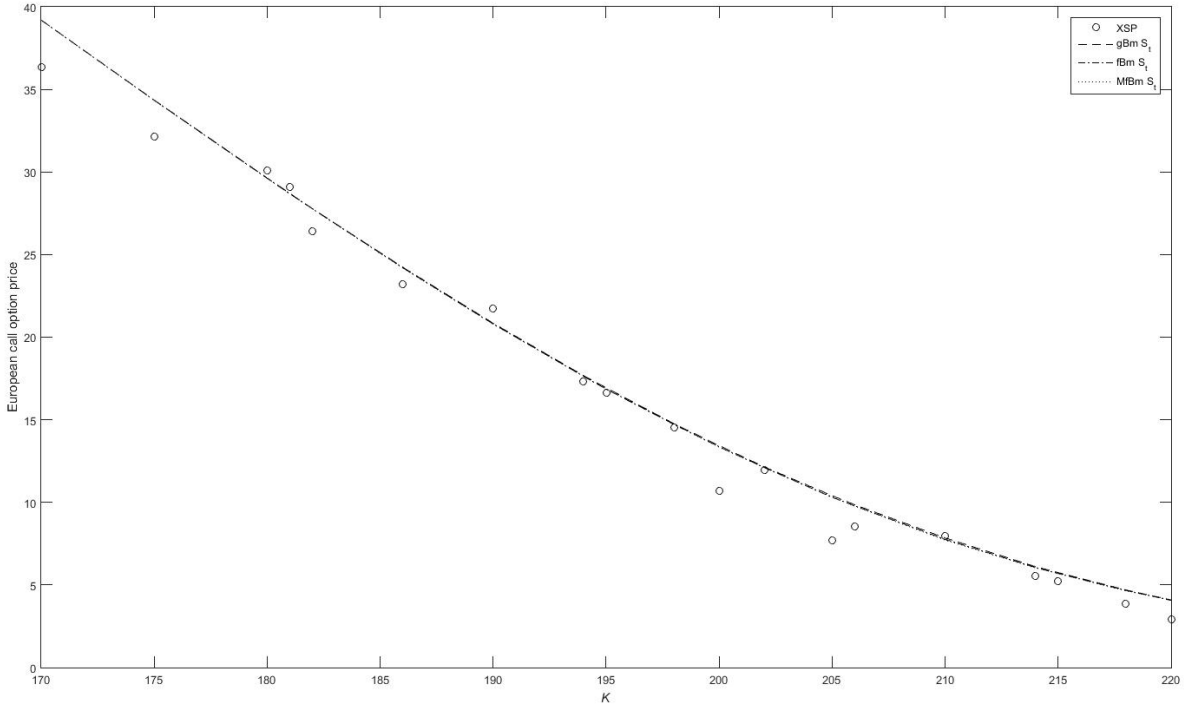

(a) $170 \leq K \leq 220$

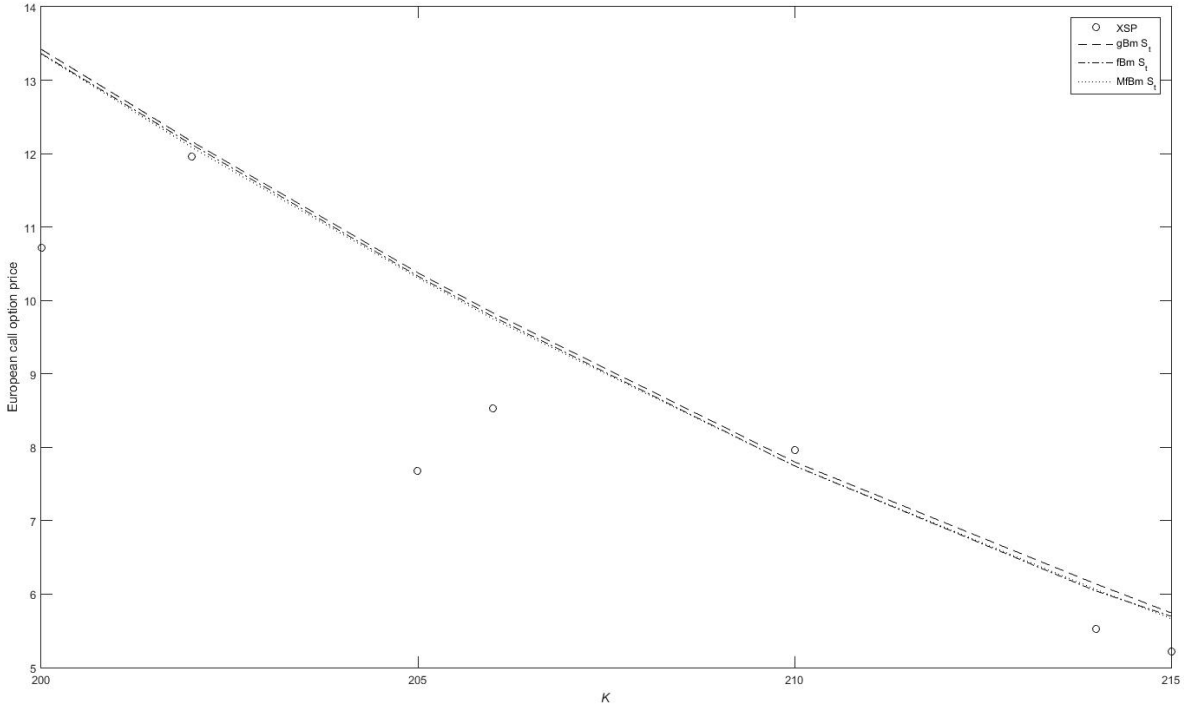

(b) $200 \leq K \leq 215$

Figure 6.8: XSP European call option data expiring as at 16 December 2016 against the calculated call option price of all three different assumptions of S_t when σ_τ follows the fBm model using the calibrated parameters as shown in Table 6.3.

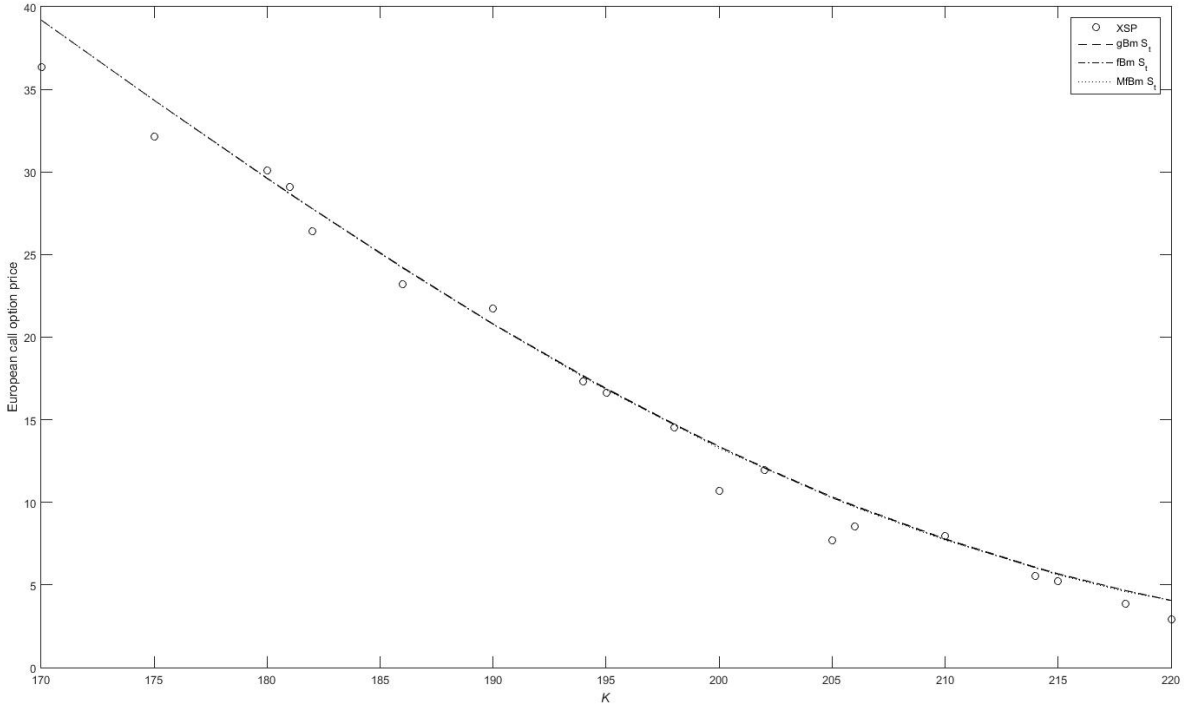

(a) $170 \leq K \leq 220$

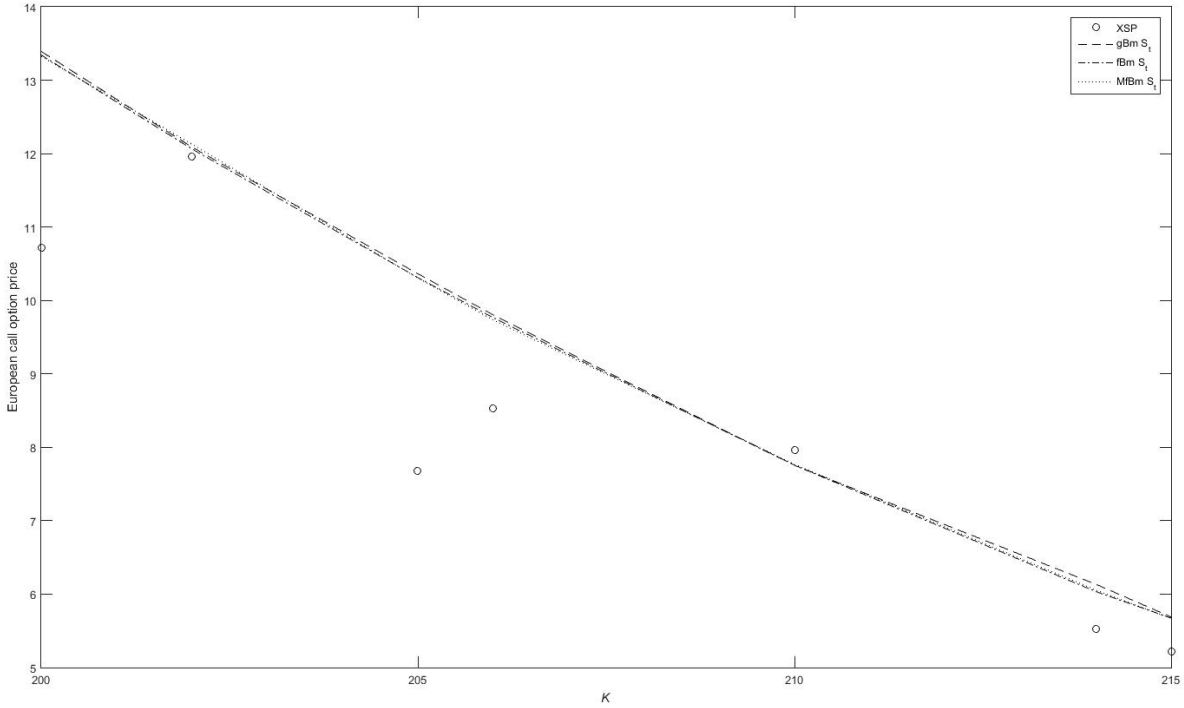

(b) $200 \leq K \leq 215$

Figure 6.9: XSP European call option data expiring as at 16 December 2016 against the calculated call option price of all three different assumptions of S_t when σ_τ follows the mfBm model using the calibrated parameters as shown in Table 6.3

6.4 Concluding remarks

This chapter investigates the performance of each model against the real Mini S&P 500 European call option (XSP) index. We first calibrate the parameters that closely describe the real market and later test it against a new set of data with longer maturity period. The results show that a stochastic volatility model performs better than a constant volatility model. This result is consistent with the literature on stochastic volatility models for option pricing. However, in this chapter, we also include the possibilities of fractal dynamics in both stock return and its volatility. The results show that when fractal dynamics are assumed only in a 1D constant volatility model, the effect of changing the stock dynamic process from gBm to fBm or even to mfBm is not significant. Although we may be able to find the combination of parameters for fBm and mfBm models which will closely reflect the market, the parameters are not realistic and inapplicable in the real world. The difference becomes more apparent when stochastic volatility models are assumed. There is a decrease in sum of squared errors when fractal dynamics are assumed in both stock return and/or the volatility process. Assuming mfBm in both stock return and its volatility gives the best combination in closely reflecting the real market. Hence, this reinforces the relevance of adopting the general stochastic option pricing model which includes fractal dynamics in both assumptions of stock return and volatility diffusion processes. Nevertheless, the consistency and authenticity of the results should be verified using other sources of data as well as calibration processes.

CHAPTER 7

Conclusions and future research directions

7.1 Main contributions of the thesis

Researchers and practitioners have, for many years, attempted to understand the financial market and more extensively the derivative market. The introduction of Black-Scholes model opened up new possibilities and understandings about the nature of derivative products, particularly options. The simplicity and elegant formula of Black Scholes comes with great trade off due to its strict assumptions.

In this thesis, we have improved the option pricing model with more realistic assumptions. Apart from adapting discrete instead of continuous hedging, we have also employed fractal stock dynamics and stochastic volatility assumptions and allowed for transaction costs. The existence of long memory in shares has been intriguing and creates new ideas on financial modeling. Despite the introduction of the fractional Brownian motion process to capture long memory in shares, there is still no definite answer on what the appropriate model to describe the financial market is. Therefore, we have constructed the general model for constant volatility and stochastic volatility model in order to distinctly analyse the effect of various parameters on the European call option and to examine which of these models is more appropriate.

We have also introduced a new parameter in the volatility diffusion process for the general stochastic volatility model so that it allows for the assumption of fractals in dynamic processes. The effect of various parameters on the European call option price is analysed to see its significance on the model itself. We have also demonstrated the use of finite element methods in solving the PDE of financial problems. The use of finite element methods in a financial context has not been widely used compared to finite difference methods of analysing PDE. However, the finite element methods may become more useful and reliable than the finite difference methods for more complex PDE problems as it allows for faster convergence. In this thesis, we have performed the numerical analysis for solving

the PDE of a European call option. Analytical solutions such as those presented by Wang *et al.* [72–74] are possible by postulating that Γ is always positive. Nevertheless, non-linear PDE problems will be unavoidable when solving for portfolios of derivatives or other types of derivatives which involve proportional transaction costs. Thus in these cases, the finite element method will be highly applicable. By performing the numerical analysis, we have also revealed the influence of the model parameters on the option price. It is apparent that these parameters depict the characteristics and behaviour of the European call option price. Furthermore, in order to determine the validity and suitability of each model, we have calibrated these with the real market data of European call option prices. We have compared our model against the S&P 500 Mini option Index (XSP) where the parameters are chosen such that the sum of squared errors between the real data and the predicted model value is minimised. We found that the stochastic volatility model performs better compared to the constant volatility model. Although the effect of altering stock dynamic to fractals in the constant volatility model is insignificant, the results in the 2D stochastic volatility model produce more promising results. The inclusion of mixed fractional Brownian motion in either stock return process or its volatility reduces the calculated sum of squared errors. Hence, the combination of both mfBm in stock return and volatility can better reflect the real financial market.

7.2 Future research directions

The research discussed in the thesis may well be improved and extended for future work. The idea of 'fractals' in finance is relatively new, hence there are still various possibilities to approach this topic. In this thesis, we have used the notion of pathwise integration in fBm as discussed in Section 2.4.2 and the inclusion of transaction cost to eliminate the no-arbitrage requirement. However, this also restricts the way we are able to construct the PDE. Others have used the strategies of semimartingale approximation as discussed in Section 2.5 to construct a long memory stochastic volatility model resembling a Heston model setting. The PDE of the general model derived in this thesis is based on the Hull-White setting assuming that the volatility function is given by $f(Y) = \sqrt{Y}$ and no correlation between the stock return and its volatility. The Heston model has been popularly known as a better stochastic volatility model compared to others. Hence, the long memory stochastic volatility model discussed in this thesis may be further extended to resemble a Heston model where mean-reverting volatility is considered.

In regards to the idea of 'fractals' in share, one may also study the notion of multifractional Brownian motion in which the Hurst parameter varies depending on time. It is a struggle to fully capture the long memory in the share market, as it would mean that we

need to consider the whole past history and not just a finite past. We have only considered mixed fractional Brownian motion in the hope that it diminishes this shortcoming, but multifractional Brownian motion may be able to play an important role in this part.

Further improvement on the numerical analysis content of this thesis may be another focus of future research. In finance, finite element method has not been extensively used compared to the finite difference method. Further work can be done to effectively and efficiently solve the non-linear PDE problems as stated in Chapter 4 and 5.

Another further research that may be of interest is the calibration and validation of the models against the real market data, as well as parameter identification. There are extensive studies that may be performed on this matter including utilising the idea of neural networks and ant colony. This line of research will assist in answering the questions of which models best reflect the real market.

Bibliography

[1] A. Assaf, "Long memory in international equity markets: Revisited," *Applied Financial Economics Letters*, vol. 4, pp. 433–437, 2008.

[2] A. Chronopoulou and F. G. Viens, "Stochastic volatility and option pricing with long memory in discrete and continuous time," *Quantitative Finance*, vol. 12, no. 4, pp. 635–649, 2012.

[3] A. Intarasit and P. Sattayatham, "An approximate formula of European option for fractional stochastic volatility jump-diffusion model," *Journal of Mathematics and Statistics*, vol. 7, no. 3, pp. 230–238, 2011.

[4] A. Melnikov and Y. Mishura, "On pricing and hedging in financial markets with long-range dependence," *Mathematics and Financial Economics*, vol. 5, no. 1, pp. 29–46, 2011.

[5] A. Tversky and D. Kahneman, "Availability: a heuristic for judging frequency and probability," *Cognitive Psychology*, vol. 5, pp. 207–232, 1973.

[6] B. B. Mandelbrot, *The fractal geometry of nature*. New York: Freeman, 1977.

[7] B. Øksendal, "Fractional brownian motion in finance," vol. 12, pp. 2441–2453, 2001.

[8] B.B. Mandelbrot, "The Pareto-Levy law and the distribution of income," *International Economi Review*, vol. 1, no. 2, pp. 79–106, 1960.

[9] ——, "Forecasts of future prices, unbiased markets and "martingale" models," *The Journal of Business*, vol. 39, no. 1, pp. 242–255, 1966.

[10] ——, "When can price be arbitraged efficiently? A limit to the validity of the random walk and martingale models," *The Review of Economics and Statistics*, vol. 53, no. 3, pp. 225–236, 1971.

[11] B.B. Mandelbrot and J.W. Van Ness, "Fractional brownian motions, fractional noises and applications," *SIAM Review*, vol. 10, no. 4, pp. 422–437, 1968.

[12] C. Bender, "Integration with respect to fractional Brownian motion and related market models," Ph.D. dissertation, University of Konstanz, 2003.

[13] ——, "An S-transform approach to integration with respect to a fractional Brownian motion," *Bernoulli*, vol. 9, no. 6, pp. 955–983, 2003.

[14] C. Bender and P. Paarczewski , "Approximating a geometric fractional Brownian motion and related processes via discrete Wick calculus," *Bernoulli*, vol. 16, pp. 389–417, 2010.

[15] C. Bender, T. Sottinen and E. Valkeila, "Arbitrage with fractional Brownian motion?" *Theory of Stochastic Processes*, vol. 13, pp. 23–34, 2006.

[16] C. Necula, "Option pricing in a fractional Brownian motion environment," *Mathematical Reports*, vol. 6, no. 3, 2004.

[17] C.R. Dominique and L.E.S. Rivera-Solis, "Mixed fractional Brownian motion, short and long-term dependence economic conditions: The case of the S&P-500 Index," *International Business and Management*, vol. 3, pp. 1–6, 2011.

[18] D. Kahneman and A. Tversky, "Prospect theory: An analysis of decision under risk," *Econometrica*, vol. 47, pp. 263–291, 1979.

[19] E. Bayraktar, H. V. Poor and K. R. Sircar, "Estimating the fractal dimension of the S&P 500 Index using wavelet analysis," *International Journal of Theoretical and Applied Finance*, vol. 7, no. 5, pp. 615–643, 2004.

[20] E. Derman and N. N. Taleb, "The illusions of dynamic replication," *Quantitative Finance*, vol. 5, no. 4, pp. 323–326, 2005.

[21] E. F. Fama, "Mandelbrot and the stable paretian hypothesis," *The Journal of Business*, vol. 36, no. 4, pp. 420–429, 1963.

[22] E. G. Haug and N. N. Taleb, "Option traders use (very) sophisticated heuristics, never the Black-Scholes-Merton formula," *Journal of Economic Behaviour & Organization*, vol. 77, pp. 97–106, 2011.

[23] E. J. Weber, *A short history of derivative security markets.* Springer, 2008.

[24] E. M. Stein and J. C. Stein, "Stock price distributions with stochastic volatility: An analytic approach," *Review of Financial Studies*, vol. 4, pp. 727–752, 1991.

[25] F. Biagini, Y. Hu, B. Øksendal and T. Zhang, *Stochastic Calculus for Fractional Brownian Motion and Applications.* London, UK: Springer, 2008.

[26] F. Black and M.S. Scholes, "The pricing of option and corporate liabilities," *Journal of Political Economy*, vol. 81, pp. 637–654, 1973.

[27] F. Comte and E. Renault, "Long memory in continuous-time stochastic volatility models," *Mathematical Finance*, vol. 8, no. 4, pp. 291–323, 1998.

[28] F. Comte, L. Coutin and E. Renault, "Affine fractional stochastic volatility models," *Annals of Finance*, vol. 8, pp. 337–378, 2012.

[29] F. Delbaen and W. Schachermayer, "A general version of the fundamental theorem of asset pricing," *Mathematische Annalen*, vol. 300, pp. 463–520, 1994.

[30] F. Y. Ren, X. T. Wang and J. R. Liang, "A proof for French's empirical formula on option pricing," *Chaos Solitons Fractals*, vol. 12, pp. 2441–2453, 2001.

[31] G. Gripenberg and I. Norros, "On the prediction of fractional Brownian motion," *Journal of Applied Probability*, vol. 33, pp. 400–410, 1996.

[32] H. E. Hurst, "Long-term storage capacity in reservoirs," *Transactions of the American Society of Civil Engineers*, vol. 116, no. 1, pp. 770–799, 1951.

[33] H. E. Hurst, R. P. Black and Y. M. Simaika, "Long-term storage: An experimental study," *Journal of the Royal Statistical Society*, vol. 129, no. 4, pp. 591–593, 1966.

[34] H. E. Leland, "Option pricing and replication with transaction costs," *The Journal of Finance*, vol. 40, pp. 1283–1301, 1985.

[35] I. Stewart. (2012, Feb. 12) The mathematical equation that caused the banks to crash. [Online]. Available: https://www.theguardian.com/science/2012/feb/12/black-scholes-equation-credit-crunch

[36] J. B. DeLong, A. Shleifer, L. H. Summers and R. J. Waldmann, "Positive feedback investment strategies and destabilizing rational speculation," *Journal of Finance*, vol. 45, no. 2, pp. 379–395, 1990.

[37] J. Gatheral, *The Volatility Surface: A Practitioner's Guide*. New Jersey: John Wiley & Sons, Inc, 2006.

[38] J. Hull and A. White, "The pricing of option on assets with stochastic volatilities," *Journal of Finance*, vol. 3, pp. 281–300, 1987.

[39] J. Pospíšil and T. Sobotka, "Market calibration under a long memory stochastic volatility model," *In review.*

[40] J. T. Barkoulas, C. F. Baum and N. Travlos, "Long memory in Greek stock market," *Applied Financial Economics*, vol. 10, pp. 177–184, 2000.

[41] L. Bachelier, "Théorie de la spéculation," Ph.D. dissertation, Annales Scientiques de l'École Normale Supérierure, 1900.

[42] L. C. G. Rogers, "Arbitrage with fractional Brownian motion," *Mathematical Finance*, pp. 95–105, 1997.

[43] L. O. Scott, "Option pricing when the variance changes randomly: theory, estimation, and an application," *The Journal of Financial and Quantitative Analysis*, vol. 22, no. 4, pp. 419–438, 1987.

[44] M. C. Mariani, I. SenGupta and G. Sewell, "Numerical methods applied to option pricing models with transaction costs and stochastic volatility," *Quantitative Finance*, vol. 15, no. 8, pp. 1417–1424, 2015.

[45] M. C. Mariani, I. SenGupta and P. Bezdek, "Numerical solutions for option pricing models including transaction costs and stochastic volatility," *Acta Applicandae Mathematicae*, vol. 118, no. 1, pp. 203–220, 2012.

[46] M. Misiran, "Modeling and pricing financial assets under long memory processes," Ph.D. dissertation, Curtin University, 2010.

[47] M. Mrázek, J. Pospíšil and T. Sobotka, "On calibration of stochastic and fractional stochastic volatility models," *European Journal of Operational Research*, vol. 254, pp. 1036–1046, 2016.

[48] M. T. Greene and B. D. Fielitz, "Long-term dependence in common stock returns," *Journal of Financial Economics*, vol. 4, pp. 339–349, 1977.

[49] N. T. Dung, "Semimartingale approximation of fractional Brownian motion and its applications," *Computers and Mathematics with Applications*, vol. 61, pp. 1844–1854, 2011.

[50] O.T. Henry, "Long memory in stock returns: some international evidence," *Applied Financial Economics*, vol. 12, pp. 725–729, 2002.

[51] P. Cheridito, "Regularizing fractional Brownian motion with a view towards stock price modelling," Ph.D. dissertation, ETH Zurich, 2001.

[52] ——, "Arbitrage in fractional Brownian motion models," *Finance Stochastics*, vol. 7, pp. 533–553, 2003.

[53] P. Grau-Carles, "Tests of long memory: a bootstrap approach," *Computational Economics*, vol. 25, pp. 103–113, 2005.

[54] P. Guasoni, "No arbitrage under transaction costs, with fractional Brownian motion and beyond," *Mathematical Finance*, vol. 16, pp. 569–582, 2006.

[55] R. C. Merton, "Theory of rational option pricing," *The Bell Journal of Economics and Management Science*, vol. 4, no. 1, pp. 141–183, 1973.

[56] R. Cont, "Long range dependence in financial markets," in *Fractals in Engineering*, E. Lutton and J. Vehel, Ed. Springer, 2012, pp. 159–180.

[57] R. Cont and P. Tankov, *Financial Modelling with Jump Processes*. Chapman and Hall, CRC Press, 2004.

[58] R.J. Elliot and J. Van Der Hoek, "A general fractional white noise theory and applications to finance," *Mathematical Finance*, vol. 13, pp. 301–330, 2003.

[59] S. Dajcman, "Time-varying long-range dependence in stock market returns and financial market disruptions - a case of eight European countries," *Applied Economics Letters*, vol. 19, pp. 953–957, 2012.

[60] S. Kasman, E. Turgutlu and D. Ayhan, "Long memory in stock returns: Evidence from the major emerging Central European stock markets," *Applied Economics Letters*, vol. 16, pp. 1763–1768, 2009.

[61] S. L. Heston, "A closed-form solution for options wth stochastic volatility with applications to bond and currency options," *Review of Financial Studies*, vol. 6, no. 2, pp. 327–343, 1993.

[62] S. Rostek, *Option pricing in fractional Brownian markets*. Berlin, German: Springer, 2009.

[63] T. Bjork and H. Hult, "A note on Wick products and the fractional Black Scholes model," *Finance and Stochastics*, vol. 9, no. 2, pp. 197–209, 2005.

[64] T. E. Duncan, Y. Hu and B. Pasik-Duncan, "Stochastic calculus for fractional Brownian motion," *SIAM Journal of Control Optimization*, vol. 38, no. 2, pp. 582–612, 2000.

[65] T. Hoggard, A.E. Whalley and P. Wilmott, "Hedging option portfolios in the presence of transaction costs," *Advances in Futures and Options Research*, vol. 7, pp. 21–35, 1994.

[66] T. Sottinen and E. Valkeila, "On arbitrage and replication in the fractional Black-Scholes pricing model," *Stat Dec*, vol. 21, pp. 93–107, 2003.

[67] T.H. Thao, "An approximate approach to fractional analysis for finance," *Nonlinear Analysis: Real World Applications*, vol. 7, pp. 124–132, 2006.

[68] Thomson Reuters Tick History. XSP. Accessed Jul. 6, 2016. [Online]. Available: Subscription Service

[69] W. Willinger, M. S. Taqqu and V. Teverovsky, "Stock market prices and long-range dependence," *Finance Stochastic*, vol. 3, pp. 1–13, 1999.

[70] X. Feng, "Pricing of Bi-direction European option under the mixed brownian-fractional Brownian model," in *Business Intelligence and Financial Engineering: Proceedings of 2011 Fourth Internatonal Conference held in Wuhan*, Oct. 2011, pp. 410–413.

[71] X. Feng and S. Quan, "Pricing of option with power payoff driven by mixed fractional Brownian motion," in *Business Intelligence and Financial Engineering: Proceedings of 2010 Third Internatonal Conference held in Hong Kong*, Aug. 2010, pp. 170–173.

[72] X. T. Wang, "Scaling and long-range dependence in option pricing I: Pricing European option with transaction costs under the fractional Black-Scholes model," *Physica A*, vol. 389, pp. 438–444, 2010.

[73] X.T. Wang, E.H. Zhu, M.M. Tang and H.G. Yan, "Scaling and long-range dependence in option pricing II: Pricing European option with transaction costs under the mixed Brownian-fractional Brownian model," *Physica A*, vol. 389, pp. 445–451, 2010.

[74] X.T. Wang, M. Wu, Z. M. Zhou, W. S. Jing, "Pricing European option with transaction costs under the fractional long memory stochastic volatility model," *Physica A*, vol. 391, pp. 1469–1480, 2012.

[75] Y. Hu and B. Øksendal, "Fractional white noise calculus and applications to finance," *Inf. Dim. Anal. Quant. Probab.*, vol. 6, pp. 1–32, 2003.

[76] Y. K. Kwok, *Mathematical models of financial derivatives*. Berlin, German: Springer, 2008.

[77] Y. Mishura and G. Shevchenko, "Mixed stochastic differential equations with long-range dependence: Existence, uniqueness and convergence of solutions," *Computers and Mathematics with Applications*, vol. 64, pp. 3217–3227, 2012.

[78] Y. S. Mishura, *Stochastic calculus for fractional Brownian motion and related processes*. Berlin, German: Springer, 2008.

[79] Yahoo! Finance. (2016, Jul. 6) S&P 500 Mini SPX Options Index (XSP). [Online]. Available: https://au.finance.yahoo.com/quote/XSP/options?p=XSP

[80] Ycharts. (2016, Jul. 6) 3 Month Treasury Bill Rate. [Online]. Available: https://ycharts.com/indicators/3monthtreasurybillratemonthly

[81] Y.W. Cheung and K.S. Lai, "A search for long memory in international stock," *Journal of International Money and Finance*, vol. 14, pp. 597–615, 1995.

[82] Z. Ding, C. W. J. Granger and R. F. Engle, "A long memory property of stock market returns and a new model," *Journal of Empirical Finance*, vol. 1, pp. 83–106, 1993.